

Aus dem Institut für Tierphysiologie der Justus Liebig Universität Gießen
und aus der Medizinischen Klinik der Justus Liebig Universität Gießen,
Innere Medizin I, Abteilung für Kardiologie/Angiologie

FoxO1a and SIRT1 in Vasculo-Proliferative Diseases: Major Roles in Regulating Smooth Muscle Cell Proliferation, Migration and Survival

Inaugural-Dissertation
zur Erlangung des Doktorgrades der
Naturwissenschaften
im Fachbereich Biologie und Chemie der
Justus-Liebig-Universität Gießen

vorgelegt von

Dipl. Biol. Heike König

aus Wien, Österreich

Wien 2009

Dekan	Prof. Dr. Volkmar Wolters
1. Gutachter	Prof. Dr. W. Clauss Institut für Tierphysiologie Justus-Liebig-Universität Gießen
2. Gutachter	Prof. Dr. H. Tillmanns Medizinische Klinik I Kardiologie - Angiologie Universitätsklinikum Gießen und Marburg, Standort Gießen
3. Gutachter	Prof. Dr. R. Dammann Institut für Genetik Justus-Liebig-Universität Gießen

Tag der Disputation: 14. Juli 2009

*dedicated to my beloved family
and Richard*

Table of Content

Table of Content	i
Table of Figures.....	vi
Table of Tables.....	viii
Table of Content	i
Table of Figures.....	vi
Table of Tables.....	viii

INTRODUCTION	1
Atherosclerosis	2
The pathogenesis of atherosclerosis.....	3
Restenosis.....	6
The pathogenesis of restenosis	6
Vascular smooth muscle cells.....	9
Response to injury and inflammation	10
Activation and migration	10
Growth factors	11
ECM and Proteinases.....	12
Cell adhesion molecules.....	13
Integrins.....	13
Proliferation.....	13
Apoptosis	14
The phosphatidylinositol 3-kinase/Akt pathway	20
The phosphatidylinositol 3-kinases	20
The Akt kinase	21
The forkhead box O (FoxO) family of transcription factors	24
The forkhead box O family of transcription factors	24
FoxO target genes and its cellular function	25
DNA repair and detoxification under stress conditions.....	26
Cell differentiation	26
Glucose metabolism.....	26
Cell death.....	27
Other functions.....	28
Protein partners of FoxOs	28
Regulation of FoxO transcriptional activity via posttranslational modifications.....	30

Regulation of FoxO function via phosphorylation.....	30
Regulation of FoxO function via acetylation and deacetylation	34
Regulation of FoxO function via ubiquitination and degradation	36
The mammalian NAD-dependent protein deacetylase SIRT1	38
The family of mammalian histone deacetylases	38
The mammalian class III histone deacetylases (sirtuins).....	38
The biological function of SIRT1	40
MATERIALS AND METHODS	43
Materials.....	44
Chemicals	44
Antibodies	46
Primary antibodies.....	46
Secondary antibodies	47
Small interfering RNAs (siRNAs).....	47
Primer	47
Methods	48
Cell culture.....	48
Human coronary artery smooth muscle cells (HCASMC)	48
Mouse embryonic fibroblasts (MEF)	48
Mouse vascular smooth muscle cells	48
Rat vascular smooth muscle cells	48
Rat pulmonary artery smooth muscle cells (PASMC)	49
Cryoconservation and thawing of cells	49
RNA interference	49
Cell transduction with adenoviruses.....	50
Quantification of cell proliferation	50
Quantification of cell numbers.....	50
Cell migration assays.....	51
Quantification of apoptotic cell death rates.....	51
Forkhead transcription factor activity assays.....	52
Flow cytometric cell cycle analysis.....	52
Fluorescence resonance energy transfer (FRET).....	53
Double-labeling immunofluorescence for FRET-CLSM analysis.....	54
FRET Detection.....	55
Statistical analyses.....	55
Mouse femoral artery angioplasty	56
Animals	56

Mouse femoral artery injury model	56
Injection of adenovirus	58
Application of Psammaplysene A	58
Vessel Harvesting	58
Morphometric Analysis	59
Histological and Immunohistochemical techniques	59
Immunocytochemical analysis of human and mouse cells.....	59
Immunohistochemical analysis of SIRT1 expression in mouse tissues.....	59
Immunohistochemical analysis of SIRT1 expression in human tissues.....	60
Hematoxylin and Eosin (H & E) Staining	60
PCNA (Proliferating Cell Nuclear Antigen) staining of mice tissue sections	61
Co-immunoprecipitation (Co-IP).....	61
Detection and analysis of proteins	62
Total protein extraction from cultured cells	62
Quantification of protein concentration according to DC Protein Assay	62
Sodium Dodecyl Sulfate -Polyacrylamide Gel Electrophoresis (SDS-PAGE).....	62
Transfer and blotting of proteins	63
Ponceau S staining of proteins	63
Immunodetection of proteins	64
Synthesis of RNA.....	64
RNA Isolation	65
Determination of RNA concentration	65
First-strand cDNA synthesis	65
Polymerase Chain Reaction (PCR)	66
Agarose gel electrophoresis	67
Statistical analysis.....	67

RESULTS

68

Psammaplysene A and its analogues regulate HCASMC behavior <i>in vitro</i> and <i>in vivo</i>	69
Expression of FoxO1a in HCASMCs.....	69
Psammaplysene A renders FoxO1a nuclear localization in HCASMCs.....	70
Psammaplysene A-treatment inhibits HCASMC proliferation	71
Psammaplysene A blocks cell cycle entry of HCASMCs in G0/G1-phase	73
Psammaplysene A does not affect FoxO1a binding to specific promoter regions.....	74
Psammaplysene A blocks growth factor-induced cyclin D1 expression.....	75
Psammaplysene A inhibits neointima formation in wire-injured mouse femoral arteries	77
Psammaplysene A-analogues modulate HCASMC proliferation	78

FoxO1a localizes to the nucleus of serum-stimulated HCASMCs upon F10-treatment	80
F10-treatment inhibits HCASMC proliferation but does not induce apoptosis.....	81
Combined treatment with Psammaplysene A and F10 inhibits HCASMC proliferation at low concentrations	82
FoxO1a regulates PASC proliferation, migration and apoptosis.....	84
FoxO1a translocates from the nucleus to the cytoplasm in response to serum stimulation.....	84
FoxO1a regulates PASC proliferation, apoptosis and migration	84
FoxO1a induces PASCs apoptosis via upregulating caveolin-1 expression	87
Active FoxO1a blocks serum-induced downregulation of p27 ^{KIP1} and Cyclin D1 expression	88
FoxO1a regulates proliferation, migration and apoptosis of PASCs from MCT-treated rats	89
The histone deacetylase SIRT1 regulates HCASMC homeostasis <i>in vitro</i> and <i>in vivo</i>	92
SIRT1 affects HCASMC proliferation and migration	92
SIRT1 is localized to the nucleus of vascular smooth muscle cells.....	92
Endogenous SIRT1 is downregulated by siRNA in HCASMCs.....	93
Serum stimulation induces an upregulation of SIRT1 levels in HCASMCs	94
Pharmacological inhibition of endogenous SIRT1 function enhances HCASMC proliferation	95
Downregulation of SIRT1 by siRNA technique enhances proliferation of HCASMCs.....	96
SIRT1 is involved in regulating cell proliferation of mouse embryonic fibroblasts	96
Activation of SIRT1 by resveratrol inhibits serum-induced HCASMCs proliferation	97
Resveratrol influences HCASMCs proliferation via manipulating SIRT1 function	98
Adenoviral transduction with either active or constitutive inactive SIRT1 affects HCASMCs proliferation	100
SIRT1 is involved in inhibiting migration of HCASMCs and MEFs	100
SIRT1 is expressed in VSMCs of the murine femoral artery vessel wall	101
Adenovirus mediated gene transfer of SIRT1 protein inhibits neointimal hyperplasia in mouse femoral artery after endothelial injury	102
SIRT1 is expressed in VSMCs of human tissues.....	104
FoxO1a is not an interaction partner of SIRT1 in serum-stimulated HCASMCs	104

SIRT1 deacetylates FoxO1a in HCASMCs.....	107
Deacetylation of FoxO1a by SIRT1 enhances its transcriptional activity.....	107
Effect of SIRT1 on HCASMC programmed cell death	109
Pharmacological inhibition of endogenous SIRT1 induces apoptosis in HCASMCs.....	110
Hydrogenperoxide treatment induces HCASMCs apoptosis.....	111
Suppression of SIRT1 by siRNA technique induces apoptosis of HCASMCs ..	112
SIRT1 protects mouse embryonic fibroblasts from H ₂ O ₂ -mediated cell death..	113
Stimulation of endogenous SIRT1 activity reduces HCASMC apoptosis in response to serum-starvation	114
Adenoviral overexpression of active or inactive SIRT1 affects HCASMC viability and apoptotic cell death	114
SIRT1 protein expression is upregulated during apoptosis induction.....	115
SIRT1 and FoxOs are localized to the nuclei of peroxide stressed HCASMCs	115
SIRT1 interacts with FoxO1a during peroxide stress	116
FoxO1a is deacetylated by SIRT1 in response to peroxide induced stress.....	118
SIRT1 enhances cell survival following exposure to oxidative stress by shifting FoxO1a- induced responses away from apoptotic cell death and towards cell- cycle arrest and survival.....	119
DISCUSSION	122
Psammaplysene A and its analogues regulate HCASMC homeostasis <i>in vitro</i> and <i>in vivo</i>	123
FoxO1a regulates PASM proliferation, migration and apoptosis.....	130
SIRT1 regulates HCASMC proliferation, migration and survival.....	134
Summary	143
REFERENCES	145
References	146
APPENDIX	I
Summary	II
Zusammenfassung	IV
Acronyms and Abbreviations	VI
Declaration	IX
Publications	X
Acknowledgements	XII

Table of Figures

Figure 1. <i>Structure of an artery</i>	2
Figure 2. <i>Endothelial dysfunction in atherosclerosis</i>	3
Figure 3. <i>Fatty-streak formation during atherosclerosis</i>	4
Figure 4. <i>Formation of an advanced, complicated athero-sclerotic lesion</i>	5
Figure 5. <i>Unstable fibrous plaques in atherosclerosis</i>	5
Figure 6. <i>Development of restenosis after angioplasty</i>	7
Figure 7. <i>Morphology of a diseased murine artery</i>	8
Figure 8. <i>VSMCs secrete various mediators affecting their own cell behavior</i>	12
Figure 9. <i>Scheme of the cell cycle</i>	15
Figure 10. <i>Death receptor-mediated apoptotic pathway</i>	18
Figure 11. <i>Mitochondrial apoptotic pathway</i>	19
Figure 12. <i>The phosphatidylinositol 3-kinase/Akt pathway</i>	23
Figure 13. <i>Different post-translational modifications of the four FoxO isoforms</i>	33
Figure 14. <i>A model for FRET acceptor bleaching</i>	53
Figure 15. <i>Schematic representation of the spectral overlap integral</i>	54
Figure 16. <i>The endovascular injury of the murine femoral artery (Part 1)</i>	57
Figure 17. <i>The endovascular injury of the murine femoral artery (Part 2)</i>	57
Figure 18. <i>The endovascular injury of the murine femoral artery (Part 3)</i>	58
Figure 19. <i>Serum induces nuclear exclusion of FoxO1a proteins in HCASMCs</i>	69
Figure 20. <i>Structure of Psammaplysene A</i>	70
Figure 21. <i>Effect of Psammaplysene A on FoxO1a localization in HCASMCs</i>	71
Figure 22. <i>Effect of Psammaplysene A on HCASMC proliferation, migration and apoptosis</i>	72
Figure 23. <i>Psammaplysene A blocks HCASMC cycle progression in G0/G1-phase</i>	74
Figure 24. <i>Effect of Psammaplysene A on FoxO1a activity</i>	75
Figure 25. <i>Effect of Psammaplysene A on different cell cycle regulators</i>	76
Figure 26. <i>Psammaplysene A prevents neointima formation in vivo</i>	77
Figure 27. <i>Psammaplysene A modulates cellular proliferation in vivo</i>	78
Figure 28. <i>Psammaplysene A-analogues modulate HCASMC proliferation</i>	79
Figure 29. <i>Effect of F10 on FoxO1a localization in HCASMCs</i>	80
Figure 30. <i>Effect of F10 on HCASMC proliferation and apoptosis</i>	81
Figure 31. <i>Effect of a Psammaplysene A /F10 combination on HCASMC proliferation</i>	82
Figure 32. <i>Intracellular expression of FoxO1a in PASMCs</i>	84
Figure 33. <i>Cloning and mutagenesis of the constitutively active FoxO1a</i>	85
Figure 34. <i>FoxO1a regulates PASMC proliferation, migration and apoptosis</i>	86
Figure 35. <i>FoxO1a regulates caveolin-1 expression</i>	87

Figure 36. <i>FoxO1a</i> modulates expression of cell cycle regulating proteins in PASMCs.....	88
Figure 37. <i>FoxO1a</i> regulates proliferation, migration and apoptosis of MCT-treated PASMCs.....	90
Figure 38. <i>SIRT1</i> expression in VSMCs from various species.....	92
Figure 39. <i>SIRT1</i> downregulation by siRNA in HCASMCs.....	93
Figure 40. Serum stimulation affects <i>SIRT1</i> expression in HCASMCs.....	94
Figure 41. Effect of pharmacological <i>SIRT1</i> inhibition on HCASMC proliferation.....	95
Figure 42. Anti-proliferative effect of <i>SIRT1</i> is partially reversed by siRNA for <i>SIRT1</i>	96
Figure 43. <i>SIRT1</i> affects proliferation in mouse embryonic fibroblasts.....	97
Figure 44. Resveratrol treatment affects HCASMCs proliferation.....	98
Figure 45. Resveratrol affects cell proliferation via regulating <i>SIRT1</i> function.....	99
Figure 46. Cloning and mutagenesis of the dominant negative <i>SIRT1</i>	100
Figure 47. Effect of <i>SIRT1</i> on cell chemotaxis.....	101
Figure 48. <i>SIRT1</i> expression in the native and injured mouse femoral artery.....	102
Figure 49. <i>SIRT1</i> prevents neointima formation in vivo.....	103
Figure 50. <i>SIRT1</i> modulates cellular proliferation in vivo.....	103
Figure 51. <i>SIRT1</i> expression in human tissues.....	104
Figure 52. Detection of close association of <i>SIRT1</i> and <i>FoxO1a</i> in HCASMCs.....	106
Figure 53. <i>FoxO1a</i> is deacetylated by <i>SIRT1</i> in HCASMCs.....	107
Figure 54. Enhancement of <i>FoxO1a</i> transcriptional activity by <i>SIRT1</i>	108
Figure 55. Effect of pharmacological inhibition of <i>SIRT1</i> on HCASMC viability and apoptosis.....	110
Figure 56. H_2O_2 induces apoptosis of HCASMCs.....	111
Figure 57. Effect of <i>SIRT1</i> downregulation on HCASMC viability and apoptosis.....	112
Figure 58. Cell viability and death in <i>SIRT1</i> $-/-$ and wild-type MEFs.....	113
Figure 59. Resveratrol protects HCASMCs from apoptotic cell death.....	114
Figure 60. <i>SIRT1</i> expression is upregulated in response to apoptotic stimuli.....	115
Figure 61. Localization of <i>SIRT1</i> and <i>FoxO1a</i> in response to peroxide stress.....	116
Figure 62. Detection of close association of <i>SIRT1</i> and <i>FoxO1a</i> in HCASMCs.....	117
Figure 63. Acetylation levels of <i>FoxO1a</i> during peroxide stress.....	118
Figure 64. <i>GADD45</i> expression in response to oxidative stress is regulated by <i>SIRT1</i>	119
Figure 65. <i>MnSOD</i> expression in response to H_2O_2 treatment is not regulated by <i>SIRT1</i>	120
Figure 66. <i>SIRT1</i> -dependent modulation of <i>FoxO1a</i>	141

Table of Tables

Table 1. <i>FoxO target genes and their cellular roles</i>	30
Table 2. <i>List of chemicals</i>	45
Table 3. <i>List of primary antibodies</i>	47
Table 4. <i>List of secondary antibodies</i>	47
Table 5. <i>List of siRNAs for transient gene downregulation</i>	47
Table 6. <i>List of primer for reverse transcriptase PCR</i>	47
Table 7. <i>List of acronyms and abbreviations</i>	VIII

Introduction

Atherosclerosis

Cardiovascular diseases, such as myocardial infarction, stroke, and peripheral vascular insufficiency are currently the leading cause of death in the United States, Europe, and part of Asia¹⁻³. Atherosclerosis, a progressive inflammatory disorder which is characterized by the accumulation of lipids and fibrous elements in the artery vessel wall, is the primary cause for this growing burden⁴⁻⁶. For a detailed composition of the vessel wall, the reader is referred to Box 1, page 2. Atherosclerosis develops over decades, however, it has its start already during childhood and young adolescence⁷. Interestingly, earliest lesions seen with atherosclerosis in arteries are distributed randomly throughout the arterial tree, whereas advanced states are commonly found at sites with turbulent blood flow, such as bifurcations and branches, as well as at curved sections⁸⁻¹⁰.

Atherosclerosis is a multifactorial disease. Identified risk factors associated with this disease include hyperlipidemia, hypercholesterolemia, hypertension, diabetes mellitus, alcohol use, tobacco use and physical inactivity, but also age, gender and genetic predisposition¹¹. More recently, different other risk factors have also been identified, such as elevated plasma levels of apolipoprotein A¹², homocysteine^{13, 14}, plasminogen activator inhibitor 1 (PAI-1)¹⁵ and fibrinogen¹⁶.

Box 1 | Structure of an artery

The arterial wall is composed of three layers consisting of different cell types and connective tissue: the tunica intima, the tunica media and the tunica adventitia.

Tunica intima:

The innermost zone consists of a single layer of endothelial cells on the luminal side, a subendothelial layer of connective tissues and a layer of elastic fibers - known as the internal elastic lamina - on the peripheral side.

Tunica media:

This layer consists of numerous layers of vascular smooth muscle cells (VSMCs) as well as elastic and collagen fibers. It is covered by the external elastic membrane, which is composed of elastic fibers and notably thinner than the internal elastic lamina.

Tunica adventitia:

The adventitia is the outer layer and consists of an extracellular connective tissue matrix containing blood vessels, some smooth muscle cells, nerve fibers and fibroblasts.

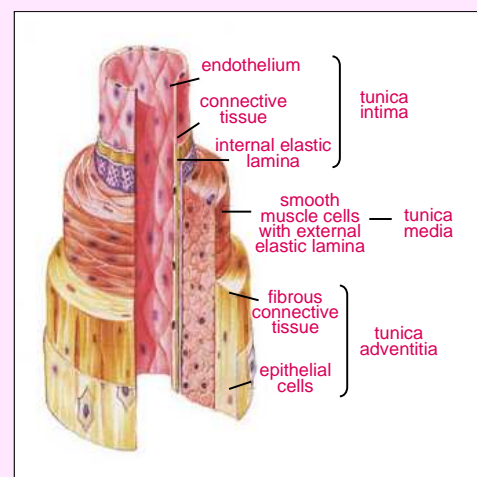


Figure 1. Structure of an artery
The picture was adapted from Fox¹⁷

The pathogenesis of atherosclerosis

In 1973, the "Response to injury hypothesis" was raised by Ross *et al.* describing the induction of atherosclerosis as a response to endothelial denudation¹⁸. This hypothesis has been tested and modified over the past 35 years and the most recent version represented in Figure 2 - Figure 5 stresses endothelial dysfunction rather than denudation initiating the chronic inflammatory process.

Endothelial injury induced by the above mentioned risk factors can lead to endothelial dysfunction^{19, 20}. This dysfunction is characterized by alteration in permeability of the lining endothelial cells which leads to an accumulation of lipids and lipoprotein particles (mainly low-density lipoprotein (LDL)) in the subendothelial space of the intima^{4, 21}. It has subsequently been shown that LDL undergoes modification by oxidation in the vessel wall²²⁻²⁴, and that the generated, minimally oxidized LDL (oxLDL) either directly attracts monocytes²⁵ or stimulates the overlying endothelial cells to produce various pro-inflammatory molecules^{22, 26}. In summary, these molecules include growth factors such as macrophage colony-stimulating factor (M-CSF), chemotactic proteins such as monocyte chemoattractant protein-1 (MCP-1), and adhesion molecules such as vascular cell adhesion molecule-1 (VCAM-1). A release of these proteins results in the recruitment of leukocytes to the vessel wall²¹ (Figure 2). VCAM-1 for example binds monocytes and T-lymphocytes, two types of leukocytes mainly found in early atherosclerotic plaques^{27, 28}.

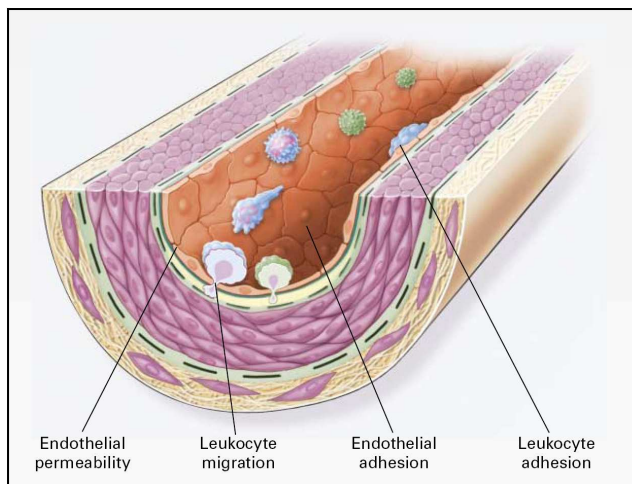


Figure 2. Endothelial dysfunction in atherosclerosis

The earliest alterations in the endothelium include enhanced permeability for LDL resulting finally in the upregulation of adhesion molecules. This then initiates the recruitment and transmigration of leukocytes into the vessel wall (see text). Picture adapted from⁴.

Once adhered to the arterial endothelium, leukocytes penetrate the endothelium lining and accumulate within the intima, a process that requires a MCP-1 gradient²⁹. OxLDL in the vessel wall stimulates the immigrated monocytes to convert into activated macrophages, which then take up the modified lipoprotein particles via their scavenger receptors, thus becoming large foam cells^{30, 31}. Experiments have shown that atherosclerotic lesions are four to ten times

smaller in mice with reduced numbers of macrophages, indicating a central role for this cell type in the development of atherosclerosis³².

The foam cells are joined by T-lymphocytes, which are activated by a series of cytokines, including tumor necrosis factor alpha (TNF- α), interleukin 2 (IL-2) and granulocyte-macrophage colony-stimulating factor (GM-CSF). Consequently, T-lymphocytes secrete chemokines such as interferon gamma (IFN- γ) and lymphotoxin by themselves. Both cytokines were verified to play important roles in the development of atherosclerotic disorders³³. The continuous accumulation of foam cells within the intima finally leads to the first ubiquitous lesion of atherosclerosis, the so-called fatty streak⁴.

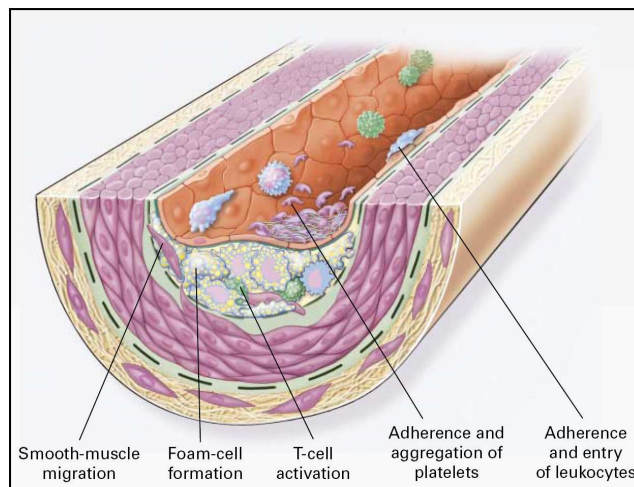


Figure 3. Fatty-streak formation during atherosclerosis

Fatty streak formation is characterized by the continuous accumulation of foam cells in the vessel wall. Foam cells derive from both monocytes and macrophages which take up oxLDL via endocytosis. Additionally, various growth factors, including PDGF and TGF, stimulate the smooth muscle cells to migrate into the fatty streak. Activated T-cells release a series of cytokines, such as IFN γ and lymphotoxin. Picture adapted from⁴.

The fatty streak can then progress to an intermediate, fibrofatty lesion if the offending risk factor(s) continue(s) to be present. At this state the macrophages and T-lymphocytes release several growth factors and cytokines, such as platelet-derived growth factor (PDGF) and transforming growth factor (TGF), thus amplifying the pro-inflammatory signals by further recruiting blood monocytes^{34, 35}. However, besides monocyte recruitment, the chemokines stimulate both endothelial cells (ECs) and vascular smooth muscle cell (VSMC) of the vessel wall to release cytokines by themselves (Figure 3). In addition, VSMCs are activated to replicate and migrate out of the media^{4, 36}.

Ultimately, the inflammatory and proliferative process leads to the progression of the atherosclerotic lesion to an advanced, complicated state called fibrous plaque (Figure 4). At that time, the lesion has a complex structure and contains multiple layers of VSMCs, both lipid-laden macrophages and VSMCs, T-lymphocytes, connective tissue, as well as lipids and varying amounts of cell debris from both apoptotic and necrotic cells in the centre of the plaque, called the lipid core. Because of remodeling processes the formation of a fibrous cap occurs which overlies the lipid core²¹.

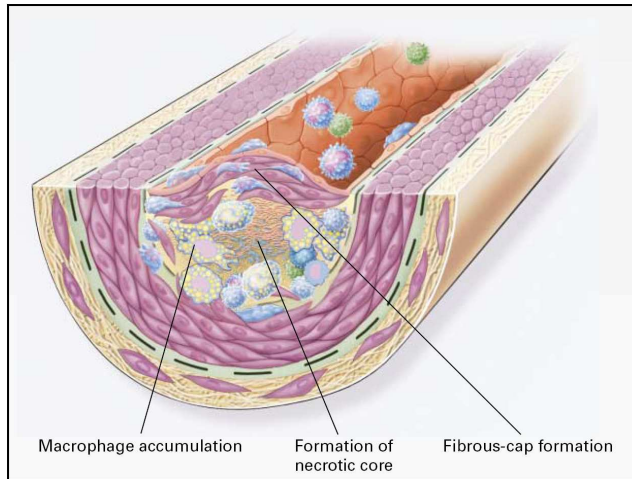


Figure 4. Formation of an advanced, complicated atherosclerotic lesion

Advanced atherosclerotic lesions are characterized by a fibrous cap - consisting mainly of VSMCs - which covers a necrotic core. The core itself mainly consists of leukocytes, lipids and cell debris. Picture adapted from⁴.

The fibrous cap consists of numerous VSMCs surrounded by a connective tissue matrix containing collagen, elastic fibers, and proteoglycans, but may sometimes also contain monocyte-derived macrophages and some T-lymphocytes³⁷. Importantly, it prevents contact between the pro-thrombotic material in the atherosclerotic lesion and the blood.

Although advanced lesions can become large enough to block blood flow (stenosis), the most important notable clinical complications are related to plaque rupture, which happens when the mechanical stresses in the fibrous cap exceed a critical level that the cap tissue can withstand³⁸. In this context, it was shown that plaques that have ruptured and caused fatal thrombosis often revealed thin fibrous caps^{39, 40}. The biomechanical strength and stability of the fibrous cap originates from interstitial collagen. However, during the inflammatory response thinning of the cap is induced on several levels: On the one hand VSMC-mediated synthesis of new collagen fibers is blocked due to the production of IFN- γ from activated T-lymphocytes, and on the other hand existing collagen is degraded via collagen-degrading enzymes (such as members of the matrix metalloproteinase (MMP) family) that are produced by macrophages

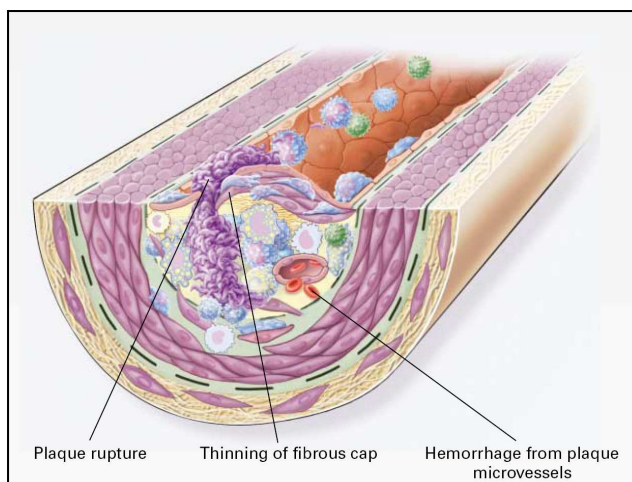


Figure 5. Unstable fibrous plaques in atherosclerosis

Rupture of the atherosclerotic plaque results due to constant thinning of the fibrous cap. Collagen-degrading enzymes as well as the reduced production of collagen fibers are responsible for the thinning of the fibrous cap. Additionally, VSMC apoptosis also contributes to this vulnerability. Picture adapted from⁴.

(reviewed in²¹). Additionally, apoptosis of VSMCs in the plaque also contributes to plaque vulnerability as described below.

Once the fibrous cap ruptures, exposure of the pro-thrombotic necrotic core content to the blood causes sudden thrombus formation and thrombus-mediated acute coronary events, as for example myocardial infarction or stroke⁴¹ (Figure 5). Responsible for this is on the one hand the collagen in the plaque's extracellular matrix, which triggers platelet activation and on the other hand the tissue factors produced by macrophages and VSMCs, which activates the coagulation cascade⁴².

Restenosis

Plaque formation during atherosclerosis does not always lead to plaque rupture and "acute coronary syndrome" (ACS) but can cause narrowing of the arteries (stenosis) resulting in an insufficient blood supply (see above). Patients suffering from coronary artery stenosis will experience angina pectoris (chest pain). Percutaneous transluminal coronary angioplasty (PTCA), also termed percutaneous coronary intervention (PCI), is a well-established technique for the treatment of vascular occlusions and was first performed in man 1977 by Andreas Grüntzig⁴³. Unfortunately, its success is often limited by the subsequent re-occlusion (restenosis) of the dilatated artery, which is primarily due to neointimal hyperplasia. Indeed, 30–40% of patients that have undergone PTCA will develop restenosis within the first 6 months upon surgery^{44, 45}, thus generating high costs for additional surgery procedures (e.g. revascularization or bypass surgery). With the deployment of stents in the mid 1980's, the incidence of restenosis is now about 20%, but still an unacceptably high rate⁴⁴. Stents are small wire-mesh tubes or "scaffolds" introduced into the blood vessel to eliminate the problem of early recoil after angioplasty (Figure 6). Unfortunately, the clinical problem of in-stent restenosis still remains⁴⁶. Recently, the concept of using drug-eluting stents coated with anti-proliferative and anti-inflammatory agents that could potentially inhibit neointimal hyperplasia has emerged⁴⁷. Use of these agents, such as macrolide sirolimus (rapamycin) and taxane paclitaxel^{48, 49}, significantly lowered the rate of in-stent restenosis (<10%), but implicated several other problems such as in-stent thrombosis, polymer hypersensitivity and retarded healing due to delayed re-endothelialization^{50, 51}.

The pathogenesis of restenosis

Mechanical injury through balloon angioplasty (with cell loss in the intima and media, elastic lamina fragmentation and a general damage of tissue architecture) triggers a healing response of the arterial wall, resulting in restenosis. The excessive pathological repair begins immediately

after the initial injury and may last for weeks or months. It has been well characterized in various animal models of balloon denudation⁵². The exact pathophysiology of restenosis has still not been fully established but it has been suggested that this disease comprises three main processes: early elastic recoil, neointimal hyperplasia and vessel remodeling⁵³⁻⁵⁵.

Elastic recoil occurs within the first hours after vessel dilation (Figure 6). In response to stretching the vessel, the elastic fibers within the vessel wall start to recoil back to their original state. This event leads to an immediate luminal diameter loss and defines the beginning of restenosis⁵⁶.

Vessel injury due to stretching results in endothelial denudation, exposing the subendothelial components of the vessel to the blood, thus promoting aggregation of leukocytes and platelets, as well as induction of the coagulation cascade⁵⁷. Activated platelets release cytokines in order to recruit leukocyte to the place of injury and additionally express adhesion molecules (e.g. P-selectin) for leukocyte binding. Consequently, mononuclear leukocytes enter the arterial wall and subsequently transform into macrophages. These activated macrophages produce cytokines and growth factors by themselves, which is pivotal for amplifying the inflammatory response⁵⁸.

Together, all inflammatory cells release chemotactic factors such as PDGF, basic fibroblast growth factor (bFGF), transforming growth factor β (TGF- β), thrombin, and angiotensin II^{59, 60} that stimulate VSMC migration out of the media within hours after arterial injury⁶¹. Once arrived in the intima, VSMCs subsequently proliferate and secrete extra-cellular matrix (ECM) proteins building up a neointimal tissue, a process which is known as neointimal hyperplasia (Figure 6)^{36, 62}. This tissue then spreads into the vessel lumen, thus narrowing the lumen diameter. Typically, intimal hyperplasia occurs in areas where re-endothelialization is retarded revealing that the endothelium modulates the migratory and proliferative activity of the underlying VSMCs⁶³.

Nevertheless, proliferation of VSMCs is not only affected by chemotactic factors, but recent publications provide evidence for mechanic stress-induced VSMC proliferation at the place of

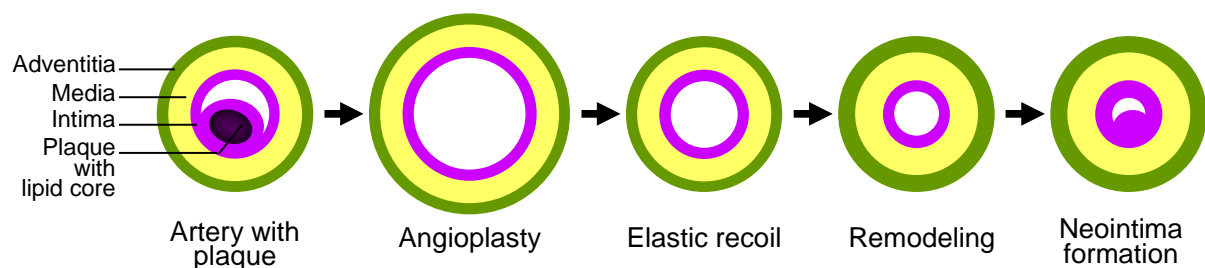


Figure 6. Development of restenosis after angioplasty

Restenosis after angioplasty comprises three processes: Early recoil within one hour after dilatation, vascular remodeling and neointima formation during the next one to six months.

endothelial denudation⁶⁴. Sedding *et al.* demonstrated that mechanical force activates integrin-mediated phosphatidylinositol 3-kinase/Akt (PI3K/Akt) signaling in VSMCs resulting in cell cycle entry and progression^{65, 66}. Interestingly, caveolin-1, a major constituent of caveolae (= invaginations of the plasma membrane), is required for efficient signaling in these cells by creating an active c-Src kinase/PI3K/Akt module⁶⁶.

The dynamic process of VSMC migration requires ECM protein degradation and re-synthesis. For example, the production of MMPs by macrophages is upregulated during the inflammatory process, leading to matrix remodeling and initiates VSMC migration⁶⁷.

Several studies have demonstrated that, additionally to VSMCs, myofibroblasts in the adventitia also respond to the inflammatory cytokines, causing their proliferation and migration into the intimal tissue. This contributes to the enlargement of the adventitia as well as to collagen synthesis within the media (Figure 6)^{68, 69}. The role of both the adventitia and collagen in the remodeling of the arterial wall has been increasingly recognized and postulated to play a key role in late lumen loss during restenosis^{70, 71}. However, still little is known about the molecular mechanisms involved in this process. Figure 7 shows the mentioned neointimal tissue within a murine artery generated upon endovascular arterial injury.

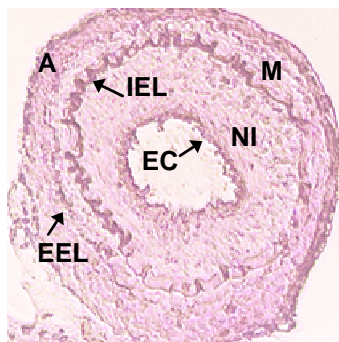


Figure 7. Morphology of a diseased murine artery

Histological transverse section of a murine femoral artery with significant luminal narrowing caused by restenosis after intravascular arterial injury. Abbreviations: A, adventitia; EEL, external elastic lamina; M, media; IEL, internal elastic lamina; NI, neointima; EC, endothelial cells. Picture from Sedding *et al.*.

Vascular smooth muscle cells

Atherosclerosis, restenosis and pulmonary hypertension (see Box 2, page 9) are complex diseases, in which VSMCs are the predominant cell type and an important actor. In healthy adult arteries, VSMCs are normally in a quiescent, fully differentiated state, and are part of the vessel wall media (see Figure 1 in Box 1). They provide structural integrity and have the ability to dilate and constrict the vessel wall, thereby regulating blood flow. Walker and coworkers first described the phenotype of VSMC obtained from the rat media as a spindle-shaped phenotype, with the classic "hill-and-valley" growth pattern⁷². Likewise, arteries of various other species - including humans - show this kind of medial VSMC phenotype.

During vessel development in the embryo, as well as in the above named disease states the situation changes and arterial VSMCs undergo a process often referred to as phenotypic

Box 2 | Pulmonary hypertension

Hyperplasia and VSMC migration are features involved in atherosclerosis/restenosis as well as in pulmonary vascular diseases, such as pulmonary hypertension (PHT). The normal pulmonary circulation is an uncommonly low pressure and low resistance system, whose function is to optimize blood and tissue oxygenation⁷³. The cardiovascular syndrome of PHT is defined clinically as a condition of elevated pulmonary arterial pressure and/or pulmonary vascular resistance due to both vessel wall remodeling and increase in vascular constriction. PHT leads to right heart failure because of right ventricular hypertrophy, which finally leads to premature death. A typical indicator for severe, advanced PHT - as it is also for atherosclerosis and restenosis - is remodeling of the arterial vessel wall⁷⁴. A variety of stimuli are known to initiate this pathophysiological process, including chronic hypoxia, increased pulmonary blood flow, anorectic and other drugs, as well as different idiopathic causes⁷³. Histologically, pulmonary vascular remodeling is displayed by intimal proliferation, medial and adventitial hypertrophy and hyperplasia, muscularization of peripheral vessels such as arterioles, and vaso-occlusive plexiform lesions⁷⁵.

Pulmonary artery smooth muscle cells (PASMCs) in the lung artery wall contribute primarily to these remodeling processes. Their function is modulated by e.g. growth factors, contractile agonists and inflammatory mediators released by different cell types in response to the above mentioned PHT triggers. First, PASMCs re-enter the cell cycle, subsequently proliferate, migrate and secrete ECM proteins. The changes within the vessel wall lead to a decrease in lumen diameter and to an increase in vascular resistance to blood flow due to an attenuated vasodilatory capacity. Consequently, this leads to a persistence of high blood pressure.

The detailed molecular mechanisms that control vascular remodeling remain unknown to date. However, recent studies by Goncharova *et al.* revealed a role for the PI3K/Akt pathway in mediating proliferation and migration of human PASMCs. This pathway is demonstrably important in a variety of vaso-proliferative disorders, as for example in the already mentioned atherosclerosis and restenosis. For a detailed description of the PI3K/Akt pathway the reader is referred to the capital "The phosphatidylinositol 3-kinase/Akt pathway" in the main text. Fouty and coworkers observed that overexpression of the Akt downstream target p27^{KIP1}, an inhibitor of cyclin-dependent kinases (see Box 3, page 15) decreased PASMC proliferation⁷³. These results were verified by other investigators⁷⁶. Unpublished data from our group revealed the involvement of FoxO transcription factor in PHT, which is not surprisingly given that FoxOs are direct Akt-targets and regulate p27^{KIP1} transcription as it is reviewed in the introduction part of this thesis (see below). The present PhD study further examines FoxO's regulatory function on PASMC behavior. Determining the molecular pathways that are responsible for mediating PASMC behavior will help us to identify new therapeutic approaches for treating PHT.

modulation. A switch from the quiescent contractile phenotype to an altered “synthetic” one characterizes this process. VSMCs of this population are present in the intima after balloon angioplasty and are morphologically distinct from their medial counterparts^{72, 77}. They show an epitheloid phenotype, and the cells grow as a monolayer exhibiting a cobblestone morphology at confluence^{72, 77}.

Functionally, these cells enter the cell cycle (see Box 3, page 15), acquire the capacity to proliferate dramatically, migrate and synthesize ECM proteins thereby generating new tissue⁷⁸. Besides these functions, this type of VSMC significantly attenuates expression of SMC-specific marker genes, such as smooth muscle α -actin, smooth muscle myosin heavy chain (MHC), caldesmon etc.⁷⁹. For further information on VSMC diversity, the reader is referred to recent reviews^{80, 81}. The activator(s) triggering the process of phenotypic modulation *in vivo* is/are still unclear. However, it is believed that injurious stimuli-mediated changes in the vessel wall environment and in the ECM are responsible for it.

The origin of intimal VSMCs has been an issue of debate and until recently, the prevailing theory was that after induction of mitogenic stimuli, VSMCs migrate out of the vessel's media into the intima^{4, 36}. However, this theory has been challenged by recent studies in animal models of vessel injury and in human allograft studies, where it is proposed that intimal VSMCs originate from diverse other sources besides the media. For example, intimal VSMCs may originate from circulating bone marrow-derived progenitor cells (see review Sata *et al.*⁸²). Work from our group could demonstrate the potential of circulating human endothelial progenitor cells (EPCs) to transdifferentiate into functionally active VSMCs *in vitro* and *in vivo* (Sedding *et al.*, personal communication). Additionally, both fibroblasts from the adventitia and ECs are able to transdifferentiate into VSMCs during restenosis, respectively⁸³. The contribution of each of these possibilities is, nevertheless, controversial and a subject of debate. The only thing that has been proven yet is that VSMCs of the arterial wall are biologically heterogeneous.

Response to injury and inflammation

Activation and migration

Activation and migration of VSMCs from the media to the intima plays an essential role in pathologic processes, such as intimal hyperplasia and atherosclerosis. For example, at least 20% to 40% of medial VSMCs are activated in response to balloon injury and enter the cell cycle⁸⁴. These cells then transmigrate through breaks in the internal elastic membrane into the innermost area of the vessel. Nearly 50% of these migrating cells continue to proliferate for several cycles and generate new tissue, whereas the rest does not synthesize DNA⁸⁵. Therefore, migration and proliferation should thus be considered as two distinct mechanisms leading to neointimal thickening⁸⁵.

Successful cell migration is induced by a myriad of extracellular influences such as growth factors, ECM proteins, and interaction with cell surface receptors - particularly integrins - which activate a complex array of intracellular signal transduction pathways⁸⁶. These processes result in VSMC focal adhesion turnover, actin filament polymerization, proteolysis of the ECM, and directed migration along gradients of different chemoattractant stimuli.

Growth factors

Multiple growth factors, which serve as mitogens and chemoattractants, have been shown to stimulate VSMC migration both in a paracrine and an autocrine mechanism^{85, 86}. Vascular injury results in the local release of these factors. The plasma contains norepinephrine, lipoprotein A, angiotensin II, epidermal growth factor (EGF) and insulin-like growth factor (IGF-1). The last three, together with bFGF, are also released by ECs. Thrombin from the thrombus formed after endothelial denudation itself has strong mitogenic properties and stimulates EC- and VSMC-mediated PDGF expression and release. Moreover, activated platelets release at least five mitogens for VSMCs, including serotonin, thromboxane A₂, TGF- β , bFGF and PDGF⁸⁷. Although they constitute a minority population in the injured vessel – in comparison to all other cell types -, macrophages synthesize a wide variety of growth factors, including PDGF, bFGF, TGF- β , TGF- α , IL-1, and EGF⁸⁵.

It is important not to underestimate the effect of the VSMCs themselves on growth factor release. TGF- β and EGF, stimulate VSMCs to secrete the potent chemoattractant fibronectin. Additionally, angiotensin II, EGF, IGF-1 and bFGF are released by VSMCs. Through the release of these factors, VSMCs may - in a paracrine fashion - indirectly induce their own migration as well as other cellular processes that are important for the pathophysiology of vascular diseases (Figure 8).

However, of all the mentioned growth factors, PDGF is the most well described and likely most important one. Sedding *et al.* reported recently, that the factor VII activating protease (FSAP), a plasma protein, reduces neointima formation in a mouse model at sites of injury via inactivating PDGF. In comparison to the wild-type FSAP, a mutated form failed to reduce VSMC migration and proliferation in the vessel wall during repair mechanisms⁸⁸.

As it was already mentioned, proliferation is also influenced by PDGF. Even so, in contrast to proliferation, migration is an earlier response to PDGF and is stimulated by lower concentrations than those needed for cell division⁸⁵.

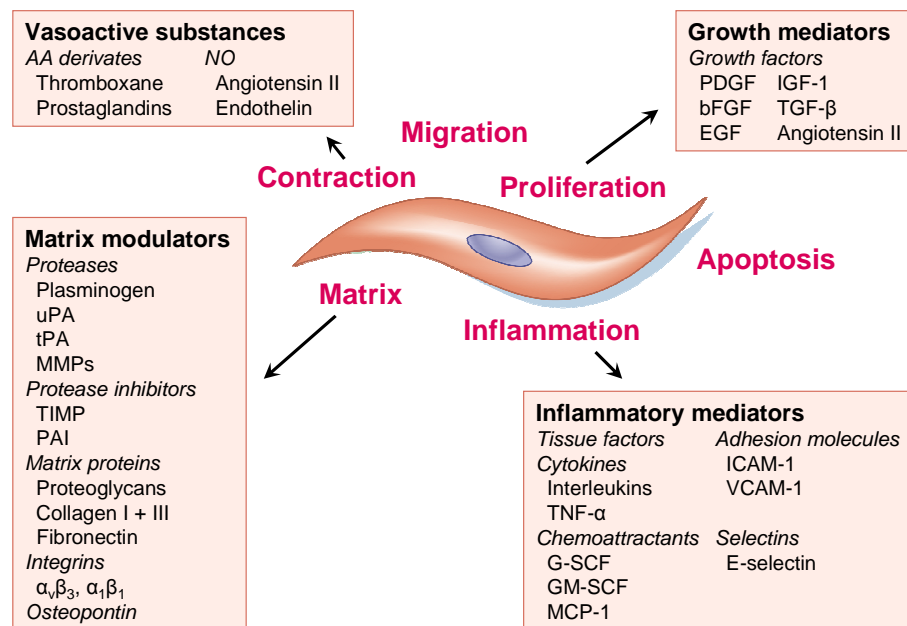


Figure 8. VSMCs secrete various mediators affecting their own cell behavior

VSMCs mediate their own migration on the one hand by releasing factors for matrix alterations and on the other hand by secreting mitogens and chemoattractants important for locomotion (see text for further information). However, many of these mediators simultaneously affect proliferation, apoptosis, inflammation and contraction of VSMCs. For example, several growth factors stimulate VSMC proliferation, migration and apoptosis. The picture was adapted from Dzau *et al.*⁴⁵.

ECM and Proteinases

Migration of VSMCs requires proteolysis or digestion and remodeling of the surrounding ECM. In the normal vessel wall ECM is composed predominately of collagen, elastin, proteoglycans, and glycoproteins. After arterial injury, the kind, quantity, and distribution of these matrix proteins changes: collagen, glycoproteins and hyaluronic acid are expressed to a greater extent. Expression of CD44 on the VSMC membrane - a receptor for hyaluronic acid - has been shown to be upregulated in the neointima, and interaction between hyaluronic acid and CD44 was proven to stimulate VSMC migration⁸⁹. In addition to CD44, migrating VSMCs express another hyaluronic receptor called receptor for hyaluronic acid-mediated motility or shortly RHAMM^{89, 90}. Apart from serving only structural function, certain ECM proteins itself, such as collagen I and IV and fibronectin, are as potent as PDGF in stimulating VSMC locomotion⁹¹.

For ECM degradation different proteolytic systems including MMPs and serine proteinases of the urokinase-type plasminogen activator system are essential. Proteinases are a family of enzymes produced by a variety of cell types and are activated in response to vascular injury. In vascular diseases MMP-2 and MMP-9 are of special interest, since type IV collagen is the main substrate of both gelatinases. Type IV collagen is a basal membrane component which has to be degraded to enable the migration of VSMCs⁸⁶. All MMPs are secreted as inactive zymogens and have to be cleaved, for example by plasmin – a serine proteinase of the urokinase-type

plasminogen activator system – in order to be activated. MMP gene expression is induced by cytokines and the growth factors bFGF and VEGF.

Besides the indirect activation of MMPs, plasmin can directly digest ECM components enzymatically, including fibrin, fibronectin, laminin and the protein core of proteoglycans. The protease is released as plasminogen into the circulation and activated by tissue-type plasminogen activator (tPA) or urokinase-type plasminogen activator (uPA). Most migrating cells express uPA and sometimes tPA, and thereby facilitating migration⁸⁵. Like MMP-expression, expression of both plasminogen activators is affected by VEGF and bFGF.

Cell adhesion molecules

A dynamic interaction between transmembrane adhesive receptors on the VSMC cell surface and ECM components is another key process in VSMC locomotion and migration. There are several cell adhesion molecules (CAMs) known which are subdivided into four protein families: the integrins, the immunoglobulin superfamily (IgSF), the cadherins and the selectins. However, the integrins were shown to be the most important subtype of CAMs involved in VSMC migration during vessel dysfunction.

Integrins

Integrins are heterodimer receptors located on almost every cell type and composed of one α - and one β -subunit, that can be combined to form more than 20 different types of integrin receptors. VSMCs are particularly known to express β_1 - and β_3 -subunits⁹². The β_1 -integrin subunit is constitutively expressed and abundant on quiescent VSMCs. The β_3 -subunit is upregulated during vascular remodeling processes as well as in the presence of TGF- β and PDGF, and focused on the leading edge of migrating cells. Several different α -subtypes are expressed including α_v and α_1 . Nevertheless, $\alpha_v\beta_3$ appears to be the major migration promoting receptor on VSMCs, attaching to osteopontin, a phosphoprotein with adhesive and chemotactic properties that is associated with arterial VSMC migration under pathological conditions⁸⁹. Osteopontin was recently shown to be expressed in diseased vessels by macrophages, VSMCs and ECs⁹³. ReoPro (also called Abciximab), an antibody against all β_3 -integrins, inhibits in-stent neointimal hyperplasia after PTCA in humans, partially by preventing VSMC migration from the media to the intima⁹².

Proliferation

After being migrated to the intima, many of the neointimal VSMCs continue to proliferate excessively for several cycles. Proliferation is characterized by the transition of cells through the cell cycle and is triggered by numerous growth factors and cytokines. Different cell types (e.g. inflammatory cells) involved in the pathological process of vasculo-proliferative diseases create

a mitogenic milieu essential for proliferation (see above). For example, activated macrophages were already mentioned to synthesize PDGF, which stimulates VSMC migration⁸⁵. However, PDGF can also directly promote excessive intimal VSMC proliferation⁹⁴. Another very important growth factor for stimulating VSMC proliferation is bFGF, which is synthesized by most of the cell types found in atherosclerotic and restenotic areas. As it was shown in the rat model by Lindner and colleagues, dying vascular cells release bFGF, which in turn initiates proliferation of VSMCs in the media⁹⁵. Previous work performed during my diploma thesis could also demonstrate the effect of bFGF on human VSMC proliferation (unpublished data). Intimal proliferation of VSMCs also occurs under the influence of numerous other growth factors as for example TGF- β , IGF-1, and angiotensin II⁴⁵.

Furthermore, cytokine- or sheer stress-induced secretion of nitric oxide (NO) by ECs results in attenuated VSMC proliferation⁹⁶. Loss of the endothelium after physical or biochemical injury results on the one hand in loss of endothelium-derived NO production and on the other hand in loss of its homeostatic function. This may explain the effect of re-endothelialization of the denuded vessel on blocking neointima formation⁶³.

Vascular proliferation requires DNA replication, and is therefore dependent on cell cycle transition (see Box 3, page 15). As in all mammalian cells, proliferation of VSMCs is primarily controlled at the site of cell cycle entry, the so-called G0/G1- to S-phase transition. Numerous growth factors, amongst them PDGF and bFGF, initiate different signaling cascades leading to transcription of early genes that allow cell cycle entry⁷⁸. Other factors, including EGF and IGF-1, however, stimulate progression of the cells toward the S-phase⁷⁸ (see Figure 9). One important signaling cascade activated by growth factors in VSMCs during proliferation is the already mentioned PI3K/Akt pathway⁹⁷, which is described in further details in chapter “The phosphatidylinositol 3-kinase/Akt pathway”. Activation of this pathway induces e.g. accumulation of cyclin D and downregulation of the “gatekeeper” p27^{KIP1}, thus, providing requirements for cell cycle progression into S phase⁹⁸. Interestingly, activation and progression of the cell cycle machinery in plaque VSMCs does not always induce cell division, but was recently also shown to induce programmed cell death⁹⁹.

Apoptosis

An outstanding feature of blood vessel remodeling, both during normal development and pathological disorders, is the apoptotic cell death of VSMCs in the vessel wall¹⁰⁰⁻¹⁰². Cell death in atherosclerotic lesions was first recognized by R. Virchow 150 years ago in 1858¹⁰³. Since 1995, several research laboratories reported on apoptosis of VSMCs implicated in atherosclerosis and restenosis^{38, 104-109}.

Box 3 | The mammalian cell cycle

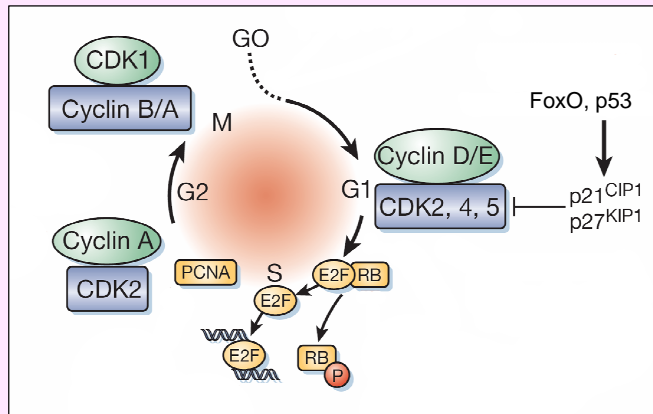


Figure 9. Scheme of the cell cycle

Cell cycle progression is regulated by holoenzymes composed of CDKs and a regulatory subunit called cyclins. CKIs negatively regulate the activation of CDKs. See text for details. Adapted from⁴⁵.

The cell cycle comprises a highly conserved, coordinated set of events resulting in cell growth and division of a mother cell into two daughter cells. It consists of four different phases: G1-phase, S-phase, G2-phase and M-phase^{45, 78}. During the S-phase (S=synthesis), the DNA is replicated, whereas during the M (Mitosis)-phase, the chromosomes and the cytoplasm are divided between the two daughter cells. G1 and G2, the so called "Gap"-phases, separate S and M and represent times where the cells carries on its normal metabolic functions. Non-dividing cells, or quiescent cells, have entered a state called G0-phase. Several checkpoints at the G1/S and G2/M transition ensure controlled cell cycle progression¹¹⁰. The one regulating S-Phase entry is called restriction point and is located at the end of the G1-phase. Here the cell decides whether it should divide, or enter a resting stage. The second checkpoint can be found at the end of G2-phase. As soon as

the cell is ready for mitosis this checkpoint triggers the start of the M-phase. Progression through each cell cycle phase depends on cyclin-dependent kinases (CDKs), which themselves have to be activated by a special class of proteins called cyclins¹¹⁰. In mammals, the cyclins have been named A, B, D and E, whereas the proteins of the CDK superfamily are indicated as CDK followed by a number. Each phase of the cell cycle involves different cyclin-CDK complexes (see Figure 9). Triggers for transition through the G1- and S-phases are both the augmented accumulation of cyclin D-CDK4 and cyclin E-CDK2 complexes, as well as rising levels of proliferating cell nuclear antigen (PCNA)¹¹⁰. Cyclin A-CDK2 and cyclin B-CDK1 complexes regulate the subsequent G2/M transition¹¹⁰. A family of regulatory proteins that plays a key role in preventing CDK activity is the cyclin-dependent kinase inhibitor family (CKI) which comprises two classes: The INK proteins, which disable activation of CDK4 and CDK6, and the CIP/KIP proteins, such as p27^{KIP1} and p21^{CIP1}, which negatively regulate cell cycle progression by targeting diverse cyclin-CDK complexes. Different transcription factors transactivate CDKs and CKIs. For example, active p53 causes G1-phase arrest by inducing expression of p21^{CIP1}, which in turn inhibits the activity of the G1-specific cyclin-CDK complexes. Conversely, the E2F family of transcription factors together with retinoblastoma (RB) protein controls expression of genes in S-phase. FoxO transcription factors are other important regulators, similar to p53, as recently shown by our group. Their influence will be discussed in more detail below.

The term of apoptosis was first introduced by Kerr and coworkers in 1972¹¹¹ and describes a special kind of spontaneous cell death, which has to be distinguished from necrosis. During the development of apoptosis, all cell types go through a series of morphological changes, beginning with shrinkage of the cell membrane and continuing with margination and condensation of the nuclear chromatin, as well as cellular fragmentation and, ultimately, the engulfment of the apoptotic bodies by adjacent neighboring cells³⁸. All three of the major cell types found in atherosclerotic lesions (macrophages, VSMCs, and ECs) can undergo apoptosis. Nevertheless, the main subject of this thesis is about VSMCs, and therefore I will focus only on VSMC apoptosis and its contribution to atherosclerosis, restenosis and PHT.

During atherosclerosis development, the frequency of apoptotic VSMC cell death seems to increase as the plaques proceeds. Early lesions tend to have only few apoptotic VSMCs as compared to normal vessels, however, the apoptotic rate further increases in advanced atherosclerotic plaques³⁸. Moreover, it has been observed that there is an exceeding number of VSMC dying of apoptosis in unstable atherosclerotic lesions than in stable lesions of human coronary arteries^{105, 112, 113}. As already mentioned above, VSMCs from atherosclerotic plaques exhibiting an epitheloid phenotype are more prone to apoptosis than normal VSMCs due to a higher sensitivity to DNA damage inducing agents. Additionally, these cells show strong expression of the pro-apoptotic protein Bax, whereas expression of anti-apoptotic members of the Bcl-2 family can only be seen in intimal VSMCs³⁸. Taken together, this may contribute to an increase of apoptosis in advanced atherosclerotic lesion.

In early atherosclerotic lesions apoptosis of VSMCs seems to be protective due to inducing regression of thickened arterial walls. Nevertheless, in an advanced state cell death of VSMCs in the fibrous cap has detrimental effects on the plaque stability^{104, 106, 108}. Responsible for a possible plaque rupture is not only a decrease in cellular density, but - because VSMCs produce collagen fibers - loss of VSMCs will reduce the biosynthesis of new interstitial collagen fibers and subsequently, the mechanical integrity will be lost with time³⁸.

In animal models, a burst of apoptotic cell death occurs as an early phenomenon in the media and as a late event in the developing neointima after balloon angioplasty¹¹⁴. Similar in humans, apoptotic VSMCs are detected in restenotic lesion following angioplasty at a greater frequency than that observed in the normal artery wall. Apoptosis of VSMCs also participates in development of aneurysms³⁸.

Several inducers of VSMC apoptosis in the mentioned diseases have been identified in the last years. These factors include mechanical force, modified lipids (oxLDL, oxysterols), free radicals (reactive oxygen species (ROS), nitric oxide (NO)), radiation (UV-, X- and γ-radiation), Fas ligand (FasL) and inflammatory cytokines produced by activated immune cells.

Atherosclerotic lesions contain oxLDL, which seems to be a major cytotoxic component in atherosclerosis²⁴. Typically, cholesterol and its esters have only little pro-apoptotic effects, however in an oxidized state they become cytotoxic. Thus, some of these oxygenated derivatives in the oxLDL particles are suggested to be at least in part responsible for the pro-apoptotic effect of oxLDL¹⁰¹. The molecular mechanisms by which oxLDL may induce apoptosis have not been completely understood, but it seems that downregulation of Bcl-2 and activation of caspase 3 plays a role in this process¹¹⁵. Interestingly, recent studies revealed that only high concentrations of oxLDL are pro-apoptotic, whereas low concentrations are mitogenic for VSMCs.

Excessive production of ROS (e.g. hydrogen peroxide (H_2O_2)) in the atheromatous plaque also induce local VSMCs to commit suicide¹¹⁶. Interestingly, some studies have shown the multiple effect of H_2O_2 on VSMCs: whereas low concentrations of H_2O_2 and short exposure promotes cell growth, prolonged exposure to higher levels of oxidant stress leads to cell death¹¹⁶.

Besides being involved in regulating VSMC proliferation⁹⁶, NO at high concentrations leads to apoptosis of the target cells¹⁰¹. NO synthesis by ECs and macrophages is induced by several cytokines from the inflammatory response. The pro-apoptotic effect of NO is noticeably augmented when NO reacts with other types of ROS and thereby creates the cytotoxic nitrogen reactive intermediate, peroxynitrite (NO_3^-)¹⁰¹. The molecules involved in NO-induced apoptotic signaling pathways are not completely known, however they include cyclic GMP and p53³⁸. Recently it was shown by Boyle *et al.*, that NO enhances Fas/FasL interaction, which is further described below¹¹⁷.

Macrophages in the atherosclerotic plaque have already been mentioned to produce pro-inflammatory cytokines, TNF and IL-1⁸⁵. However, INF- γ is also released by activated T-lymphocytes³³. Together, these cytokines can synergistically induce apoptosis in VSMCs, as well as migration and proliferation (see above) by activating several intracellular pathways¹⁰¹.

Additionally to these cytokines, macrophages and T-lymphocytes can produce other bioactive substances, such as granzymes and perforin, which induce death of target cells¹⁰¹.

Macrophages and T-lymphocytes can promote VSMC apoptosis also by direct cell-cell interaction. Both cell types release FasL, which binds to its receptor Fas (CD95), a member of the TNF receptor superfamily, on the VSMC membrane. Surface Fas antigen ligation with FasL leads to the subsequent activation of the Fas/FasL-caspase death pathway resulting in apoptosis^{101, 102} (Figure 10). Interestingly, VSMCs were also displayed to express FasL which is believed to be responsible for the elimination of T cell in atherosclerotic lesions^{100, 118}.

Two other receptor-ligand couples play also important roles in modulating apoptotic processes in VSMCs: TNF- α and its receptor TNF receptor-1 (TNFR1)^{101, 102}, as well as TRAIL (TNF-related apoptosis-inducing ligand) and its receptor TRAIL-R2 (DR5)¹¹⁹. Like FasL, both receptors belong to the TNF receptor superfamily. Ligand binding activates the initiator molecule caspase 2 and 8, respectively (Figure 10). Caspases form a family of highly conserved aspartate-specific cysteinyl proteases that initiate and execute the program of cell death¹²⁰. Activated caspase 2 and 8 activate other downstream effector caspases (caspase 3, 6, 7) that are directly responsible for the proteolytic cleavage of cytoskeletal components, nuclear proteins and lamins. Digestion of these factors leads to changes characteristic for apoptosis and, finally, to cell disassembly (Figure 10).

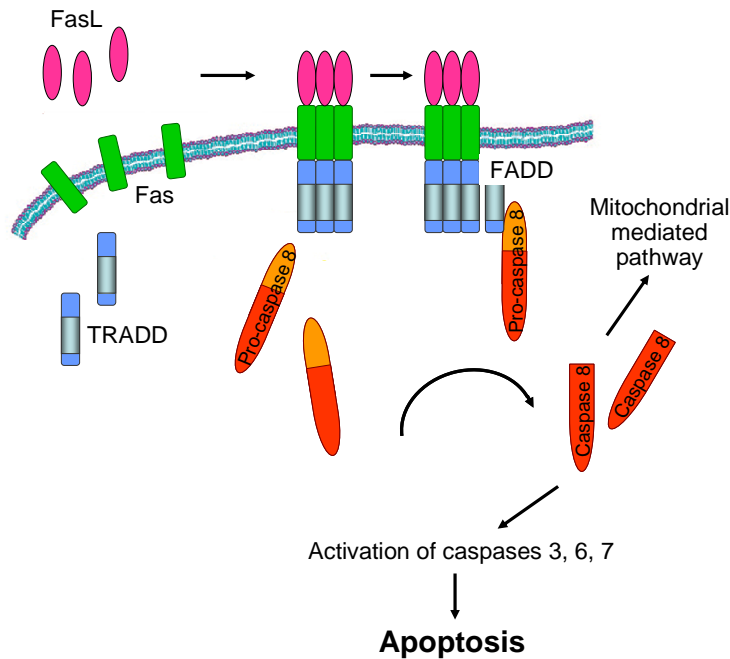


Figure 10. Death receptor-mediated apoptotic pathway

Activation of the cell membrane receptor FasL, TNFR1 and DR5 by their ligands leads to adaptor protein (e.g. FADD)-mediated recruitment and subsequent activation of initiator caspase 8. Active caspase 8 then activates downstream effector caspases (3, 6 and 7), which are responsible for the proteolytic cleavage of cytoskeletal components, nuclear proteins and lamins, leading to changes characteristic for apoptosis and, finally, to cell disassembly. Caspase 8 activation also leads to cleavage of Bid, which in turn translocates to the mitochondria and there interacts with other Bcl-2 family members (see Figure 11).

Besides this extrinsic pathway another major pathway initiates apoptosis too: the mitochondrial or intrinsic pathway. In the mitochondrial pathway, apoptosis is initiated by the release of mitochondrial cytochrome c (cyt-c) and other pro-apoptotic molecules into the cytoplasm^{101, 102}. The association of cyt-c with an adaptor molecule called Apaf-1 and pro-caspase 9 leads to the formation of active caspase 9. Together, these three proteins generate a so called "apoptosome", which orchestrates activation of several other caspases and, additionally, the biochemical execution of apoptotic cell death. The release of cyt-c from mitochondria is regulated by the balance of the pro- and anti-apoptotic proteins of the Bcl-2 superfamily. Inhibitors of apoptosis are proteins such as Bcl-2, Bid and Bcl-x_L, whereas Bax, Bad and Bim are inducers. Apoptotic stimuli attenuate Bcl-2 function and shift the balance within the Bcl-2 family towards the pro-apoptotic members (see Figure 11). It should be considered that even though the intrinsic and the extrinsic pathway are parallel and distinct, there is crosstalk between them¹²¹.

Apart from death receptors and mitochondrial pathways, other signal transduction pathways, such as JNK, MAPK and PI3K are able to mediate apoptosis by affecting secondary signaling pathways which control cell-cycle regulators. Thereby, survival factors, such as PDGF, IGF-1 and bFGF can affect both processes - cell proliferation and apoptosis -. However, interaction with the cell cycle in VSMCs of advanced lesions does not lead to proliferation, but to apoptotic cell death, partially by favoring the anti-apoptotic potential of the Bcl-2 family of proteins¹¹⁵. Low concentrations of various survival factors were shown to induce VSMC apoptosis, too¹⁰⁶.

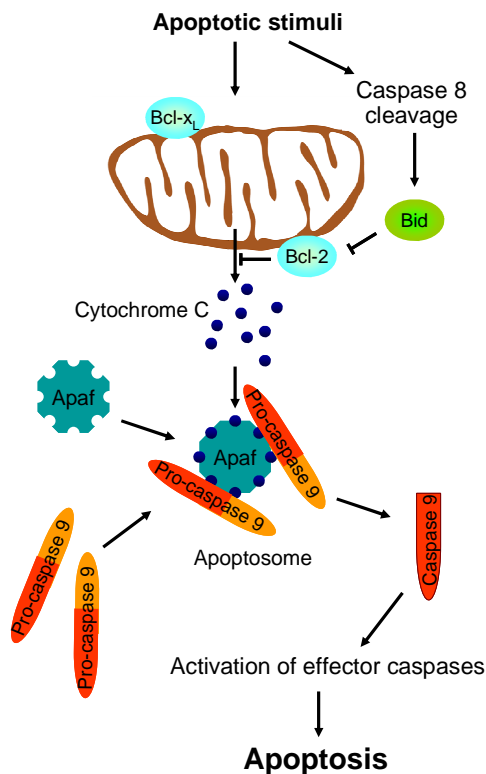


Figure 11. Mitochondrial apoptotic pathway

Anti-apoptotic members of the Bcl-2 family, such as Bcl-2 and Bcl-x_L are located on the outer mitochondrial membrane. Apoptotic stimuli induce for example binding of pro-apoptotic Bid (after cleavage by caspase 8) to Bcl-2, thereby inhibiting its protective function. This shift in balance between pro- and anti-apoptotic Bcl-2 family member leads to the release of mitochondrial cytochrome c. Cytochrome C, in concert with the adaptor protein Apaf binds pro-caspase 9 forming an apoptosome, which cleaves pro-caspase 9. Activated caspase 9 activates caspase 3 and triggers the downstream caspase cascade leading to apoptosis.

Among the common cell cycle regulators are the tumor suppressor gene p53 and the proto-oncogene c-myc. p53 activity is associated with the upregulation of apoptotic cell death, thus having the function of an anti-oncogene. Wild-type p53 represses cell proliferation by maintaining cells with DNA damage in G1-phase allowing them to repair damaged DNA¹⁰¹. If DNA repair is inexecutable, p53-expressing cells resist the G1 block and enter the pathway leading to cell death¹²². Deletion of p53 inhibits apoptosis and strongly exacerbates atherosclerosis in different atherosclerosis-susceptible mouse models¹⁰¹.

Depending on the levels of expression, the proto-oncogene c-myc has been implicated to both cell death and proliferation¹⁰¹. In VSMCs from human atherosclerotic plaques the c-myc oncogene is overexpressed resulting in a diminished growth rate as compared to “normal” VSMCs¹¹⁵. Bennett and colleagues revealed that a deregulated expression of c-myc can promote apoptosis of VSMCs¹²³, thus, c-myc has an important impact on the pathogenesis of atherosclerosis.

Apoptosis of VSMCs itself has a number of deleterious effects¹⁰². First, apoptotic VSMCs expose phosphatidylserine (PS) on the cell surface, which is a critical event in their recognition by macrophages. Unfortunately, PS can promote both thrombin generation and activation of the coagulation cascade. Second, membrane-derived microparticles are released into the circulation by the apoptotic VSMCs. These microparticles remain pro-coagulant and are thrombogenic both locally and systemically. In patients with ACS, plasma levels of pro-

coagulant microparticles were shown to be increased and thus may be linked with coronary re-occlusion^{102, 115}. Third, VSMC apoptosis causes release of e.g. IL-1, MCP-1 and bFGF causing further stimulation of the inflammatory response.

The phosphatidylinositol 3-kinase/Akt pathway

VSMC growth, cell cycle entry, migration, and survival in vasculo-proliferative diseases are influenced by various environmental inducers, e.g. growth factors as reviewed in the previous three sections. But how do all these factors stimulate VSMCs and activate a coordinated set of events leading to changes in cell behavior?

The phosphatidylinositol 3-kinases

The trigger for stimulus-induced intracellular signal events is the acute phosphorylation of phosphatidylinositol lipids (PIs) at the D-3 hydroxyl group position of the inositol ring. The phosphorylated form then functions as a signaling intermediate in signal transduction cascades. A family of related enzymes that are able to phosphorylate PIs are the phosphatidylinositol 3-kinases (PI3Ks) (reviewed in¹²⁴). Various forms of PI3Ks exist in higher eukaryotes. Based on their structural and functional homologies they are divided into three classes: Class I, II and Class III. Class I enzymes are generally considered to preferentially phosphorylate the plasma lipid phosphatidylinositol-4,5-bisphosphate (PI(4,5)P₂) and, hence, synthesize phosphatidylinositol-3,4,5-trisphosphate (PI(3,4,5)P₃) on the inner leaflet of the plasma membrane (Figure 12).

Class I enzymes are further subdivided into two groups of PI3Ks, class Ia and Ib¹²⁵. Whereas class Ia enzymes transmit regulatory signals which they receive from receptor protein tyrosine kinases, class Ib enzymes are linked to G-protein-coupled receptor systems¹²⁵. Class Ia PI3Ks are cytosolic heterodimers composed of a p110 catalytic subunit and a regulatory subunit (p85, p55 or p50) with two Src-homology 2 (SH2)-domains. In quiescent cells, the regulatory subunit maintains the catalytic subunit in an inactive state. As soon as the SH2 domains of either p85, p55 or p50 directly interact with phospho-tyrosine residues of activated growth factor receptors or adaptor proteins, PI3K is targeted to the plasma membrane and p110 is activated to convert PI(4,5)P₂¹²⁵ (Figure 12).

Growth factor receptors belong to the large family of receptor tyrosine kinases. Conformational changes within the intracellular domains of the receptor after ligand binding induce activation of intrinsic tyrosine kinases, thus leading to the auto-phosphorylation of tyrosine residues in the carboxy-terminal part of the receptor. These phosphotyrosine residues create new SH2-binding sites for e.g. binding of PI3K.

Recently, the potential role of PI3K as a mediator of restenosis has been depicted by Braun-Dullaeus *et al.*. They found PI3K to increase protein levels of several cell cycle proteins in smooth muscle cells from coronary arteries upon growth factor stimulation and vessel denudation⁹⁷.

Hyperactivation of the PI3K pathway contributes to human cancers and plays an important role in diabetes mellitus type-II¹²⁴. The tumor suppressor protein PTEN (phosphatase and tensin homologue deleted on chromosome 10) - a phosphatase that dephosphorylates PI(3,4,5)P3 at position 3 - antagonizes PI3K signaling (Figure 12). It was discovered to be a tumor-suppressor gene that is often mutated in different types of cancer, as for example in high-grade glioblastoma, breast and prostate cancer¹²⁵. Another protein counterbalancing PI3K activity by dephosphorylating PI(3,4,5)P3 at the 5-position is SHIP (SH2-containing inositol phosphatase)¹²⁵.

Although the focus of this thesis deals with the stimulation of PI3K in response to mitogen-induced receptor tyrosine kinases activation, the influence of mechanical forces on PI3K pathway stimulation should not be disregarded. Data from our group published within the last 4 years indicate, that mechanical force rapidly activates the PI3K/Akt pathway in VSMCs and thereby triggers forkhead transcription factor-mediated downregulation of the cell cycle inhibitor p27^{KIP1}⁶⁵ (for further detail see chapter “The Forkhead box O (FoxO) family of transcription factors”). In an advanced study, it was shown that the functional signaling complexes resulting in PI3-K/Akt activation during cyclic stretch are composed of the integrin receptor $\alpha_v\beta_3$ (see “Integrins”), caveolin-1, PI3K, and the non-receptor tyrosine kinase c-Src⁶⁶. Nevertheless, the mechanosensitive signaling pathways being responsible for regulation of the cell cycle mechanisms are still poorly understood.

The Akt kinase

Generated PI(3,4,5)P3 acts as a intracellular second messenger molecule that allows the activation of PI-dependent kinases, such as the protein serine-threonine kinases Akt (also called protein kinase B (PKB)) and phosphoinositide-dependent kinase-1 (PDK-1), as well as activators of Rho family GTPases¹²⁶. The proteins are recruited to the membrane by direct binding of their pleckstrin-homology (PH) domains to PI(3,4,5)P3 (Figure 12). Association of both proteins, Akt and PDK-1, with PI(3,4,5)P3 brings both proteins into close proximity and facilitates phosphorylation of Akt on threonin residue 308 (Thr308) by PDK-1. A second kinase recently discovered called PDK-2 triggers the phosphorylation of Ser473 in Akt. Phosphorylation of both residues leads to an increase in the catalytic activity of Akt¹²⁷.

Recently, the role of tyrosine phosphorylation on Akt regulation was investigated. It was provided evidence, that the Src family of non-receptor tyrosine kinases are also involved in Akt activation due to phosphorylating tyrosine residues in the C-terminal motif of Akt^{128, 129}.

Because Akt activity is dependent on PI3K, stimuli, which induce PI3K activity automatically, activate Akt as well. Active Akt triggers signals by phosphorylating a myriad of other proteins that affect cell cycle entry, cell growth and survival (see below). Most of these proteins are located into the cytoplasm. Nevertheless, phosphorylated Akt was shown to translocate to the nucleus within 5-10 min upon activation where it phosphorylates different intranuclear targets. Most of the known Akt-protein targets become inactivated by the phosphorylation event (for overview, see Figure 12). For example, Akt-mediated phosphorylation of the pro-apoptotic protein Bad creates a binding site for the 14-3-3 family of chaperon proteins and inhibits Bad from binding to Bcl-2 family members Bcl-2 and Bcl-x_L. Thus Bcl-2 and Bcl-x_L can execute their pro-survival function and Bad-induced apoptosis is inhibited¹³⁰.

Similarly, phosphorylation of the Forkhead box O (FoxO) family of transcription factors by Akt creates a binding site for the 14-3-3 proteins¹³⁰ (for further details see "Regulation of FoxO function via phosphorylation"). Interestingly, Akt is also able to directly phosphorylate p27^{KIP1}, a cell cycle inhibitor known to be transcriptionally regulated by the FoxO transcription factors¹³¹. Phosphorylation of p27^{KIP1} causes its cytoplasmic sequestration and this limits the availability of p27^{KIP1} proteins to inhibit cell cycle progression.

Controversial studies exist concerning the Akt-mediated phosphorylation of the cell cycle regulatory protein p21^{CIP1}. Whereas one report suggested that p21^{CIP1} phosphorylation by Akt leads to its cytoplasmic sequestration¹³², two other groups confirmed p21^{CIP1} to be an Akt substrate, but – in contrast - did not observe cytoplasmic translocalization of p21^{CIP1} upon Akt activation^{133, 134}. Thus, Akt promotes cell cycle progression on the one hand by inhibiting FoxO transcription factors and on the other hand by inhibiting their FoxO targets, such as p27^{KIP1} and p21^{CIP1}.

Another Akt substrate identified is glycogen synthase kinase 3 (GSK3). Phosphorylation inactivates GSK3, and therefore stabilizes or activates GSK3 targets such as cyclin D, c-Myc and glycogen synthase¹²⁴.

Phosphorylation and thereby activation of the serin/threonin kinase mammalian target of rapamycin (mTOR) has also been suggested by Akt¹²⁵. Upon phosphorylation, mTOR arranges the release of eIF-4E (translation initiation factor), which leads to initiation of translation. In addition, activated mTOR catalyzes phosphorylation of the ribosomal S6 kinase p70S6K which in turn activates ribosomal S6 proteins and thereby enhances protein translation.

Akt does not only directly phosphorylate activator proteins, but also modifies other signaling pathways regulating proliferation, apoptosis and differentiation. For example, Akt interacts and phosphorylates Raf¹³⁵, a key mediator that triggers signals from the GTP-binding protein Ras to MEK and ERK. Raf phosphorylation inhibits its activity due to the phosphorylation-dependent binding of 14-3-3 and thereby induces activation of the Raf-MEK-ERK signaling pathway. Through regulating Raf, Akt provides the opportunity for the PI3K pathway to interact with the Ras/MAPK pathway¹³⁶. Recently, this inter-pathway crosstalk was presented evidence to guide the phenotypic modulation of VSMCs¹³⁷.

Additionally, Akt has also been implicated in the regulation of the NF- κ B transcriptional pathway. Akt directly phosphorylates IKK (I κ B kinase)¹³⁸, which in turn phosphorylates I κ B, a protein keeping the transcription factor NF- κ B in an inactive state. Phosphorylated I κ B releases

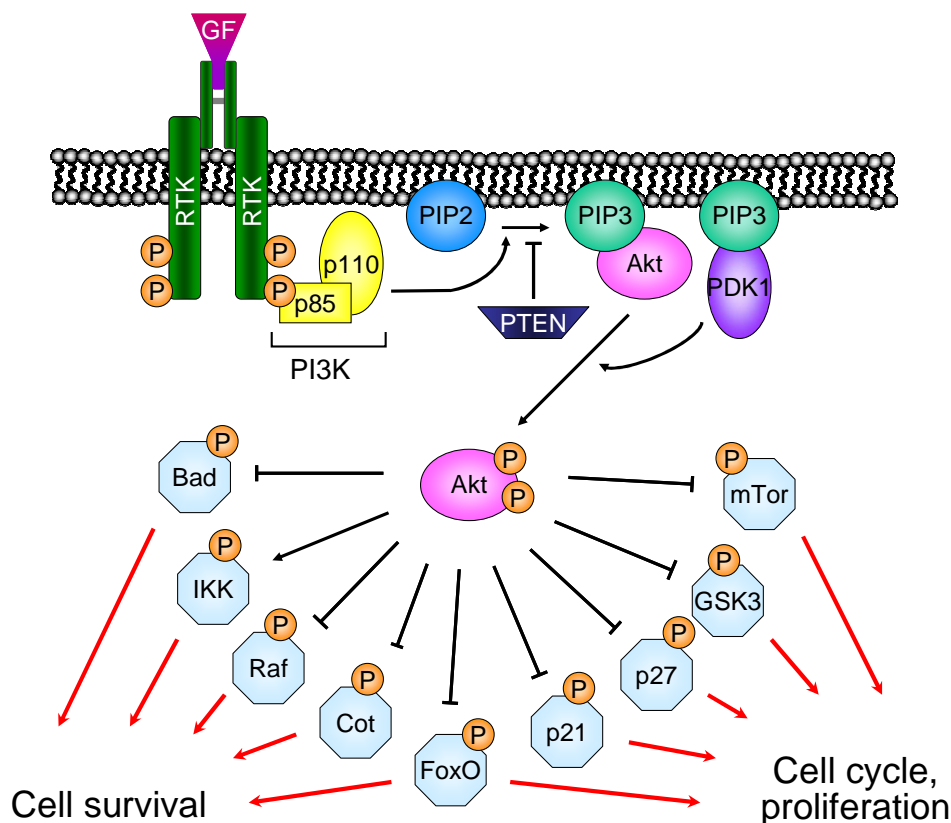


Figure 12. The phosphatidylinositol 3-kinase/Akt pathway

Upon e.g. growth factor stimulation PI3K is activated and converts PIP2 to PIP3, therefore generating lipid second messengers. PIP3 triggers the phosphorylation and activation of Akt. Activated Akt regulates downstream target proteins that mainly act on cell survival and/or cell cycle progression/proliferation. Note that the figure shows only a small number of Akt targets. Cot, cancer Osaka thyroid; FoxO, forkhead transcription factor; GF, growth factor; GSK3, glycogen synthase kinase 3; IKK, I κ B kinase; mTOR, mammalian target of rapamycin; PDK1, phosphoinositide-dependent kinase-1; PI3K, phosphatidylinositol 3-kinase; PIP2, phosphatidylinositol-4,5-bisphosphate; PIP3, phosphatidylinositol-3,4,5-trisphosphate; PTEN, phosphatase and tensin homologue deleted on chromosome 10; RTK, receptor tyrosine kinase.

NF- κ B and is further rapidly degraded by the proteasome. Akt can also phosphorylate Cot (cancer Osaka thyroid)¹³⁹, a MAP kinase kinase kinase. This phosphorylation does not affect its kinase activity but leads to activation of IKK kinases.

Despite phosphorylating and regulating all these important factors, my thesis deals preferentially with the Akt-target proteins of the FoxO family. Their role and functions are further introduced in the next chapter.

The forkhead box O (FoxO) family of transcription factors

An important Akt target is the forkhead box O (FoxO) family of transcription factors. They have important functions in processes like development, differentiation, proliferation, metabolism, apoptosis, DNA repair and stress resistance (reviewed in Burgering and Kops¹⁴⁰). The importance of the different processes that are regulated by FoxO implicates that FoxO transcription factors are central players in controlling cell behavior.

The forkhead box O family of transcription factors

Forkhead box O (FoxO) transcription factors include an important subfamily within the superfamily of winged helix/forkhead class of transcription factors, which is characterized by a 110-amino-acid, monomeric DNA binding domain termed the “forkhead box” or “Fox”¹⁴¹. In 1989, Weigel and Jackle identified the first member of this class, a protein which was shown to be involved in *Drosophila melanogaster* embryonic development¹⁴². The Forkhead family can be found in all eukaryotes and plays a major role in central processes of life (reviewed in¹⁴³). In humans, the forkhead transcription factor family is composed of 39 distinct members, that have been splitted into 19 subgroups classified from FoxA to FoxS. They regulate a wide range of processes, from organogenesis (FoxC) to language acquisition (FoxP)¹⁴⁴. Interestingly, all members of class ‘O’ (FoxO) are regulated by the insulin/PI3K/Akt signaling pathway¹⁴⁵. The first member of this class was identified in the nematode *Caenorhabditis elegans* (*C. elegans*) and named DAF-16. In this animal, the transcription factor has been investigated for its regulatory role in longevity and dauer formation^{146, 147}. For further information on DAF-16 signaling in *C. elegans* see “Regulation of FoxO function via phosphorylation”.

In mammals, DAF-16 has four described orthologues: FoxO1a (forkhead related transcription factor; FKHR), FoxO3a (FKHR-like1; FKHL1), FoxO4 (ALL1-fused-gene-from-chromosome-X; AFX) and the recently cloned FoxO6¹⁴⁸ comprising the FoxO subgroup. FoxO1a, FoxO3a and FoxO4 proteins are expressed to varying degrees in all mammalian tissues and have a predominant cytosolic localization upon Akt inactivation¹⁴⁹⁻¹⁵¹, whereas

FoxO6 is mostly nuclear and mainly expressed in the brain^{148, 152}. In humans, FoxO1a, FoxO3a and FoxO4 are ascribed to have tumor-suppressor functions, since all FoxO isoforms were identified at chromosomal translocations in different human tumors^{149, 153-157}. The presence of multiple FoxO factors in mammals suggests possible redundancy among the family members.

The *in vivo* physiological importance of FoxO transcription factors was shown to be functionally diverse in mammals as concluded from loss- and gain-of-function experiments in both transgenic and knockout mice¹⁵⁸. Interestingly, the different FoxO-knockout mice generated until now show very distinct phenotypes. FoxO1a-deficient mice die on embryonic day 10.5 as a consequence of incomplete vascular development of both the embryo and yolk sac, thus indicating a fundamental role for FoxO1a in vasculogenesis^{158, 159}. On the contrary, FoxO3a- and FoxO4-null mice were viable and showed no obvious failures compared to their littermate controls, indicating these two FoxO members not to be necessarily involved in the development of the vasculature¹⁵⁸. Nevertheless, female FoxO3a-knockout mice suffer from age-related progressive infertility since a premature follicle activation causes early reduction of fertile oocytes^{158, 160}. Additionally, these mice show less unimportant defects such as anemia and glucose uptake defects, as well as an increase in neutrophil apoptosis. No defects have been observed in FoxO4^{-/-} mice yet¹⁵⁸. FoxO6 knockout mice have not been developed to date.

Besides containing the characteristic DNA-binding forkhead domain, the FoxOs harbor a transactivation domain, located in the N-terminal and C-terminal parts of the protein, respectively, as well as a nuclear localization signal (NLS) located in the C-terminal end of the forkhead domain^{161, 162}, and a nuclear export signal (NES) (Figure 13). FoxO1a has an additional NLS¹⁶³. Furthermore, all FoxOs contain multiple conserved Akt phosphorylation motifs. Interestingly, one of the Akt phosphorylation motifs is located within the conserved NLS region. Attaching a phosphate group to it inhibits re-import of FoxO factors to the nucleus, which has a major impact on FoxOs functional abilities (see below).

FoxO target genes and its cellular function

FoxO forkhead transcription factors have been shown to control different cell processes such as cell proliferation, differentiation, metabolism and survival or apoptosis via regulation of cell cycle progression¹⁶⁴. They do so by regulating gene expression through binding to DNA promoter sequences related to the consensus sequence 5'-TTGTTTAC-3' via their forkhead box¹⁵⁰. This sequence was identified for DAF-16 for the first time and is therefore termed DBE for "DAF-16 family protein-binding element". Bioinformatic evidence indicates that a variety of FoxO target genes, which are depicted in Table 1 and described in more detail below, contain DBEs in their promoter regions¹⁶⁵. FoxO factors bound to DNA typically act as potent transcriptional

activators^{166, 167}, however, Ramaswamy and coworkers could also verify a repressing functions of these transcription factors¹⁶⁸.

DNA repair and detoxification under stress conditions

Consistent with the hypothesis that FoxO-mediated cell cycle stop may allow time for repairing damaged DNA, the expression of active FoxO isoforms in mammalian cells leads to upregulation of several genes being involved in DNA repair^{168, 169}, such as GADD45. Besides stimulating repair of damaged DNA, GADD45 also controls cell cycle transition at the G2/M boundary (see above). FoxO transcription factors were also shown to induce transcription of genes encoding free radical scavenging enzymes (e.g. catalase and manganese superoxide dismutase (MnSOD))¹⁶⁸⁻¹⁷¹. MnSOD catalyzes the conversion of superoxide radicals into hydrogen peroxide, whereas catalase converts H₂O₂ into H₂O and oxygen. With this, FoxOs enable detoxification of destructive ROS.

Taken together, FoxO transcription factors increase cellular stress resistance by controlling two aspects: 1) repair of damages caused by ROS and 2) detoxification of ROS (reviewed in¹⁷²).

The protective effect of FoxO proteins against oxidative stress can perhaps best be observed during human pregnancy, when human endometrial stromal cells are exposed to a tremendous amount of ROS due to major fluctuations in oxygen concentration¹⁷³. Through a process called decidualization, the human endometrial stroma transforms itself and thereby becomes resistant to oxidative stress-induced apoptosis. This differentiation process enables implantation of the embryo and depends on the induction of FoxO1a, which in turn upregulates expression of MnSOD¹⁷³.

Cell differentiation

In differentiating erythroid cells, FoxO3a was revealed to promote differentiation, partially by inducing B-cell translocation gene 1 (BTG1) expression¹⁷⁴. Furthermore, latest studies demonstrated FoxO3a to act as a transcriptional repressor due to the fact that this protein directly binds to the Id1 (inhibitor of differentiation 1) gene, a suppressor of erythroid differentiation¹⁷⁵. However, in adipocytes and myoblasts, expression of a constitutively active FoxO1a form inhibits differentiation *in vitro*^{176, 177}, revealing an opposite role of FoxO isoforms in the regulation of differentiation in different cell types.

Glucose metabolism

Forkhead transcription factors are also critical regulators of various enzymes involved in glucose metabolism (reviewed in^{178, 179}). For instance, FoxO family members elicit gluconeogenesis by binding to the DBE located within the promoter regions of glucose-6-

phosphatase (G6Pase)^{180, 181}, as well as to the DBEs in phosphoenolpyruvate carboxykinase (PEPCK)¹⁸² leading to their upregulation. Whereas G6Pase is responsible for dephosphorylating glucose-6-phosphate, PEPCK decarboxylates oxaloacetate to phosphoenolpyruvate (PEP) in a GTP-dependent manner. During energy deprivation, FoxO1a increases pyruvate dehydrogenase kinase 4 (PDK4) expression¹⁸³. In liver as well as in the skeletal and heart muscle this enzyme helps to save glucose under fasting conditions.

The mitochondrial 3-hydroxy-3-methylglutaryl-CoA synthase (HMGCS2), an enzyme involved in ketone body synthesis in the liver, is another recently identified FoxO target involved in metabolism¹⁸⁴. Ketone bodies originate from plasma triglycerides, which are converted into fatty acids in part by the enzyme lipoprotein lipase (LPL), whose expression is in turn increased by FoxO1a¹⁸⁵.

Peroxisome proliferator-activated receptor (PPAR)- γ coactivator 1 (PGC-1), a transcriptional co-activator induced in the liver on fasting, also has a major role in gluconeogenesis. FoxO1a directly binds to the PGC-1 promoter, thus inducing PGC-1 expression¹⁸⁶. PGC-1 itself regulates expression of e.g. PEPCK and G6Pase via coactivating FoxO1a^{187, 188}. With having this information in mind, it can be concluded that FoxO1a and PGC-1 interact and together regulate gluconeogenesis.

Recent literature shows that FoxO1a is also able to bind sequences in the IGF-binding protein 1 (IGFBP1) promoter, thus stimulating transcription of this gene¹⁸⁹. Since FoxOs control expression of genes that are involved in gluconeogenesis and - in addition - suppress gene expression of essential regulators of glycolysis, pentose shunt and lipogenesis¹⁹⁰, it can be hypothesized that FoxO activity induces a metabolic switch that is similar to low glucose and fasting conditions.

Cell death

FoxO transcription factors mediate regulation of various pro-apoptotic genes^{166, 191-195}, thereby controlling the process of programmed cell death. Thus, one possible way by which cell survival can be promoted is by departing FoxO proteins away from death genes. As already mentioned above, apoptosis can be induced upon activation of FasL (or other receptors belonging to the TNF receptor superfamily) and upon release of cyt-c from mitochondria, respectively (Figure 10 and Figure 11). FoxO3a binds to the promoter region of the FasL gene via three putative binding sites, thereby initiating increased FasL transcription¹⁶⁶. Additionally, FoxO3a also enhances expression of TRAIL, another ligand for the apoptosis-inducing receptor DR5¹⁹³ (see above). Subsequently to inducing activity of these receptors, caspases are stimulated which trigger the execution of programmed cell death. Functional active FoxO1a upregulates TRADD, the TNF receptor-associated death domain¹⁹⁶. Together with other adaptor proteins, TRADD can lead to caspase 8 activation and thereby inducing apoptotic cell death.

Besides apoptosis-triggering receptors, mitochondrial release of cyt-c leads to subsequent apoptosis. Cyt-c release is induced by an imbalance of pro- and anti-apoptotic proteins of the Bcl-2 superfamily, with activated FoxOs shifting the balance towards the pro-apoptotic site. Bim, a pro-apoptotic Bcl-2 family member, is under direct transcriptional control of FoxO3a in different cell types^{191, 194}. Another pro-apoptotic member of the Bcl-2 family identified as a FoxO target gene is bNIP3L (Bcl-2/adenovirus E1B 19 kDa interacting protein 3-like)¹⁹⁵. In addition, FoxO4 binds and activates the promoter of the transcriptional repressor Bcl-6¹⁹². Upregulation of Bcl-6 expression leads to a subsequent transcriptional downregulation of Bcl-x_L, thereby inducing cyt-c release from the mitochondria. Depending on the stimulus and cell-type, FoxO transcription factors initiate apoptotic cell death either via the intrinsic mitochondria-dependent mechanism or via the extracellular death receptor-dependent pathway.

The reasons why some cell types generally committing suicide upon FoxO activation and others are going into cell cycle arrest^{164, 197} are not clear at the moment, and further studies need to be done on this subject to clear this problem.

Other functions

FoxO transcription factors are further involved in various processes, such as skeletal muscle atrophy originating from FoxO3a activated Atrogin-1¹⁹⁸, neovascularisation and repressed endothelial nitric oxide synthase (eNOS) expression¹⁹⁹.

Recently, van der Heuvel and coworkers demonstrated a direct effect of FoxOs on caveolin-1 expression, a constituent of caveolae²⁰⁰. Results from our group suggest that caveolin-1 expression by activated FoxO1a may desensitize neointimal VSMCs to apoptotic stimuli, thereby contributing to the prevention of neointima formation and restenosis (Sedding *et al.*, unpublished data).

Protein partners of FoxOs

During the last years it was shown that besides directly binding to specific promoter sequences, FoxO factors alter gene expression via interacting with other transcription factors. For example, FoxOs interact with CREB-binding protein (CBP) (see above) as well as with steroid receptor coactivator. However, until now these interactions were only demonstrated *in vitro* but not *in vivo*²⁰¹.

Recent research revealed that FoxO factors are also able to bind to nuclear hormone receptors including the androgen receptor (AR) and estrogen receptor (ER)²⁰²⁻²⁰⁴. FoxO proteins also interact with Smad transcription factors thereby regulating cellular processes²⁰⁵. In cooperation with FoxO, the Smad3/Smad4 complex can lead to p21^{CIP1} gene expression. STAT3-mediated expression is also controlled by FoxO factors. FoxO1a can interact with STAT3 thus enhancing STAT3-mediated expression²⁰⁶.

Target Gene	Regulation	Process	Reference
4EBP1	+	cell growth	207, 208
Atrogin-1	+	muscle atrophy	198, 209, 210
Bcl-6	+	apoptosis	192
Bim	+	apoptosis	191, 194
bNIP3L	+	apoptosis	195
BTG1	+	cell cycle/differentiation	174
catalase	+	oxidative stress	171
caveolin-1	+	signaling	200, 211
Chop	+	cellular stress	212
collagenase	+	extracellular matrix degradation	213
Cyclin B	+	cell cycle	214
Cyclin D	-	cell cycle	168, 215
Cyclin G2	+	cell cycle	216
DDB1	+	DNA repair	172
eNOS	-	neovascularization	199
ER α	+	cell cycle, apoptosis	204
FasL	+	apoptosis	166
G6Pase	+	metabolism	180, 217
GADD45	+	DNA repair/cell cycle	169, 218
GILZ	+	apoptosis	219
Glutathione transferase	+	oxidative stress	220
HIF1	-	angiogenesis/metabolism	221
HMGCS2	+	metabolism	184
HSP70	+	apoptosis	222
Id	-	differentiation	175
IGFBP1	+	metabolism	189
InsR	+	signaling	208, 223
LPL	+	lipid metabolism	185
MafA	+	oxidative stress	224
MnSOD	+	oxidative stress	170
MuRF1	+	muscle atrophy	210
NeuroD	+	oxidative stress	224
OLD1	+	longevity	225
p130	+	cell cycle/quiescence	164
p21 ^{CIP1}	+	cell cycle/differentiation	205
p27 ^{KIP1}	+	cell cycle	226-228
PA26	+	oxidative stress	172
PDK4	+	metabolism	183
PEPCK	+	metabolism	182, 217
PGC-1	+	glucose metabolism	186

PGC1	+	hepatic metabolism	186, 229
Plk	+	cell cycle	214
PPAR γ 1 and 2	-	glucose metabolism	230
Scl-1	+	longevity/stress resistance	231
SCP	+	lipid metabolism/stress resistance	232
SMURF2	+	ubiquitin-mediated degradation	221
TRADD	+	apoptosis	196
TRAIL	+	apoptosis	193

Table 1. FoxO target genes and their cellular roles

FoxO transcription factors regulate the transcription of numerous target genes either positively (+) or negatively (-). Note that this figure is expandable and does not include all known FoxO target genes.

In response to different stress stimuli including nutrient deprivation, FoxO3a interacts with the tumor suppressor p53 both *in vitro* and *in vivo*^{233, 234}. Based on the evidence that FoxO and p53 interact with each other, and the discovery of p53 and FoxO sharing several downstream targets such as p21^{CIP1} and GADD45, it can be suggested that these two proteins may modulate tumor suppression.

Other transcription factors, such as Myc and NF- κ B have also been implicated in regulating FoxO activity and target gene specificity to mediate cell fate decisions¹⁷².

Last but not least, β -catenin has been shown to bind to FoxO transcription factors²³⁵. The binding of β -catenin to FoxO enhances the transcriptional activity of FoxO proteins, thereby inhibiting progression through the cell cycle²³⁵. Under conditions of oxidative stress, the interaction of β -catenin with FoxO transcription factors has been reported to increase²³⁵.

Regulation of FoxO transcriptional activity via posttranslational modifications

FoxO transcriptional regulators control diverse cell functions such as cell cycle progression, defense against oxidative damage, repair of damaged DNA and apoptotic cell death (see above). These divergent functions of FoxO proteins are tightly controlled by signal-induced, post-transcriptional modifications, including Akt-mediated and non-Akt-mediated phosphorylation, acetylation and ubiquitination, which have been reviewed extensively^{172, 236, 237}.

Regulation of FoxO function via phosphorylation

FoxO transcription factors have been implicated with multiple signaling pathways, however in mammals modified FoxO function was mostly observed upon growth factor-induced signaling via the conserved PI3K/Akt pathway^{166, 167, 238-241} (for further details on PI3K/Akt signaling pathway see chapter “The phosphatidylinositol 3-kinase/Akt pathway”).

The initial evidence implicating FoxOs as a target of Akt came from genetic studies carried

out in *C. elegans*. DAF-16, the roundworm FoxO orthologues and direct downstream target of the PI3K/Akt signaling pathway, markedly extends lifespan in the nematode^{146, 147}. Under unfavorable environmental conditions such as low food or high population density, *C. elegans* can enter a so-called dauer stage. Dauer stage is a phase of developmental arrest, which is characterized by low metabolic activity and enhanced resistance to stress. Entering this stage allows the nematode to live up to ten times longer than a “normal” littermate does. A pathway that regulates dauer stage in this animal was identified to be the growth factor receptor induced PI3K/Akt pathway (reviewed in Guarente and Kenyon²⁴²). Loss-of-function mutations in the insulin-receptor DAF-2, a known regulatory protein involved in activating the PI3K/Akt cascade, double the lifespan of the animal²⁴³. Nevertheless, life span extensions caused by *daf-2* mutations required the activity of DAF-16²⁴³. Several analyses indicated the transcriptional activity of DAF-16 to be repressed by the phosphorylative activity of the PI3K/Akt pathway, and that the DAF-16 sequence revealed four consensus sites for Akt phosphorylation¹⁴⁰. Further studies in *Drosophila melanogaster* and different mammals have revealed identical pathways to that in the nematode. Thus, it can be concluded that PI3K/Akt/FoxO signaling pathways are conserved throughout evolution (reviewed in¹⁴⁰).

Akt regulates FoxO activity in mammals via phosphorylation of three conserved residues (one threonine and two serine) in FoxO1a, 3a and 4 (FoxO1a: Thr24, Ser256, Ser319²³⁸⁻²⁴⁰; FoxO3a: Thr32, Ser253, Ser315¹⁶⁶; FoxO4: Thr28, Ser193, Ser258^{167, 241} and on two residues (one threonine Thr26 and one serine Ser184) in FoxO6²⁴⁴, respectively (Figure 13). Under conditions when Akt is inactive, FoxOs either interact with diverse DNA promoter sequences or shuttle between the cytoplasm and nucleus through an importin- and exportin-dependent nuclear transport mechanism¹⁶¹. Phosphorylation of the three residues in FoxO1a, FoxO3a and FoxO4 induces inhibition of FoxO transcriptional activity on the one hand by reducing the DNA binding capacity of the transcription factor and on the other hand by exclusion of the transcription factor from the nucleus via binding to 14-3-3 proteins.

14-3-3 chaperone proteins are ubiquitously expressed conserved scaffolding proteins, which are able to bind many functionally diverse proteins, including enzymes, receptors and transcription factors, usually when they contain phosphorylated serine or threonine residues. In its unbound state, 14-3-3 can dynamically transit the nucleus²⁴⁵. Akt-mediated phosphorylation of FoxO transcription factors generates two consensus-binding sites for 14-3-3¹⁶¹. Exportins in the nuclear membrane mediate export of 14-3-3 proteins from the nucleus and therefore may also export FoxOs to the cytosol.

Nevertheless, binding of the chaperone 14-3-3 seems not to be sufficient for nuclear export, but efficient translocation requires both active intrinsic NES sequences within the bound ligand and phosphorylation/14-3-3 binding²⁴⁵. Since one phosphorylation motif of the FoxOs is located

within the NLS sequence (as already mentioned above, Figure 13a), binding of the chaperone to the transcription factor does not only contribute to nuclear exclusion but also masks the NLS. Thus, once translocated to the cytoplasm 14-3-3 can sequester FoxO in that compartment^{166, 246}. Further details on FoxO shuttling from the nucleus to the cytoplasm and back are reviewed in¹⁶².

For the constitutive nuclear transcription factor FoxO6, phosphorylation at the two specific Akt phosphorylation sites appears to decrease the transcriptional activity only by reducing DNA binding²⁴⁴.

In addition to Akt, SGK (serum and glucocorticoid inducible kinase) - another serine/threonine-kinase activated by PDK-1 in response to growth factor/PI3K stimulation - is involved in phosphorylating FoxOs²⁴⁷ (Figure 13a). Surprisingly, Akt preferentially phosphorylates FoxO factors at different sites than SGK²⁴⁷.

Insulin and other growth factors also induce the phosphorylation of adjacent on multiple other sites of FoxO transcription factors both *in vitro* and *in vivo*. For example, FoxO1a is phosphorylated at Ser329 by the dual tyrosine phosphorylated and regulated kinase 1 (DYRK1)²⁴⁸, member of the MAP kinase family (Figure 13a). Phosphorylation upon growth factor stimulation “primes” FoxO1a for phosphorylation of two other serin residues (Ser322 and Ser325) by casein kinase (CK1)²⁴⁹ (Figure 13a). Interestingly, both phosphorylation events accelerate the Akt/SGK-induced FoxO-relocalization to the cytoplasm by increasing interaction of FoxO with Ran and Exportin/Crm1, two proteins responsible for nuclear export²⁴⁹. Nevertheless, FoxO function is only 'fine-tuned' by the CK1 and DYRK1, whereas the PI3K pathway remains the main regulator of FoxO function¹⁶².

More recently, it has been shown that the IκB kinase (IKK) enzyme complex (part of the upstream NF-κB signal transduction cascade) induces the phosphorylation of FoxO3a at Ser644 (Figure 13a). This phosphorylated residue in the C-terminal of the transcription factor maps the protein for proteolytic degradation via the ubiquitin-dependent proteasome pathway leading to its inhibition²⁵⁰. However, Ser644 is only present in FoxO3a and since this residue is not present in other FoxO isoforms the influence of IKK on controlling other FoxOs still remains to be established.

In addition to induction of phosphorylation by insulin or other growth factor signaling, the cyclin-dependent kinase 2 (CDK2) - a key regulator of DNA damage - also phosphorylates and thereby inactivates FoxO transcription factors²⁵¹ (Figure 13a). However, this modification seems to be FoxO1a-specific. CDK2 functionality is often eliminated after DNA damage, thus leading to an increase in functionally active FoxO1a. Since activation of FoxO1a is essential for inducing transcription of pro-apoptotic genes such as Bim, TRAIL and FasL, inhibition of CDK2-

dependent FoxO1a-phosphorylation represents a new pathway linking DNA damage to cell death²⁵¹.

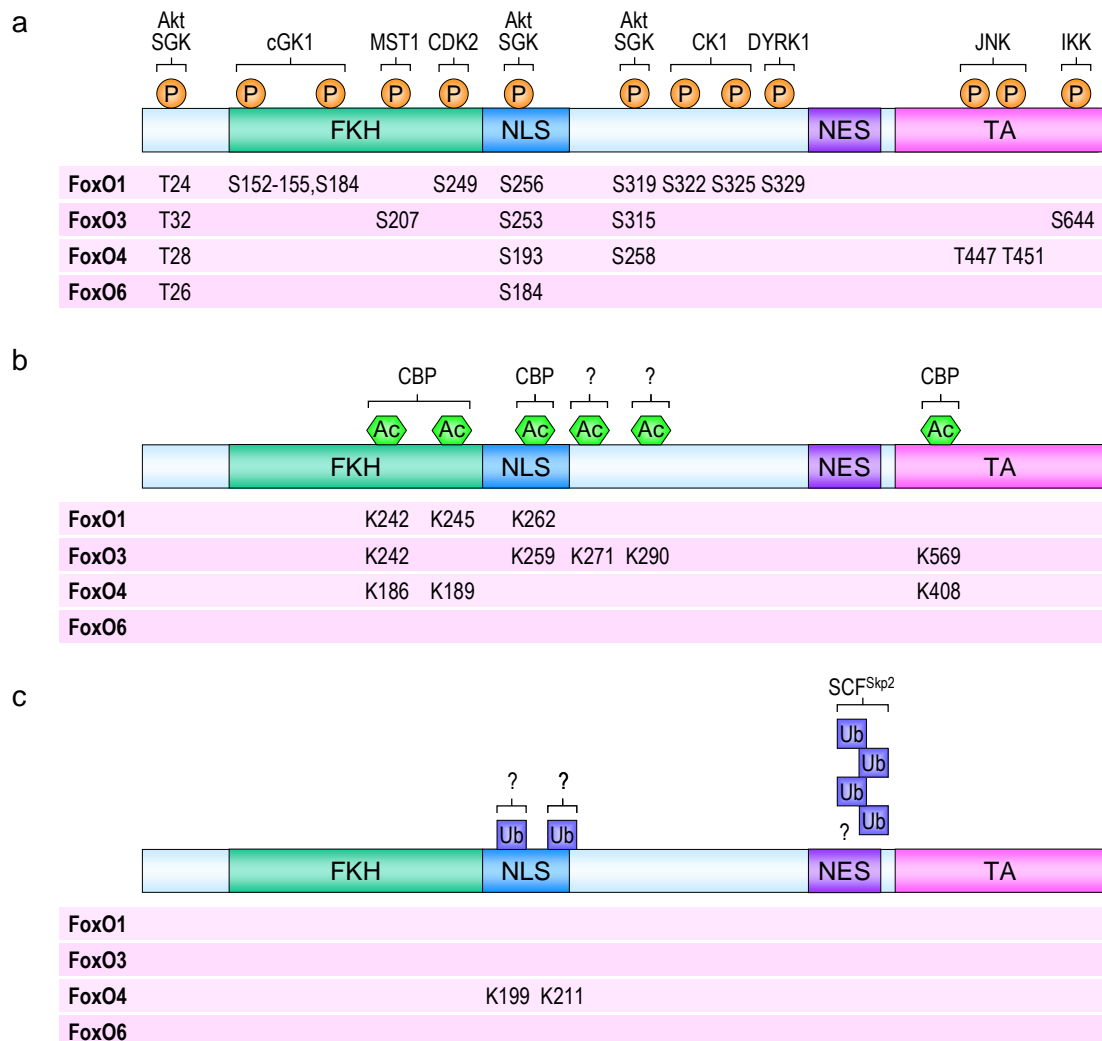


Figure 13. Different post-translational modifications of the four FoxO isoforms

FoxO transcription factor activity is regulated by phosphorylation and acetylation upon stress stimuli and growth factor stimulation. The forkhead box O transcription factors (FoxO) contain various domains: a forkhead or DNA-binding domain (FKH), a nuclear localization sequence (NLS) and a nuclear export sequence (NES) as well as a transactivation domain (TA). Modified residues are indicated and amino-acid numbers are given for the individual isoforms. **a)** FoxO phosphorylation: The kinases responsible for the various phosphorylation events are indicated above the schematic protein structure. For further detail see text. **b)** FoxO Acetylation: Acetylation of specific FoxO residues has only been studied for the cyclic-AMP responsive element binding (CREB)-binding protein (CBP) and not for other histone acetyl transferases. **c)** FoxO ubiquitination: Two potential monoubiquitination sites on FoxO4 are indicated. Unknown ubiquitinating or acetylating enzymes are indicated by question marks. Ac, acetylation; CDK2, cyclin-dependent kinase-2; cGK1, cGMP-dependent protein kinase-1; CK1, casein kinase-1; DYRK1, dual-specificity tyrosine (Y)-phosphorylation-regulated kinase-1; IKK, IKB kinase; JNK, c-Jun N-terminal kinase; MST1, mammalian sterile 20 kinase-1; P, phosphorylation; SCF^{Skp2}, the SKP1/cullin-1/F-box protein complex that contains the specific substrate-targeting F-box protein SKP2; SGK, serum- and glucocorticoid-inducible kinase; Ub, ubiquitination.

Research in mammalian myoblast revealed a regulatory activity of FoxO1a during myogenesis. In these cells, FoxO1a was shown to directly control expression of cyclic GMP-dependent protein kinase I (cGKI)²⁵². However, in an autoregulatory loop cGKI itself phosphorylates FoxO1a leading to an abolished DNA binding capacity of the transcription factor (Figure 13a), thus exhibiting a novel feedback mechanism in myoblast cell fusion²⁵².

After having introduced all the phosphorylation events leading to FoxO inactivity and nuclear exclusion, it is noteworthy to mention that recently the phosphorylation of FoxO by JNK (c-Jun N-terminal kinase) was shown by Essers *et al.* to have the opposing effect: JNK-mediated phosphorylation induces FoxO-translocation from the cytoplasm to the nucleus²⁵³. Once in the nucleus, FoxO4 can upregulate stress-resistance genes such as MnSOD and catalase, by binding to its specific promoter regions. JNK belongs to the family of MAPK kinases and is activated upon stress stimuli. Mammalian FoxO4 is phosphorylated on Thr447 and Thr451 by the activated JNK²⁵³ (Figure 13a). Interestingly, these sites are neither conserved in other mammalian FoxO isoforms nor in the worm orthologue, even though all these FoxOs were demonstrated to be phosphorylated by JNK *in vitro*^{253, 254}. Thus, it seems that JNK phosphorylates other FoxO transcription factors at sites that need to be investigated in the future.

The opposing effect of growth factors and oxidative stress on FoxO subcellular localization is controlled by the phosphorylation of FoxO at different sites. Brunet and colleagues identified stress stimuli to override the effect of growth factors in mammalian cells when applied simultaneously, so that FoxO transcription factors are localized to the nucleus under these circumstances²³³. The detailed activities by which stress stimuli and JNK lead to FoxO relocalization to the nucleus are not yet known, however, recent studies identified 14-3-3 proteins to play a role in this phenomenon. Upon phosphorylation by JNK, 14-3-3 chaperons release all their bound substrates, including FoxO transcription factors which then have the prerequisite to re-enter the nucleus^{255, 256}.

Lehtinen and coworkers could show that the mammalian sterile 20-like kinase 1 (MST1) mediates oxidative stress-induced cell death in primary mammalian neurons by binding and phosphorylating FoxOs directly *in vitro* and *in vivo*²⁵⁷ (Figure 13a). MST1 phosphorylation, exactly like JNK phosphorylation, activates FoxO, but how this activation occurs is still unclear. Additionally, MST1 regulates p38 and JNK pathways²³⁷, thus MST1 regulation of FoxO may also be mediated indirectly through JNK.

Regulation of FoxO function via acetylation and deacetylation

In addition to regulation via phosphorylation, a second important posttranslational modification pathway that regulates FoxO transcriptional activity has been identified:

Acetylation/deacetylation. Acetylation is characterized through transfer of an acetyl moiety from acetyl-CoA to a substrate. Many proteins that can become acetylated belong to the family of histones and transcription factors. Since these proteins are involved in the regulation of transcription, enzymes controlling the acetylation/deacetylation status - the so-called acetyltransferases and deacetylases, respectively - have major roles in the control of cell fate (reviewed in Legube and Trouche, 2003²⁵⁸).

In the past years, numerous enzymes that are able to catalyze the transfer of an acetyl group to a lysine residue in a substrate were discovered²⁵⁹. These acetylases can be subdivided into another group called histone acetyltransferases (HATs). For example CBP, p300 and PCAF (CBP-associated factor) belong to this group, even they were shown to acetylate non histone proteins, too.

For mammalian FoxO transcription factors, several acetylases have been identified until today influencing the transcriptional regulation of FoxO downstream target genes *in vitro* and *in vivo*^{233, 260-265}. The already mentioned, CBP, p300 and PCAF are able to directly acetylate FoxO factors at several conserved lysine residues, whereas p300 is also able to acetylate FoxO indirectly by recruiting PCAF. FoxO1a is acetylated at Lys242, Lys245, and Lys262²⁶¹, whereas Fukuoka *et al.* identified three lysine residues Lys186, Lys189, and Lys408 in FoxO4 being acetylated²⁶⁰ (Figure 13b). FoxO3a is acetylated at 5 residues in the carboxyterminal part of the protein²³³ (Figure 13b). Several other FoxOs lysine residues have been determined by mass-spectrometric analysis of being possible acetylation targets for yet unidentified HATs²⁶⁴. Some of these residues are conserved among all FoxO members. However, acetylation of most of these residues did not change FoxO transcriptional activity considerably^{260, 266}.

Acetylation of FoxO transcription factor occurs in response to insulin stimulation²⁶⁴ as well as after oxidative stress treatment^{233, 262, 263}. In conclusion it can be said that both stimuli contribute to FoxO acetylation, although the kinetics of insulin-induced and stress-induced acetylation appear to differ²³⁷.

The molecular mechanisms whereby HATs bind and modify FoxO factors are still unclear. However, it was shown that acetylation of FoxO proteins weakens their transactivation capacity. For example, acetylation of Lys242, Lys245 and Lys262 of FoxO1a has been shown to attenuate its sequence-specific DNA binding *in vitro*, whereas these modifications affected PI3K/Akt-mediate phosphorylation at Ser253 *in vivo*²⁶⁷. Several other studies also suggest that acetylation inhibits and deacetylation activates FoxO^{261, 263, 268-270}. Thus, acetylation of proteins involved in the transcription process may lead to attenuated transcription. Paradoxically, under some circumstances acetylation of FoxO factors appears to induce their transcriptional activity, leading to an advanced FoxO target gene expression^{262, 271}. Whether this effect is dependent on

the stimulus or is target gene specific needs to be determined. Nevertheless, this interesting observation accommodate with the next mentioned point.

Alternatively to acetylate FoxOs, the acetyltransferases CBP, p300 and PCAF also function as transcriptional coactivators for FoxOs modulating its DNA binding ability. This leads to an increase in FoxO-dependent transcription. Both proteins interact with the C-terminal transactivator domain in the FoxO transcription factors. Binding to CBP/p300 is an initial step in assembling the transcriptional activation complex of FoxO, thus providing a connection between the basal transcriptional machinery and their regulators^{260, 263, 271}.

Histone deacetylases (HDACs) are enzymes that remove acetyl residues from proteins, thus inverting the acetylation process. Acetylated mammalian FoxOs are deacetylated *in vitro* and *in vivo* by SIRT1, a member of the mammalian Class III deacetylases (for details see “The mammalian NAD-dependent protein deacetylase SIRT1”). The lysine residues of FoxO1a that seem to be preferentially deacetylated by SIRT1 are Lys242, Lys245, and Lys262²⁶¹.

In addition to SIRT1, other histone deacetylases from HDACs class I and II may regulate FoxO activity because treatment of cells with inhibitors for these classes induces FoxO acetylation^{233, 262, 263, 267, 269} and affects FoxO localization²⁶⁹ as it was shown by others and by our group (for further detail see “Results”).

Besides the two opposing concepts that FoxO acetylation either activates or inactivates FoxO function, a recent study declares that SIRT1 influences FoxO transcription factors in a context-specific manner, thus regulating the balance between pro-apoptotic and cell cycle arrest genes²³³. For example, it has been reported that SIRT1-activated FoxO promotes cell-cycle arrest by inducing p27^{KIP1} expression and cellular resistance to oxidative stress by upregulating levels of MnSOD and GADD45^{169, 218} (see above). Results verifying this concept were achieved in this thesis. However, the detailed mechanism by which SIRT1 differentially controls FoxO functions is not yet known and more work is needed to elucidate conclusively the role of acetylation and SIRT1 on FoxO function.

Regulation of FoxO function via ubiquitination and degradation

FoxO shuttling to the cytoplasm exposes FoxO proteins to a third system irreversible regulating their activity post-transcriptionally: The ubiquitination-dependent proteasomal degradation^{250, 272-274}. This system can be induced by growth factors through PI3K/Akt signaling^{272, 273} and also through IKK (see above)²⁵⁰ leading to polyubiquitination of FoxO transcription factors (see Figure 13c). The ubiquitin ligase acting on FoxO1a has been identified as Skp2, a member of the SCF (Skp1/Cul1/FoxO1a-box) E3 ubiquitin ligase complex²⁷⁴. Akt-mediated phosphorylation of Ser256 in FoxO1a is the primary event that generates a binding site for Skp2 (see Figure 13a). After interaction with FoxO1a, Skp2 polyubiquitinates the transcription factor and thereby

induces its degradation leading to a dramatic decrease in the FoxO1a level. As a result of Skp2-mediated proteosomal degradation, FoxO1a transcriptional activity is downregulated. Nevertheless, Skp2 does not act on all FoxO members.

For FoxO3a, the crucial kinase is IKK rather than Akt, and the relevant target residue is Ser644, attracting an yet unidentified ubiquitin ligase²⁵⁰ (Figure 13a). As already mentioned above, this serine residue is not conserved in other FoxO isoforms and organisms. Thus, there is no evidence for IKK of phosphorylating and controlling other FoxO proteins. However, the essential steps - phosphorylation-dependent ubiquitination followed by proteasomal degradation - are the same for all FoxO factors.

Since cytosolic localization is the prerequisite for optimal degradation of FoxO1a, FoxO3a and FoxO4, the question arises how degradation of FoxO6 - the constitutive nuclear FoxO factor - occurs. It seems possible that FoxO6 is degraded by another system than the proteasome system, for example by protease cleavage (see below). However, the exact mechanisms remain to be identified.

Degradation of polyubiquitinated FoxO is a constitutive, but slow process^{272, 273} with polyubiquitination detectable after ~12 hours. Recent research could show that FoxOs are not only polyubiquitinated but are also influenced by monoubiquitination, which is triggered by rising stress levels²⁶⁶. Monoubiquitination is an immediate process (~5 minutes after exposure to stress) leading to FoxO nuclear localization and stimulates its transcriptional activity. However, the mechanism that mediates this nuclear localization is unclear and the ubiquitin ligase (E3) catalyzing monoubiquitination has not been identified yet. USP7 (also known as herpesvirus-associated ubiquitin-specific protease (HAUSP)) was shown to remove monoubiquitin but not polyubiquitin moieties from FoxOs²⁶⁶. Interestingly, acetylation and ubiquitination target the same amino-acid residues in FoxO transcription factors. For example, the lysine residues 199 and 211 in FoxO4 can become both acetylated and ubiquitinated²⁶⁶ (Figure 13c), which suggests that competition between different lysine modifications can occur. If acetylation of FoxO lysines is the first event, functionality of the transcription factor is inhibited due to a weakened DNA-binding and/or renewed monoubiquitination is prevented²⁶⁷.

Another system for degrading FoxO transcription factors - besides being processed by the ubiquitin system - is protease cleavage. FoxO3a can be cleaved by caspase 3-like proteases, yielding an NH₂-terminal, and a COOH-terminal domain. A similar proteolytic-dependent way has been shown for FoxO1a regulation²⁷⁵. Similar to FoxO3a and FoxO1a, a proteolytic cleavage site has also been identified in FoxO4, but interestingly not in FoxO6²⁷⁶.

The current findings on FoxO regulation by posttranslational modification reveal that mitogens and oxidative stress counterbalance FoxO function through multiple mechanisms and dependent on the context the outcome may vary.

The mammalian NAD-dependent protein deacetylase SIRT1

The family of mammalian histone deacetylases

The post-translational modification of FoxO transcription factors via acetylation is a dynamic process and the enzymes catalyzing the removal of acetyl moieties on FoxO lysines are called HDACs (see above). Originally, these proteins were identified for their ability to catalyze histone deacetylation and are therefore named histone deacetylases. Deacetylation of histones elevates the positive charge within the histone tails. In conclusion, this intensifies the histones' affinity for DNA leading to gene silencing. However, in addition to histones, recent research identified several other proteins that can be deacetylated by HDACs, such as p53, E2F and the already mentioned FoxOs.

To date, more than 12 human HDACs have been identified and are divided in 4 subgroups: class I, class II, class III and class IV HDACs²⁷⁷. The class I HDACs consists of HDAC1, 2, 3 and 8, whereas HDAC4, 5, 6, 7, 9 and 10 belong to the class II HDACs. Class III HDACs are yeast Sir2 (silent mating type information regulator 2)-like sirtuins, which will be discussed later in this chapter²⁷⁸. HDAC11 is at the moment the only known member of class IV HDACs (for a review see Blander *et al.*²⁷⁹).

Class I HDACs (the yeast Rpd3-like histone deacetylases) show a predominant nuclear localization and because of their ubiquitous expression pattern seem to be involved in general cellular processes^{277, 280}. Class II enzymes shuttle between the cytoplasm and the nucleus via an interaction with 14-3-3 proteins (see above), and have a more restricted expression pattern suggesting to have tissue-specific functions during development of organisms. They show strong homology to yeast Hda1 family^{277, 280}. Both, class I and II HDAC function can be potently inhibited by the small molecule inhibitor TSA (Trichostatin A), with an IC₅₀ at low nanomolar concentrations for all classes of HDACs^{277, 280}.

The mammalian class III histone deacetylases (sirtuins)

The Sir2 family of histone deacetylases (typed class III HDACs) are structurally different from the other two HDAC classes, and are insensitive to TSA²⁷⁸. The Sir2 family is highly conserved in organisms ranging from bacteria to complex eukaryotes as e.g. humans²⁸¹. In humans, the class III HDAC is comprised of seven members called SIRT1 (sirtuin1) to SIRT7²⁸². Each

member of this family shows sequence conservation in the 250 amino acid core domain^{281, 282}, and some contain additional N- or C-terminal sequences. Out of all seven family members, SIRT1 is the closest homologue of yeast Sir2. SIRT1 is ubiquitously expressed and has been believed to be a nuclear protein. Nevertheless, recent reports also verified the cytoplasmic localization of SIRT1 in various tissues and cells. For example findings by Tanno and coworkers indicate a nucleocytoplasmic shuttling of SIRT1 during different stages of development and in response to physiological and pathological stimuli²⁸³. SIRT2, which is a cytosolic enzyme, controls mitotic exit and is involved in tubulin deacetylation. SIRT3, 4 and 5 are all three localized to mitochondria²⁷⁹. SIRT6 and SIRT7 are found in the nucleus, where SIRT6 is associated with heterochromatin and SIRT7 accumulates in nucleoli²⁷⁹. In summary, it is interesting to see that some of the mammalian Sir2-like proteins still have histone deacetylase activity, whereas other family member use non-histone proteins as a substrate.

Sirtuins, as compared to Class I and II HDACs, have recently been shown to belong to a group of enzymes called ADP-ribosyl transferases: They possess nicotinamide adenine dinucleotide (NAD⁺)-dependent protein and histone deacetylation activity *in vitro*^{278, 284}. Sirtuins couple deacetylation to the hydrolysis of NAD⁺, transferring the acetyl group from their protein substrate to ADP-ribose, thereby generating nicotinamide (NAM) and a novel metabolite, O-acetyl-ADP-ribose^{285, 286}. O-acetyl-ADP-ribose itself may have a unique cellular function and seems to be an important regulator of physiology^{287, 288}. Indeed, recent studies in yeast revealed that O-acetyl-ADP-ribose can initiate structural reorganization of the Sir complex that is responsible for silencing of chromatin²⁸⁸.

Since SIRT1-mediated deacetylation is NAD⁺ dependent, it is linked to the metabolic state of the cell and can be regulated by environmental circumstances influencing NAD⁺/NADH ratio, or the NAM levels. For example caloric restriction affects the metabolic process by increasing the NAD⁺/NADH ratio, thus extending lifespan in a wide range of organisms from yeast to mammals²⁸⁹. This led to the hypothesis that caloric restriction may act via SIRT1 to enhance longevity. Fulco *et al.* showed that during human muscle differentiation the NAD⁺/NADH ratio diminishes thus leading to modified SIRT1 deacetylase activity²⁹⁰. Interestingly, not only SIRT1 activity, but also SIRT1 levels were found to be increased upon caloric restriction in mammalian cells²⁹¹.

Studies from the Sinclair group have identified NAM as a potent inhibitor of SIRT1 both *in vivo* and *in vitro*^{292, 293}. Unfortunately, as this compound is directly incorporated into the cell metabolism, it is not clear whether it is specific for a given sirtuin. High-throughput screenings have discovered several different chemical compounds specific for Sir2/SIRT1. For example, splitomicin²⁹⁴ as well as sirtinol²⁹⁵ are potent inhibitor of human sirtuins. For a review the reader is referred to²⁹⁶.

As mentioned above, elevated Sir2 activity promotes longevity. The plant polyphenol resveratrol being abundant for example in red wine, was discovered by Howitz and coworkers to increase SIRT1 activity in the budding yeast *Saccharomyces cerevisiae* resulting in increased yeast life span by 70%²⁹⁷. Since these observations in 2003, resveratrol has been revealed to extend the lifespan of different other species including *C. elegans* and *D. melanogaster* in a Sir2-dependent manner^{298, 299}. A recent study identified resveratrol to improve health and survival of mice³⁰⁰. In human cell lines, treatment with low concentrations of resveratrol increased cell survival upon ionizing radiation-induced DNA damage²⁹⁷. Moreover, the acetylation of p53 at the known SIRT1 lysine residue 382, was decreased following resveratrol treatment²⁹⁷. Experiments presented in this study suggest that even in human tissues resveratrol activates SIRT1, thus amplify its protective effect (see “Results”-part of this thesis).

These data suggest that even general health and lifetime extension by mitigation of age-related diseases (e.g. cardiovascular diseases) in humans using resveratrol are attainable goals³⁰¹. Since resveratrol is found in red wine this could be the explanation for the “French paradox”, the fact that red wine drinking people in France have relatively low coronary heart disease rates. Also for those who seek the “fountain of youth”, resveratrol or any other activator of SIRT1 is of special interest. Nevertheless, the mechanism of resveratrol - and other polyphenols – as well as its physiologic impact on SIRT1 activity is poorly understood and needs to be determined in the future.

The biological function of SIRT1

A role for Sir2 as a transcriptional silencer was unraveled by genetic studies in yeast. However, the deacetylase also enhances lifespan in yeast by inhibiting production of toxic extrachromosomal rDNA circles³⁰². The replicative life span of the yeast was extended by 30% after introduction of a second copy of Sir2 into the genome³⁰³. Interestingly, subsequent studies revealed that the *C. elegans* Sir2-homologue also affects lifespan of the nematode, but by totally different mechanism. In *C. elegans*, an extra copy of Sir2 enhances longevity by stimulating the activity of the worm FoxO-homologue DAF-16^{304, 305} (see above). It does so by directly binding to DAF-16³⁰⁶, and not as previous studies suggested by downregulating insulin signaling³⁰⁴. Likewise, overexpression of the Sir2 protein in *Drosophila* significantly extended the lifespan of the fly³⁰⁷, however, the mechanism remain unknown. After mammalian SIRT1 has already been implicated in stress resistance and numerous metabolic pathways, it will be interesting to know whether Sir2 also regulates the aging process of higher eukaryotes.

As the name histone deacetylase implicates, SIRT1 was shown to deacetylate histones, such as histones H3 and H4²⁷⁹. Nevertheless, today more than 15 non-histone substrates are also known, of which some are further described below. However, even though SIRT1 deacetylates a vast amount of proteins and was shown to have substrate specificity *in vivo*, a

recent study could not identify a specific amino acid sequence close to the acetylated lysines that are being catalyzed by the enzyme³⁰⁸. Thus, substrate recognition by SIRT1 does not depend on the DNA sequence of the substrate but depends on other yet unknown principles. A review about the chemical and structural characteristics of SIRT1 was written by Sauve *et al.*²⁹⁶.

SIRT1 targets participate in important biological processes as for example fat mobilization and differentiation. Recent studies revealed the repression of the fat regulator PPAR- γ by SIRT1 via interaction with the PPAR- γ cofactors NCoR (nuclear receptor co-repressor) and SMRT (silencing mediator of retinoid and thyroid hormone receptors) which leads to fat mobilization in white adipose tissue and reduced fat cell formation³⁰⁹. Since fat reduction is well-known to extend mouse lifespan, the above mentioned influence of SIRT1 may contribute to the prolongation of lifespan.

Also skeletal muscle differentiation is regulated by SIRT1. MyoD function, a muscle transcriptional regulator, is either directly attenuated by the sirtuin or via SIRT1-mediated deacetylation of another histone acetyltransferase called PCAF²⁹⁰. SIRT1 also controls glucose metabolism in the liver through deacetylating PGC-1³¹⁰. Last but not least, SIRT1 function is also important in B cell differentiation (reviewed in²⁷⁹).

Axonal protection and survival of neurons are other processes affected by SIRT1³¹¹. Transcription of human genes is repressed by SIRT1 at different levels: At the level of polymerase apparatus (TAFI68), as well as at the level of basal transcription factor (HES1 and HEY2) and repressor activity (CTIP2)²⁷⁹.

SIRT1 promotes cell survival under stress conditions by deacetylating and repressing the proto-oncogene p53³¹²⁻³¹⁴. Results from these indicated studies were verified recently by new findings in SIRT1 knockout mice created by Cheng *et al.*: SIRT1-deficient animals show hyperacetylated p53 after DNA damage and display increased thymocyte apoptosis³¹⁵. Two other independent groups also created SIRT1 knockout mice³¹⁶. Both groups showed that SIRT1 $-/-$ mice were viable but significantly smaller than their wildtype littermates at birth, and most of these animals did not reach adulthood due to early postnatal death. Once born, SIRT1 null mice often survived to adulthood but had obvious developmental defects, such as delay in eyelid opening at time of birth. Knockout mice also revealed several organ defects: Whereas SIRT1 $-/-$ mice generated by Cheng *et al.* showed cardiac and retina defects, McBurney and coworkers found defects in lung and pancreas³¹⁶. Interestingly, both sexes of the knockout animals were sterile. Infertility in female SIRT1 null animals appeared to be due to failure in ovulation, whereas male infertility originated from a significant low number of mature sperms.

Besides promoting cell survival, activation of SIRT1 can inhibit cell senescence by both repressing the tumor and growth suppressor promyelocytic leukemia protein (PML) and by

activating the catalytic subunit of hTERT (human telomerase reverse transcriptase)²⁷⁹. In addition, SIRT1 can modulate survival and cellular stress response through regulation of NF- κ B signaling³¹⁷, Ku70^{291, 318} and FoxO transcription factors^{233, 262}. SIRT1-mediated deacetylation of FoxO by seems to mostly induce FoxO transcriptional activity or at least determines gene specificity of FoxO (as discussed above).

SIRT1 does not only have a direct role on FoxO activity but also regulates PGC-1, p300/CBP and possibly PPAR which function as FoxO cofactors as mentioned in the chapter “The Forkhead box O (FoxO) family of transcription factors”. Notably, these proteins also affect gene transcription on their own as described in the above examples. SIRT1-mediated deacetylation of these cofactors affects their activity and seems to be context-dependent.

Taken together, it can be said that activation of SIRT1 seems to work in various ways to reduce cell ageing, and increases cell survival by attenuating apoptosis and elevating defense and repair mechanisms.

Cellular aging and cellular stresses cause diminished function of all organs, including the heart and the vasculature³¹⁹. Thus, with age the incidence of cardiovascular diseases increases dramatically. In the blood vessels, medial VSMCs are especially affected by aging. Change of their properties (proliferation, migration and apoptosis) contributes to vascular remodelling and atherosclerosis (see chapter “Vascular smooth muscle cells”).

Since SIRT1 – as it was shown above - is involved in controlling both cellular aging and stresses, studying its function in VSMCs with regard to cardiovascular diseases seems to be promising for a more detailed understanding of the pathophysiology of the vasculature as well as for determining future therapeutic strategies.

Materials and Methods

Materials

Chemicals

Product	Source	Cat.No.
10% Non-immune goat serum	Zymed Laboratories Inc, San Fransisco, CA, USA	50-197
2-Mercaptoethanol	Sigma-Aldrich Chemie GmbH, Munich, Germany	M-3148
2-Propanol	Riedel-de Haën Sigma-Aldrich Laborchemikalien GmbH, Seelze, Germany	59304
5x siRNA Buffer	Dharmacon, Inc., Chicago, IL, USA	B-002000-UB-100
Acetic acid 100%	Merck KGaA, Darmstadt, Germany	1.00063
Acetone	Riedel-de Haën Sigma-Aldrich Laborchemikalien GmbH, Seelze, Germany	32201
Albumin Fraktion V	Carl Roth GmbH + Co. KG, Karlsruhe, Germany	8076.2
Antibody diluent	Zymed Laboratories Inc, San Fransisco, CA, USA	00-3118
Aqua ad iniectionabilia (H ₂ Odd)	Baxter Deutschland GmbH, Unterschleißheim, Germany	001428
Blotting Grade Blocker Non-fat dry milk	Bio-Rad Laboratories, Hercules, CA, USA	170-6406
Bovine serum albumine (Fraction V)	Carl Roth GmbH + Co. KG, Karlsruhe, Germany	8076.2
Bromphenol blue	Sigma-Aldrich Chemie GmbH, Munich, Germany	B-8026
Calcium chloride (CaCl ₂)	Merck KGaA, Darmstadt, Germany	1.02382.1000
Chloroform	Sigma-Aldrich Chemie GmbH, Munich, Germany	C7559
Complete™ Protease Inhibitor Cocktail Tablets	Roche Diagnostic GmbH, Mannheim, Germany	1697498
Dimethylsulfoxide (DMSO)	Sigma-Aldrich Chemie GmbH, Munich, Germany	D-4540
DL-Dithiothreitol	Sigma-Aldrich Chemie GmbH, Munich, Germany	D-9163
Dulbecco's phosphate buffered saline (PBS) 10x	PAA Laboratories GmbH, Pasching, Austria	H15-011
Dulbecco's phosphate buffered saline (PBS) 1x	PAA Laboratories GmbH, Pasching, Austria	H15-002
Dynabeads Protein G	Dynal Biotech GmbH, Hamburg, Germany	100.03
Eosin Y Disodium salt	Sigma-Aldrich Chemie GmbH, Munich, Germany	E-4382
Ethanol	Riedel-de Haën Sigma-Aldrich Laborchemikalien GmbH, Seelze, Germany	32205
Fetal bovine serum (FBS)	Invitrogen GmbH, Karlsruhe, Germany	10500-064
Gelatin	Sigma-Aldrich Chemie GmbH, Munich, Germany	G-2500
Glycerol	Sigma-Aldrich Chemie GmbH, Munich, Germany	G-6279
Glycine	Carl Roth GmbH + Co. KG, Karlsruhe, Germany	3908.2
Hematoxylin solution	Merck KGaA, Darmstadt, Germany	1.05174
Hepes	Sigma-Aldrich Chemie GmbH, Munich, Germany	H-3375
Histofix 4 % (PFA)	Carl Roth GmbH + Co. KG, Karlsruhe, Germany	P087.3
Hoechst 33342 (10 mg/ml)	Molecular Probes, Eugene, Oregon, USA	H-3570
Hydrochloric acid (HCl)	Merck KGaA, Darmstadt, Germany	1.09057
Hydrogen Peroxide (H ₂ O ₂) 3%	Otto Fischer GmbH & Co. KG, Saarbrücken, Germany	6305046
L-Glutamine	PAA Laboratories GmbH, Pasching, Austria	M11-004
Lipofectamine 2000	Invitrogen GmbH, Karlsruhe, Germany	52758
Magnesium chloride (MgCl ₂)	Sigma-Aldrich Chemie GmbH, Munich, Germany	M8266

Methanol	Riedel-de Haën Sigma-Aldrich Laborchemikalien GmbH, Seelze, Germany	65543
Nicotinamide (NAM)	Sigma-Aldrich Chemie GmbH, Munich, Germany	N-3376
Normal goat serum (NGS)	Invitrogen GmbH, Karlsruhe, Germany	16210-064
OptiMEM I	Invitrogen GmbH, Karlsruhe, Germany	31985-047
Penicillin / Streptomycin	PAA Laboratories GmbH, Pasching, Austria	P11-010
Phloxine B	Sigma-Aldrich Chemie GmbH, Munich, Germany	P-4030
Ponceau S Solution	Sigma-Aldrich Chemie GmbH, Munich, Germany	P-7170
Potassium chloride (KCl)	Sigma-Aldrich Chemie GmbH, Munich, Germany	P9333
Propidium Iodide Solution (PI) (1.0 mg/ml)	Sigma-Aldrich Chemie GmbH, Munich, Germany	P-4864
Psammaphysene A	kindly provided by J. Clardy, Harvard Medical School, Boston, MA, USA	
Recombinant Human PDGF-BB	R&D Systems GmbH, Wiesbaden, Germany	220-BB
Resveratrol	Sigma-Aldrich Chemie GmbH, Munich, Germany	R5010
RNAse A	Invitrogen GmbH, Karlsruhe, Germany	12091-039
RNAse ZAP	Sigma-Aldrich Chemie GmbH, Munich, Germany	R-2020
Sirtinol	Axxora Deutschland GmbH, Grünberg, Germany	ALX-270-308
Sodium azide (NaN ₃)	Sigma-Aldrich Chemie GmbH, Munich, Germany	S-2002
Sodium chloride (NaCl)	Carl Roth GmbH + Co. KG, Karlsruhe, Germany	3957.1
Sodium chloride solution	Baxter Deutschland GmbH, Unterschleissheim, Germany	001498
Sodium deoxycholate	Sigma-Aldrich Chemie GmbH, Munich, Germany	D6750
Sodium dodecyl sulfate (SDS)	Carl Roth GmbH + Co. KG, Karlsruhe, Germany	2326.2
Sodium dodecyl sulfate solution 10% (w/v)	Bio-Rad Laboratories, Hercules, CA, USA	161-0416
Sodium hydroxide solution (NaOH)	Merck KGaA, Darmstadt, Germany	1.09137
Splitomicin	Axxora Deutschland GmbH, Grünberg, Germany	ALX-270-380
Sulfuric acid (H ₂ SO ₄)	Sigma-Aldrich Chemie GmbH, Munich, Germany	433217
Tissue Tek™	Sakura Finetek Europe B.V., Zoetenwoude, Netherlands	4583
Trichostatin A (TSA)	Sigma-Aldrich Chemie GmbH, Munich, Germany	T8552
Tris	Carl Roth GmbH + Co. KG, Karlsruhe, Germany	4855.2
Triton X 100	Sigma-Aldrich Chemie GmbH, Munich, Germany	T-9284
Trizma® hydrochloride (Tris-HCl)	Sigma-Aldrich Chemie GmbH, Munich, Germany	T5941
Trypan blue solution (0.4%)	Sigma-Aldrich Chemie GmbH, Munich, Germany	T-8154
Trypsin/EDTA	Cambrex BioScience, Inc, Walkerville, MD, USA	CC-5012
Tween 20	Sigma-Aldrich Chemie GmbH, Munich, Germany	P-1379
Ultrapure DNase/RNase-Free Distilled Water	Invitrogen GmbH, Karlsruhe, Germany	10977-035
Vectashield Mounting Medium	Vector Laboratories, Inc., Burlingame, CA, USA	H-1000
Xylenes	Riedel-de Haën Sigma-Aldrich Laborchemikalien GmbH, Seelze, Germany	95692

Table 2. List of chemicals

Antibodies

Primary antibodies

Antibody	Source	Isotype	Company	Cat.No.
α -Smooth Muscle Actin	mouse	IgG monoclonal Cy3 conjugated	Sigma-Aldrich Chemie GmbH, Munich, Germany	C 6198
β -tubulin	mouse	IgG monoclonal	Sigma Chemical Co, St Louis, MO, USA	T 4026
Acetylated-Lysine	rabbit	IgG polyclonal	Cell Signaling Technology, Inc., Beverly, MA, USA	9441
Acetylated-p53 (Lys382)	rabbit	IgG polyclonal	Cell Signaling Technology, Inc., Beverly, MA, USA	2525
Bim (H-191)	rabbit	IgG polyclonal	Santa Cruz Biotechnology Inc., Santa Cruz, CA, USA	sc-11425
Caveolin-1 (N-20)	rabbit	IgG polyclonal	Santa Cruz Biotechnology Inc., Santa Cruz, CA, USA	sc-894
CDK4 (C-22)	rabbit	IgG polyclonal	Santa Cruz Biotechnology Inc., Santa Cruz, CA, USA	sc-260
Cleaved Caspase-3 (Asp175)	rabbit	IgG polyclonal	Cell Signaling Technology, Inc., Beverly, MA, USA	9661
Cleaved PARP (Asp214)	rabbit	IgG Polyclonal	Cell Signaling Technology, Inc., Beverly, MA, USA	9541
Cyclin A	rabbit	IgG polyclonal	Santa Cruz Biotechnology Inc., Santa Cruz, CA, USA	sc-751
Cyclin B	rabbit	IgG polyclonal	Santa Cruz Biotechnology Inc., Santa Cruz, CA, USA	sc-595
Cyclin D1	rabbit	IgG polyclonal	Santa Cruz Biotechnology Inc., Santa Cruz, CA, USA	sc-753
Cyclin E	rabbit	IgG polyclonal	Santa Cruz Biotechnology Inc., Santa Cruz, CA, USA	sc-481
FasL	rabbit	IgG polyclonal	Santa Cruz Biotechnology Inc., Santa Cruz, CA, USA	sc-834
FoxO1a	rabbit	IgG polyclonal	Cell Signaling Technology, Inc., Beverly, MA, USA	9462
FoxO3a	rabbit	IgG polyclonal	Cell Signaling Technology, Inc., Beverly, MA, USA	9467
GADD45 α (C-20)	rabbit	IgG polyclonal	Santa Cruz Biotechnology Inc., Santa Cruz, CA, USA	sc-792
MnSOD	rabbit	IgG polyclonal	Santa Cruz Biotechnology Inc., Santa Cruz, CA, USA	sc-30080
p21 (C-19)	rabbit	IgG polyclonal	Santa Cruz Biotechnology Inc., Santa Cruz, CA, USA	sc-397
p27 (F-8)	mouse	IgG monoclonal	Santa Cruz Biotechnology Inc., Santa Cruz, CA, USA	sc-1641
p53 (FL-393)	rabbit	IgG polyclonal	Santa Cruz Biotechnology Inc., Santa Cruz, CA, USA	sc-6243
PARP	rabbit	IgG polyclonal	Cell Signaling Technology, Inc., Beverly, MA, USA	9542
phospho-Akt (Ser475)	rabbit	IgG polyclonal	Cell Signaling Technology, Inc., Beverly, MA, USA	9271
phospho-FoxO1a (Ser256)	rabbit	IgG polyclonal	Cell Signaling Technology, Inc., Beverly, MA, USA	9461
phospho-Rb	rabbit	IgG polyclonal	Cell Signaling Technology, Inc., Beverly, MA, USA	9308

SIRT1	mouse	IgG monoclonal	Upstate Biotechnology, Lake Placid, NY, USA	05-707
SIRT1 (H-300)	rabbit	IgG polyclonal	Santa Cruz Biotechnology Inc., Santa Cruz, CA, USA	sc-15404
SIRT1 (H-300)	rabbit	IgG polyclonal biotin conjugated	Santa Cruz Biotechnology Inc., Santa Cruz, CA, USA	sc-13404
Vinculin (H-300)	rabbit	IgG polyclonal	Santa Cruz Biotechnology Inc., Santa Cruz, CA, USA	sc-5573

Table 3. List of primary antibodies**Secondary antibodies**

Antibody	Source	Conjugate	Company	Cat.No.
Anti-mouse IgG	sheep	HRP	Santa Cruz Biotechnology Inc., Santa Cruz, CA, USA	sc-2005
Anti-mouse IgG	goat	Alexa Fluor 488	Molecular Probes, Eugene, Oregon, USA	A-11029
Anti-rabbit IgG	goat	HRP	Santa Cruz Biotechnology Inc., Santa Cruz, CA, USA	sc-2004
Anti-rabbit IgG	goat	Alexa Fluor 488	Molecular Probes, Eugene, Oregon, USA	A-11034
Anti-rabbit IgG	donkey	Cy5	Dianova GmbH, Hamburg, Germany	711-176-152
Streptavidin-Cy3 (ZyMax Grade)		Cy3	Zymed Laboratories Inc, San Francisco, CA, USA	43-8315

Table 4. List of secondary antibodies**Small interfering RNAs (siRNAs)**

Gene	Species		siRNA-duplex sequence
SIRT1	human	FWD REV	5' -TTG AGG CCA GAG TCT GAG GT- 3' 5' -CTC CGA GAT AGC AGG GAA TG- 3'
siCONTROL Non-Targeting siRNA #2	human		www.dharmacon.com

Table 5. List of siRNAs for transient gene downregulation**Primer**

Gene	Species		Primer sequence for reverse transcriptase PCR
SIRT1	human	FWD REV	5' -GTC GTA CAA GTT GTC GGC CAG - 3' 5' -CCC ATT GTC TCC TTC CCC AG- 3'
18S	human	FWD REV	5' -TTG AGG CCA GAG TCT GAG GT- 3' 5' -CTC CGA GAT AGC AGG GAA TG- 3'

Table 6. List of primer for reverse transcriptase PCR

Methods

Cell culture

All cells were cultured in an incubator at 37°C and 5% CO₂. For harvesting and passaging, cells were washed twice with PBS and detached using trypsin/EDTA. All plastic ware was purchased from Costar (Cambridge, MA, USA) and NUNC (Wiesbaden, Germany), respectively.

Human coronary artery smooth muscle cells (HCASMC)

Human coronary artery smooth muscle cells (HCASMC) were purchased from Clonetics (Cat.No. CC-2683, Cambrex, Walkersville, MD, USA) and were cultured by using Smooth Muscle Cell Growth Medium 2 (Cat.No. C-22262, PromoCell, Heidelberg, Germany) supplemented with penicillin (10'000 U/ml) and streptomycin (10'000 µg/ml). For some experiments silencing of cells for 72 h in Smooth Muscle Cell Basal Medium 2 (Cat.No. C-22062, PromoCell, Heidelberg, Germany) was necessary. The cells were used exclusively until passage 6.

Mouse embryonic fibroblasts (MEF)

Mouse embryonic fibroblasts (MEF) derived from SIRT1 knockout mice (S1KO) or from wild-type littermates (WT) were generously provided by Dr. Raul Mostoslavsky (Howard Hughes Medical Institute, Children's Hospital, Center for Blood Research, and Department of Genetics, Harvard University Medical School, Boston, MA, USA). The cells were grown in DMEM/HAM's F-12 with L-Glutamine supplemented with 10% FBS and penicillin/streptomycin (10'000 U/ml und 10'000 µg/ml) and 0.0008% 2-Mercaptoethanol. In case of starvation, the cells were kept in DMEM/HAM's F-12 with L-Glutamine without FBS for 12 h before use.

Mouse vascular smooth muscle cells

Mouse vascular smooth muscle cells were derived from male C57/BL6 mice and isolated by the explant method, as previously described⁶⁶. Cells were cultured in DMEM/HAM's F-12 supplemented with 10% FBS and penicillin/streptomycin (10'000 U/ml and 10'000 µg/ml). For all experiments reported in this study, only passages 4 to 10 were used. Quiescence, when indicated, was achieved by serum withdrawal for 48 h.

Rat vascular smooth muscle cells

Primary cultures of rat vascular smooth muscle cells were isolated by enzymatic dissociation from the aorta of non-treated or monocrotaline-treated Sprague-Dawley rats as described elsewhere³²⁰. Studies were conducted on cells (passage 4 to 10) after they had achieved confluence in 10% FBS/DMEM/HAM's F-12 medium plus penicillin/streptomycin (10'000 U/ml and 10'000 µg/ml). To achieve quiescence, serum withdrawal for 48 h was performed.

Rat pulmonary artery smooth muscle cells (PASMC)

Rat pulmonary artery smooth muscle cells (PASMC) were kindly provided by Dr. Soni Pullamsetti (University of Giessen Lung Center (UGLC), Medical Clinic II/V, Giessen, Germany). The cells were cultured in DMEM/HAM's F-12 supplemented with L-Glutamine, 10% FCS and penicillin/streptomycin (10'000 U/ml and 10'000 µg/ml), and used between passage 3-6. Serum-starvation was performed for 24 h in DMEM/HAM's F-12 plus L-Glutamine.

Cryoconservation and thawing of cells

For deep-freezing, cells in passage 3 grown in a 75 cm² tissue culture flask were trypsinized with 1 ml trypsin/EDTA, neutralized with 10 ml serum-containing medium and centrifuged for 5 min at 1000 rpm. Supernatant was discarded completely and the cell-pellet was resuspended in "freezing" medium (growth medium + 5% DMSO). 2.5 ml "freezing" medium was used for one 75 cm² flask. Cryogenic vial with 0.8 ml aliquots (~ 5x 10⁵ cells) were frozen first at -80°C and then transferred to -120°C after 24 h.

For thawing, one vial was taken out of -120°C, its content was melt as soon as possible and plated in pre-warmed growth medium at 37°C into a 75 cm² tissue culture flask. After attached of the cells, the medium was changed to remove the remaining DMSO.

RNA interference

HCASMCs at ~50% confluency were transiently transfected with the indicated siRNA duplex by using Lipofectamine 2000 (Cat.No. 11668-027; Invitrogen GmbH, Karlsruhe, Germany) according to the manufacturer's instructions. For one well of a 24-well plate, siRNA was diluted in 50 µl in OptiMEM I Reduced Serum Medium. Regarding to its silencing efficiency, siRNA was used at a final concentration of 10 nM. The amount of Lipofectamine 2000 used for one transfection was 0.5 µl diluted in 50 µl OptiMEM I. After a 15 min incubation time, the diluted siRNA was combined with diluted Lipofectamine 2000, and incubated for an additional 15 min at room temperature. The 100 µl complex-solution was afterwards combined with 400 µl growth medium (without antibiotics) and added to each well containing cells. After 24 h, medium was changed. Recommended transfection controls were performed with each siRNA experiment: a) non transfected cells; b) mock transfection (without siRNA, but with lipid carrier) for detection of cellular effects caused by the transfection event itself and c) transfection with a non-targeting siRNA (siControl) for detecting off-target effects. Experiments with transfected cells were performed between 48-72 h post-transfection. Transfection conditions used for all experiments were established by me in preparation to the final experiments.

Cell transduction with adenoviruses

Rat PSMCs cultured in growth medium were infected with a non-replicative control-adenovirus (Ad-GFP), or Ad-FoxO1a;AAA (encoding a constitutive inactive FoxO1a form plus GFP-tag) at 100 multiplicity of infection (MOI) after reaching 70% confluency. Both types of adenovirus were a gift from Prof. William Sellers, (Dana-Farber Cancer Institute, Boston, MA, USA). Cells were grown for an additional 48 h in serum-containing medium and afterwards used for the assays indicated in the text.

Quantification of cell proliferation

The quantification of cell proliferation was determined by measuring the incorporation of the pyrimidine analogue 5-bromo-2'-deoxyuridine (BrdU) instead of thymidine into the genomic DNA of proliferating cells. Therefore, the colorimetric Cell Proliferation ELISA from Roche (Cat.No. 11647229001, Roche Diagnostics, Mannheim, Germany) was used according to the manufacturer's instruction. In brief, cells grown in 96-well plates were incubated with BrdU labeling solution (final concentration: 10 μ M) for the last 6 h of their cultivation. The labeling medium was then removed by tapping off and the cells were fixed with FixDenat for 30 min at room temperature. After thoroughly removing FixDenat solution by flicking off and tapping, the cells were stored at either 4°C or the assay was carried on immediately with incubating the cells with anti-BrdU-POD working solution for 2 h at room temperature. After removal of the antibody conjugate by flicking off, the cells were rinsed three times with washing solution before substrate solution was added and then incubated at room temperature until color development was sufficient for photometric detection. 1 M H_2SO_4 was added to each well and after gently shaking for 20 sec the absorbance was measured in an ELISA reader at 450 nm against blank measurements (BrdU-medium), with a reference wavelength of 620 nm.

Quantification of cell numbers

The quantification of cell population numbers was colorimetrically assayed by using the Cell Proliferation Reagent WST-1 from Roche (Cat.No. 11644807001, Roche Diagnostics, Mannheim, Germany). WST-1 is a stable tetrazolium salt which is cleaved to a soluble formazan by a complex cellular mechanism that occurs only in healthy, metabolically active cells. Therefore, the amount of formazan dye formed directly correlates to the number of viable cells in the culture. For the experiments, cells grown in 96-well microtiter plates were incubated to 70% confluency and then treated with different agents as indicated. After treatment, the ready-to-use WST-1 reagent was added to the wells at a 1:10 dilution and incubated at 37°C until color development was sufficient for photometric detection. Absorbance was measured at 450 nm against WST-1-containing medium as a blank, with a reference wavelength of 620 nm.

Cell migration assays

Chemotactic cell migration was studied by using a 12-well modified Boyden Chamber Migration Assay. This system consists of 8 µm-pore size porous transwell polycarbonate membrane inserts from Corning (Cat.No. 3468098; Fisher Scientific GmbH, Schwerte, Germany) which were coated with 1.5% gelatin for 2 h at 37°C from both sides before use. The transwells were washed once with PBS and placed into a 12-well plate (Cat.No. 3468071; Fisher Scientific GmbH, Schwerte, Germany) containing 600 µl serum-free medium supplemented with the chemoattractant PDGF-BB (20 ng/ml) and 20% FBS, respectively. Addition of the chemoattractant only to the lower compartment establishes a gradient and cell migration through the pores of the membrane is stimulated.

Cells grown in 100-mm dishes were washed twice with PBS and harvested by trypsinization. The cell suspension was centrifuged for 5 min and 1000 rpm at room temperature. The cell pellet was resuspended in 10 ml serum free medium and centrifugation step was repeated. Afterwards the cell pellet was resuspended in 1 ml serum free medium and cell number was counted using a standard hemocytometer. Cellular density was adjusted to 5×10^5 cells/ml and 100 µl cell suspension (=50'000 cells) was added to the upper compartment. Migration was allowed to proceed for the indicated time points at 37°C, 5% CO₂ in a humidified incubator. After incubation, non-migrated cells located on the upper side of the membrane were scraped off with cotton swabs and remaining medium on the lower side of the insert membranes was carefully dapped off. The inserts were then transferred into a new 12-well plate containing 150 µl growth medium supplemented with 10% WST-1. It had to be taken care that the whole membrane was submerged in the medium. The plate was incubated at 37°C and 5% CO₂ until yellow color development of the medium was sufficient for photometric detection. The amount of formazan dye directly correlates to the number of migrated cells. 50 µl of the cell medium was then transferred to a fresh 96-er well plate and measurement was done at 450 nm against medium containing WST-1 as a blank, with a reference wavelength of 620 nm.

Quantification of apoptotic cell death rates

Apoptotic cells were analyzed using the Cell Death Detection ELISA Plus (Cat.No. 11774425001, Roche Diagnostics, Mannheim, Germany) which is a photometric enzyme-immunoassay kit for *in vitro* qualitative and quantitative determination of apoptotic cells. The assay was performed according to the manufacturer's instructions. In brief, cells grown in 96-well plates (under the conditions indicated) were centrifuged at 200 x g for 10 min at room temperature. Supernatants were carefully aspired without shaking the pellet at the bottom and cells were lysed with Lysis Buffer for 30 min at room temperature. This step was followed by centrifugation at 200 x g for 10 min at room temperature. 20 µl of the lysate was then transferred into the microtiter plate provided with the assay and 80 µl of freshly prepared

Immunoreagent was added. The plate was incubated at room temperature for 2 h under gently shaking. The solution was then removed by tapping and each well was rinsed 3x with 250 μ l of the provided Incubation Buffer. Afterwards 100 μ l ABTS solution was pipetted into each well and incubated on a plate shaker until color development was sufficient for photometric analysis. Measurement was done at 405 nm against ABTS solution as a blank, with a reference wavelength of 490 nm.

Forkhead transcription factor activity assays

In vitro FoxO activity assay was performed by using the commercially available activity assay TransAMTM FKHR Transcription Factor Assay Kit (Cat.No. 46396; Active Motif Europe, Rixensart, Belgium). Briefly, HCASMCs or PASMCs were grown on 100-mm dishes and treated as indicated. Nuclear extract was prepared by using NE-PER[®] Nuclear and Cytoplasmic Extraction Reagents (Cat.No. 78833, Pierce Biotechnology/Perbio Science Deutschland GmbH, Bonn, Germany) and protein concentrations were measured with the DC Protein Assay (see below). The activity assay was performed as described in the manual. In brief, 40 μ l Complete Binding Buffer was added to each well of the provided microwells and 10 μ l of nuclear extract (= 15 μ g nuclear extract) was added followed by incubation for 1 h at room temperature with mild agitation. For blank controls, 10 μ l of Complete Lysis Buffer was added. Each well was washed 3x with 200 μ l Wash Buffer before adding 100 μ l diluted FoxO1a (1:500). The wells were incubated for 1 h at room temperature. After another washing step, 100 μ l of diluted HRP-conjugated antibody was added to all wells being used for 1 h. The wells were washed 4x and 100 μ l Developing Solution was added per well and incubated until color development was sufficient. 100 μ l Stop Solution was added and absorbance was measured at 450 nm with a reference wavelength of 620 nm. The plate reader was blanked using the blank wells.

Flow cytometric cell cycle analysis

Cell cycle distribution (G_0/G_1 , S, and G_2/M phases) was analyzed by flow cytometry (FACS). HCASMCs and PASMCs, respectively, grown on 100 mm-dishes, were treated as indicated and harvested by trypsinization. The cells were washed once with ice-cold PBS, fixed in 10 ml 75% ice-cold methanol and kept frozen at -20°C until FACS analysis. Two hours prior to FACS analysis, the cells were spun down, washed 1x with PBS and incubated for 1 h at 37°C in PBS containing 100 μ g/ml RNase A, 10 μ g/ml propidium iodide (PI) and 3% FBS. After two washing steps with PBS, cells were resuspended in 500 μ l PI-PBS and analyzed for DNA content. Samples were analyzed using standard methods on a BD FACScanTM flow cytometer (BD Biosciences, Becton Dickinson GmbH, Heidelberg, Germany). Duplet discrimination prior to cell cycle analysis was performed by blotting fluorescence-width vs. fluorescence-area. Data were

computer analyzed using commercially available “BD CellQuest™ Pro” Version 5.2.1 software (BD Biosciences, Becton Dickinson GmbH, Heidelberg, Germany).

Fluorescence resonance energy transfer (FRET)

Fluorescence resonance energy transfer (FRET), also named Foerster-resonance-energy-transfer, is a powerful technique for detecting molecular interactions of two proteins during biological reactions both *in vivo* and *in vitro*³²¹. FRET describes the non-radiative energy transfer from an excited donor fluorophore to a second fluorophore (acceptor fluorophore). Excitation of a donor fluorophore elevates it to a higher energy state and its subsequent return to the ground state normally leads to emission of light at a characteristic emission spectrum. If another fluorophore is in close proximity to the donor (1 - 10 nm) - and its absorption spectrum overlaps the emission spectrum of the donor - energy from the donor is possibly transferred to the so-called acceptor fluorophore³²².

There are 22 different techniques for quantifying FRET signals³²², however, for my experiments the method of “FRET acceptor bleaching” was used. This method involves the measurement of changes in donor fluorescence, both in the presence and absence of an acceptor. It is performed by comparing the intensity of donor fluorescence in the same sample before and after destroying the acceptor fluorophore by laser-mediated photo bleaching. If a FRET signal was initially measured, an augmentation in donor fluorescence will emerge upon photo bleaching of the acceptor³²³ (Figure 14). The change in fluorescence-intensity can be described either as FRET efficiency (FRET_{eff}) or as increase in donor fluorescence (ΔIF).

The transfer efficiency of energy is measured as: $\text{FRET}_{\text{eff}} = ((D_{\text{post}} - D_{\text{pre}}) / D_{\text{post}}) \times 100$;

the increase in donor fluorescence as: $\Delta\text{IF} = D_{\text{post}} - D_{\text{pre}}$

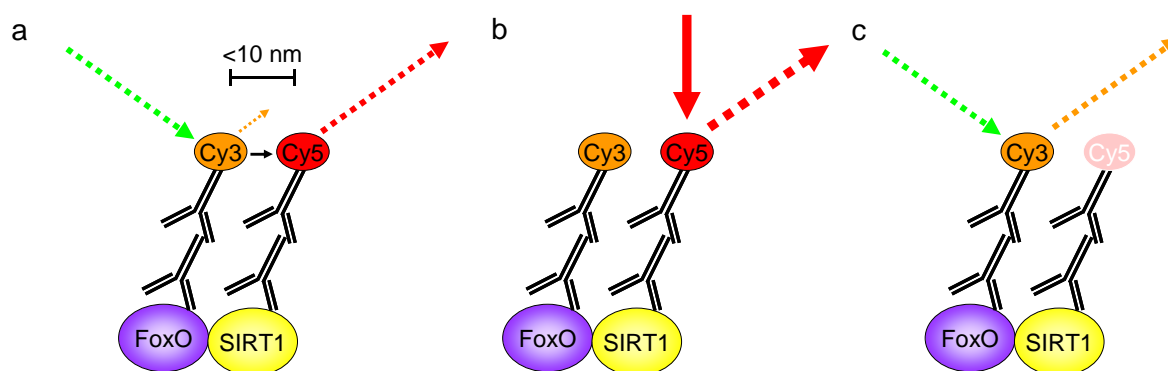


Figure 14. A model for FRET acceptor bleaching

a) Excitation of the donor at a wavelength of 543 nm. If the distance between donor and acceptor is less than 10 nm, non-radiative energy transfer occurs and the acceptor emits light at 639-738 nm. The donor emits only some light at 555–620 nm. **b)** Bleaching of the acceptor. **c)** The bleached acceptor-fluorophore is not able to accept light from the donor. Therefore, the emitted light from the donor strongly increases.

D_{post} is the intensity of the donor fluorescence after photo bleaching of the acceptor, and D_{pre} the intensity of donor fluorescence before acceptor photo bleaching. Positive FRET_{eff} and ΔIF are noted when $D_{\text{post}} > D_{\text{pre}}$.³²⁴ For my experiments, always ΔIF is indicated to describe FRET signal, because compared to FRET_{eff} , ΔIF has a higher specificity and sensitivity than FRET_{eff} , and therefore can better distinguish between a real FRET phenomenon and control experiments (Dr. Gabi Krasteva, personal communication).

For FRET analysis, the native proteins have to be labeled with fluorophore-coupled antibodies for the specific proteins. It is important to choose an acceptor fluorophore whose absorption spectrum overlaps the fluorescence emission spectrum of the donor (see above, and

Figure 15). For my experiments, the Cy3-Cy5 donor-acceptor pair, which was already shown to be reliable and relatively stable^{325, 326}, was used.

Figure 15 shows the overlap of the Cy3 emission spectrum and the red Cy5 absorption spectrum; this pair supports a strong FRET interaction.

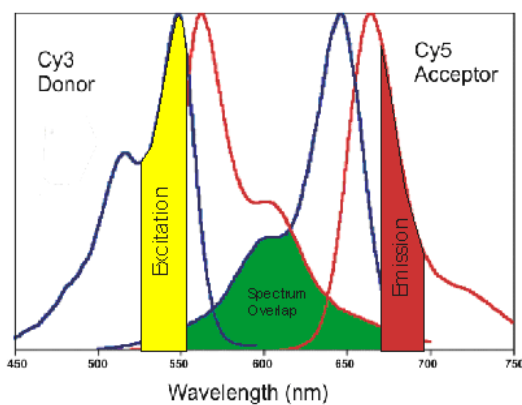


Figure 15. Schematic representation of the spectral overlap integral

Cy3 has its absorption maximum at 550 nm (blue line) and an emission-maximum at 570 nm (red line), whereas Cy5 has an absorption maximum at 650 nm (blue line) and emits maximal light at 670 nm (redline). The absorption spectrum of the acceptor fluorophore must overlap the emission spectrum of the donor fluorophore. By using appropriate filter-sets, both spectra can easily be separated from each other (picture see ³²⁷).

Double-labeling immunofluorescence for FRET-CLSM analysis

HCASMCs were grown on 8-well chamberslides until 70% confluency. All chambers were then maintained in serum free medium for 72 h to silence the cells. After serum starvation, HCASMCs were stimulated with either 20% FBS in growth medium, 1 mM H_2O_2 in serum-free medium or kept quiescent for 30 min. The chamberslides were fixed with 4% Histofix for 10 min, washed 3x 10 min with PBS and 5 min with H_2O . The cells were dried at room temperature for 10 min and then incubated for 1 h in blocking solution (5% normal goat serum containing 1% BSA in PBS). Primary antibodies against FoxO1a or FoxO3a were diluted in dilution buffer (PBS containing 0.01 % NaN_3 and 4.48 g/l NaCl) 1:25 and 1:100, respectively, and applied overnight at room temperature. After a washing step of 3x 10 min in PBS, Cy5-conjugated donkey anti-rabbit-Ig (1:500) was applied in dilution buffer for 1 h at room temperature. This incubation was followed by a second washing step of 3x 10 min with PBS, a post-fixation step for 5 min in 4% P Histofix, and a third washing step of 3x 10 min with PBS. The slides were then

incubated overnight at room temperature with a biotin-conjugated antibody for SIRT1 diluted 1:10 in the buffer described above. The species-specificity of this secondary reagent was controlled by overnight incubation of some slides with PBS instead of anti-SIRT1 antibody. Omission of the primary antibody for SIRT1 excludes cross-reactivity of both secondary antibodies with each other. The next day the slides were washed 3x 10 min with PBS (control slides and FRET slides in separate cuvettes), and the Cy3-conjugated anti-biotin-IgG was applied 1:2'500 in dilution buffer for 30 min at room temperature. Again, the slides were rinsed 3x 10 min with PBS, post-fixed for 5 min in 4% PFA followed by 3 washing steps à 10 min in PBS. The cells were coverslipped with Mowiol 4-88, pH 8.6 (kindly provided by Dr. Gabi Krasteva).

FRET Detection

Slides with double-labeled HCASMCs were analyzed with an epifluorescence microscope (Zeiss, Jena, Germany) using suitable filter sets for both Cy3 and Cy5, and with a confocal laser scanning microscope (CLSM; Leica-TCS SP2 AOBs; Leica, Mannheim, Germany). FRET was quantified upon acceptor photo bleaching at a 63x magnification using the CLSM. The CLSM was adjusted as follows: Excitation of Cy3: 51% He/Ne-laser power (543 nm), detection at 555-620 nm; Excitation of Cy5: 20% He/Ne-laser power (633 nm), detection at 639-738 nm. A region of interest ("ROI") was determined and in that region the acceptor fluorophore (Cy5) was photobleached 10x using the 633 nm He/Ne-laser at 100% activity and maximal zoom thus destroying Cy5. Pictures of the Cy3- and Cy5-fluorescence were taken simultaneously before and after bleaching. To reduce the background noise, the pictures were scanned three times and the mean in signal intensity was calculated. Changes in the Cy3 signal (ΔIF) were evaluated in the photobleached area (see above). To control the stability of the system, fluorescence of adjacent regions of the bleached ROI region was determined. If a $FRET_{eff} \geq 2\%$ was measured, this run was excluded from further analysis. For each condition at least 20 measurements out of 5 independent immunocytochemistry-experiments were performed.

Statistical analyses

Differences among two experimental groups and their appropriate control groups in the FRET-experiments were evaluated with the Kruskal-Wallis test subsequently followed by Mann-Whitney test using software SPSS, version 11.5.1 (SPSS GmbH Software, Munich, Germany), with results being highly significant at $p \leq 0.001$.

Mouse femoral artery angioplasty

Animals

Adult male C57/BL6 mice were purchased from Charles River (Quebec, Canada). All procedures involving experimental animals were performed in accordance with protocols approved by the institutional committee for animal research of the Giessen University and complied with the “Guide for the Care and Use of Laboratory Animals” (NIH publication No. 86-23, revised 1985).

Mouse femoral artery injury model

Mice used for surgical procedures were anesthetized by intramuscular injection of 2.5 µg xylazine (Rompun® 2%, Bayer Vital GmbH, Leverkusen, Germany), 3 mg ketamine (Ketamine Inresa 50 mg/ml; INRESA Arzneimittel GmbH, Freiburg; Germany) and 5 µg atropine (Atropinsulfate-solution 0.5 mg/ml, Fresenius KABI Deutschland GmbH, Bad Homburg, Germany) diluted in 0.9% sodium chloride solution into the right upper leg. Surgery was carried out using a dissecting microscope (Leica S4 E, Leica Mikrosysteme Vertrieb GmbH, Bensheim, Germany). Following anesthesia, the mice were fixed with tape and underwent transluminal mechanical injury of the left femoral artery by insertion of a straight spring wire (0.38 mm in diameter, Cook, Bloomington, IN, USA) for > 5 mm towards the iliac artery. This method was previously described by Sata *et al.*³²⁸ and modified by our group as described below. In brief, the fur on the left hind limb in the region of operation was carefully removed with a scissor and afterwards the region of operation was disinfected. The skin was cut off from the distal end of the leg in proximal direction for approximately 1 cm. Then the preparation of the femoral vessel/nerve strand was carried out. First of all the accompanying femoral nerve was carefully separated, and then the femoral vein was isolated from the artery by blunted dissection up to where the profunda femoris artery branches off the femoral artery. Therefore connective tissues around the artery was carefully removed with microsurgery forceps (Dumont S.A., Switzerland). This process was followed by preparation of the profunda femoris artery towards the external iliac artery. The nerve and vein accompanying the A. profunda femoris were also separated from the artery to prevent their injury during operation. The profunda femoris artery was then ligated distally (Ligation I) with Ethilon 6-0 silk sutures (Johnson & Johnson Intl, St-Stevens-Woluwe, Belgium) after isolation from nerve and vein (Figure 16). In addition, the femoral artery was looped proximally (Ligation III) and distally (Ligation II) with 6-0 silk suture for temporally controlling blood flow during the dilatation process (Figure 16). As with all ligations it had to be taken care that the blood flow was not interrupted untimely and as a result ischemia would occur in the distal tissue regions of the vessel. In preparation of the following dilatation, the ligations were stretched to prevent blood flow. The exposed A. profunda femoris branch was dilated by topical application of xylocaine (Xylocain® 2 %, AstraZeneca GmbH, Wedel,

Germany). Transverse arteriotomy was performed in the A. profunda femoris with Vannas style iris spring scissor (Aesculap AG & Co KG, Tuttlingen, Germany) (Figure 16).

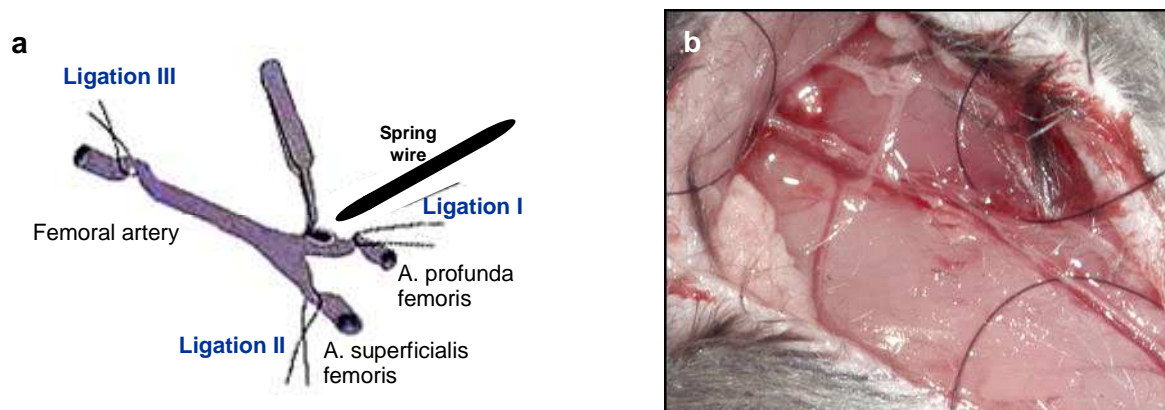


Figure 16. The endovascular injury of the murine femoral artery (Part 1)

The left femoral artery was exposed by blunt dissection, looped proximally and distally with a 6-0 silk suture for temporally controlling blood flow during the dilatation process (a, b). The femoralis profunda branch was isolated and ligated distally. Transverse arteriotomy was performed in the femoralis profunda branch (Picture modified after Sata *et al.*³²⁸)

Microsurgery forceps (Aesculap AG & Co. KG, Tuttlingen, Germany) were used to extend the arteriotomy through which a straight spring wire (0.38 mm in diameter, No. C-SF-15-15, COOK, Bloomington, IN, USA) was carefully introduced into the femoral artery for more than 5 mm toward the iliac artery (Figure 17).

The wire was left in the artery for approximately 1 min to denude and dilate the artery. After removal of the wire, the profunda femoris artery was secured at its proximal end with a silk suture (Figure 17). Subsequently, blood flow in the femoral artery was reconstituted by unfasten

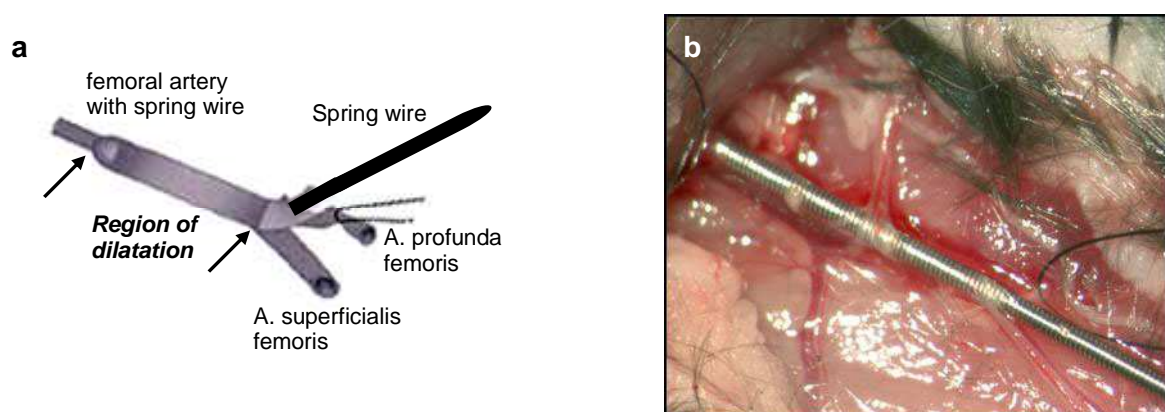


Figure 17. The endovascular injury of the murine femoral artery (Part 2)

Microsurgery forceps were used to extend the arteriotomy through which a 0.38 mm straight wire was introduced for more than 5 mm into the femoral artery toward the iliac artery (a, b). The wire was left in the artery for 1 minute to denude and dilate the artery. (Picture modified after Sata *et al.*³²⁸)

the silk sutures in the proximal (Ligation III) and distal (Ligation II) part of the artery. The skin transection was sealed with a 6-0 Prolene® silk suture (Figure 18).

During the whole surgery it was necessary to take care that the tissue was moistened with xylocaine. After surgery the mouse was defixed and awaked under red light.

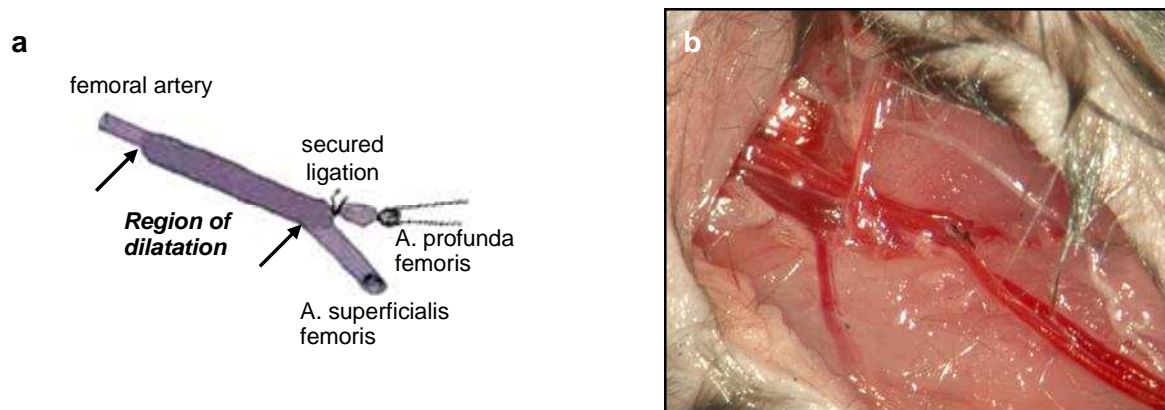


Figure 18. The endovascular injury of the murine femoral artery (Part 3)

After removal of the wire, the proximal part of the A profunda femoris was tied off. Blood flow of the femoral artery was restored (a, b). (Picture modified after Sata *et al.*³²⁸)

Injection of adenovirus

After removal of the wire out of the femoral artery and restoration of blood flow, replication-incompetent adenovirus encoding SIRT1, a constitutively inactive SIRT1-mutant H355A (recently generated by our group) or a control-adenovirus was mixed with 45 μ l of a 20% thermosensitive polymer (Pluronic F-127, Cat.No. P2443, Sigma Aldrich; Munich, Germany) to a final concentration of 1×10^8 pfu/ml. The gel was placed around the dilatated artery and left. The adenoviruses had been previously tested for efficient infection and transgene expression in VSMCs and in HEK cells.

Application of Psammaphysene A

Immediately after dilatation, the artery was covered with 45 μ l of a 20% thermosensitive polymer (Pluronic F-127, Cat.No. P2443, Sigma Aldrich; Munich, Germany) containing 10 μ M Psammaphysene A (kindly provided by J. Clardy, Harvard Medical School, Boston, MA, USA). The gel was left around the artery and released its substrate over the next 21 days.

Vessel Harvesting

At the timepoints indicated below, the mice were killed by an overdose of isoflurane (Isofluran-Baxter, Baxter Deutschland GmbH, Unterschleissheim, Germany). At death, the mice were perfused via the left ventricle with 2% PFA in PBS (pH 7.4). The femoral arteries were carefully

excised, rinsed in PBS to remove remained blood and post-fixed in 2% PFA overnight at 4°C. The following day, the dilated arteries were embedded in Tissue Tek[®] snap-frozen in liquid nitrogen and stored at -80°C until use.

Morphometric Analysis

Frozen and embedded arteries were sectioned on a Leica cryostat (LEICA CM 1900, Leica Mikrosysteme Vertrieb GmbH, Bensheim, Germany). The cross-sections (6 µm) were placed on poly-L-lysine coated slides for subsequent immunohistochemical stainings. For morphometric analyses, hematoxylin and eosin staining was performed (for protocol see below). All sections were examined under a Leica DMRB microscope (Leica Mikrosysteme Vertrieb GmbH, Bensheim, Germany) and morphometric analysis was performed using KS300 imaging software (Carl Zeiss, Hallbermoos, Germany). The external elastic lamina, internal elastic lamina, and the lumen circumferences, as well as medial and neointimal area of three sections per artery were measured.

Histological and Immunohistochemical techniques

Immunocytochemical analysis of human and mouse cells

Immunocytochemical analysis was used for detecting SIRT1 or FoxOs in human and mouse cells. Cells grown on coverslips were fixed in 4% PFA for 10 min at room temperature, rehydrated and permeabilized with 0.3% Triton-X in PBS for 15 min, and blocked for 1 h with 10% ready-to-use normal goat serum solution. The primary antibody was diluted in read-to-use antibody diluent (SIRT1 1:100, FoxO1a 1:50, FoxO3a 1:100) and incubated overnight at room temperature. Subsequently to rinsing 3x 5 min with PBS, cells were incubated with secondary antibody (anti-rabbit Alexa 488 or anti-mouse Alexa 488) diluted 1:200 in antibody diluent for 1 h at room temperature in the dark. Prior to mounting with Vectashield[®] Mounting Medium, cells were stained with Dapi. Cells were analyzed by fluorescent light microscopy (DMRB, Leica, Mannheim, Germany).

Immunohistochemical analysis of SIRT1 expression in mouse tissues

SIRT1 expression in cells of the mouse femoral artery was detected by fluorescence staining. Cryosection slides were fixed in 4% PFA for 15 min at room temperature, rehydrated and permeabilized with 0.3% Triton-X in PBS for 15 min and blocked for 1 h with 10% ready-to-use normal goat serum solution. The primary antibody was diluted in read-to-use antibody diluent (SIRT1 1:50) and incubated overnight at room temperature. Subsequently to rinsing 3x 5 min with PBS, cells were incubated with a mix of secondary antibody (anti-rabbit Alexa 488, 1:200) and Cy3-coupled anti-smooth muscle cell actin antibody (1:200) diluted in antibody diluent for 1 h at room temperature in the dark. Prior to mounting with Vectashield[®] Mounting Medium, cells

were washed 3x 5 min with PBS and stained with Dapi. Cells were analyzed by fluorescent light microscopy (DMRB, Leica, Mannheim, Germany).

Immunohistochemical analysis of SIRT1 expression in human tissues

SIRT1 expression in diverse human tissues was analyzed using broad spectrum Histostain-SAP Kit from Zymed Laboratories (Cat.No. 95-9842, Zymed Laboratories Inc, South San Fransisco, Ca, USA). Cryosection slides from the indicated tissues were fixed with acetone at 4°C for a period of 10 min and then stained according to manufacturers instructions. In brief, slide were rehydrated with PBS for 15 min and incubated with Blocking Solution (Reagent 1A) for 10 min at room temperature. Primary rabbit anti-SIRT1 antibody was applied in ready-to-use antibody diluent (1:100) and incubated in a moist chamber overnight at room temperature. The slides were then rinsed with PBS (3x 2 min). Biotinylated Second Antibody (Reagent 1B) was added to each section and incubated for 10 min at room temperature followed by a washing step (3x 2 min). Enzyme Conjugate (Reagent 2) was applied to the tissues for 10 min, slides were rinsed 3x 2 min with PBS and Substrate-Chromogen Mixture was then added for 10 min. Each section was washed well with H₂Odd and counterstained with Counterstain (Reagent 4). The slides were rinsed twice with 100% ethanol, cleared in xylene and coverslipped with Mounting Solution (Reagent 5). Stainings were evaluated using an epifluorescence microscope (DMRB, Leica, Mannheim, Germany). Negative controls were performed using only the secondary antibody.

Hematoxylin and Eosin (H & E) Staining

Hematoxylin and eosin staining was used on tissues for staining nuclei (blue, hematoxylin) and cytoplasm (red, eosin). Cryoslides were fixed in 4% PFA at room temperature for 10 min and rehydrated with PBS for 15 min. Hematoxylin staining was performed using Gill's hematoxylin III (Cat.No. 5174, Merck, Darmstadt, Germany) for 6 sec and non-specific hematoxylin staining was removed by a rinse of the slides with acetic acid. The slides were washed in running tap water for 10 min and then immersed in eosin stain for 5 sec. The eosin staining solution was prepared as follows:

Eosin Staining Solution (for 1 l)	100 ml Eosin (1 g Eosin Y on 100 ml H ₂ Odd), 10 ml Phloxin (1 g Phloxin B on 100 ml H ₂ Odd), 780 ml 95% ethanol, 4 ml acetic acid
--------------------------------------	---

This step was followed by dehydration in ascending alcohol solutions: 2 min 96% isopropyl alcohol supplemented with 0.6% acetic acid and twice with 100% isopropyl alcohol for 2 min each. The slides were mounted with Vectashield Mounting Medium and observed under the microscope (DMRB, Leica, Mannheim, Germany).

PCNA (Proliferating Cell Nuclear Antigen) staining of mice tissue sections

To detect proliferating VSMCs in neointimal tissue, mouse artery cross-sections were stained for the proliferating cell nuclear antigen (PCNA) by using Zymed's PCNA staining kit (Cat.No. 93-1143, Zymed Laboratories Inc, South San Francisco, Ca, USA) according to the manufacturers instructions. In brief, tissue cross-sections were fixed in 4°C acetone for 10 min and then blocked with Blocking Solution (Reagent 1) for 10 min at room temperature. The biotinylated mouse anti-PCNA primary antibody (Reagent 2) was applied for 60 min at room temperature to the sections. This step was followed by rinsing with PBS 3x 2 min and application of the Streptavidine Peroxidase (Reagent 3) for 10 min at room temperature. The slides were washed 3x 2 min with PBS and the DAB chromogen mix was added for 5 min. For hematoxylin counterstaining, the slides were covered with Reagent 5 for 2 min and subsequently washed with H₂O until sections turn blue. The slides were dehydrate in a graded series of alcohol, and cleared with xylene before covered with Histomount (Reagent 6) and coverslip.

Co-immunoprecipitation (Co-IP)

HCASMCs were cultured in 100-mm dishes until 80% confluency and then incubated for 12 h in the absence or presence of the compounds/H₂O₂ indicated. For cell lysate preparation, dishes were washed 2x with ice-cold PBS and lysed with 500 µl of Co-IP lysis buffer on ice for 30 min. Samples were centrifuged at 13'000 rpm for 15 min at 4°C and supernatants were collected.

Co-IP Lysis Buffer	50 mM Tris HCl pH 8.2, 100 mM NaCl, 2 mM EGTA, 10 mM NaF, 40 mM β-glycerophosphate, 0.4% Triton-X, 10 mM NAM, 10 µM TSA, 1% freshly prepared Complete Protease Inhibitor Cocktail
-----------------------	---

Protein concentrations were measured and samples were adjusted to 300 µg protein in 400 µl lysis buffer per sample. The samples were precleared with 5 µl Dynabeads® Protein G (Cat.No. 100.03; Dynal Biotech GmbH, Hamburg, Germany) and incubated with rotating mixing for 30 min at 4°C. The supernatant was afterwards transferred to a new tube and incubated with an antibody for acetylated-lysines (1 µg antibody per 100 µl lysate) or with a normal rabbit IgG control antibody (Cat.No sc-2027, Santa Cruz Biotechnology Inc., Santa Cruz, CA, USA) under the same conditions as before. After incubation for 2.5 h, 15 µl of the beads were added for an additional hour. The immune complexes were collected using a magnet and supernatant was discarded. After washing 3x with 1 ml lysis buffer the immune complexes were collected and finally resuspended in 40 µl lysis buffer. The samples were separated on SDS-PAGE after boiling for 5 min. The blots were probed with an antibody for FoxO1a.

Detection and analysis of proteins

Total protein extraction from cultured cells

For whole-cell extracts, adherent cells grown on 60-mm and 100-mm dishes, respectively, were washed twice with ice-cold PBS and lysed on ice with RIPA Lysis Buffer. Cells were then collected by scraping, transferred to a prechilled microcentrifuge tube, homogenized by vortexing and incubated on ice for 30 min.

RIPA Buffer	PBS, 1% NP-40, 0,5% sodium deoxycholate, 0.1% SDS, 1% freshly prepared Complete Protease Inhibitor Cocktail
-------------	---

Cell lysates were clarified by centrifugation (15 min, 13'000 rpm, 4°C) and supernatants containing total protein extracts were either stored at -80°C or used immediately for further experiments.

Quantification of protein concentration according to DC Protein Assay

Protein concentrations were determined using the colorimetric assay DC Protein Assay from BioRad (Cat.No. 500-0111, BioRad, Munich, Germany), according to manufacturer's instructions. Briefly, 2.5 µl protein solution was mixed with 2.5 µl H₂O and pipetted into one well of a 96-well microplate. 25 µl of Working Reagent (20 µl Reagent S per each ml Reagent A) was added. Finally 200 µl Reagent B was added per well and the plate was incubated at room temperature with mild agitation for 10 min. Absorbance was read at 620 nm. The whole assay used is based upon the Lowry assay and uses BSA as a standard. The absorbance values of different amounts of BSA were used to generate a standard calibration curve. Concentrations of the unknown protein samples were determined by comparison with the standard curve.

For avoiding inexactness each measurement was carried out in duplicate and the mean value was generated.

Sodium Dodecyl Sulfate -Polyacrylamide Gel Electrophoresis (SDS-PAGE)

Denaturing Sodium Dodecyl Sulfate polyacrylamide gel electrophoresis (SDS-PAGE) was performed essentially as described by Laemmli *et al.* 1970³²⁹ for separating proteins according to their molecular weight. Ready Gel Tris-HCl gels compatible for Mini Protean 3 Electrophoresis Cell (BioRad, Munich, Germany) were purchased from BioRad (5%: Cat.No. 161-1154; 7.5%: Cat.No.161-1154; 12%: Cat.No. 161-1156, BioRad, Munich, Germany). The acrylamide content of SDS-PAGE gels was varied according to the size of the protein being examined. 10-30 µg protein were denaturated by boiling at 99°C for 5 min in 10x SDS PAGE Loading Buffer before separation on an SDS-PAGE gel.

Samples and pre-stained protein marker standard (Cat.No. 27-2110, Peqlab Biotechnologie GmbH, Erlangen, Germany) were loaded simultaneously on the same gel and electrophoresis was performed for approximately 1 h at 120 V in electrophoresis buffer.

10x SDS-PAGE
Loading Buffer

625 mM Tris-HCl pH 6.8, 20% SDS, 50% glycerol,
0.3% bromophenol blue, 9% 2-mercaptoethanol

1x SDS-PAGE
Electrophoresis
Buffer

25 mM Tris, 250 mM glycine pH 8.3, 1% SDS

Transfer and blotting of proteins

Following electrophoresis, proteins separated by SDS-PAGE were transferred from the gel to a PVDF-Plus Membrane (0.45 μ m) (Cat.No. PV4HY320F2, Osmonics Inc., Moers, Germany). The membrane was pre-treated with 100% methanol for 1 min, rinsed with water and subsequently soaked with Transfer Buffer together with two fiber pads (Cat.No. 170-3933, BioRad, Munich, Germany) and two thick whatman papers (Cat.No. 3030-6185, Whatman plc, Kent, UK). The gel was pre-equilibrated in Transfer Buffer prior to electrophoretic transfer.

1x Transfer Buffer

25 mM Tris, 192 mM glycine pH 8.3, 20% methanol,
0.1% SDS

The transfer was performed using a wet transfer system (Mini Trans-Blot Cell, Cat.No. 170-3930, BioRad, Munich, Germany). In this system gel, membrane, fiber pads and whatman papers were arranged as a sandwich in a cassette which is placed in a module compatible with the Mini Trans-Blot Cell. The complete tank was filled with Transfer Buffer and transfer was run for 1 h at 100 V.

Ponceau S staining of proteins

After blotting, the membrane was stained with Ponceau S reagent (Cat.No. P-7170, Sigma-Aldrich Chemie GmbH, Munich, Germany) to ensure proper transfer of proteins onto the membrane. The membrane was destained with H₂O and rinsed several times with PBS-T solution.

PBS-T

PBS, 0.1% Tween 20

Immunodetection of proteins

After decolorization the membrane was blocked with 5% Skim Milk Solution for 1 h at room temperature with mild agitation.

5% Skim Milk Solution	PBS, 0.1% Tween 20, 5% Skim Milk Powder
-----------------------	---

This step was followed by incubation with the primary antibody against the desired protein in 5% Skim Milk Solution overnight with gentle shaking at 4°C. The following day the membrane was washed three times for 10 min at room temperature with PBS-T. Detection was performed with HRP-conjugated secondary antibody in 5% Skim Milk Solution. After incubation for 1 h at room temperature, three washing steps of 10 min with PBS-T and rinsing with PBS were followed. The membrane was incubated for 5 min with chemiluminescence ECL Plus Western Blotting Detection Solution (Cat.No. RPN2132, Amersham Biosciences Europe GmbH, Freiburg, Germany). Membranes were exposed to audiographic films (Hyperfilm ECL, Cat.No. RPN3103K, Amersham Biosciences Europe GmbH, Freiburg, Germany) or X-Ray films (Cat.No. Agfa Curix HT 1.000G Plus, Agfa-Gevaert N.V., Mortsel, Belgium) using a Hypercassette (Cat.No. RPN12649, Amersham Biosciences Europe GmbH, Freiburg, Germany). The membrane was reprobbed several times and therefore needed to be stripped of bound antibody by submerging in Restore Western Blotting Stripping Buffer (Cat.No. 21059, Pierce Biotechnology Inc., Rockford, IL, USA) for 30 min at 37°C according to manufacturer's instructions. Afterwards the membrane was blocked again with 5% Skim Milk Solution and incubated with a new antibody as described before.

For detection of phosphorylated proteins the buffers were substituted. Instead of using PBS-T for washing, TBS-T was used.

TBS-T	20 mM Tris pH 7.6, 140mM NaCl, 0.1% Tween 20
-------	--

Likewise, the membrane was blocked with 5% BSA in TBS-T and the antibodies were diluted in 5% BSA in TBS-T.

Synthesis of RNA

All works, which were necessary for *in vitro*-synthesis of RNA, were done under RNase-free conditions. All liquid solutions used were DEPC-treated.

RNA Isolation

RNA of cells grown in 60-mm dishes was extracted using peqGOLD RNAPure™ (Cat.No. 30-1020, Peqlab Biotechnologie GmbH, Erlangen, Germany). Therefore, the cell medium was aspirated under the hood and cells were lysed in 1 ml peqGOLD RNAPure™. Afterwards, the samples were incubated at room temperature for 5 min to permit complete dissociation of nucleo-protein complexes. Then 0.2 ml chloroform was added and tubes were shaken vigorously by hand for 15 sec. After incubating the samples for 10 min at room temperature, they were centrifuged at 13'000 x g for 5 min at room temperature. Following centrifugation, the mixture separates into a lower yellow phenol-chloroform phase, an interphase, and a colorless upper aqueous phase, which exclusively contains the RNA. The aqueous phase was transferred to a fresh tube and RNA was precipitated by mixing with 0.5 ml isopropyl alcohol. The samples were incubated at room temperature for 10 min and then centrifuged at 13'000 x g for 10 min at 4°C. The RNA precipitated and formed a gel-like pellet on the bottom of the tube. The supernatant was removed and the RNA pellet was washed twice with 1 ml cold 75% ethanol followed by centrifugation at 13'000 x g for 10 min at 4°C. At the end of the procedure, the RNA pellet was air-dried for 5-10 min. For redissolution, total RNA was dissolved 1:30 in RNase/DNase-free water and stored at -80°C until use.

Determination of RNA concentration

The concentration of isolated RNA was determined by measuring the absorbance at 260 nm in a spectrophotometer. Therefore, 6 µl of the RNA-solution were diluted in 294 µl RNase/DNase-free water and RNA concentration was measured using quartz cuvettes versus 300 µl water as blank.

First-strand cDNA synthesis

For analyzing gene expression, the RNA of interest first needs to be reverse transcribed into cDNA. First strand cDNA was synthesized by using Moloney Murine Leukemia Virus Reverse Transcriptase (M-MLV) Kit (Cat.No. 28025-013, Invitrogen GmbH, Karlsruhe, Germany). 1 µg of total RNA was diluted with DEPC-treated water to a final volume of 13.5 µl and 10.5 µl of cDNA Synthesis-Mix was added.

Finally, 1 µl M-MLV Reverse Transcriptase was added per sample and the mixture was incubated at 37°C for 1 h. The reaction was stopped by incubation for 15 min at 99°C and samples were stored at -80°C.

cDNA Synthesis-Mix (1x)	5 µl	First-Strand Buffer
	2.5 µl	0.1 M DTT
	0.5 µl	RNasin (Cat.No. N2511, Promega GmbH, Mannheim, Germany)
	1.5 µl	primer "random" (Cat.No. 11034731001, Roche Diagnostics GmbH, Mannheim, Germany)
	1 µl	10 mM dNTP Mix (Cat.No. 11581295001, Roche Diagnostics GmbH, Mannheim, Germany)

Polymerase Chain Reaction (PCR)

Expression of endogenous mRNA was determined by reverse transcription of total RNA followed by Polymerase Chain Reaction Analysis (PCR) using Taq-DNA Polymerase. The method of polymerase chain reaction is used for amplification of specific cDNAs.

The Taq DNA polymerase was already part of a commercially available ready-to-use PCR-Master-Mix S from Peqlab (Cat.No. 01-1410, Peqlab Biotechnology GmbH, Erlangen, Germany). PCR-Master-Mix S is supplied at 2x final concentration, with the final reaction concentrations as follows: 5 units/µl Tag-DNA-Polymerase, 0.4 mM dNTPs, 20 mM Tris-HCL (pH 8.8 at 25°C), 100 mM KCl, 0.02% Tween 20 and 3 mM MgCl₂.

The PCR-reaction mix was prepared as follows:

PCR-Reaction Mix (1x)	5 µl	PCR-Master-Mix S
	0.7 µl	primer forward (10 pmol/µl)
	0.7 µl	primer reverse (10 pmol/µl)
	2.6 µl	DEPC-treated H ₂ O

1 µl cDNA was added to a total reaction volume of 10 µl.

Primer, number of PCR cycles and annealing temperatures chosen for PCR depended on the cDNA sequence to be amplified.

One representative PCR cycle for SIRT1 is shown below:

Preheating	94 °C	2 min	} 25 cycles
Denaturation	94 °C	20 sec	
Annealing	56 °C	20 sec	
Elongation	68 °C	30 sec	
Extension	68 °C	7 min	
	4 °C	∞	

All Polymerase Chain Reaction amplifications were carried out on a thermocycler GeneAmp® PCR System 2400 (PerkinElmer LAS (Germany) GmbH, Rodgau, Germany).

Agarose gel electrophoresis

Analysis of DNA fragments from PCR were performed by agarose gel electrophoresis. 1% agarose gels were prepared by dissolving 0.5 g agarose (Cat.No. 155109-027, GibcoBRL, Eggenstein, Germany) in 50 ml of TAE Buffer.

1x TAE Buffer	0.04 M Trisacetate, 0.0001 M EDTA
---------------	-----------------------------------

The agarose was melted using a microwave oven. After the agarose was cooled down to approximately 50°C, 0.5 µl ethidium bromide was added and the whole fluid was poured into a gel-cast for letting it solidify. PCR products were combined with 2.5 µl 5x DNA Loading buffer. EZ Load™ DNA molecular weight marker (Cat.No. 170-8353, BioRad) was used as loading marker.

5x DNA Loading Buffer	625 mM Tris-HCl pH 6.8, 20% SDS, 50% glycerol, 0.3% bromophenol blue, 9% 2-mercaptoethanol
-----------------------	--

Electrophoretic separation was carried out at 133 V and 200 mA on a Consort E452 power supply. The PCR products were visualized on an ultraviolet transilluminator TM-36 (UVP, Upland, CA, USA) and images captured using a Polaroid GelCam (Polaroid GmbH, Dreieich-Sprendlingen, Germany).

Statistical analysis

Data were stored and analyzed on personal computers using Excel 2003 (Microsoft) and Sigma Plot 8.0 with Sigma Stat 2.03 (Systat Software GmbH, Erkrath, Germany). Data between the study groups were analyzed by ANOVA followed by pairwise comparison with Fisher's least significance test. All data are represented as mean and standard deviation. Probability values are indicated for each experiment.

Results

Psammallysine A and its analogues regulate HCASMC behavior *in vitro* and *in vivo*

Recently we were able to demonstrate the forkhead transcription factor FoxO1a to be a key regulator of arterial VSMC proliferation, migration and apoptosis *in vitro* and *in vivo* (Sedding *et al.*, unpublished data). Especially the impact of phosphorylated FoxO1a on VSMC homeostasis was demonstrated. My thesis now further implies FoxO1a to represent an attractive target for future therapeutic strategies in the prevention of vasculo-proliferative diseases. In the first part of my thesis, I demonstrate the effect of potential FoxO1a-targeting drugs on VSMC behavior both *in vitro* and *in vivo* and reveal the importance of FoxO1a's nuclear localization for its activity.

Expression of FoxO1a in HCASMCs

Previous studies in various cell types reported growth factor-induced phosphorylation of FoxO1a transcription factors via the intracellular phosphatidylinositol 3-kinase (PI3K)/protein kinase B (Akt)-signaling pathway^{166, 167, 238, 239}. Akt-mediated phosphorylation leads to translocation of FoxO1a from the nucleus to the cytoplasm followed by its inactivation. To my

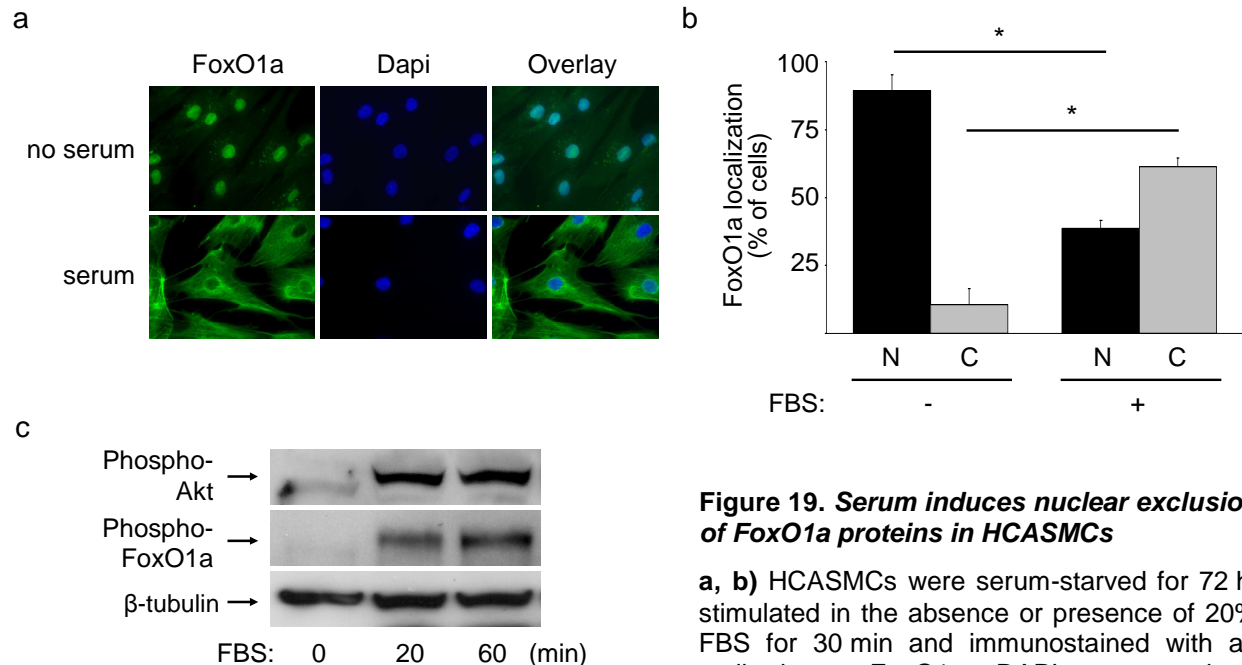


Figure 19. Serum induces nuclear exclusion of FoxO1a proteins in HCASMCs

a, b) HCASMCs were serum-starved for 72 h, stimulated in the absence or presence of 20% FBS for 30 min and immunostained with an antibody to FoxO1a. DAPI was used to visualize nuclear DNA. **a)** Representative

images of FoxO1a's cellular distribution in HCASMCs. Immunofluorescence experiments were carried out at least in triplicate. **b)** Quantification of FoxO1a nuclear-cytoplasmic distribution in HCASMCs treated with or without serum for 30 min. Mean percentage values and standard deviations from > 300 cells out of three independent experiments are shown (* $p < 0.001$ vs respective serum-starved control (t-test)). N, nucleus; C, cytoplasm. **c)** Cell lysates of HCASMCs held quiescent for 72 h in basal medium or exposed to 20% FBS in growth medium for the indicated timeperiods were processed to Western blot analysis for phospho-Akt and phospho-FoxO1a. Detection of β -tubulin served as loading control. The blot shown is representative of three independent experiments.

knowledge, there are no publications demonstrating FoxO1a function in the human vascular system yet, thus, first the cellular distribution of FoxO1a in quiescent and serum-stimulated HCASMCs was determined by immunocytochemistry. FoxO1a localized primarily to the nucleus in the absence of serum (89% nuclear and 11% cytoplasmic), whereas in the presence of FBS the cellular distribution is almost reversed (39% nuclear and 61% cytoplasmic) (Figure 19a, b). These data are consistent to unpublished data from our group concerning FoxO1a localization in mouse VSMCs.

To gain more insight in whether the observed translocation in response to serum stimulation correlates with FoxO1a phosphorylation in a PI3K/Akt-dependent manner, phosphorylation of both Akt and FoxO1a was analyzed in cultured HCASMCs stimulated with 20% FBS. Within 20 min upon serum-stimulation, phosphorylation of Akt and FoxO1a was initiated (Figure 19c). These effects were PI3K dependent because inhibition of PI3K using the pharmacological inhibitors LY294002 or wortmannin blocked FoxO phosphorylation and nuclear export (Sedding *et al.*, unpublished data).

Together my data indicate that FoxO1a's subcellular localization is regulated by post-transcriptional modification (phosphorylation) in HCASMCs.

Psammaplysene A renders FoxO1a nuclear localization in HCASMCs

Recently, Psammaplysene A, a natural product from the marine sponge *Psammaplysilla* sp. was identified in a high-throughput screen to promote retention of FoxO1a in the nucleus of cells with PTEN loss-of-function mutations^{330, 331} (Figure 20). Psammaplysene A was shown to be PI3K/Akt signaling pathway specific in these cells, however, the targets as well as possible cellular impacts of the sponge compound have not been studied yet. Since we previously identified FoxO1a to have a central role in the pathogenesis of neointima formation (Sedding *et al.*, unpublished data), stabilization of this transcription factor may represent a new therapeutic strategy towards the prevention of vasculo-proliferative diseases.

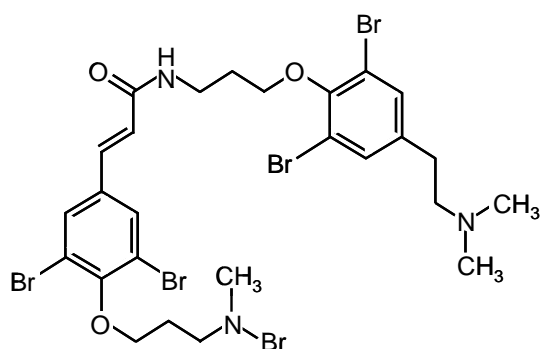


Figure 20. Structure of Psammaplysene A

In order to determine whether Psammaplysene A promotes retention of FoxO1a in the nucleus of growing HCASMCs, cells were serum-starved to allow for adequate silencing and then pre-treated with the Psammaplysene A at the concentrations indicated. Stimulation of the cells was performed with 20% FBS followed by immunostaining and imaging. Despite serum-stimulation, which was previously shown to stimulate FoxO1a translocation to the cytoplasm (Figure 19a, b and Figure 21a, b), endogenous FoxO1a was localized partially to the nucleus of Psammaplysene A-treated HCASMCs (Figure 21a, b). This effect was stronger with increasing Psammaplysene A concentrations (5 μ M and 10 μ M) (Figure 21a, b).

These data indicate that treatment of serum-stimulated HCASMCs with Psammaplysene A results in FoxO1a nuclear sequestration.

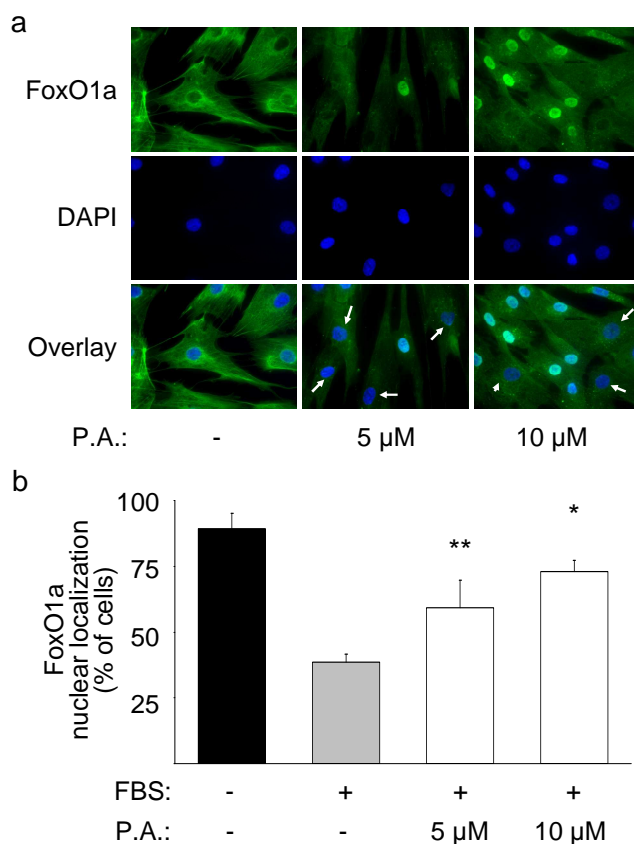


Figure 21. Effect of Psammaplysene A on FoxO1a localization in HCASMCs

HCASMCs were serum-starved for 72 h in basal medium and pre-incubated for 1 h with or without Psammaplysene A (P.A.) at different concentrations (5 μ M, 10 μ M). Subsequently, cells were stimulated with 20% FBS for 30 min and cellular distribution of endogenous FoxO1a was determined by immunostaining with a specific antibody for FoxO1a **(a)**. A co-staining with DAPI was used to visualize nuclei. Pictures were made using a fluorescence microscopy. ICC experiments were carried out at least in triplicate. **b)** Based on FoxO1a immunostaining, quantitative analysis of FoxO1a's nuclear distribution was performed by counting at least > 200 nuclei from two independent preparations. Data represent mean and error bars. Statistical significance was determined by ANOVA (* p < 0.001, ** p < 0.02 vs FBS-stimulated HCASMCs).

Psammaplysene A-treatment inhibits HCASMC proliferation

Since Psammaplysene A-treatment inhibited translocation of FoxO1a from the nucleus to the cytoplasm in FBS-stimulated HCASMCs, the question arose whether Psammaplysene A-mediated FoxO1a retention modulates HCASMC homeostasis. First of all, Psammaplysene A was tested at different concentrations for its ability to influence HCASMC growth. Interestingly, treatment with increasing concentrations of Psammaplysene A resulted in a dose-dependent decrease in cell number (Figure 22a).

Furthermore, different Psammaplysene A concentrations were analyzed for their effect on inhibiting DNA replication of HCASMCs. Figure 22b illustrates results from BrdU incorporation assays. Treatment with 5 μ M Psammaplysene A inhibited DNA synthesis by ~45% as compared to non-treated FBS-stimulated HCASMCs, therefore almost halved the proliferation rate. Treatment with 10 μ M Psammaplysene A completely abolished BrdU incorporation. These data are consistent with studies from Kau *et al.* in cells with PTEN loss-of-function mutations, where

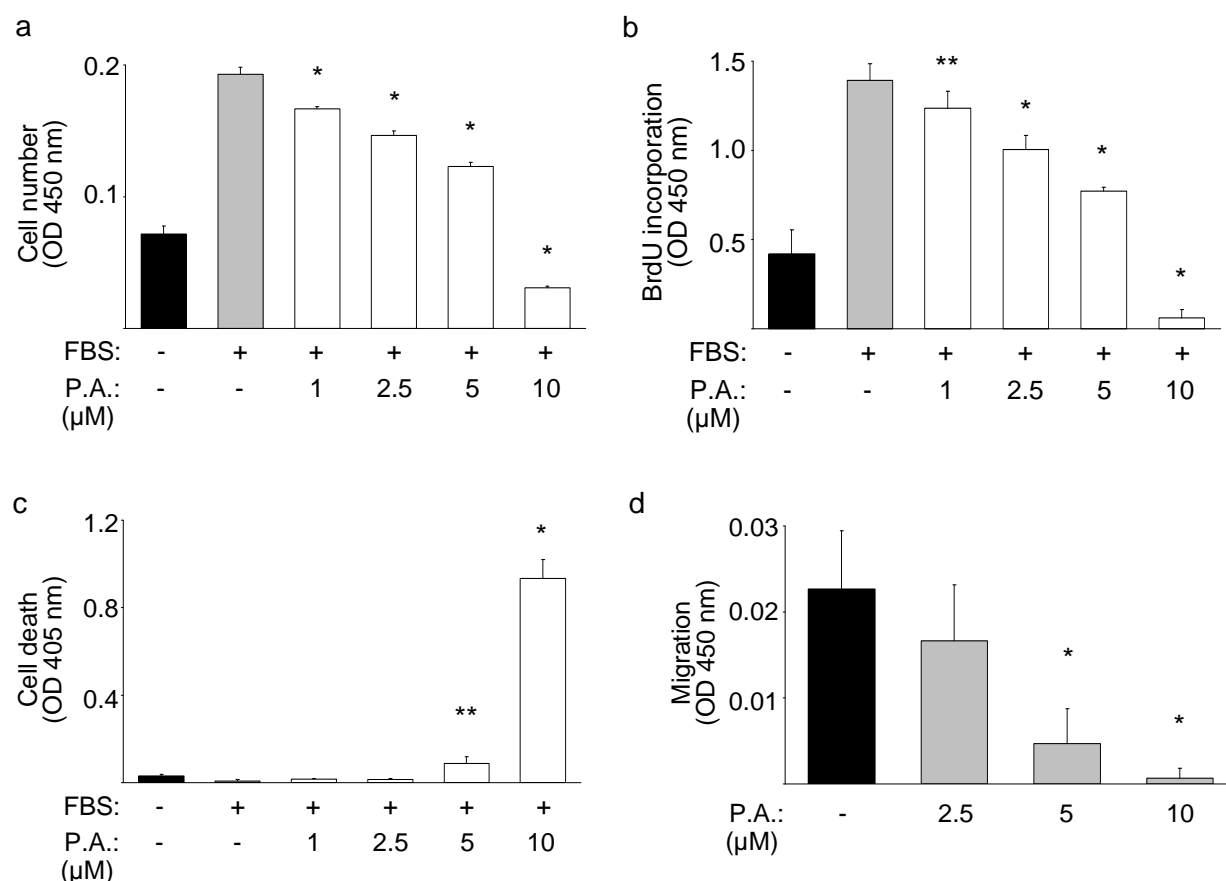


Figure 22. Effect of Psammaplysene A on HCASMC proliferation, migration and apoptosis

a) HCASMCs were plated and grown for 20 h in medium supplemented with 20% FBS plus various concentrations of Psammaplysene A (P.A.). Quiescent cells were used as control. Cell numbers were analyzed by WST-1 assay. Data represent mean OD values of four measurements plus standard deviations. Statistical significance was determined by ANOVA (* p < 0.001 vs FBS). **b)** Cells were treated as in (a) and grown for 14 h in FBS- and Psammaplysene A-containing medium. Afterwards, BrdU was added to the medium of both starved and stimulated cells for 6 h and its incorporation was measured by ELISA. Data of the graph represent mean OD values of BrdU-positive cells. The same experiment was performed at least trice with the same results. The standard error for each value is shown. Statistical significance was determined by ANOVA (* p < 0.001, ** p < 0.01 vs FBS alone; n =4). **c)** HCASMCs were cultured as in a) and cytoplasmic accumulation of mono- and oligonucleosomes was quantified by ELISA. Mean OD values of both untreated serum-starved and FBS-stimulated HCASMCs were designated as controls (* p < 0.001, ** p < 0.02 vs FBS; n =3). The experiment was repeated trice with the same results. **d)** HCASMCs were silenced for 60 h and pre-incubated with or without the indicated concentrations of Psammaplysene A for additional 12 h. The cells were allowed to migrate along a 20% FBS-gradient for 6 h in a modified Boyden-chamber model. The amount of migrated cells was evaluated by WST-1 assay. Data shown are representatives of three independent experiments with similar results and represent mean OD values and standard deviations. Statistical significance was determined by ANOVA (* p < 0.01 vs FBS; n =3).

Psammaplysene A was able to inhibit cell proliferation with an IC_{50} of 5-10 μM ³³⁰.

Taken together, I consider that the observed decrease in HCASMC growth released by increasing Psammaplysene A concentrations is, at least partially, due to a Psammaplysene A-dependent inhibition of DNA replication.

Moreover, cell death detection ELISAs revealed that the observed reduction in HCASMC cell number in response to a 5 μM Psammaplysene A-treatment was not due to an strong increase in apoptotic cell death (Figure 22c), suggesting that at this concentration Psammaplysene A is mainly responsible for inhibiting cell proliferation (Figure 22b), but not for inducing apoptosis. At 10 μM , the situation changed and lack of HCASMC growth (Figure 22a) was due to both a strong inhibition of cell cycle progression (Figure 22b) and a significant increase in apoptotic cell death (Figure 22c). Complementing the assay's results, HCASMCs treated with 10 μM Psammaplysene A revealed the presence of intracellular blebbing, cell shrinkage and detachment (data not shown).

The significant increase in apoptotic cell fragmentation in response to 10 μM Psammaplysene A-treatment was also documented by FACS analysis as shown in Figure 23e: The amount of small DNA fragments was visibly increased after treatment with 10 μM Psammaplysene A as compared to treatment with 5 μM Psammaplysene A.

In order to investigate whether Psammaplysene A inhibits chemotactic cell migration, migration assays were performed with HCASMCs incubated in the presence or absence of Psammaplysene A. FBS was used for stimulating directed cell migration. The marine sponge extract significantly attenuated FBS-induced HCASMC migration along the chemotactic gradient in a dose-dependent manner, with Psammaplysene A at 10 μM almost completely inhibiting chemotaxis (Figure 22d).

Altogether, these results demonstrate Psammaplysene A to have a regulatory function on HCASMC behavior, simultaneously modulating proliferation, migration and apoptosis. Whether FoxO1a's nuclear retention plays a role in this observation will be explored in the later parts of the thesis.

Psammaplysene A blocks cell cycle entry of HCASMCs in G0/G1-phase

To further examine the role of Psammaplysene A on cell cycle progression, serum-stimulated HCASMCs were exposed to different concentrations of Psammaplysene A for 24 h. Serum-starvation was used to arrest cell cycle. Fluorescence-activated cell sorting (FACS) analyses of quiescent HCASMCs revealed a block in G0/G1-phase (Figure 23a). FBS-stimulation did not affect progression of HCASMCs through G1/S, therefore the cells subsequently enter the G2/M-phase of the cell cycle (Figure 23b). Importantly, FACS analyses of HCASMCs incubated with

increasing concentrations of Psammaplysene A showed that treatment of the cells with the marine sponge compound led to the accumulation of cells in G1 dose-dependently, even if the cells were stimulated by serum to enter the cell cycle (Figure 23c-e). Thus, these cells failed to progress through the G1/S transition as growth factor stimulated cells usually do. Psammaplysene A at a concentration of 10 μ M showed the strongest effect.

With this experiment, earlier results determined by BrdU incorporation were confirmed and altogether, the results suggest that Psammaplysene A inhibits HCASMC proliferation primarily by inhibiting S-phase entry.

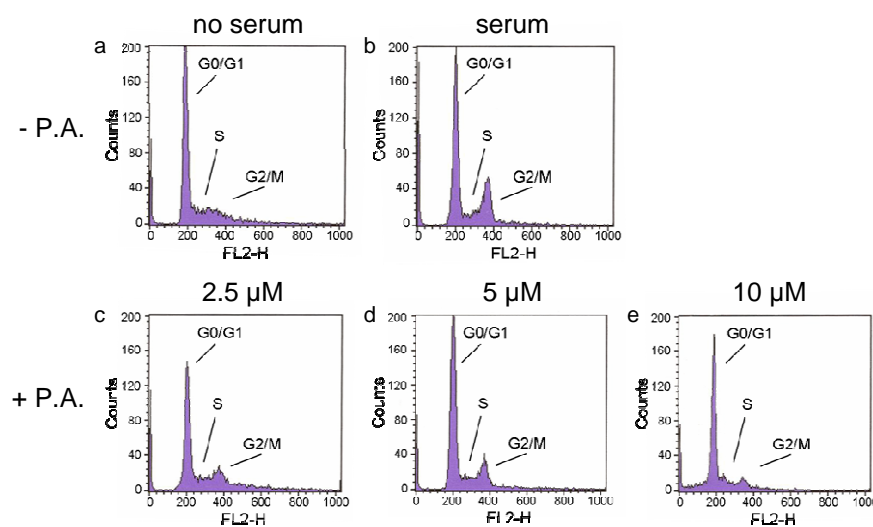


Figure 23. Psammaplysene A blocks HCASMC cycle progression in G0/G1-phase

HCASMCs were cultured as indicated below and subsequently fixed with methanol. Quiescent cells were used as controls. Fixed cells were stained with propidium iodide, and cell cycle progression was analyzed by fluorescence-activated cell sorting (FACS) as described in “Materials and Methods”. Typical cell cycle histograms are recorded. (a) Silenced HCASMCs. Different cells were released from G0/G1-phase block by culturing for 24 h in the absence (b) or presence (c-e) of Psammaplysene A (P.A.; 2.5 μ M, 5 μ M and 10 μ M) in 20% FBS-supplemented growth medium.

Psammaplysene A does not affect FoxO1a binding to specific promoter regions

In order to gain deeper insight into the mechanism by which Psammaplysene A affects FoxO1a function, endogenous FoxO1a activity was determined using a commercially available FoxO1a activity assay for measuring the binding capacity of FoxO1a to its specific promoter sequences. Quiescent HCASMCs revealed strong FoxO1a binding activity as shown in Figure 24a and b. Stimulation of HCASMCs with FBS resulted in a decline of FoxO1a activity as compared to silenced ones (Figure 24a, b). Since Psammaplysene A was able to both retain FoxO1a in the nucleus of serum-stimulated HCASMCs and mimicking a silenced cell state, I expected FoxO1a, at least partially, maintained bound to its specific promoters regions under Psammaplysene A-treatment. Thus, genes such as p27^{KIP1} should be transcribed despite serum stimulation, and its product should contribute to cell cycle arrest in G0/G1 as observed by FACS

(Figure 23). Surprisingly, Psammaplysene A did not increase FoxO1a activity in Psammaplysene A-treated HCASMCs as compared to untreated stimulated ones - neither at a concentration of 5 μ M (Figure 24a) nor at 10 μ M (Figure 24b).

These data indicate that Psammaplysene A-mediated nuclear localization of FoxO1a is not sufficient to re-establish direct binding of FoxO1a to promoter regions of known target genes.

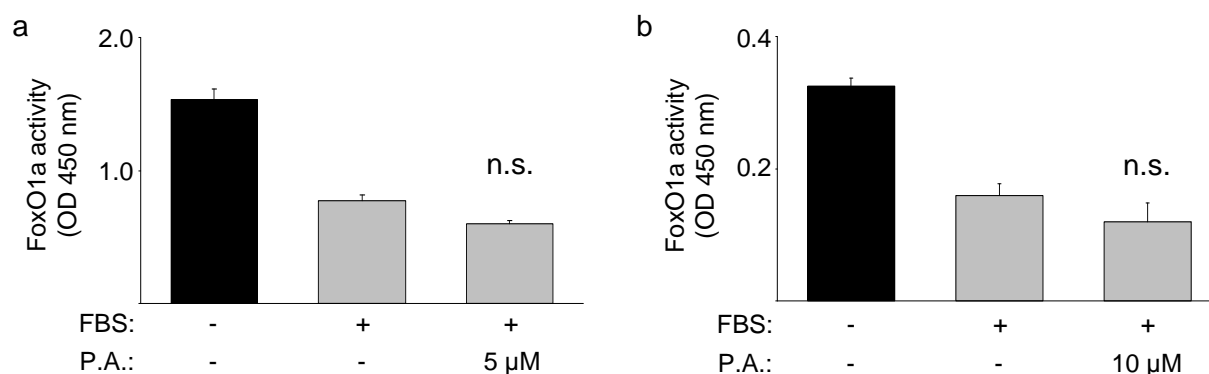


Figure 24. Effect of Psammaplysene A on FoxO1a activity

Endogenous FoxO1a activity was measured with a commercially available *in vitro* assay using nuclear HCASMC lysates. Briefly, HCASMCs were serum-starved for 60 h, pre-treated with or without Psammaplysene A (P.A.; 5 μ M, 10 μ M) for 16 h, and subsequently stimulated with 20% FBS for 30 min. Nuclear extracts were prepared as described elsewhere and 15 μ g per condition was used to analyze FoxO1a activity. Results are means and standard deviations from duplicate measurements, and representative of at least two independent experiments. Data were analyzed by ANOVA (non-significant (n.s.) > 0.08 vs FBS alone). **a)** HCASMCs were treated with Psammaplysene A at 5 μ M. **b)** HCASMCs were treated with Psammaplysene A at 10 μ M.

Psammaplysene A blocks growth factor-induced cyclin D1 expression

Earlier experiments demonstrated the marine sponge compound Psammaplysene A to undoubtedly affect HCASMC cell cycle progression. In order to understand how Psammaplysene A inhibits G1/S-phase transition without affecting FoxO1a promoter binding, expression levels of numerous cell cycle regulators were analyzed. Total cellular proteins were prepared and subjected to immunoblotting assays for p27^{KIP1}, cyclin D1, CDK4, cyclin A and B, phospho-retinoblastoma protein (phospho-pRb) and proliferating cell nuclear antigen (PCNA). p27^{KIP1} as a direct FoxO1a target gene was efficiently downregulated as FBS-stimulated cells progressed through G1-phase (Figure 25a). Likewise, Psammaplysene A-treated cells showed significant downregulation of p27^{KIP1} (Figure 25a), which was not surprisingly, since the compound was demonstrated not to increase binding of FoxO1a to its specific promoter sequences despite serum stimulation (Figure 24). CDK4 levels remained unchanged under all tested conditions (Figure 25a). Cyclin D1 was strongly expressed in FBS-stimulated HCASMCs, as well as in growing HCASMCs treated with 2.5 μ M and 5 μ M Psammaplysene A, respectively (Figure 25a). In sharp contrast, cyclin D1 was almost undetectable in cells treated with 10 μ M of

the marine sponge compound (Figure 25a). Since the phosphorylation of pRb is initiated by cyclin D1-CDK4 complexes, decreases in cyclin D1-CDK4 levels due to low cyclin D1 levels in 10 μ M Psammaplysene A-treated cells resulted in hypo-phosphorylated pRb levels (Figure 25a). However, even in HCASMCs treated with 2.5 μ M or 5 μ M Psammaplysene A, a slight decrease in phospho-pRb levels as compared to FBS alone was observed. Hypo-phosphorylated pRb binds and inhibits E2F transcription factors. Consequently, expression of the E2F-dependent target cyclin A was inhibited too (Figure 25a). Cyclin B, a critical regulator of the G2/M transition was also undetectable in cells incubated with 10 μ M Psammaplysene A (Figure 25a). The expression of PCNA as a DNA synthesis marker was also analyzed in HCASMCs to demonstrate proliferation (Figure 25a).

To determine whether Psammaplysene A was likely to act upstream of FoxO1a in the PI3K/Akt/FoxO1a signaling pathway, cell extracts were analyzed by immunoblotting for phospho-Akt (Figure 25b). None of the compounds concentrations inhibited FBS-induced Akt phosphorylation, suggesting that Psammaplysene A does not affect the pathway upstream of FoxO1a. Likewise, changes in the expression level of phospho-FoxO1a were not observed after Psammaplysene A-treatment (Figure 25b).

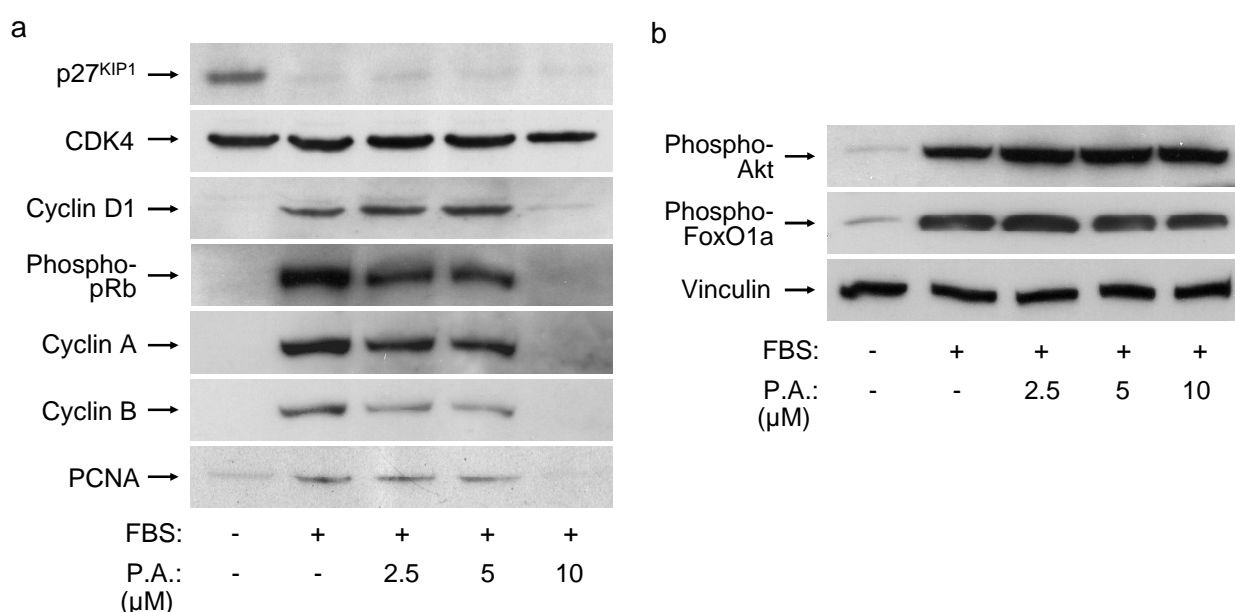


Figure 25. Effect of Psammaplysene A on different cell cycle regulators

a) HCASMCs were subjected to serum starvation for 60 h, pre-treated with or without Psammaplysene A (P.A.; 2.5 μ M, 5 μ M or 10 μ M) for 12 h, and subsequently exposed to medium containing 20% FBS and/or Psammaplysene A at the indicated concentrations for 24 h. Total cellular protein extracts were prepared and subjected to immunoblot assay. Protein expression associated with cell cycle progression was studied by using specific antibodies for p27^{KIP1}, CDK4, cyclin D1, cyclin A and B, phospho-Rb, and PCNA. **b)** HCASMCs were cultured as in (a), however, cells were lysed already after 20 min of stimulation with FBS +/- Psammaplysene A. Phospho-Akt and phospho-FoxO1a expression levels were analyzed by Western blot with specific antibodies. Vinculin was used as loading control.

Taken together, the Western blot results are consistent with data revealing Psammaplysene A to downregulate HCASMC growth by attenuating cell cycle progression. Treatment with Psammaplysene A at 10 μ M negatively regulates expression of cyclin D1, thus, Psammaplysene A-induced decreases in cyclin D1 levels consequently inhibit G₁ cell cycle progression and therefore also affect protein expression of other downstream cell cycle regulators. Since FoxO1a is known to be involved in regulating cyclin D1 expression indirectly^{168, 215, 332}, an effect of Psammaplysene A on FoxO1a activity with regard to cyclin D1 regulation seems to be possible, even this Psammaplysene A-mediated modification does not affect direct target gene expression.

Psammaplysene A inhibits neointima formation in wire-injured mouse femoral arteries

Psammaplysene A was recently shown to inhibit VSMC proliferation *in vitro* by decreasing cyclin D1 protein levels. Next, the marine sponge extract was analyzed for influencing neointimal hyperplasia in an *in vivo* mouse femoral artery model. Psammaplysene A was directly delivered to the wire-denudated mouse femoral artery. Representative photomicrographs of hematoxylin/eosin-stained femoral artery cross-sections 21 days following injury are shown in Figure 26. A significant concentric neointima was evident in non-treated arteries, clearly defined by the internal and external elastic laminae. Psammaplysene A-treatment at a concentration of 10 μ M significantly attenuated neointima formation in this *in vivo* model. Histomorphological analysis of neointima/media (I/M) ratios of six independent experiments was performed (data not shown), however, since out of six animals two comprised thrombotic clots within their denudated vessels – which makes an exact analysis impossible – a significant result could not be made. Nevertheless, preliminary data out of 4 animals revealed that the I/M ratio of Psammaplysene A-treated arteries was apparently reduced as compared to control vessels, possibly due to diminished VSMC proliferation upon Psammaplysene A-treatment.

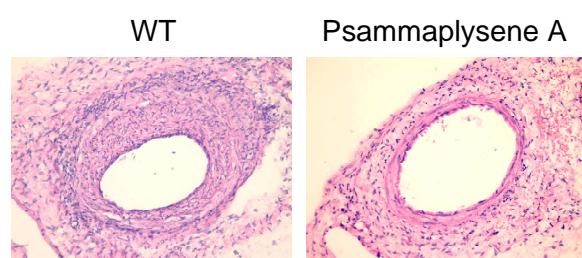


Figure 26. Psammaplysene A prevents neointima formation *in vivo*

a) Representative cross sections of mouse femoral arteries of both control-mice and Psammaplysene A-treated mice 21 days after dilatation are shown. The sections were stained with hematoxylin and eosin, and examined by light microscopy.

As suggested by the *in vitro* data, Psammaplysene A's potency to prevent neointima formation seemed to result from an anti-proliferative effect as determined by qualitative PCNA-staining of Psammaplysene A-treated arteries 21 days following injury (Figure 27). In comparison

to control arteries, the number of PCNA-positive VSMCs in Psammaplysene A arteries was significantly decreased.

Taken together, these data suggest that attenuation of neointimal hyperplasia by treatment with Psammaplysene A is mediated, at least partially, through inhibition of VSMC proliferation.

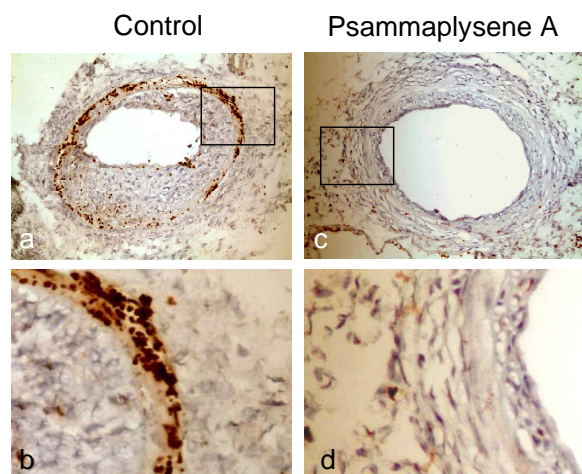
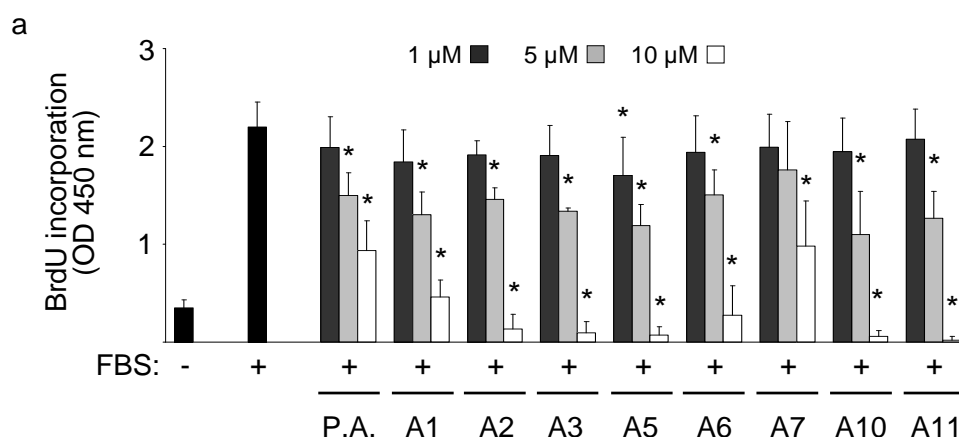


Figure 27. Psammaplysene A modulates cellular proliferation in vivo

In vivo cell proliferation was detected by using Zymed's PCNA staining kit in femoral artery sections of non-treated (a and b) and Psammaplysene A-treated (10 μ M) vessels (c and d) at day 21 after wire-injury. c and d are high-magnification images of the boxed regions shown on low magnification images of the complete vessel (a and c).

Psammaplysene A-analogues modulate HCASMC proliferation

Psammaplysene A was shown in the above experiments to modulate the PI3K/Akt/FoxO1a pathway and therefore treatment with this compound may represent a new therapeutic strategy towards the prevention of vasculo-proliferative diseases. Unfortunately, there is only limited supply of this marine sponge extract. To overcome this problem Georgiades *et al.* developed a method to efficiently synthesize this compound³³³. With the development of this strategy, it was also possible to synthesize different Psammaplysene A-analogues³³⁴. In cooperation with our lab, a focused library of 28 Psammaplysene-like molecules was screened in diverse biological assays. First of all, the 28 compounds were analyzed for modulating BrdU incorporation into the DNA of serum-stimulated HCASMCs. Since the aim of this experiment was to identify molecules



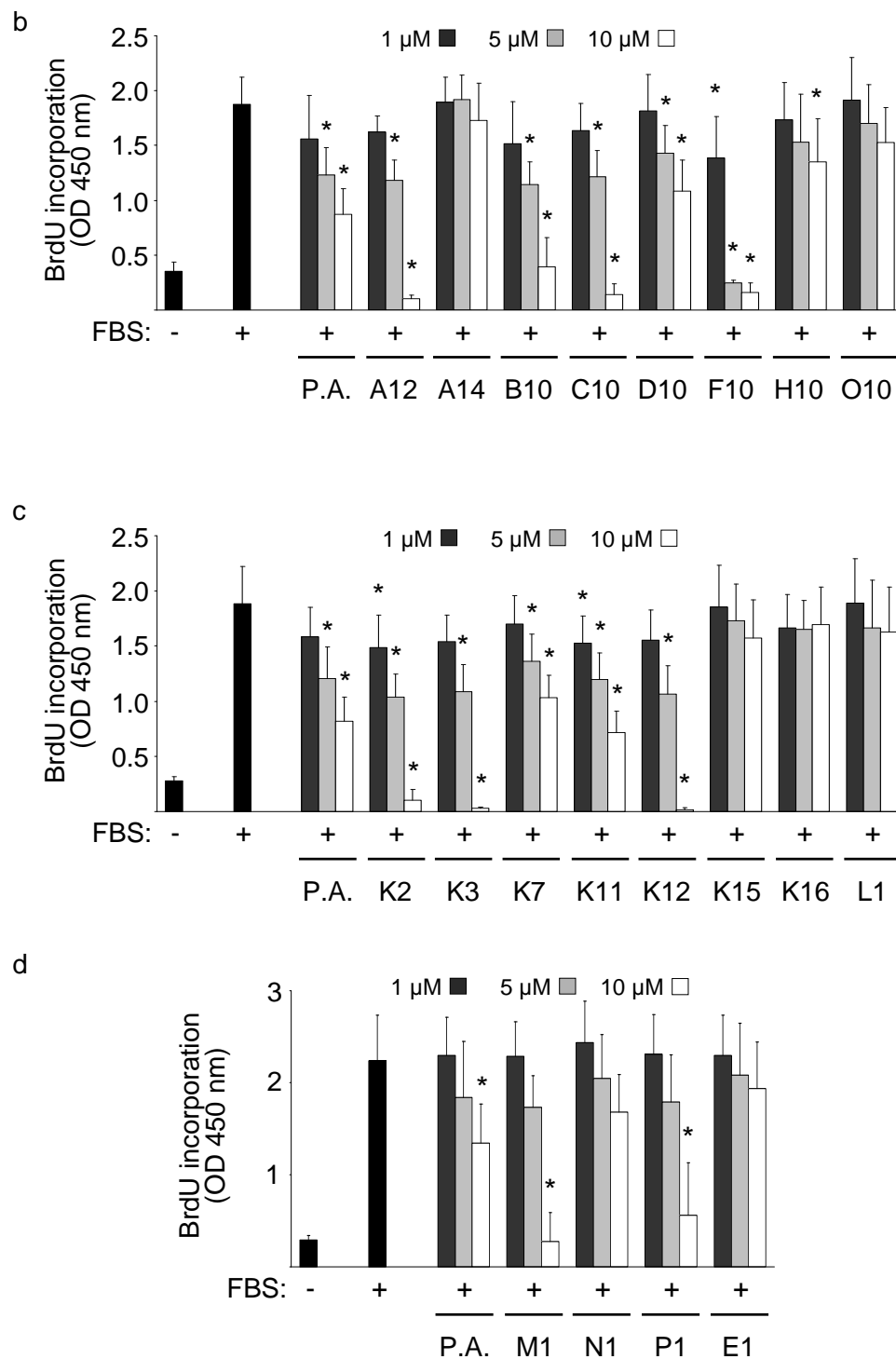


Figure 28. Psammaplysene A-analogues modulate HCASMC proliferation

HCASMCs were cultured in serum-containing medium for 20 h with or without the different Psammaplysene A-like molecules or Psammaplysene A (P.A.) at the indicated concentrations. Quiescent cells were used as control. BrdU incorporation was determined by ELISA. Mean absorbance values plus standard deviation of three independent experiments are presented in the graphs. Statistical significance was determined by ANOVA (* $p < 0.001$ vs FBS alone; $n=12$).

that are more potent than Psammaplysene A, each compound was tested at the concentrations which were earlier shown for Psammaplysene A to affect DNA synthesis: 1 μ M, 5 μ M and 10 μ M. Some of the Psammaplysene A-analogues showed almost no effect on inhibiting cell cycle progression at the tested concentrations, such as A14, K15, K16 and L1. Most of the compounds inhibited BrdU incorporation comparable to Psammaplysene A. Only a compound named F10 was able to decrease HCASMC proliferation significantly at a concentration of 1 μ M and more importantly, completely inhibited proliferation already at a concentration of 5 μ M. Thus, this compound was the only one out of the 28 tested which was able to inhibit HCASMC proliferation more potently than Psammaplysene A does.

Therefore, my further studies concentrated on examining the effect of F10 on modulating HCASMCs behavior in more detail.

FoxO1a localizes to the nucleus of serum-stimulated HCASMCs upon F10-treatment

In order to determine whether F10, similar to Psammaplysene A, promotes retention of FoxO1a to the nuclei of growing HCASMCs, silenced HCASMCs were treated with either 2.5 μ M F10 or 5 μ M F10 and stimulated with 20% FBS before immunostaining and imaging. As it was previously shown for Psammaplysene A, F10 inhibited FBS-mediated FoxO1a translocation to the cytoplasm, at least partially, at a concentration of 2.5 μ M (Figure 29a). The effect of 5 μ M F10 in retaining FoxO1a's nuclear localization was significantly higher to that of the lower

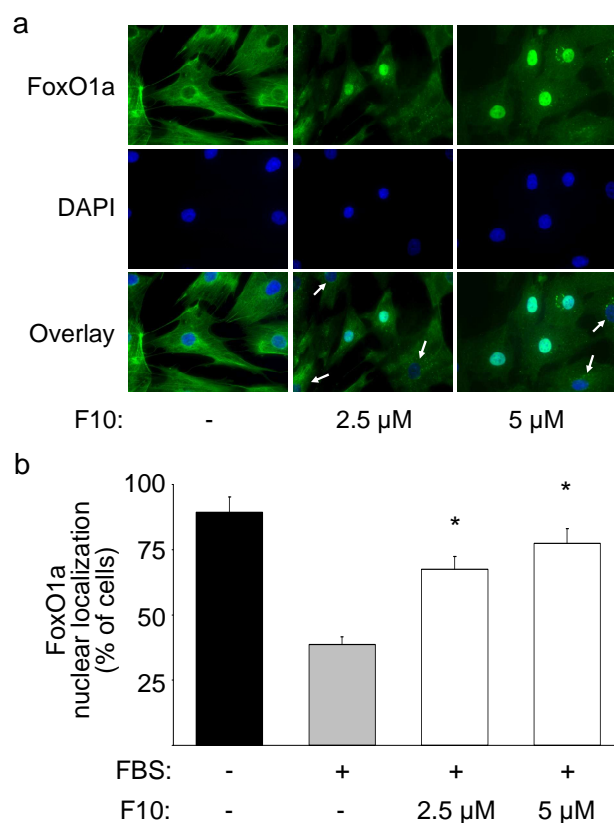


Figure 29. Effect of F10 on FoxO1a localization in HCASMCs

HCASMCs were silenced for 72 h in basal medium, treated for 1 h with or without 2.5 μ M and 5 μ M F10, respectively, and then stimulated for 30 min with 20% FBS. Each ICC experiment was repeated trice **a**) Cellular distribution of endogenous FoxO1a was determined by immunostaining with a specific antibody for FoxO1a and co-staining with DAPI was used to visualize nuclei. Images were made by using a fluorescence microscopy. **b**) Quantitative analysis of FoxO1a's nuclear distribution was performed by counting at least 200 nuclei from two independent preparations. Data represent mean and error bars. Statistical significance was determined by ANOVA (* p <0.001 vs FBS-stimulated HCASMCs).

concentration (Figure 29b): Approximately 77% of the cells treated with 5 μ M F10 express FoxO1a within their nuclei despite the presence of serum in the medium.

These data reveal that besides Psammaplysene A, the Psammaplysene A-analogue F10 is also able to inhibit FoxO1a translocation in serum-stimulated HCASMCs.

F10-treatment inhibits HCASMC proliferation but does not induce apoptosis

Since F10-treatment was already shown in the Psammaplysene A-analogues-screening to inhibit BrdU-incorporation into the DNA of HCASMCs, I next analyzed its attenuating effect on HCASMC proliferation in more detail. F10 at the indicated concentration was applied to HCASMCs and cell numbers were examined 24 h post-treatment using WST-1 assays (Figure 30a). Treatment with the Psammaplysene A-analogue attenuated HCASMC growth dose-dependently, with concentrations > 5 μ M revealing cell numbers comparable to silenced cells.

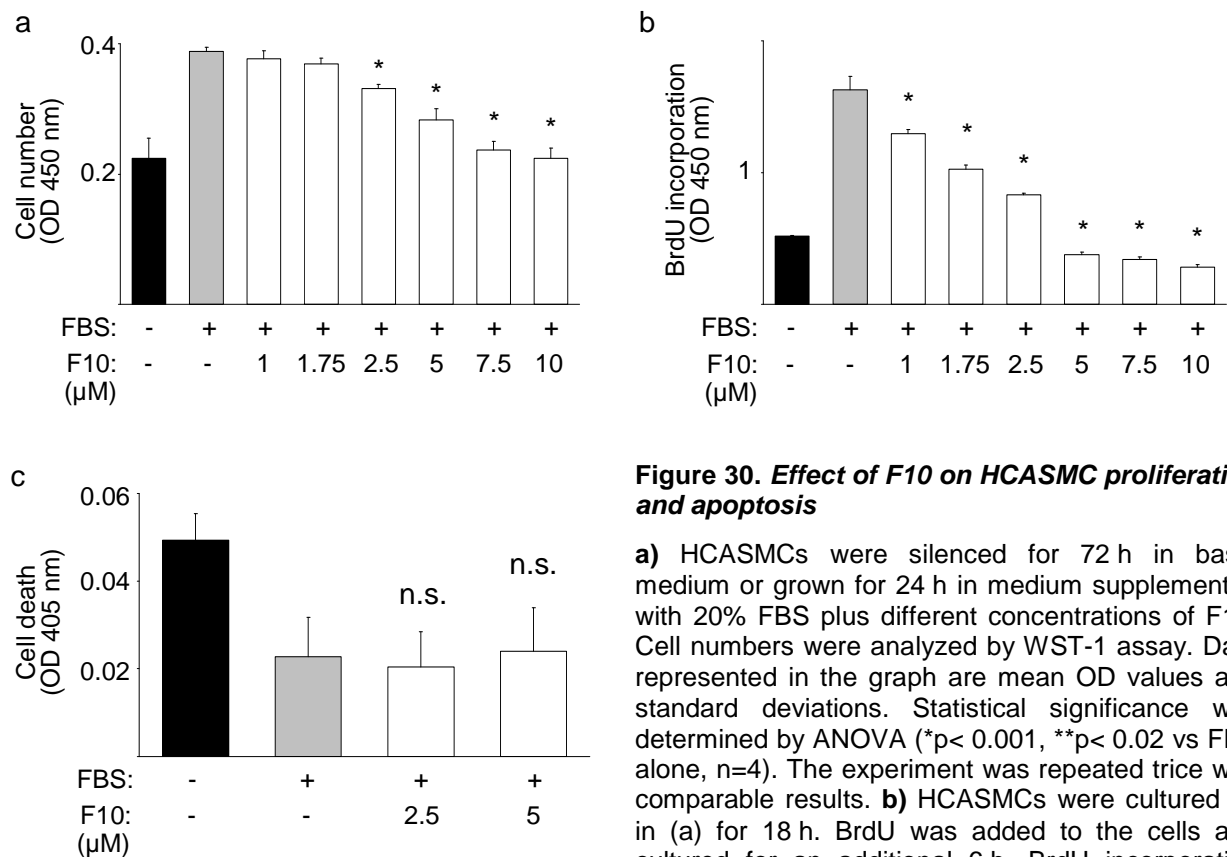


Figure 30. Effect of F10 on HCASMC proliferation and apoptosis

a) HCASMCs were silenced for 72 h in basal medium or grown for 24 h in medium supplemented with 20% FBS plus different concentrations of F10. Cell numbers were analyzed by WST-1 assay. Data represented in the graph are mean OD values and standard deviations. Statistical significance was determined by ANOVA (* p < 0.001, ** p < 0.02 vs FBS alone, n =4). The experiment was repeated trice with comparable results. **b)** HCASMCs were cultured as in (a) for 18 h. BrdU was added to the cells and cultured for an additional 6 h. BrdU incorporation was measured by ELISA. Data represent mean

OD values and standard errors of BrdU-positive cells of one representative experiment, which was repeated three times with the same results. Statistical significance was determined by ANOVA. (* p < 0.001, ** p < 0.02 vs FBS alone; n =3). **c)** HCASMCs were cultured as in a) and cytoplasmic accumulation of mononucleosomes and oligonucleosomes was quantified by Cell Death Detection ELISA. Mean OD values of both untreated serum-starved and FBS-stimulated HCASMCs were designated as controls. Statistical significance was determined by ANOVA (non-significant (n.s.) > 0.5 vs FBS-control; n =3).

To investigate whether reduction in cell numbers upon F10-treatment was due to a decrease in cell proliferation, BrdU incorporation was examined after application of F10. As previously shown, already at low concentrations F10 significantly attenuated DNA synthesis of FBS-stimulated HCASMCs. 2.5 μ M F10 decreased FBS-induced proliferation by ~ 50% (Figure 30b) whereas concentrations above 5 μ M inhibited BrdU incorporation completely (Figure 30b).

To exclude F10 of inducing apoptotic cell death at the concentrations previously tested on manipulating HCASMC proliferation and cell number, the compound was applied to HCASMCs and amounts of mono- and oligonucleosomes within the cells cytoplasm were measured using commercially available cell death detection ELISAs (Figure 30c). Interestingly, F10 neither at 2.5 μ M nor at 5 μ M significantly induced apoptosis in HCASMCs.

Thus, in contrast to what was shown for Psammaplysene A, a decrease in HCASMC cell numbers upon F10-treatment is only due to reduced DNA synthesis rates but not to apoptotic cell death.

Combined treatment with Psammaplysene A and F10 inhibits HCASMC proliferation at low concentrations

Both Psammaplysene A and the Psammaplysene A-like compound F10 were shown to inhibit HCASMC proliferation. Next, I was interested in the combinative effect of both agents on modulating HCASMC proliferation. Therefore, HCASMCs were treated with different compositions of the two compounds and DNA replication was measured by BrdU incorporation ELISA. As it was illustrated in Figure 31, HCASMCs treated with a combination of 2.5 μ M Psammaplysene A and 2.5 μ M F10 revealed BrdU incorporation rates similar to that of quiescent cells. It is noteworthy to mention that neither 2.5 μ M Psammaplysene A alone nor 2.5 μ M F10 alone completely inhibited cell proliferation. However, a combinative treatment with both agents was able to prevent HCASMC proliferation to almost 100%.

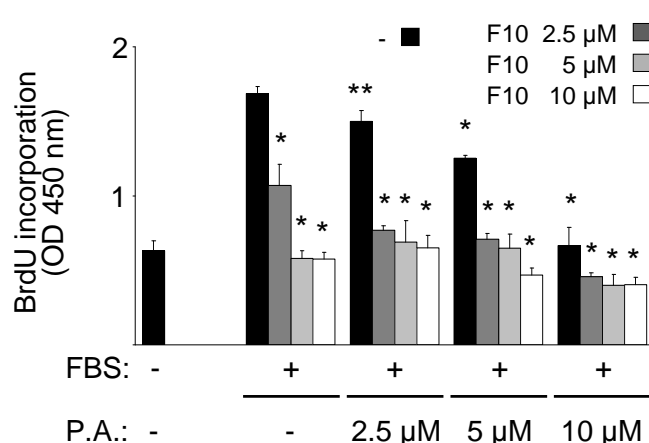


Figure 31. Effect of a Psammaplysene A /F10 combination on HCASMC proliferation

HCASMCs were treated with or without different combinations of Psammaplysene A (P.A.) and F10 in 20% FBS-containing medium for 16 h, before BrdU was added for additional 6 h. BrdU incorporation was measured by ELISA. Silenced cells were used as controls. Data in the graph represent the mean OD values and error bars. Statistical significance was determined by ANOVA (* $p < 0.001$, ** $p < 0.01$ vs FBS-stimulated HCASMCs; $n=4$).

Thus, single doses of each compound can be reduced by applying Psammaplysene A and F10 simultaneously.

With this part of my thesis I was able to show recent discoveries concerning the inhibition of VSMC proliferation *in vitro* and *in vivo* by the natural product Psammaplysene A from the marine sponge *Psammaplysilla* sp.. The Psammaplysene A-analogue F10 similarly affects VSMC behavior and importantly, both compounds are specific to the PI3K/Akt/FoxO1a signaling pathway and regulate FoxO1a's nucleocytoplasmic localization. It seems that both molecules somehow influence FoxO1a function since cyclin D1 is downregulated in serum-stimulated cells upon Psammaplysene A-treatment. Nevertheless, the direct target of Psammaplysene A and F10 is still unknown, and further studies need to explore their detailed molecular mode of action.

FoxO1a regulates PASMC proliferation, migration and apoptosis

Besides atherosclerosis and restenosis, pulmonary hypertension (PHT) is another progressive, proliferative vascular disorder resulting from continuous vasoconstriction and structural remodeling of artery vessels (see Introduction)⁷⁵. The structural changes occurring in the vessel include, among other things, VSMC migration and proliferation. The major signaling pathway being responsible for initiating pathological changes in VSMC behavior was recently shown to be PI3K/Akt-dependent^{73, 335}. Since our group previously demonstrated FoxO1a's regulatory function on HCASMCs (Sedding *et al.*, unpublished data), its effect on pulmonary artery smooth muscle cells (PASMCs) was investigated in close collaboration with Dr. Soni Pullamsetti from the University of Giessen Lung Center (UGLC). Our latest results are comprised in the next part of this thesis.

FoxO1a translocates from the nucleus to the cytoplasm in response to serum stimulation

The expression level of endogenous FoxO1a in rat PASMCs was analyzed by immunocytochemistry and, as it was previously shown for VSMCs from coronary arteries (Figure 19), FoxO1a is expressed in the nucleus of silenced PASMCs and translocates to the cytoplasm in response to serum stimulation (Figure 32). *In vivo* expression of FoxO1a in nuclei of VSMCs of native pulmonary vessels was also immunohistochemically identified (Dr. Pullamsetti, personal communication).

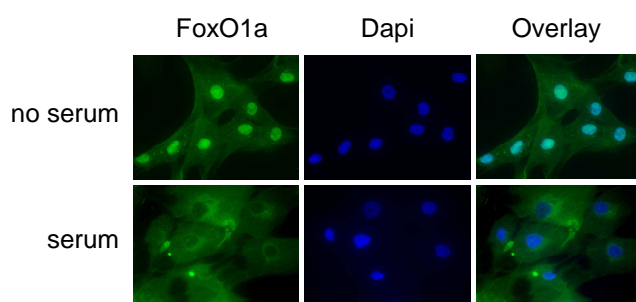


Figure 32. Intracellular expression of FoxO1a in PASMCs

Rat PASMCs were serum-starved (24 h) or cultured in serum containing medium. Immunostaining with a specific antibody for FoxO1a revealed FoxO1a distribution within the cells. Nuclear DNA was stained with DAPI. The pictures shown are representative photographs

FoxO1a regulates PASMC proliferation, apoptosis and migration

To study the function of FoxO1a in PASMCs, the cells were transduced with recombinant adenoviruses encoding a non-phosphorylatable, constitutively active mutant of FoxO1a (Ad-FoxO1a;AAA). The inactive FoxO1a mutant was created by alanine substitution of the three Akt phosphorylation sites (T24A, S256A, S319A = FoxO1a;AAA) as previously described¹⁶⁸ (Figure 33). The amount of replication defective adenoviral vector necessary for efficient transient expression of FoxO1a;AAA was carefully evaluated previously by our group (Sedding *et al.*,

unpublished data). Additionally, Sedding *et al.* provided evidence that expression of the adenoviral construct was detectable in VSMCs at least 72 h post-transduction.

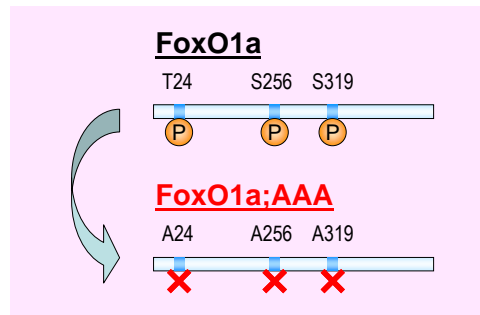


Figure 33. Cloning and mutagenesis of the constitutively active FoxO1a

A non-phosphorylatable, constitutively active mutant of FoxO1a was created by alanine substitution of the three Akt phosphorylation sites (T24A, S256A, S319A = FoxO1a;AAA). Subsequently, recombinant Ad-FoxO1a;AAA adenovirus was generated.

PASMC cultures were transduced either with Ad-FoxO1a;AAA or a GFP-encoding control adenovirus (Ad-GFP). Non-transduced PASMCs, either serum-starved or cultured in FBS-containing medium, were used as controls. The effect of Ad-GFP- and Ad-FoxO1a;AAA-transduction on PASMC number was investigated by using WST-1 assay. Results are shown in Figure 34a. While upon serum stimulation cell numbers significantly increased in both control cells and cells expressing GFP, PASMCs transduced with Ad-FoxO1a;AAA failed to grow. Furthermore, serum-starved PASMCs revealed only a marginally fewer amount of viable cells than Ad-FoxO1a;AAA-transduced cells do in response to FBS stimulation (Figure 34a).

The observed reduction in cell number of PASMCs forced to express FoxO1a;AAA as compared to Ad-GFP-transduced cells was, at least partially, due to a FoxO1a;AAA-dependent inhibition of cell proliferation as it was measured by BrdU incorporation assays. 48 h post-transduction, FoxO1a;AAA-expressing PASMCs showed a decline in DNA replication by 71% as compared to Ad-GFP-transduced cells (Figure 34b). Since the measured BrdU incorporation rate of Ad-GFP-transduced PASMCs is comparable to growing control PASMCs, it was provided evidence that the transduction-process itself had no impact on the cells ability to replicate DNA (Figure 34b).

Furthermore, migration along a chemotactic PDGF-BB-gradient was examined by using a modified Boyden chamber model. PDGF-BB induced chemotaxis of non-transduced PASMCs, whereas absence of the chemoattractant resulted in an almost complete loss of PASMC migration (Figure 34c). Ad-FoxO1a;AAA but not Ad-GFP significantly inhibited PDGF-BB-induced PASMC chemotaxis; the migration rate of PASMCs overexpressing the constitutive active FoxO1a was comparable to that of non-migrating cells (no chemoattractive stimuli) (Figure 34c).

In order to ask whether, in addition to suppressing proliferation, FoxO1a affects apoptotic cell functions too, cytoplasmic accumulation of mono- and oligonucleosomes in both transduced and non-transduced PSMCs was measured using Cell Death Detection ELISAs. Cells expressing FoxO1a;AAA revealed significant high numbers of cleaved DNA particles as compared to Ad-GFP- and non-transduced controls (224% increase compared to Ad-GFP) (Figure 34d). As it will be shown for HCASMCs later (Figure 56), stressing PSMCs by serum-deprivation enhanced apoptotic cell death rates (Figure 34d). Completing these results, PSMCs expressing FoxO1a;AAA consistently indicated the presence of intracellular cytoplasmic blebbing, cell shrinkage, nuclear condensation and membrane detachment from the surrounding cells as determined by morphology (data not shown).

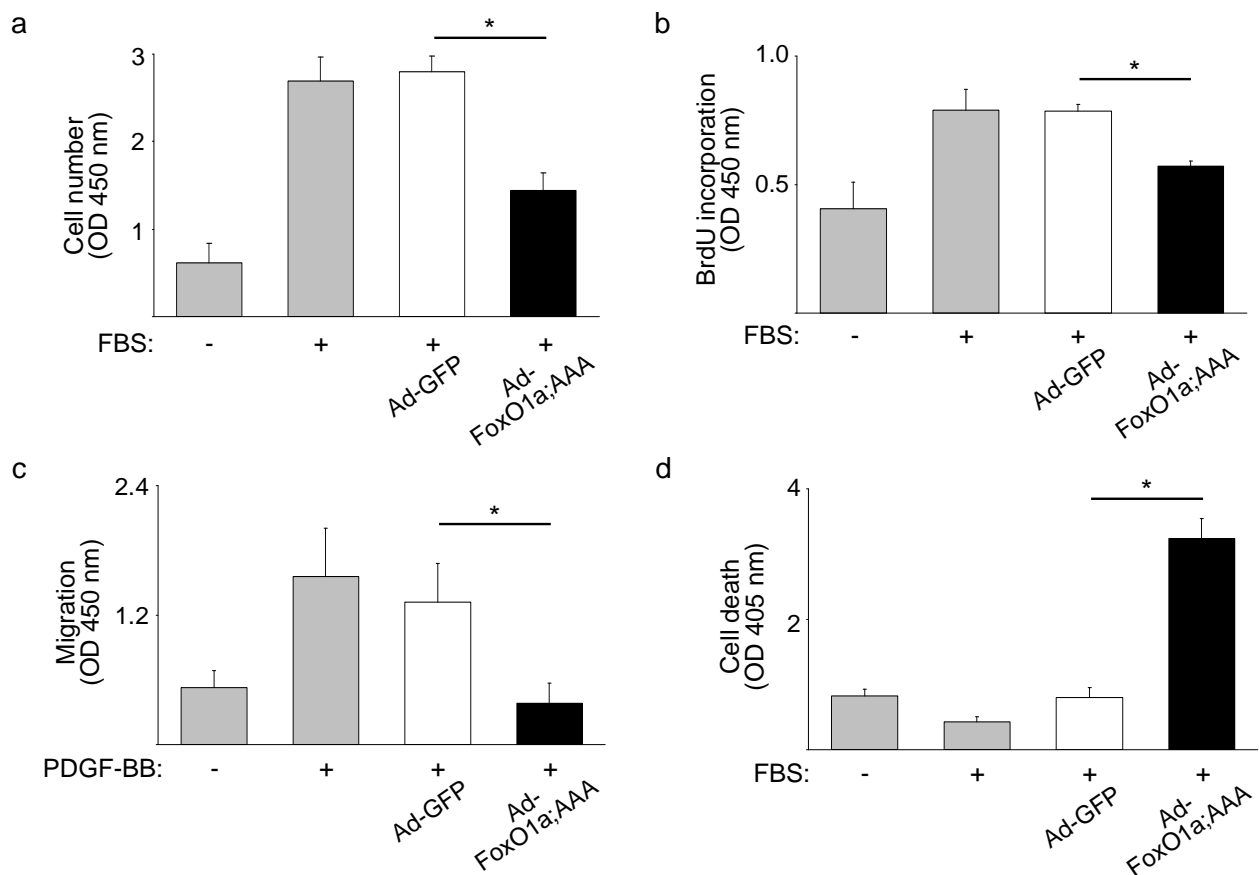


Figure 34. FoxO1a regulates PSMC proliferation, migration and apoptosis

PSMCs transduced with FoxO1a;AAA or a control vector (Ad-GFP) were incubated in growth medium for 48 h. Non-transduced PSMCs either serum-starved for 24 h or growing were used as controls. Data represent mean and standard deviations of three to six measurements. Each experimental set was repeated at least three times with similar results. Statistical significance was determined by ANOVA. **a)** Total cell numbers were evaluated 48 h post-transduction by WST-1 assay (* $p < 0.001$; $n=6$). **b)** 48 h post-transduction, PSMCs were grown for 6 h in the presence of BrdU and proliferation was measured by ELISA (* $p < 0.001$; $n=4$). **c)** 48 h post-transduction PSMCs were plated on gelatine-coated polycarbonate membranes and allowed to migrate for 24 h along a PDGF-BB gradient (20ng/ml). Cell number of migrated cells was determined by WST-1 assay (* $p < 0.02$; $n=3$). **d)** Cytoplasmic accumulation of mono- and oligonucleosomes was evaluated by Cell Death Detection ELISA of the four different already mentioned cell populations 48 h post-transduction (* $p < 0.001$; $n=3$).

Taken together, these results suggest that FoxO1a is a key-regulator of PASMC function, simultaneously modulating proliferation, apoptosis and migration. Furthermore, the presented absence of high cell numbers in Ad-FoxO1a;AAA-transduced PASMC cultures seems to be due to a combined effect of growth inhibition and an augmented apoptotic rate.

FoxO1a induces PASMCs apoptosis via upregulating caveolin-1 expression

Recently Sedding et al. could identify caveolin-1 to be transcriptionally regulated by FoxO1a in VSMCs of coronary arteries, and that the pro-apoptotic effect of activated FoxO1a is, at least partly, mediated by upregulating caveolin-1 protein levels in these cells (Sedding et al., unpublished data). Thus, I hypothesized FoxO1a to control programmed cell death in PASMCs via regulating caveolin-1 as well. Following Ad-FoxO1a;AAA transduction, caveolin-1 protein levels significantly increased as determined by immunoblotting (Figure 35). Other genes potentially involved in PASMC apoptosis were evaluated too. Interestingly, neither death effector ligand FasL nor Bim, both proteins recently shown to be transcriptionally regulated by FoxO transcription factors^{166, 191}, were elevated in FoxO1a;AAA expressing PASMCs (Figure 35). However, both proteins were upregulated upon stress caused by serum-starvation. Thus slight increases in cell death rates of quiescent cells (see Figure 34d) might be due to increased expression of pro-apoptotic FasL and Bim. Apoptosis itself was monitored by immunostaining for cleaved caspase 3.

Together, these results indicate that FoxO1a's pro-apoptotic effect in PASMCs seems to be mediated by a transcriptional upregulation of caveolin-1.

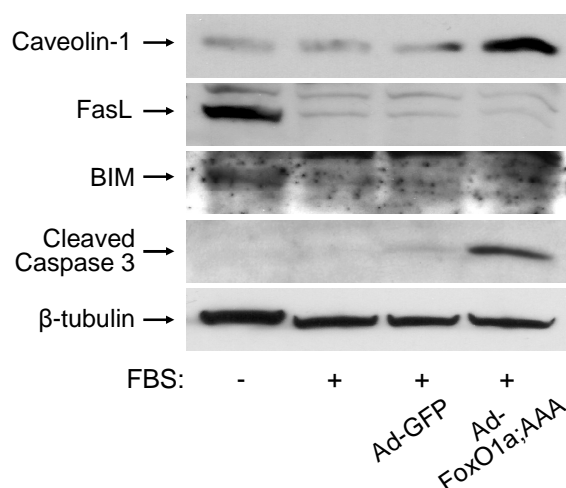


Figure 35. FoxO1a regulates caveolin-1 expression

PASMCs were transduced with adenoviruses encoding GFP (Ad-GFP) or FoxO1a;AAA (Ad-FoxO1a;AAA). Quiescent and growing PASMCs were used as controls. Expression of caveolin-1, FasL and Bim was determined 72 h post-transduction by immunoblot analysis using specific antibodies. Apoptosis induction was monitored with an anti-cleaved caspase 3-antibody. β-tubulin served as control for equal protein loading.

Active FoxO1a blocks serum-induced downregulation of p27^{KIP1} and Cyclin D1 expression

To further study the mechanisms of FoxO1a's anti-proliferative effect, analysis of cell cycle regulating proteins was undertaken. PSMCs were transduced with adenoviruses (Ad-GFP or Ad-FoxO1a;AAA) or left untreated and protein expression levels were detected 72 h post-transduction by Western blot analysis (Figure 36). The decrease in DNA synthesis in PSMCs forced to express FoxO1a;AAA as seen above (Figure 34b) was attributed to a sustained upregulation of the cyclin-dependent kinase inhibitor p27^{KIP1} and a decline in Cyclin D1 levels (Figure 36). Whereas proliferation block in FoxO1a;AAA-expressing PSMCs was accompanied by a sustained upregulation of p27^{KIP1} and a downregulation of Cyclin D1 (Figure 36), infection with the adenovirus containing the reporter gene only (Ad-GFP) did not alter p27^{KIP1} and Cyclin D1 expression levels as compared to non-transduced FBS-stimulated PSMCs (Figure 36). Regulation of both p27^{KIP1} and Cyclin D1 in serum-deprived VSMCs was already implicated earlier to a blockade at G1, which is responsible for a prevented S-phase entry of these cells compared to serum-stimulated ones (Figure 36a). Thus, inhibition of PSMC proliferation by active FoxO1a is due to a blockade of cell cycle progression in G1. Any changes in the expression levels of other cyclin-dependent kinase inhibitor (p21^{CIP1}) or other cyclins (Cyclin E) were not observed (Figure 36). Further evidence for reduced cell proliferation of Ad-FoxO1a;AAA-transduced PSMCs was the reduction of hyperphosphorylated retinoblastoma gene product (pRb) in these cells.

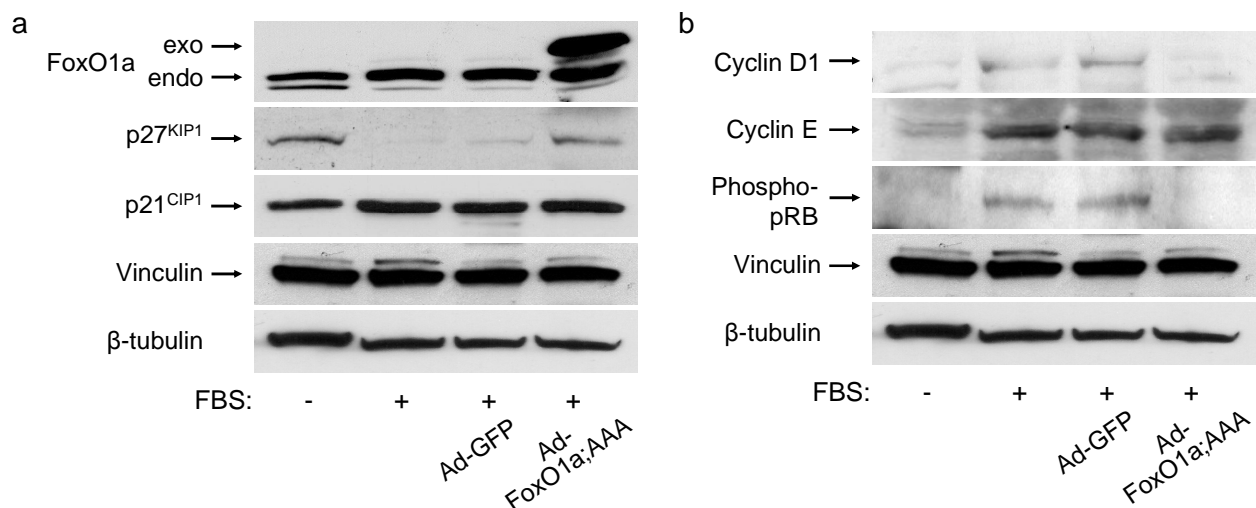


Figure 36. FoxO1a modulates expression of cell cycle regulating proteins in PSMCs

PSMCs, either transduced with Ad-GFP, Ad-FoxO1a;AAA or left untreated, were cultured in serum-containing medium. Control cells were serum-starved for 24 h in basal medium. Expression of cell cycle regulating proteins was monitored by Western blot analysis with specific antibodies for p27^{KIP1}, p21^{CIP1}, Cyclin D1, Cyclin E and phospho-pRb. Analysis of FoxO1a protein levels revealed expression of both endogenous and exogenous FoxO1a in Ad-FoxO1a;AAA-transduced PSMCs. Stainings for vinculin and β-tubulin were performed for loading control.

These data indicate that FoxO1a is involved in modulating Cyclin D1 and p27^{KIP1} expression in PASMCs, thereby attenuating FBS-induced cell cycle progression due to cell cycle arrest.

FoxO1a regulates proliferation, migration and apoptosis of PASMCs from MCT-treated rats

Monocrotaline (MCT), a toxin isolated from plants of the *Crotalaria* species, is used to intentionally induce severe pulmonary hypertension (PHT) in animals in order to generate an experimental model for exploring the pathophysiology of PHT and the development of pharmacological means of treating it³³⁶. Pulmonary vessels from MCT-treated rats show significant increases in media thickness similar to neointimal thickening during restenosis. Pullamsetti *et al.* recently investigated the effect of MCT on increased PASMC migration and proliferation as well as matrix remodeling, which represent key features of MCT-induced PHT³³⁷. Since my previous results exhibit the involvement of FoxO1a in regulating PASMC behavior, I next investigated the impact of this transcription factor on pathologically modified PASMCs.

First, cell numbers of both Ad-FoxO1a;AAA-transduced and Ad-GFP-transduced PASMCs from MCT-treated rats were analyzed by WST-1 assay. Transduction of PASMCs with the FoxO1a encoding adenovirus significantly decreased the number of viable cell as compared to PASMCs expressing the GFP-control vector (Figure 37a). Serum-deprivation of non-transduced MCT-PASMCs resulted in low cell numbers, whereas stimulation with FBS significantly enhanced the amount of viable cells (Figure 37a).

The cells ability to incorporate labeled BrdU during DNA synthesis was measured 48 h post-transduction by ELISA. As it was previously shown for PASMCs from healthy rats, MCT-PASMCs expressing FoxO1a;AAA showed a decline in DNA replication as compared to Ad-GFP-transduced cells (Figure 37b). Non-transduced, growing PASMCs from MCT-rats showed higher DNA replication rates as compared to serum-starved ones (Figure 37b).

Furthermore, the chemotactic response of both adenovirus- and non-transduced PASMCs from MCT-treated rat was examined using modified Boyden chamber migration assays. The chemoattractant PDGF-BB was used to excite chemotactic cell migration. PDGF-BB caused strong chemotaxis of non-transduced and Ad-GFP-transduced PASMC along the chemoattractive gradient, whereas significant less cell migration was observed when analyzing PASMCs expressing active FoxO1a (82% less compared to Ad-GFP) (Figure 37c). Thus, it seems that FoxO1a reconstitution reverses PDGF-BB-induced PASMC migration (Figure 37c). In earlier studies Pullamsetti *et al.* were able to demonstrate that the migration rate of PASMCs derived from MCT-rats ranged at 155% of that of PASMCs derived from control rats³³⁷.

As it was already shown earlier for PASCs from healthy rats, transduction with Ad-FoxO1a;AAA significantly enhanced the apoptosis rate of MCT-treated PASCs as measured by Cell Death Detection ELISA (~ 300% increase compared to Ad-GFP) (Figure 37d). Transduction with Ad-GFP revealed only a slight increase in apoptosis, therefore the transduction process itself was demonstrated not to be responsible for increasing cell death rates. Stressing non-transduced MCT-PASCs by truncating serum supply for 24 h also resulted in an increase in apoptosis rate as compared to cells grown in serum-containing medium (Figure 37d). Thus, it seems that recovering FoxO1a function in MCT-treated PASCs by adenovirally increasing expression of FoxO1a attenuates their survival rate under growth conditions. Completing these results, PASCs expressing FoxO1a;AAA showed the

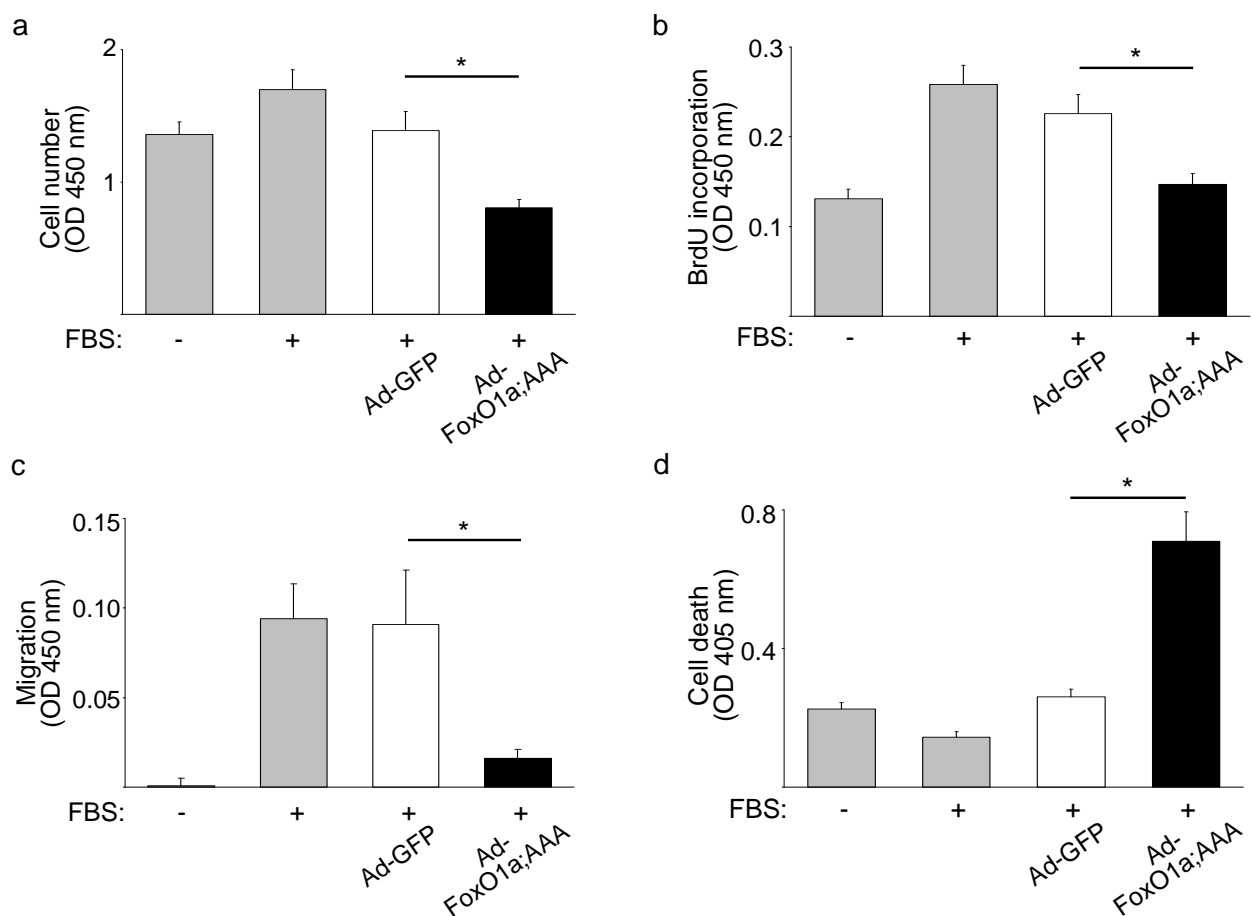


Figure 37. FoxO1a regulates proliferation, migration and apoptosis of MCT-treated PASCs

PASCs derived from MCT-treated rats were transduced with FoxO1a;AAA or a control vector (Ad-GFP) and grown in FBS-supplemented medium for 48 h. Non-transduced PASCs were either serum-starved for 24 h or cultured in growth medium before use. Data represent mean absorbance values plus error bars. One representative experiment from at least three separate ones is shown per experimental set-up. Statistical significance was determined by ANOVA. **a)** Total cell number was evaluated 48 h post-transduction by WST-1 assay (* $p < 0.001$; $n=6$). **b)** 48 h post-transduction, MCT-PASCs were grown for 6 h in the presence of BrdU and proliferation was measured by ELISA (* $p < 0.001$; $n=4$). **c)** PASC migration towards 20ng/ml PDGF-BB was measured by modified Boyden chamber. After 24 h, cell number of migrated cells was determined by WST-1 assay (* $p < 0.001$; $n=3$). **d)** Apoptosis rates of serum-starved MCT-PASCs as well as of growing non-treated, Ad-GFP- and Ad-FoxO1a;AAA-transduced MCT-PASCs were measured by ELISA (* $p < 0.001$; $n=3$).

characteristic morphology of cells undergoing apoptotic cell death: Cell shrinkage, bebbing, membrane detachment and nuclear fragmentation (data not shown).

Together, the results suggest that FoxO1a is a key regulator of cell function in pathologically modified PSMCs, simultaneously modulating proliferation, migration and apoptosis. Furthermore, prevention of serum-induced cell number increase in FoxO1a;AAA-transduced cells seems to be due to a combined effect of growth inhibition and augmented apoptotic rate.

In summary, the data derived from studies with PSMCs indicate a central role of FoxO1a in modulating cell behavior of these cells *in vitro*. Further studies need to explore FoxO1a's effect on PSMCs *in vivo* and in the pathogenesis of PHT. Nevertheless, my data imply that FoxO1a may represent an attractive target for future therapeutic strategies in the prevention of different vascular proliferative diseases, such as atherosclerosis, restenosis and PHT.

The histone deacetylase SIRT1 regulates HCASMC homeostasis *in vitro* and *in vivo*

SIRT1 affects HCASMC proliferation and migration

Mammalian FoxO transcription factors control various biological functions, including cell cycle arrest in various cell types^{169, 215, 226}. Recently, the effect of phosphorylated FoxO1a on cell cycle progression, proliferation and migration of VSMCs *in vitro* and *in vivo* was discovered (see above and Sedding *et al.*, unpublished data) revealing a critical role for FoxO1a in vascular remodeling processes. However, the effect of Foxo1a acetylation remains elusive. Since the mammalian histone deacetylase SIRT1 has been shown to be involved in manipulating FoxO function in several cell lines^{233, 262}, I sought to determine the effect of SIRT1 and FoxO1a deacetylation on VSMC function in the present study.

SIRT1 is localized to the nucleus of vascular smooth muscle cells

The deacetylase SIRT1 was recently published to play major roles in diverse cell types ranging from pro- to eukaryotes^{303, 304, 307}. However, to my knowledge no one ever studied its function in the vascular system, or more precisely in VSMCs of coronary arteries. Therefore, I was interested whether SIRT1 is expressed in VSMCs deriving from different species and if though, how the intracellular distribution of SIRT1 would be. For this purpose, indirect immunofluorescence studies on human VSMCs (HCASMCs), rat VSMCs and mouse VSMCs were performed with specific antibodies for SIRT1. Microscopy analyses revealed a relatively

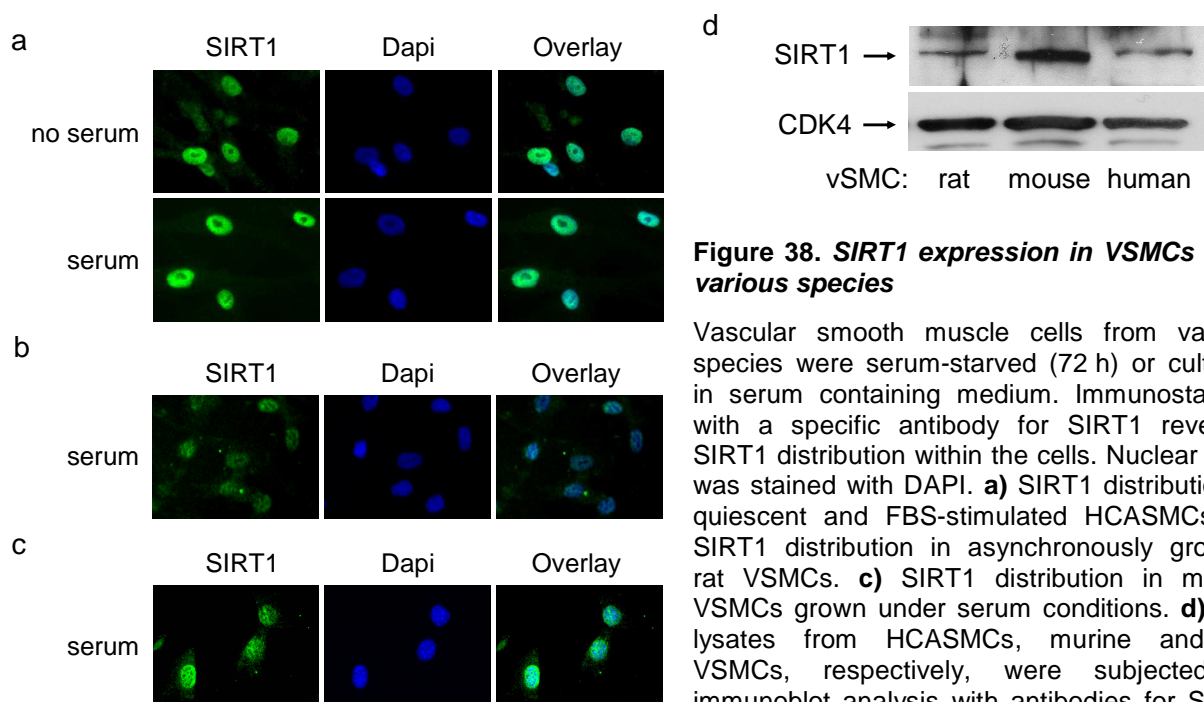


Figure 38. SIRT1 expression in VSMCs from various species

Vascular smooth muscle cells from various species were serum-starved (72 h) or cultured in serum containing medium. Immunostaining with a specific antibody for SIRT1 revealed SIRT1 distribution within the cells. Nuclear DNA was stained with DAPI. **a)** SIRT1 distribution in quiescent and FBS-stimulated HCASMCs. **b)** SIRT1 distribution in asynchronously growing rat VSMCs. **c)** SIRT1 distribution in murine VSMCs grown under serum conditions. **d)** Cell lysates from HCASMCs, murine and rat VSMCs, respectively, were subjected to immunoblot analysis with antibodies for SIRT1 and CDK4 (loading control).

homogenous nuclear distribution of endogenous SIRT1 in both serum-starved and growing HCASMCs (Figure 38a). Similarly, VSMCs from rat and mouse synthesize SIRT1, and in both species the deacetylase was predominantly localized to the nucleus (Figure 38b, c). Western blot analysis additionally demonstrated SIRT1 expression in VSMCs of all three species (Figure 38d).

Together these results reveal that SMCs from the vascular system, independent of the species, synthesize SIRT1 and that the deacetylase seems to be constantly nuclear.

Endogenous SIRT1 is downregulated by siRNA in HCASMCs

Transfection of HCASMCs with siRNA for SIRT1 (siSIRT1) was used for mimicking loss-of-function studies in this cell type. Non-targeting control siRNA (siControl) was used to detect off-target effects. Non-transfected cells (NT) as well as mock-transfected ones (lipid carrier only) provided the possibility to detect cellular effects caused by the delivery process itself. During extensive studies, I established optimal transfection conditions in advance to all siRNA

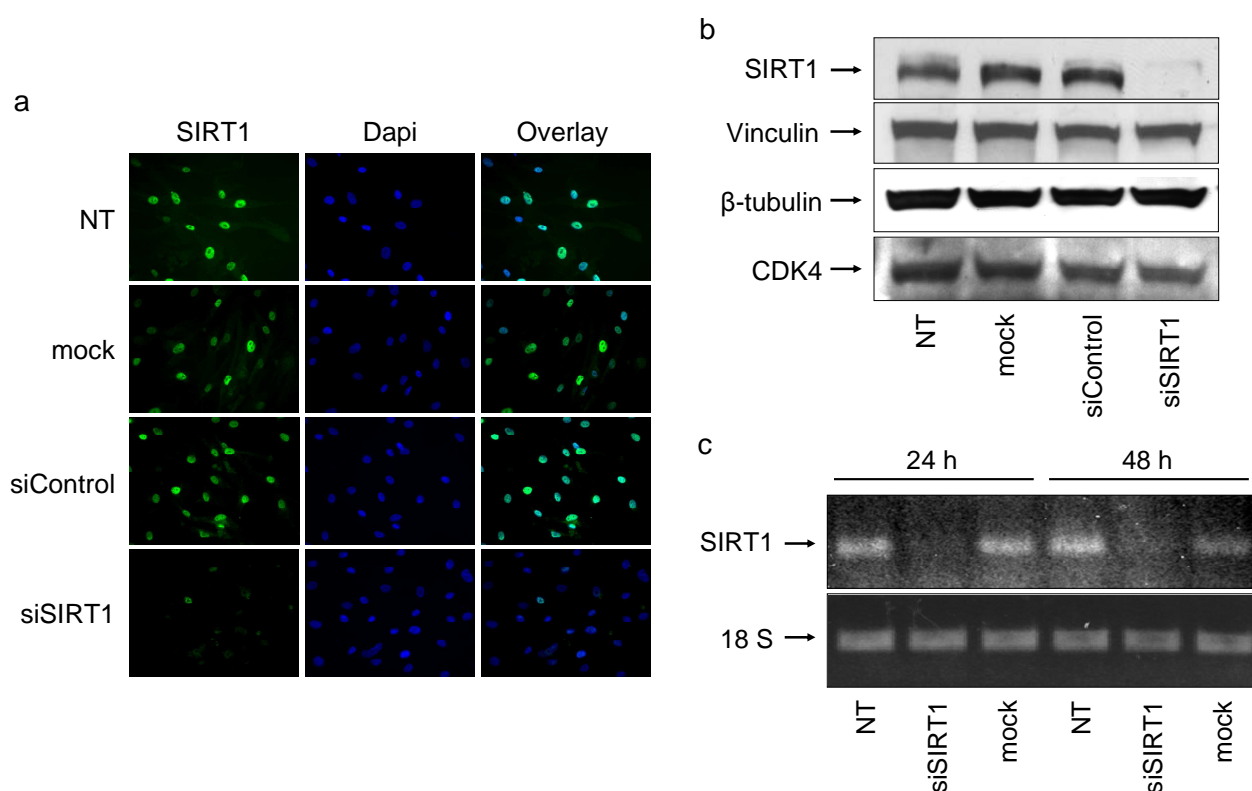


Figure 39. SIRT1 downregulation by siRNA in HCASMCs

HCASMCs were either mock-transfected (lipid-carrier only), transfected with control siRNA (siControl) or siRNA for SIRT1 (siSIRT1). Control cells were left untreated (NT). **a)** 48 h post-transfection SIRT1 expression was determined by immunostaining with an antibody for SIRT1. Nuclear DNA was stained with DAPI. **b)** Protein lysates from transfected HCASMCs were subjected to immunoblot with antibodies for SIRT1, vinculin, β-tubulin, and CDK4. **c)** SIRT1 mRNA levels from transfected HCASMCs were analyzed by semiquantitative reverse transcriptase PCR 24 h and 48 h post-transfection. 18S was used as an internal positive control. All experiments were conducted at least in duplicate using always independent HCASMC cultures.

experiments (data not shown). Downregulation of SIRT1 protein level was confirmed by immunocytochemistry (Figure 39a) as well as by immunoblotting (Figure 39b). siSIRT1-transfected HCASMCs showed only sporadic SIRT1 expression within their nuclei (Figure 39a). Western blot experiments additionally revealed siRNA-mediated downregulation of SIRT1 (Figure 39b), thus confirming previous immunoblot results. Since none of the tested housekeeping protein levels was influenced by siRNA for SIRT1 (Figure 39b), the specificity of the siRNA was verified. Examination of mRNA levels by our group using reverse transcriptase PCR indicated a downregulation of SIRT1 mRNA by siRNA 24 h and 48 h post-transfection, respectively (Figure 39c).

In the end of this experiments I conclude that transient downregulation of SIRT1 can be achieved by the use of specific siRNA.

Serum stimulation induces an upregulation of SIRT1 levels in HCASMCs

To determine whether serum stimulation modulates the expression levels of SIRT1 in HCASMCs, Western blot analysis of HCASMCs treated for various times with serum was carried out. As shown in Figure 40a, incubation of silenced HCASMCs with 20% FBS in growth medium resulted in an upregulation of SIRT1 protein levels after approximately 4 to 6 h. Induction of proliferation was determined by immunoblot analysis for Cyclin D1 expression, a cell cycle regulatory protein that is upregulated during cell cycle progression (Figure 40a). Reverse transcriptase PCR analysis of serum-treated HCASMCs indicated an increase in SIRT1 mRNA levels already 1 to 2 h following FBS treatment (Figure 40b). Interestingly, SIRT1 mRNA levels truncated over time to their starting levels (Figure 40b). Similarly, SIRT1 protein levels returned to baseline levels and even dramatically decreased at later timepoints following mitogenic stimulation (data not shown).

Taken together, these data indicate that serum stimulation induces a transient increase in SIRT1 expression followed by a later dramatic decrease in HCASMCs.

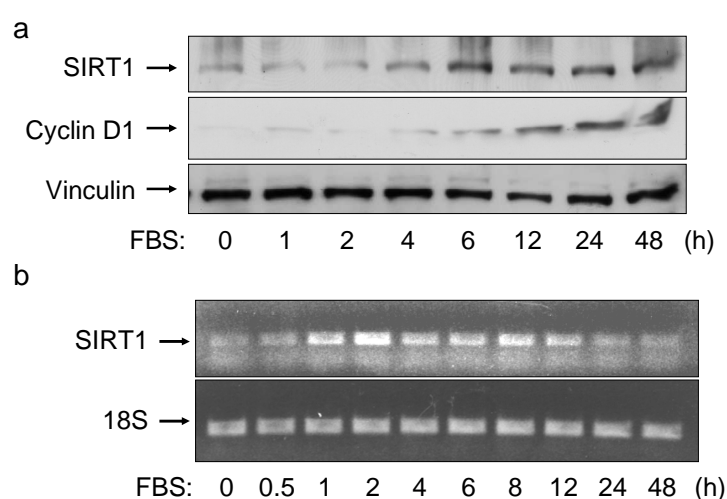


Figure 40. Serum stimulation affects SIRT1 expression in HCASMCs

HCASMCs were serum-starved for 72 h in basal medium and subsequently stimulated with 20% FBS in growth medium for the indicated timeperiods. **a)** Cell lysates were processed to Western blot analysis for SIRT1, cyclin D1 and vinculin (loading control). The blot shown is representative of three independent experiments. **b)** SIRT1 mRNA levels were analyzed by semiquantitative reverse transcriptase PCR 48 h post-transfection. Quantifying 18S mRNA was used as a loading control. PCR experiments were conducted at least in triplicate using always independent HCASMC cultures.

Pharmacological inhibition of endogenous SIRT1 function enhances HCASMC proliferation

After having shown that SIRT1 is upregulated in response to serum stimulation, I was interested in the influence of endogenous SIRT1 on HCASMC proliferation. For analyzing this, HCASMCs were either serum-starved or incubated with 20% FBS. Serum treatment significantly induced HCASMC replication as determined by BrdU incorporation (Figure 41a, b and earlier results). Pharmacological inhibition of SIRT1 function by treatment with either NAM or splitomicin, both agents often utilized for downregulating SIRT1 activity²⁹²⁻²⁹⁴, significantly increased FBS-mediated DNA synthesis as compared to non-treated serum-stimulated cells (Figure 41a, b).

Next, I was interested whether both molecules were able to induce proliferation in silenced HCASMCs. As seen in Figure 41c and d, even quiescent cells were animated to enter the cell cycle and duplicate themselves upon drug treatment. Optimal concentrations of both agents

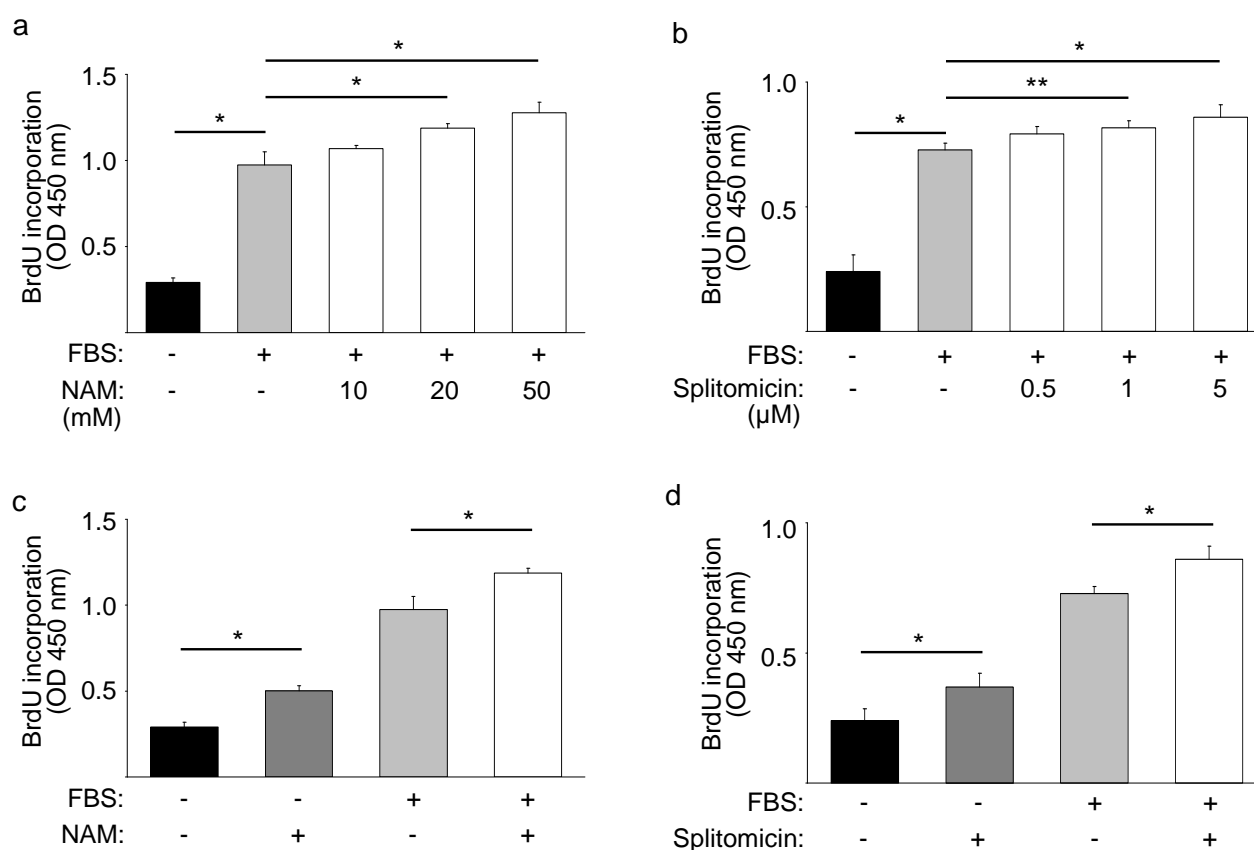


Figure 41. Effect of pharmacological SIRT1 inhibition on HCASMC proliferation

HCASMCs were cultured in growth medium supplemented with 20% FBS, and treated without or with pharmacological SIRT1 inhibitors (NAM or splitomicin) for 20 h. Some cells were serum-starved for 72 h. BrdU incorporation was measured by ELISA. Data represent means and standard deviations of three to six measurements. Each experimental set was repeated at least three times with similar results. **a)** HCASMCs were treated with different concentrations of NAM (* $p < 0.001$; $n = 6$). **b)** HCASMCs were treated with different concentrations of splitomicin (* $p < 0.001$, ** $p < 0.01$; $n = 4$). **c, d)** Both serum-starved and proliferating HCASMCs were treated with 20 mM NAM (* $p < 0.001$; $n = 6$) and 5 μM splitomicin (* $p < 0.001$; $n = 4$), respectively. Statistical significance of all experiments was determined by ANOVA.

(NAM and splitomicin) for influencing HCASMC behavior were carefully determined in the run-up to all experiments (data not shown).

Since DNA synthesis of HCASMCs is upregulated by the use of SIRT1 inhibitors, the latest experiments reveal the involvement of SIRT1 in controlling excessive proliferation and regulating HCASMC dormancy.

Downregulation of SIRT1 by siRNA technique enhances proliferation of HCASMCs

Given that there is no clear evidence for the used pharmacological agents of inhibiting SIRT1 function specifically, proliferation of HCASMCs was also measured in SIRT1-deprived cells. For this experiment, HCASMCs were transfected with either siRNA for SIRT1 or a non-silencing control siRNA, cultured in the absence or presence of 20% FBS, and then assayed for cell proliferation by ELISA 72 h post-transfection. siRNA efficiency and specificity for SIRT1 was demonstrated in previous experiments (see Figure 39). As shown in Figure 42, FBS-mediated HCASMC proliferation was enhanced by siRNA-mediated downregulation of SIRT1. Interestingly, downregulation of SIRT1 had also a small but significant effect on BrdU incorporation into cellular DNA of silenced HCASMCs as compared to control transfected serum-starved cells (Figure 42).

Together these results confirm the inhibitory effect of SIRT1 on HCASMC proliferation and support my previous results.

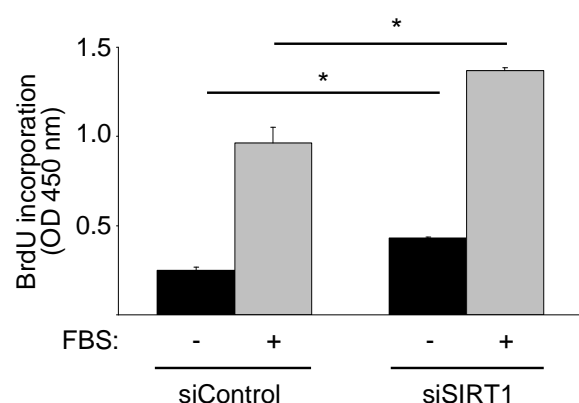


Figure 42. Anti-proliferative effect of SIRT1 is partially reversed by siRNA for SIRT1

HCASMCs were transfected with siRNA for SIRT1 (siSIRT1) or control siRNA (siControl). 24 h post-transfection the cells were incubated for additional 48 h in the absence or presence of 20% FBS. BrdU incorporation was measured by ELISA. Data represent means and error bars of OD values (* $p < 0.001$, ** $p < 0.01$; $n = 4$). Data depicted are representative of five independent experiments from different HCASMC aliquots. Statistical significance was determined by ANOVA

SIRT1 is involved in regulating cell proliferation of mouse embryonic fibroblasts

Due to the finding that endogenous SIRT1 inhibits cell cycle progression in HCASMCs, I assumed that SIRT1 could also modulate proliferation of mouse embryonic fibroblasts (MEFs). MEFs were derived either from SIRT1-null mice or from their wild-type littermates. First, endogenous SIRT1 was revealed by immunoblotting with an antibody for SIRT1 and, as expected, SIRT1-knockout MEF do not express the deacetylase (Figure 43a).

Proliferation of both types of MEFs was revealed by measuring BrdU incorporation into the cells DNA (Figure 43b). In serum-cultured SIRT1-null MEFs, the ability to replicate DNA was enhanced as compared to cells capable of synthesizing SIRT1 (Figure 43b). Interestingly, as it was demonstrated earlier with SIRT1-knockdown HCASMCs, BrdU incorporation rates of silenced MEFs deprived of SIRT1 were little but significantly higher to that of quiescent wild-type MEFs, indicating an increase in proliferation in SIRT1-null MEFs as compared to wild-type MEFs (Figure 43b).

In agreement with the previous results, I could show that functional active SIRT1 attenuates cell proliferation in both quiescent and growing cells, independent of the cell type examined.

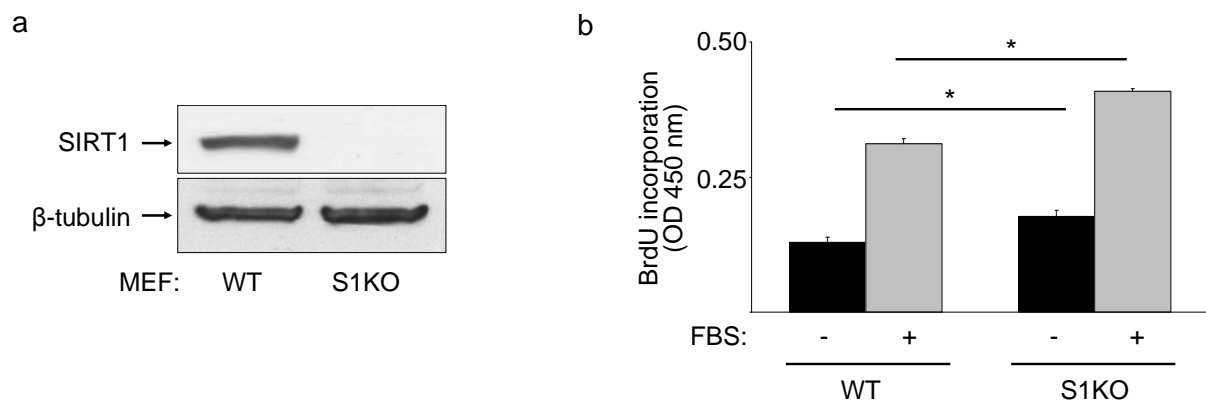


Figure 43. SIRT1 affects proliferation in mouse embryonic fibroblasts

a) Mouse embryonic fibroblasts (MEF) from SIRT1-knockout mice (S1KO) or from their wild-type littermates (WT) were analyzed for SIRT1 expression by western-blotting with an antibody for SIRT1. Equal protein loading was confirmed using anti-β-tubulin antibody. **b)** WT MEFs and SIRT1-null MEFs were either cultured in serum-containing medium or were serum-starved for 14 h before incubating with BrdU for 6 h. BrdU incorporation was analyzed by ELISA and data given represent mean absorbance values and standard deviations of four measurements (* $p < 0.001$). Statistical significance was determined by ANOVA. The experiment was repeated six times with same results.

Activation of SIRT1 by resveratrol inhibits serum-induced HCASMCs proliferation

Recently, Howitz *et al.* described the substance resveratrol, a plant polyphenol, being a specific small molecule activator of SIRT1²⁹⁷. As I could show that SIRT1 inhibits HCASMC proliferation, I was interested in whether activation of SIRT1 by resveratrol would attenuate serum-induced proliferation in this cell type. First, HCASMCs cultured in growth medium were treated with different amounts of resveratrol for a total of four days. Cell numbers were counted every 24 h using a hemocytometer. Activation of SIRT1 by resveratrol reduced HCASMCs proliferation dose-dependently, with 50 μM resveratrol completely inhibiting DNA replication (Figure 44a). It is note worth to mention that treatment with 50 μM resveratrol partially induced cell death as it was seen by changes in cell morphology and cell detachment (data not shown).

Similar results were obtained using WST-1 assays: Quantitative analysis of HCASMC cell numbers revealed a dose-dependent decrease of viable cells after treatment with increasing

concentrations of resveratrol (Figure 44b).

To further demonstrate inhibition of proliferation, BrdU incorporation in response to resveratrol treatment was measured by ELISA (Figure 44c). The pro-proliferative effect of 20% FBS was partially inhibited by 10 μ M resveratrol, and 20 μ M resveratrol almost completely compensated it (Figure 44c). Treatment with 50 μ M resveratrol extremely reduced BrdU incorporation suggesting, that at this concentration the plant polyphenol did not only inhibit proliferation but also induced cell death (Figure 44c).

Taken together, this part of my thesis demonstrates that resveratrol-treatment reverses FBS-induced DNA synthesis in HCASMCs. Whether the observed effect is SIRT1 specific will be explored in the following part.

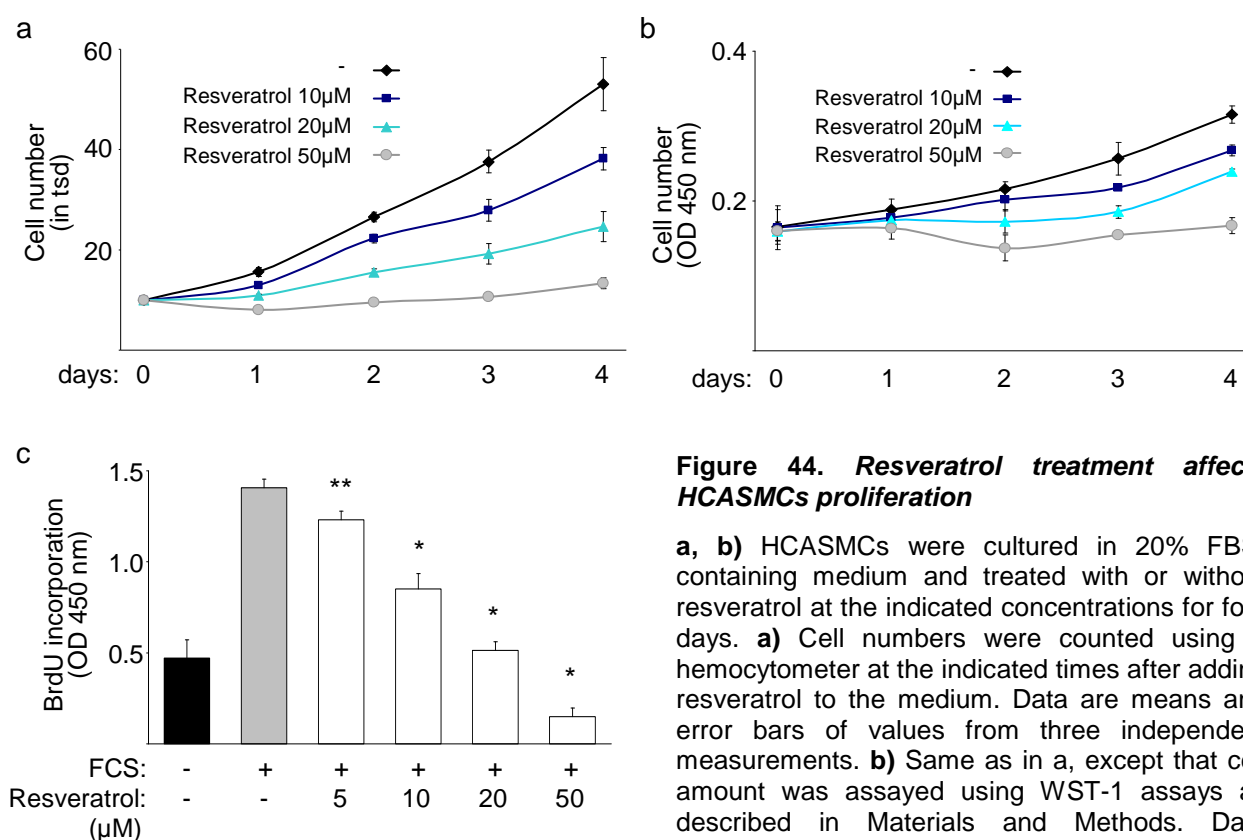


Figure 44. Resveratrol treatment affects HCASMCs proliferation

a, b) HCASMCs were cultured in 20% FBS-containing medium and treated with or without resveratrol at the indicated concentrations for four days. **a)** Cell numbers were counted using a hemocytometer at the indicated times after adding resveratrol to the medium. Data are means and error bars of values from three independent measurements. **b)** Same as in a, except that cell amount was assayed using WST-1 assays as described in Materials and Methods. Data represent means and standard deviation of four measurements. **c)** HCASMCs were incubated for

20 h with the indicated concentrations of resveratrol in growth medium supplemented with 20% FBS. Control cells were left untreated and serum-starved for 72 h. BrdU incorporation into the DNA was measured by ELISA and data represent means and standard deviations of one representative experiment (* $p < 0.001$, ** $p < 0.001$ vs. FBS; $n=4$). Statistical significance was determined by ANOVA. All experiments were repeated three times with similar results.

Resveratrol influences HCASMCs proliferation via manipulating SIRT1 function

After having shown that resveratrol affects HCASMC proliferation, I was interested in whether this molecule directly alters SIRT1 function or whether its effect on cell proliferation was exerted by manipulating other proteins within the cells. To clarify this question, HCASMCs were

transfected with siRNA targeting SIRT1 mRNA or a non-silencing siRNA (Figure 45a). 48 h post-transfection, cells were incubated in the presence or absence of resveratrol. Proliferation, as determined by BrdU incorporation, was significantly decreased in control-transfected HCASMCs after resveratrol treatment (Figure 45a), whereas SIRT1-deprived cells showed no relevant attenuation in DNA synthesis (Figure 45a).

To assess whether the effect of resveratrol on activating SIRT1 was cell type specific, MEFs from wild-type and SIRT1-knockout mice were treated with or without the polyphenol before measuring the cells DNA replication rates (Figure 45b, c). Wild-type MEFs showed a significant decrease in FBS-induced DNA synthesis upon treatment with increasing concentrations of resveratrol (Figure 45b), whereas MEF from SIRT1-knockout mice did not (Figure 45c).

Taken together these data indicate that resveratrol inhibits serum-mediated cell cycle progression in various cell types via manipulating SIRT1 function. Thus, administering resveratrol could be a promising approach for combating with vasculo-proliferative diseases.

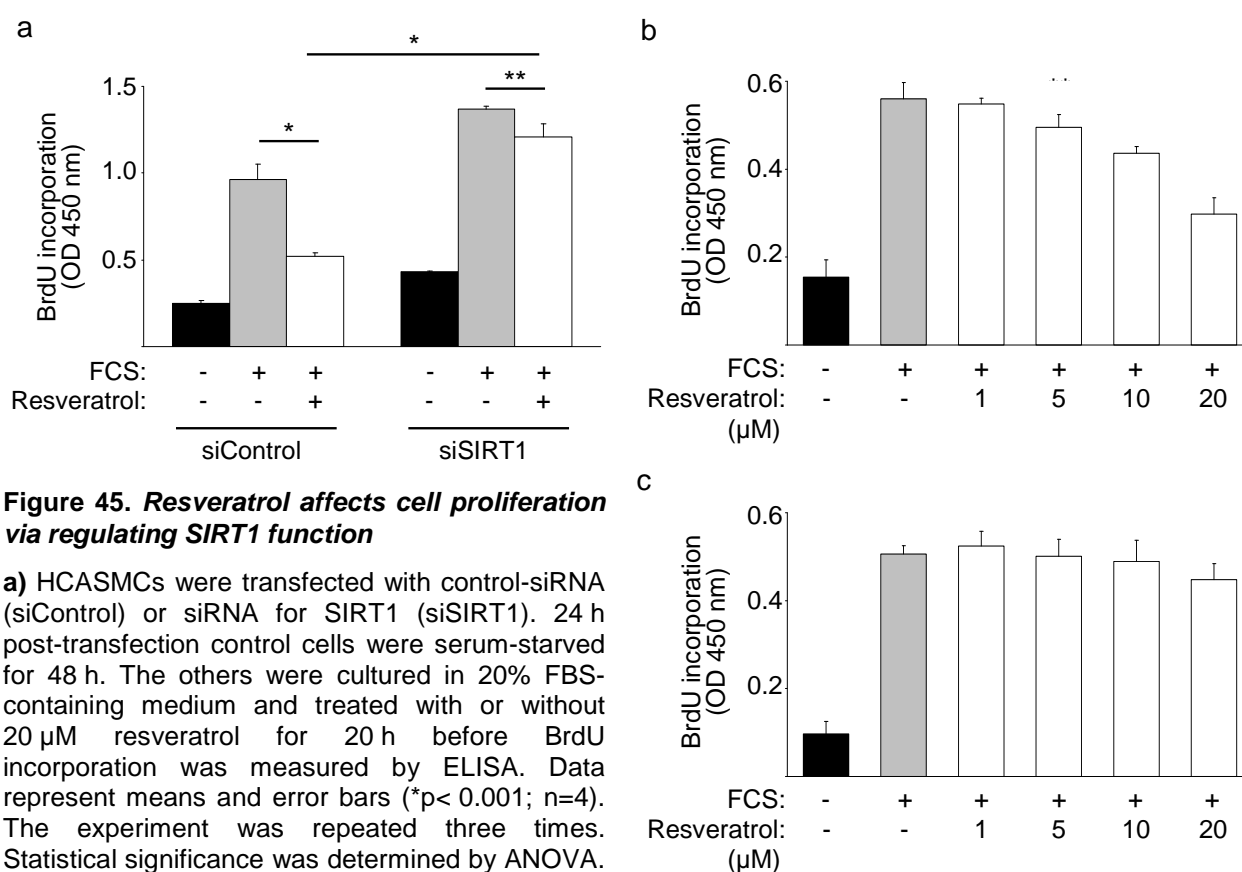


Figure 45. Resveratrol affects cell proliferation via regulating SIRT1 function

a) HCASMCs were transfected with control-siRNA (siControl) or siRNA for SIRT1 (siSIRT1). 24 h post-transfection control cells were serum-starved for 48 h. The others were cultured in 20% FBS-containing medium and treated with or without 20 μM resveratrol for 20 h before BrdU incorporation was measured by ELISA. Data represent means and error bars (* $p < 0.001$; $n = 4$). The experiment was repeated three times. Statistical significance was determined by ANOVA. MEF from wild-type mice **(b)** and SIRT1-knockout mice **(c)** were cultured in growth medium supplemented with 20% FBS and treated with the indicated concentrations of resveratrol for 20 h. Proliferation was determined by BrdU ELISA. Absorbance values and standard deviations of 4 measurements are indicated (b: * $p < 0.001$, ** $p < 0.05$ vs. FBS; c: non-significant (n.s.) > 0.02 vs FBS). Statistical significance was determined by ANOVA. The experiment was repeated twice times with similar results.

Adenoviral transduction with either active or constitutive inactive SIRT1 affects HCASMCs proliferation

Besides using resveratrol, another approach for studying excessive SIRT1 function is transduction of HCASMCs with an adenovirus encoding wildtype SIRT1 (Ad-SIRT1). Transduction with an adenoviral construct expressing a constitutive inactive mutant of SIRT1 (Ad-SIRT1-H335A) was used for competitive inhibition of SIRT1 activity. This dominant-negative form was created by site-directed mutagenesis and is characterized by substitution of a conserved histidine to arginin in the catalytic region of the protein (Figure 46). To complete my results, transduction of HCASMCs with both adenoviruses, as well as with a control virus, was performed by our group. Overexpression of functional active SIRT1 decreased HCASMC proliferation as compared to control-transduced cells (data not shown). Transduction of the cells with Ad-SIRT1-H335A resulted in DNA replication levels similar to that of control cells (data not shown).

Taken together, increasing SIRT1 activity in HCASMCs – either by forced SIRT1 expression or by pharmacologically augmenting SIRT1 function – results in attenuated DNA replication levels. Thus, my previous findings of SIRT1 being an important regulator of VSMC proliferation has been confirmed once more.

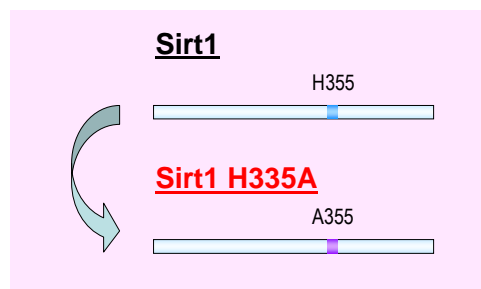


Figure 46. Cloning and mutagenesis of the dominant negative SIRT1

A constitutively inactive mutant of SIRT1 was created by mutating histidine 355 in the catalytic region of SIRT1 to alanine (H335A = SIRT1 H335A). Subsequently, recombinant SIRT1 H335A adenovirus was generated.

SIRT1 is involved in inhibiting migration of HCASMCs and MEFs

A central observation in vascular biology has been that cell cycle progression and cell migration upon mitotic stimulation are linked⁸⁵. Since SIRT1 was proven to play a role in cell cycle progression and proliferation as shown above, the question arose, whether SIRT1 is also involved in regulating HCASMC migration. siRNA-transfected HCASMCs were used for migration assays 72 h post-transfection. Migration of both control-transfected and siSIRT1-transfected cells along a PDGF-BB chemotactic gradient was examined by using a modified Boyden-chamber model. PDGF-BB induced chemotaxis of both siSIRT1- and control-transfected HCASMCs, whereas absence of the growth factor resulted in complete loss of migration (Figure 47a). Interestingly, the amount of migrated siSIRT1-transfected cells along the chemotactic gradient was significantly higher to that of control cells. Treatment of control-

transfected cells with the SIRT1 activator resveratrol interfered with chemotaxis, whereas SIRT1-depleted cells did not respond to resveratrol (Figure 47a). This again indicated resveratrol to act specifically via manipulating SIRT1 function.

To assess whether SIRT1's effect on chemotaxis is cell type specific, a similar experiment using wild-type MEFs and MEFs derived from SIRT1-knockout mice was performed. For both cell types, 20% FBS was chemotactic (Figure 47b). Nevertheless, loss of SIRT1 resulted in a significant increase in serum-induced migration as compared to the wild-type situation. As it was already shown for HCASMCs, absence of the chemotactic stimuli almost completely inhibited migration of both MEF types (Figure 47b).

In conclusion, these data reveal that SIRT1 does not only have an impact on FBS-induced proliferation but also affects chemotaxis of different cell types.

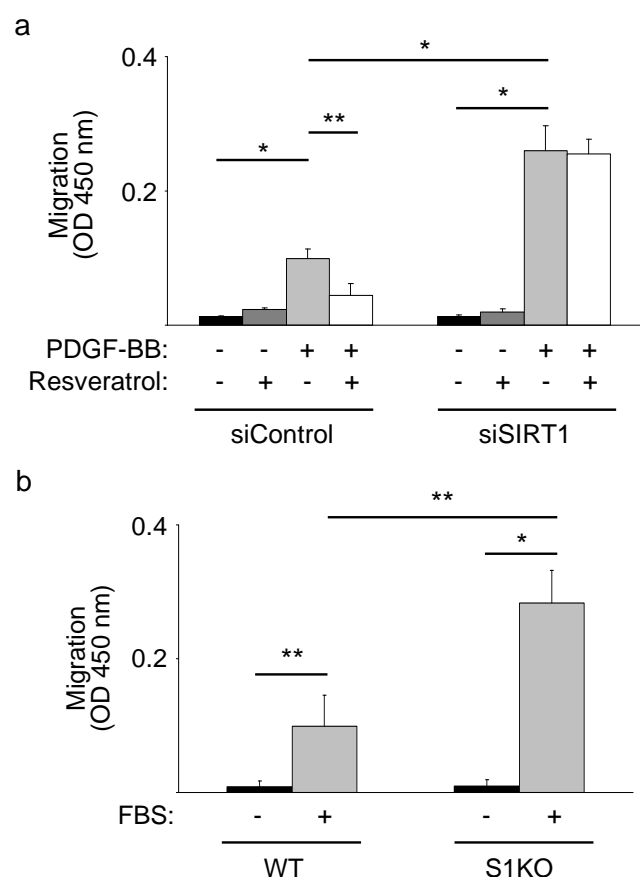


Figure 47. Effect of SIRT1 on cell chemotaxis

a) HCASMCs were transfected with siRNA for SIRT1 (siSIRT1) or non-targeting control siRNA (siControl). 24 h post-transfection cells were serum-starved for 48 h. 12 h before measuring chemotaxis, cells were treated with or without resveratrol (20 μ M). Subsequently, cells were plated on gelatine-coated polycarbonate membranes and allowed to migrate for 6 h along a 0ng/ml and a 20ng/ml PDGF-BB gradient, respectively. Numbers of migrated cells were analyzed using WST-1 assays. Data are plotted as means of triplicate samples and standard deviations (* p < 0.001, ** p < 0.01; n = 3). Data represent one experiment of four performed and statistical analysis was performed by ANOVA. **b)** MEFs derived from SIRT1-knockout mice (S1KO) or wild-type littermates (WT) were serum-starved for 24 h and then allowed to migrate along either a 0% or a 20% FBS gradient. Migrated cells were incubated with WST-1. Absorbance values plus error bars are presented in the graph (* p < 0.001, ** p < 0.01; n = 3). Data shown are representative of one experiment from four separate ones with similar results. Statistical significance was determined by ANOVA.

SIRT1 is expressed in VSMCs of the murine femoral artery vessel wall

As SIRT1 is expressed within the nuclei of mouse VSMCs *in vitro* (Figure 38), its *in vivo* expression level and distribution pattern was monitored in native mouse femoral arteries, as well as during the development of the neointima after wire-injury (Figure 48). Immunostaining of mouse femoral artery cross-sections from native mice revealed strong SIRT1 expression in the

nuclei of medial VSMCs (Figure 48a). Double-staining with an antibody for α -smooth muscle actin determined SIRT1-positive cells to be VSMCs. Dilatation of mouse femoral arteries resulted in neointima development over time (Figure 48b). Immunofluorescence studies of injured vessels at day 7 and day 21 post-dilatation confirmed expression of endogenous SIRT1 in medial cells of the femoral artery, as well as low expression in cell providing the neointimal tissue (Figure 48b). As shown by double-staining with an antibody for α -smooth muscle actin, the neointimal tissue consists of mainly α -smooth muscle actin-expressing VSMCs (Figure 48b).

Together with previous data these results indicate a SIRT1 expression not only *in vitro* but also *in vivo* in VSMCs of mouse arteries.

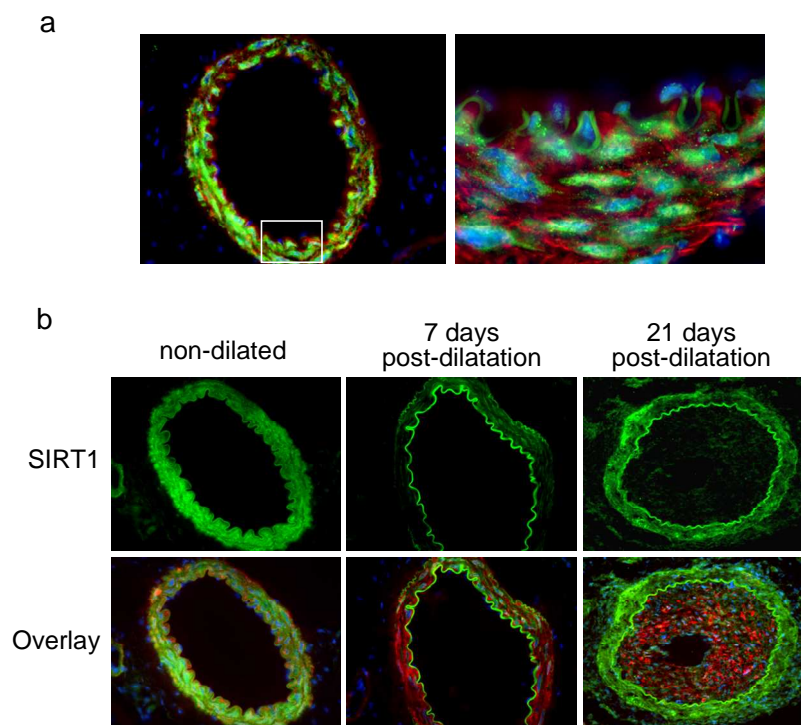


Figure 48. SIRT1 expression in the native and injured mouse femoral artery

Mouse femoral artery cross-sections were stained with specific antibodies for SIRT1 (green fluorescence) and α -smooth muscle actin (red fluorescence). DAPI was used for staining cell nuclei (blue fluorescence). **a)** A representative low magnification picture of a complete native vessel stained for SIRT1, α -smooth muscle actin and DAPI. The boxed region is highly magnified in the second image. **b)** Representative sections of native or injured mouse femoral arteries 7 days and 21 days post-injury, respectively. The lower row shows merged pictures from the same sections stained for SIRT1, α -smooth muscle actin and DAPI.

Adenovirus mediated gene transfer of SIRT1 protein inhibits neointimal hyperplasia in mouse femoral artery after endothelial injury

Since SIRT1 was recently shown to inhibit VSMC proliferation and migration *in vitro*, the clinical relevance of SIRT1 in the development of vasculo-proliferative restenosis was studied by our group using a mouse femoral artery injury model for neointimal hyperplasia. Adenoviruses expressing native SIRT1 (Ad-SIRT1), dominant-negative SIRT1 (Ad-SIRT1-H335A), or a control adenovirus (Ad-Control) was delivered to the wire-denudated mouse femoral artery. Previous studies by our group (Sedding *et al.*, unpublished data) verified efficient gene expression from localized luminal gene delivery up to 4 weeks after injury. Representative photomicrographs of hematoxylin/eosin-stained femoral artery cross-sections 21 days following injury are shown in Figure 49a. Significant neointimal hyperplasia was observed in the presence of control

adenovirus transduction (n=18), or in the presence of Ad-SIRT1-H335A (n=18) with intima over media ratios (I/M) reaching 1.93 ± 0.31 and 2.04 ± 0.24 , respectively (Figure 49b). Overexpression of Ad-SIRT1 (n=18) attenuated neointimal hyperplasia with I/M ratio 0.56 ± 0.49 (Figure 49b).

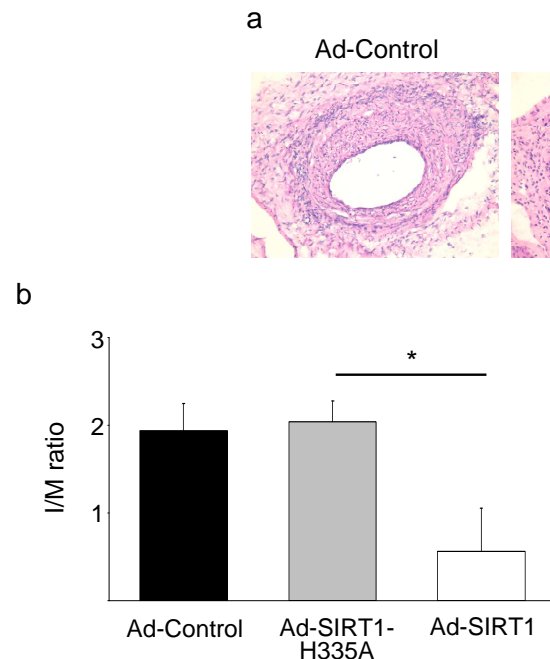


Figure 49. SIRT1 prevents neointima formation in vivo

a) Representative cross sections of mouse femoral arteries transduced with control vector (Ad-control), a constitutive inactive form of SIRT1 (Ad-SIRT1-H335A), or a wildtype SIRT1 (Ad-SIRT1) 21 days after dilatation are shown. The sections were stained with hematoxylin and eosin, and examined by light microscopy. **b)** Quantification of neointima/media (I/M) ratio of injured mouse femoral arteries, transduced with Ad-control, Ad-SIRT1-H335A or Ad-SIRT1 21 days after dilatation. Data represent means and standard deviations of 3 sections from 6 mice/group (* $p < 0.001$).

To gain insight into the mechanism of Ad-SIRT1-mediated inhibition of neointimal hyperplasia, mouse femoral artery sections were assayed for proliferation *in vivo*, using PCNA staining (Figure 50). At day 21 following injury, PCNA expression was significantly reduced in Ad-SIRT1-transduced arteries (Figure 50e, f) as compared to both Ad-Control virus-transduced vessels (Figure 50a, b) and arteries transduced with Ad-SIRT1-H335A (Figure 50c, d). Please note the PCNA positive cells being located in the media, a vessel layer known to consist of

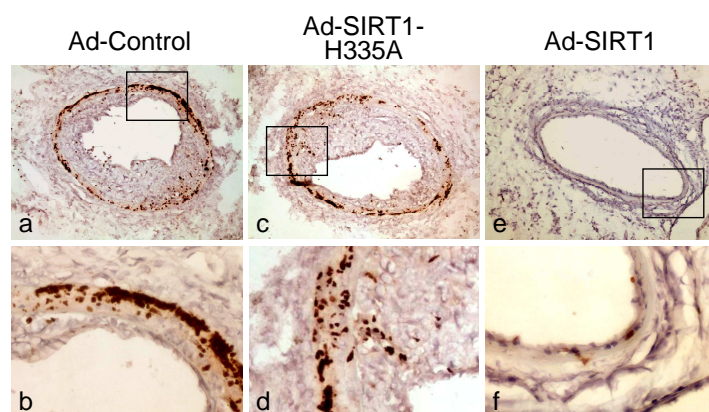


Figure 50. SIRT1 modulates cellular proliferation in vivo

In vivo cell proliferation was detected by using Zymed's PCNA staining kit in femoral artery sections of Ad-Control (**a** and **b**), Ad-SIRT1-H335A (**c** and **d**) and Ad-SIRT1-transduced vessels (**e** and **f**) at day 21 after endothelial denudation. **c**, **d** and **f** are high-magnification images of the boxed regions shown on low magnification images of the complete vessel (**a**, **c**, and **e**).

VSMCs, a cell type contributing mainly to the generation of neointimal tissue via proliferation (see “Introduction”).

Taken together, these data suggest that the deacetylase SIRT1 participates in protecting from neointimal hyperplasia by mediating inhibition of cell proliferation.

SIRT1 is expressed in VSMCs of human tissues

After having shown that SIRT1 is expressed in mouse arteries and that the deacetylase affects neointimal hyperplasia, I was interested in its distribution in human vessels and tissues generated during vasculo-proliferative diseases. Immunohistochemical analyses were performed on human aorta cross-sections as well as on sections from human atherectomy samples (representing removed atherosclerotic plaques from arteries). As presumed, human aortic VSMCs express SIRT1 within their nuclei (Figure 51a, b). Additionally, some plaque cells were SIRT1 positive, too (Figure 51c, d).

These staining demonstrate SIRT1 to be expressed not only in mouse cells and tissues but also in humans. Thus, SIRT1 seems to be a potential new target involved in the development of atherosclerosis and restenosis, and future investigations need to explore its detailed mechanism of action.

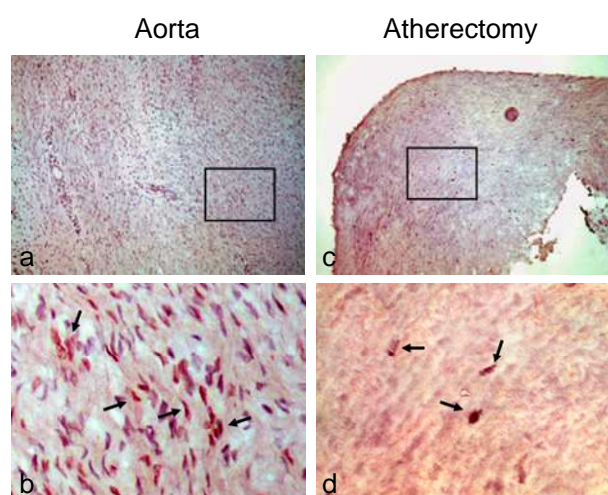


Figure 51. SIRT1 expression in human tissues

Cross-sections from a human aorta (a, b) and sections from human atherectomy samples (c, d) were stained for SIRT1 by immunohistochemistry using a broad spectrum Histostain-SAP Kit. Images a, and c are representative low-magnification images of the whole tissue, whereas b and d are high-magnification images of the boxed regions.

FoxO1a is not an interaction partner of SIRT1 in serum-stimulated HCASMCs

The previous extensive studies pointed out an important role for the deacetylase SIRT1 on regulating HCASMC proliferation *in vitro* and *in vivo*. A signaling pathway involved in regulating cell cycle progression and replication that is highly conserved among vertebrates is the insulin/IGF-1 signaling pathway. The FoxO transcription factors have been identified as a negative regulator of this pathway (see “Introduction”). Interestingly, publications of the last three years revealed a connection between the deacetylase SIRT1 and FoxO transcription

factors^{233, 262, 263}, however, these results were controversial. Nevertheless, FoxO transcription factors are promising interaction partners of SIRT1 in VSMCs of the artery system. Since we recently revealed FoxO1a's importance in regulating proliferation and migration in both HCASMCs and PASMCs (see above; Sedding *et al.*, unpublished data), SIRT1's influence on FoxO1a was investigated in the next part of this thesis.

As it was shown in Figure 38a and Figure 19a, both SIRT1 and FoxO1a localized to the nucleus under serum-free conditions. In response to FBS stimulation SIRT1 maintained its nuclear localization (Figure 38a), whereas ~ 51% of FoxO1a transcription factors translocated to the cytosol (Figure 19b). However, some FoxO1a proteins still remained in the nucleus. Since SIRT1 was shown to be responsible for inhibiting HCASMCs proliferation both under serum and non-serum conditions, the question arose whether endogenous FoxO1a is a direct substrate of SIRT1 within these cells *in vivo*. To test this, HCASMCs were grown on chamberslides and serum starved for 72 h for mimicking the quiescent state. Partially, chambers were treated with serum for 30 min pre-experimentally. Determination of close SIRT1/FoxO1a association (indicating an interaction of both proteins) was conducted by conventional double-labeling immunofluorescence followed by FRET-CLSM analysis. For analyzing interaction in serum-treated HCASMCs, FRET was measured only in cells where both proteins remained within the nucleus. A distinct increase in fluorescence (ΔIF) was detected in the bleached area of quiescence HCASMCs (mean $\Delta IF = 4.96$) (Figure 52f), revealing a close interaction between endogenous SIRT1 and FoxO1a. To exclude a false-positive FRET signal which might be caused by antibody cross-reactivity, both secondary antibodies were applied to sections that were incubated with the primary anti-FoxO1a antibody only (mean $\Delta IF = 0.28$). For measuring FRET in silenced HCASMCs, 54 regions of interest (ROIs) representing 54 nuclei of HCASMCs were observed, whereas for their corresponding control 44 ROIs were analyzed. The difference between both ΔIF s was highly significant (Figure 52f). Under serum stimulation, the mean FRET signal out of 52 ROIs decreased significantly ($\Delta IF = 3.26$) (Figure 52f), representing a highly significant loss of SIRT1/FoxO1a interaction in these cells. The ΔIF measured in the corresponding control group was low (mean $\Delta IF = 0.23$; 44 ROI) and highly significant to the experimental group.

To exclude SIRT1 to influence other FoxO isoforms, FRET analysis of FoxO3a and SIRT1 in HCASMCs was additionally performed. As it was already shown for FoxO1a, FoxO3a and SIRT1 closely interact in quiescent cell but loose their contact in response to FBS stimulation (data not shown).

Taken together, the close physiological interaction between endogenous human FoxO1a and SIRT1 in quiescent HCASMCs *in vivo* was demonstrated. However, serum stimulation

highly reduced their interaction, not only by inducing translocation of the FoxOs to the cytoplasm but also by loosening contact as determined by FRET. Thus, the effect of SIRT1 on attenuating HCASMC proliferation in growing cells is **not** due to a direct influence on FoxO1a function as it was suggested previously. It rather seems that SIRT1 controls HCASMC behavior under growth conditions by influencing other interaction partners besides FoxOs, which in turn themselves affect physiological processes. For further analyzing this hypothesis of yet unknown SIRT1 interaction partners in proliferating cells, our group used Antibody Arrays for screening protein-protein interactions. Several promising proteins were identified and one of those was already shown to directly interact with FoxO transcription factors. Further analysis will now be necessary to determine the molecular interactions and pathways of the newly found protein partners of SIRT1.

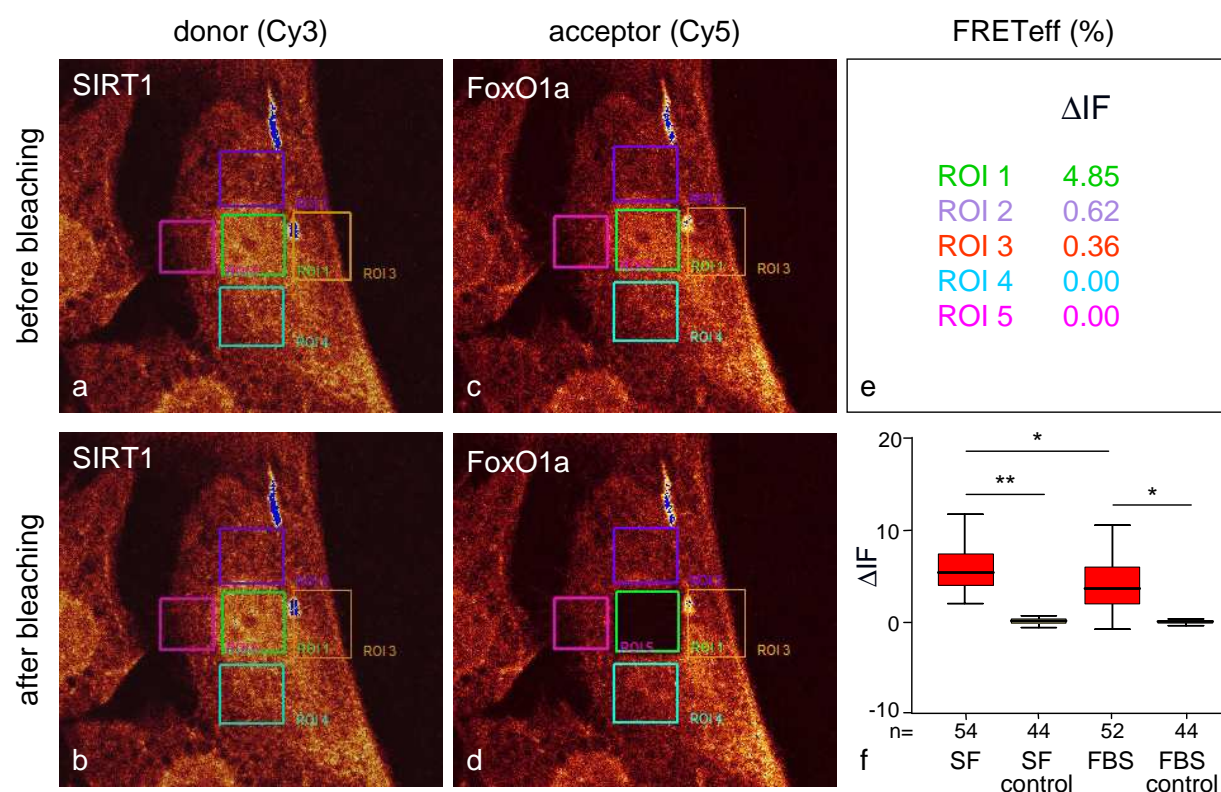


Figure 52. Detection of close association of SIRT1 and FoxO1a in HCASMCs

Close association between SIRT1 and FoxO1a in the nucleus of serum starved (SF) or FBS-stimulated HCASMCs was determined by double-labeling indirect immunofluorescence with subsequent FRET analysis. Representative images of donor (SIRT1 labeled with Cy3-conjugated antibody, **a**, **b**) and acceptor (FoxO1a labeled with Cy5-conjugated antibody, **c**, **d**) fluorescence of a FBS-treated nucleus. Cy5 was bleached in a region of interest 1 (compare ROI 1 in c and d). **e**) Increases in fluorescence (Δ IF) after bleaching for each ROI of one representative measurement are shown. ROI 1: bleached area (compare c-d). ROI 2-6: control area outside the bleached area. **f**) Δ IF in the nuclei of serum starved (SF) and FBS-treated HCASMCs as compared to their respective control group. Data represent mean values of 5 independent experiments. At least 44 ROIs were measured per condition (*p < 0.000, **p < 0.001, Mann-Whitney test; n=number of measurements). Boxplots: percentiles 0, 25, median, 75, 100.

SIRT1 deacetylates FoxO1a in HCASMCs

Given that SIRT1 functions as an NAD-dependent deacetylase and that it interacts with FoxO1a in quiescent cells, I investigated whether SIRT1 catalyzes the deacetylation of this transcription factor directly in serum-deprived HCASMCs. Therefore silenced HCASMCs were incubated for 16 h with or without NAM (SIRT1-specific) and Trichostatin A (TSA; a class I and II HDAC inhibitor^{277, 280}) for inhibiting all endogenous deacetylases. Subsequently, acetylated-lysines were immunoprecipitated from cell lysates and immune complexes were analyzed for FoxO1a by Western blot. Treatment with SIRT1 inhibitor NAM alone or with TSA alone had no visible effect on FoxO1a acetylation (Figure 53). By contrast, incubation of cells with a mix of TSA and NAM prevented deacetylation of endogenous FoxO1a, thus levels of acetylated FoxO1a augmented (Figure 53, Figure 63).

This result suggests that SIRT1 as well as Class I and II HDACs contribute to FoxO1a's deacetylation within HCASMCs.

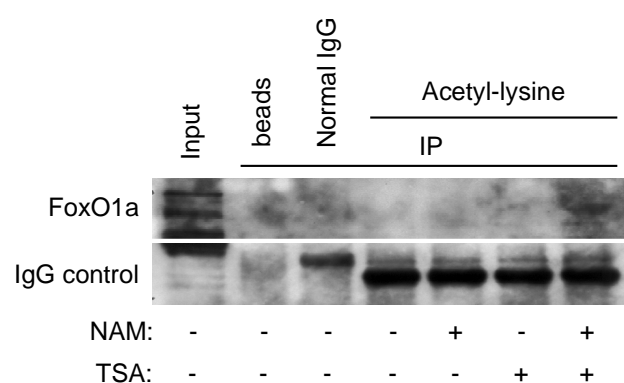


Figure 53. FoxO1a is deacetylated by SIRT1 in HCASMCs

HCASMCs were serum starved for 60 h followed by 16 h incubation with or without NAM (50 mM) and TSA (10 μ M) as indicated. Cell lysates were subjected to immunoprecipitation with an antibody for acetylated-lysines and immune complexes were analyzed by Western blot for FoxO1a. The IgG control panel indicates the IgG that correlates to the anti-acetylated antibodies and monitors the addition of the same quantity of anti-acetylated antibodies in every sample.

Deacetylation of FoxO1a by SIRT1 enhances its transcriptional activity

In the next set of experiments, I investigated whether SIRT1-mediated deacetylation of FoxO1a in quiescent HCASMCs stimulates FoxO transcriptional and biological activity. The transcriptional activity of FoxO1a from different nuclear extracts was analyzed using a commercially available FoxO1a activity assay. Consistent with their capacity to increase the abundance of acetylated FoxO1a in silenced HCASMCs, treatment with TSA/NAM significantly decreased FoxO1a activity (Figure 54a). A distinct loss in FoxO1a activity was seen in HCASMCs stimulated with serum (Figure 54a). Although NAM alone did not affect the amount of acetylated FoxO1a in immunoprecipitation experiments (Figure 53), treatment with the SIRT1 inhibitor significantly attenuated FoxO1a binding to its specific promoter element (Figure 54b).

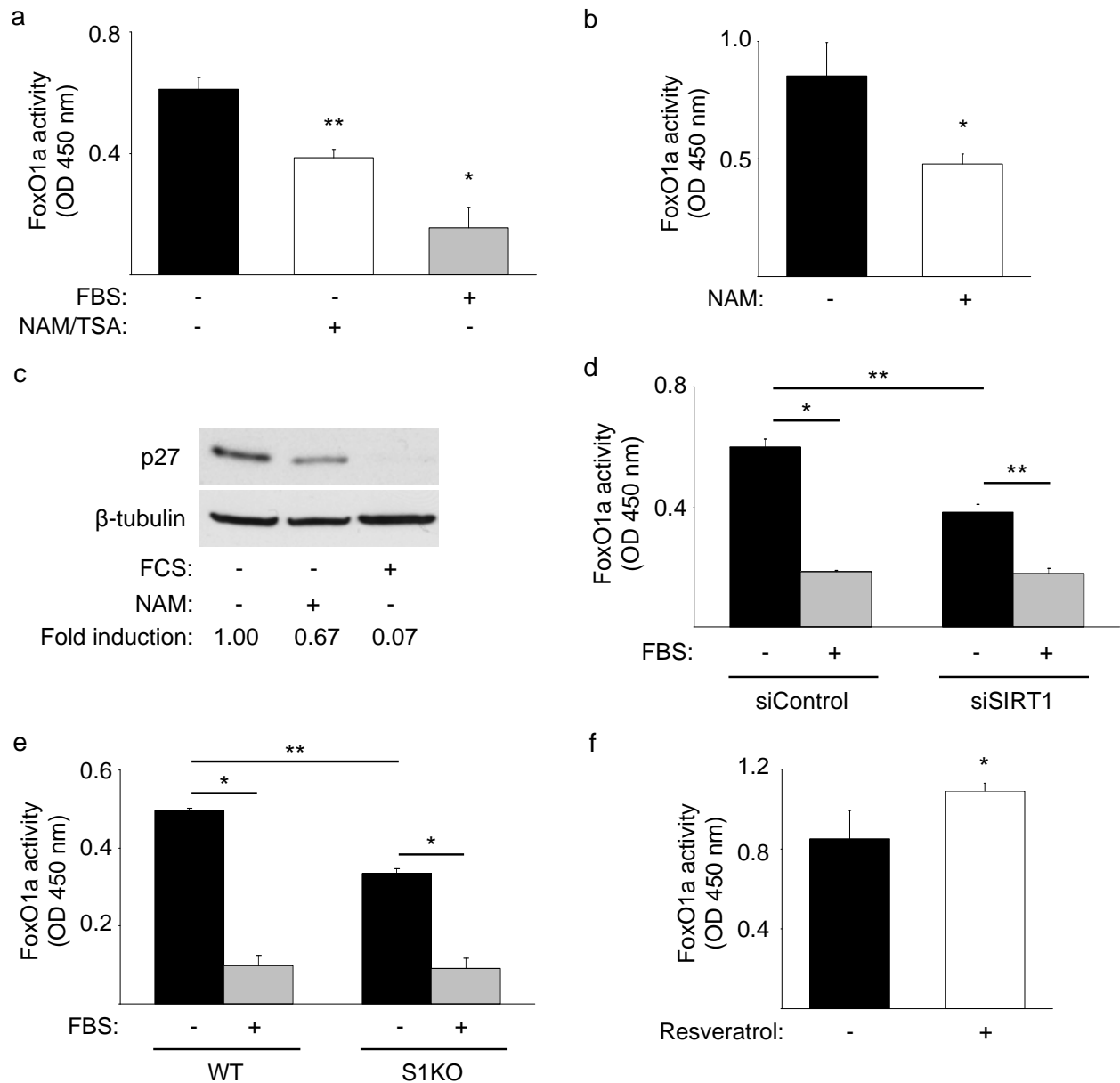


Figure 54. Enhancement of FoxO1a transcriptional activity by SIRT1

HCASMCs were serum-starved for 60 h followed by incubation with or without the indicated agents for 16 h. Nuclear extracts were extracted and FoxO1a's transcriptional activity was measured by ELISA (a,b, f). **a)** Silenced HCASMCs were treated with or without a mix of NAM (50 mM) and TSA (10 μ M). Non-treated cells stimulated with 20% FBS 30 min post-experimentally were used for control. (* p < 0.01, ** p < 0.02 vs. serum-free control; n =2). **b)** Quiescent HCASMCs were incubated with or without NAM (50 mM) and assayed for FoxO1a activity. (* p < 0.05 vs. non-treated control; n =2). **c)** HCASMCs were treated as in b) and whole cell lysates were subjected to immunoblotting with antibodies for p27^{KIP1} and β -tubulin. **d)** HCASMCs were transfected with non-silencing siRNA or siRNA targeting SIRT1. 24 h post-transfection, cells were set on serum-free medium for 48 h. 30 min before extracting nuclear lysates and determining FoxO1a activity using an ELISA, part of the cells were stimulated with 20% FBS (* p < 0.001, ** p < 0.01; n =2). **e)** MEF deriving from SIRT1-knockout mice or from their wild-type littermates (WT) were serum-starved for 12 h and stimulated for 30 min with or without 20% FBS. FoxO1a activity in the nuclear extracts was determined by ELISA (* p < 0.001, ** p < 0.01; n =2). **f)** Quiescent HCASMCs were incubated in the presence or absence of resveratrol (20 μ M) for 16 h and subjected to FoxO1a activity ELISA (* p < 0.07 vs. non-treated control; n =2). All data are mean absorbance values and standard deviations from experiments repeated at least twice with similar results. Statistical significance of all experiments was determined by ANOVA.

Moreover, NAM-mediated inhibition of SIRT1 function resulted in a reduced transactivation activity of FoxO1a: Expression of endogenous human p27^{KIP1} is decreased upon NAM treatment as determined by Western blot (Figure 54c). Previously, I demonstrated FoxO1a to be involved in the transcriptional activation of this cell-cycle inhibitor gene (Figure 25), therefore outcome of this protein is appropriate for analyzing FoxO1a transactivity.

Furthermore to pharmacologically inhibiting SIRT1, transient downregulation of SIRT1 by siRNA resulted in decreased FoxO1a activity in quiescent HCASMCs as compared to cells transfected with a non-targeting control siRNA (Figure 54d). Similar results were obtained with SIRT1-knockout MEFs and their wild-type littermates (Figure 54e). Once SIRT1 function was downregulated (either by siRNA or in SIRT1-knockout MEF), FoxO1a activity in serum-stimulated cells was not significantly further attenuated, indicating an independency of residual FoxO1a function from SIRT1.

As shown in Figure 54f, the transactivation activity of FoxO1a in quiescent HCASMCs was slightly increased in the presence of the SIRT1 activator resveratrol. Thus, increasing SIRT1 function seems to increase transactivation activity of FoxO1a. This observation fits to further results of mine, however appears to be uncommonly due to the knowledge of FoxO1a being highly activated under serum-free conditions. However, as it will be shown in the later part of the thesis, different stimuli are able to further increase SIRT1/FoxO1a interaction in quiescent HCASMCs and thus, an increase in FoxO1a activity seems to be possible upon resveratrol treatment.

In the end of this part, it can be summarized that SIRT1 contributes to proliferation inhibition in silenced HCASMCs *in vitro* and *in vivo* by deacetylating FoxO1a and thereby enhancing its transcriptional activity resulting in induced gene expression of p27^{KIP1}.

Effect of SIRT1 on HCASMC programmed cell death

Besides controlling cell cycle arrest^{169, 215, 226}, FoxO transcription factors have been shown to be involved in cell processes such as detoxification of reactive oxygen species (ROS)^{170, 171}, repair of damaged DNA¹⁶⁹, and apoptosis^{191, 194}. The deacetylase SIRT1 was shown to play a key role in resistance to stress in *C. elegans* contributing to an increase in longevity. It does so by stimulating the activity of FoxO-homologues^{304, 305} through direct binding³⁰⁶. Research represented in this thesis now demonstrates FoxO1a's contribution to HCASMC apoptotic cell death *in vitro* and *in vivo*. Since these cells have a predominant role in vascular disorders such as atherosclerosis, and apoptosis of these cells can lead to plaque rupture (see "Introduction"), modulating FoxO1a activity by SIRT1 could represent an effective approach for targeting CAD. Thus, the next part of my thesis deals with the influence of SIRT1 on VSMC apoptosis and clarifies the effect of SIRT1 on FoxO1a function in response to stress stimuli.

Pharmacological inhibition of endogenous SIRT1 induces apoptosis in HCASMCs

To examine the function of SIRT1 on HCASMCs cell viability, quiescent HCASMCs were incubated with either NAM or sirtinol, both agents known inhibitors of SIRT1 function²⁹²⁻²⁹⁵. Treatment with NAM for 48 h caused intracellular cytoplasmic blebbing, cell shrinkage and membrane detachment dose-dependently as determined by morphology (Figure 55a). Comparable findings were gained with sirtinol. Cell death induced by each agent was not caused by increased vehicle concentrations since the same concentrations of DMSO alone did not lead to cell death (data not shown).

Cell viability of HCASMCs was detected by WST-1 assays and absorbance values are expressed in Figure 55b. Treatment with NAM and sirtinol, respectively, significantly decreased the numbers of viable cell as compared to non-treated control cells. These results suggest that the enzymatic activity of SIRT1 is involved in cell survival, and that inhibition of SIRT1 by pharmacological drugs leads to reduced cell numbers.

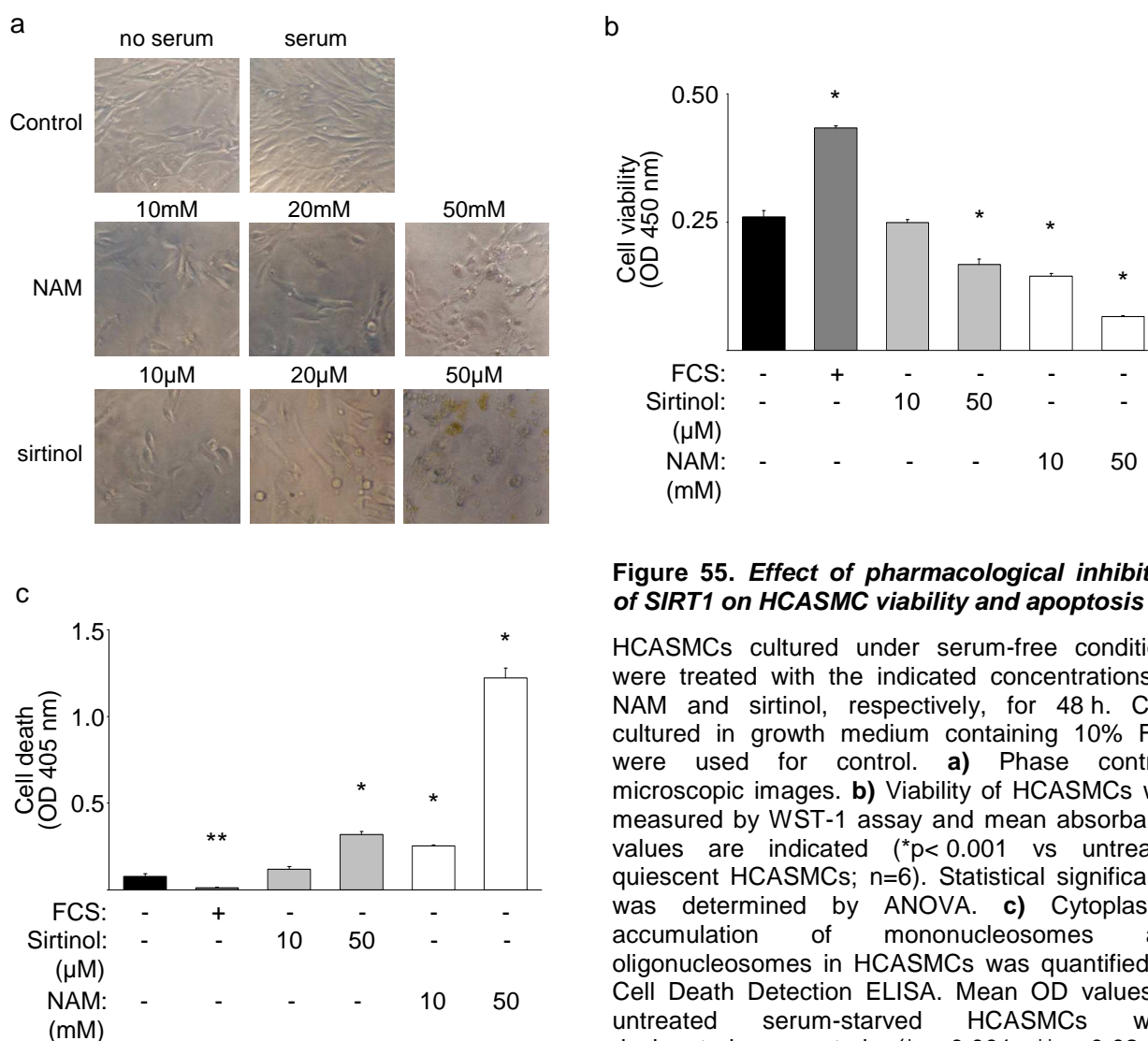


Figure 55. Effect of pharmacological inhibition of SIRT1 on HCASMC viability and apoptosis

HCASMCs cultured under serum-free conditions were treated with the indicated concentrations of NAM and sirtinol, respectively, for 48 h. Cells cultured in growth medium containing 10% FBS were used for control. **a)** Phase contrast microscopic images. **b)** Viability of HCASMCs was measured by WST-1 assay and mean absorbance values are indicated (* $p < 0.001$ vs untreated quiescent HCASMCs; $n=6$). Statistical significance was determined by ANOVA. **c)** Cytoplasmic accumulation of mononucleosomes and oligonucleosomes in HCASMCs was quantified by Cell Death Detection ELISA. Mean OD values of untreated serum-starved HCASMCs were designated as controls (* $p < 0.001$, ** $p < 0.02$ vs. untreated quiescent HCASMCs; $n=3$). Statistical significance was determined by ANOVA.

A reduction in cell number can be caused on the one hand by inhibition of cell cycle progression and proliferation (Figure 41, ff) and on the other hand by an increase in cell death induced by apoptosis or necrosis. To examine whether SIRT1-inhibitor-induced HCASMC cell reduction is attributable to apoptosis, Cell Death Detection ELISAs were performed. After treatment with either NAM or sirtinol for 48 h, HCASMCs significantly accumulated mononucleosomes and oligonucleosomes in the cytoplasm. The presence of both kinds of nucleosomes is a sensitive marker of apoptosis (Figure 55c). As it was previously shown for pulmonary VSMCs (Figure 34d), stressing HCASMCs by serum- deprivation slightly but significantly enhanced apoptotic cell death rates as compared to apoptosis rates of FBS-stimulated cells.

Together, these results indicate that HCASMC survival seems to be, at least partially, dependent on SIRT1 function and that inhibition of SIRT1 activity results in apoptotic cell death.

Hydrogenperoxide treatment induces HCASMCs apoptosis

To determine whether oxidative stress induces apoptosis of HCASMCs, HCASMCs were treated for different times with 0.5 mM of H_2O_2 , a known oxidative stressor. Based on morphology, apoptotic morphological changes such as increased cell shrinkage and membrane detachment from the surrounding cells was noted after an incubation with H_2O_2 for at least 4 h (Figure 56a). Cell Death Detection ELISAs of HCASMCs cultured under peroxide stress revealed significant increases of DNA cleavage as compared to non-stressed serum-starved cells (Figure 56b). Actinomycin D, an anti-neoplastic antibiotic that induces apoptosis through inhibiting RNA synthesis, was used as pro-apoptotic control agent (Figure 56b).

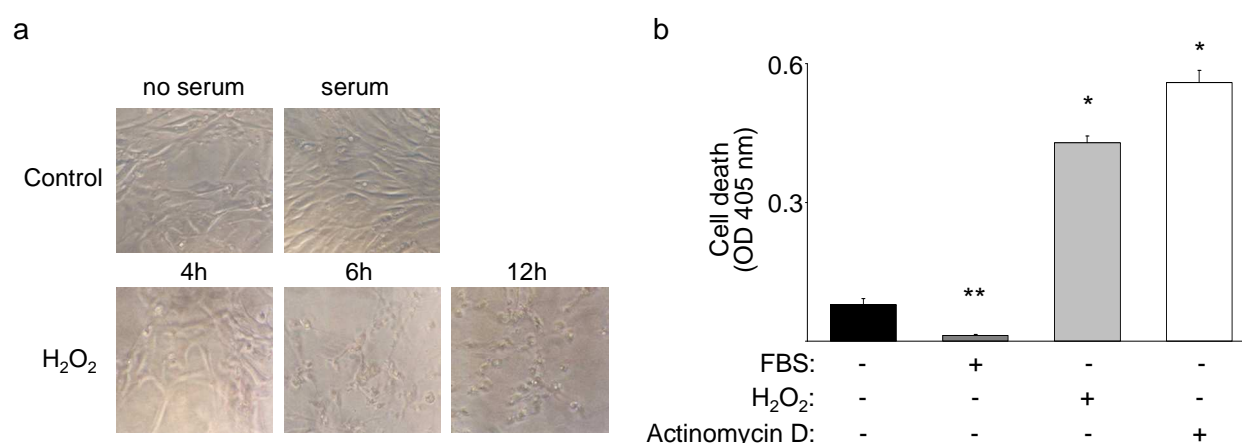


Figure 56. H_2O_2 induces apoptosis of HCASMCs

HCASMCs treated with 0.5 mM H_2O_2 for the indicated periods. **a**) Cell morphology was determined by phase contrast microscopy. **b**) Apoptosis rates of serum-starved HCASMCs were measured by ELISA after a 16 h treatment with either H_2O_2 (0.5 mM) or Actinomycin D (1 μ g/ml). Data are means plus standard deviations of three measurements. Apoptosis rates of serum-stimulated cells were used as controls (* p < 0.001, ** p < 0.01 compared to serum-free control). Statistical significance was determined by ANOVA. Results were verified by two independent experiments.

Suppression of SIRT1 by siRNA technique induces apoptosis of HCASMCs

Inhibitors of SIRT1 are shown to affect HCASMC function, however, there is no real evidence for these substances of being 100% SIRT1-specific. To overcome this problem, HCASMCs were transfected with either non-targeting control siRNA or siRNA for downregulating SIRT1 mRNA. The specificity of SIRT1 siRNA on SIRT1 downregulation was shown elsewhere (Figure 39). Cell viability was measured by WST-1 assays (Figure 57a). As previously demonstrated, hydrogen peroxide (H_2O_2) is a potent inducer of apoptosis in HCASMCs (Figure 56). To examine the influence of SIRT1 on H_2O_2 -induced apoptosis, transfected HCASMCs were treated with H_2O_2 (0.5 mM). Downregulation of SIRT1 resulted in a significant attenuation of HCASMC viability as compared to control-transfected cells (Figure 57a). Treatment with H_2O_2 exacerbated the situation by further decreasing cell viability of both SIRT1-deprived HCASMCs and control-transfected cells (Figure 57a).

Using these same cells in Cell Death Detection ELISA, I determined whether SIRT1 is responsible for modulating both starvation- and H_2O_2 -induced HCASMC apoptosis (Figure 57b). In the absence of SIRT1, HCASMCs showed significantly increased apoptosis rates in response to serum-withdrawal as compared to control-transfected cells grown under the same culturing conditions (Figure 57b). H_2O_2 -induced apoptotic cell death rates of SIRT1-deprived HCASMCs were also significantly higher to that of control-transfected cells (Figure 57b), revealing an increase in oxidative stress sensitivity in the absence of SIRT1.

Thus, these results confirm the earlier observations made by downregulating SIRT1 function pharmacologically. SIRT1 function seems to somehow protect HCASMCs from apoptosis both under serum-free conditions and in response to oxidative stress.

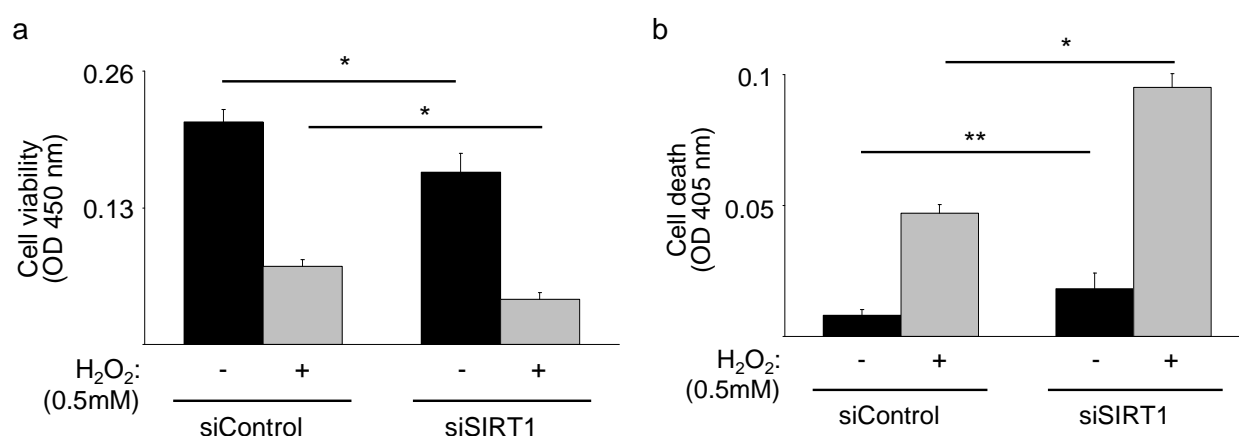


Figure 57. Effect of SIRT1 downregulation on HCASMC viability and apoptosis

HCASMCs were transfected with siRNA for SIRT1 (siSIRT1) or a non-targeting siRNA (siControl). 24 h post-transfection HCASMCs were serum-starved for 48 h and treated with or without 0.5 mM H_2O_2 for 16 h pre-experimentally. **a)** Cell viabilities were detected by WST-1 assay, and mean absorbance values plus standard deviations are shown (* $p < 0.001$; $n = 6$). **b)** Apoptosis rates of siControl and siSIRT1-transfected HCASMCs were analyzed by ELISA. Data represent means and error bars of OD values (* $p < 0.001$, ** $p < 0.05$; $n = 3$). Data depicted are representative of at least three independent experiments from different HCASMC aliquots. Statistical significance of both experiments was determined by ANOVA.

SIRT1 protects mouse embryonic fibroblasts from H₂O₂-mediated cell death

To further assess the role of endogenous SIRT1 on H₂O₂-mediated cell death in non-vascular cell types, I studied the impact of SIRT1 on MEFs - either derived from wild-type or SIRT1-knockout mice - upon peroxide treatment. The MEFs were analyzed concerning cell viability and apoptosis. Wild-type and SIRT1-null MEFs were kept under serum-free conditions and treated with or without H₂O₂. WST-1 assays revealed that MEFs from SIRT1-knockout mice showed slight decreases in cell viability as compared to MEFs from wild-type mice - both under serum-free and peroxide conditions (Figure 58a).

Cell Death Detection ELISAs further supported these results (Figure 58b). In the presence of oxidative stress stimuli such as H₂O₂, apoptosis rates of both SIRT1-knockout MEFs and wild-type MEFs were significantly augmented as compared to that of their respective serum-starved controls. Furthermore, serum-starvation alone strongly triggered apoptotic DNA cleavage in SIRT1-null MEF as compared to wild-type MEFs indicating the high sensitivity of SIRT1-knockout MEF to many types of stress stimuli (Figure 58b).

These findings are consistent with findings by Brunet *et al.*²³³ and indicate that SIRT1-null MEFs are more sensitive to both serum-starvation and H₂O₂-induced cell death than wild-type MEFs. Taken together, my results demonstrate that endogenous SIRT1 contributes to cell survival not only in human VSMCs but also in mouse fibroblasts.

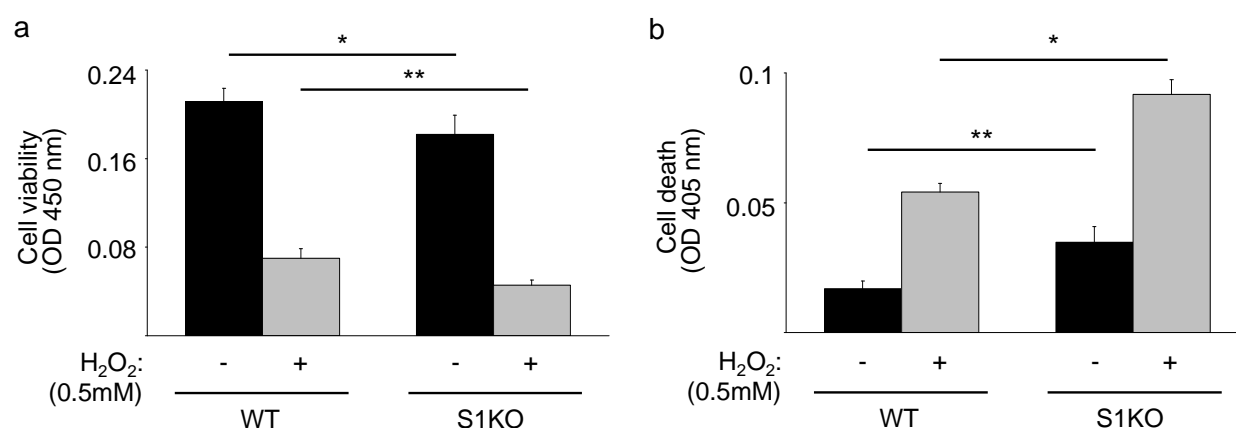


Figure 58. Cell viability and death in SIRT1 ^{-/-} and wild-type MEFs

MEFs from both wild-type (WT) and SIRT1-knockout mice were serum-starved for 14 h and subsequently incubated with or without H₂O₂ (0.5 mM) for 2 h. **a)** MEF viabilities were analyzed by WST-1 assays. Mean absorbance values and error bars are indicated (*p < 0.001, **p < 0.01; n=6). **b)** Apoptosis rates of WT MEFs and SIRT1-null MEFs were assessed by Cell Death Detection ELISA. Data presented represent means and error bars of three measurements (*p < 0.001, **p < 0.01). All experiments were performed at least five times with similar results and statistical significance was determined by ANOVA.

Stimulation of endogenous SIRT1 activity reduces HCASMC apoptosis in response to serum-starvation

Since inhibition of SIRT1 function increases HCASMC apoptosis, the question arose whether stimulation of SIRT1 function can prevent HCASMC apoptosis induced by serum-starvation. Therefore silenced HCASMCs were stimulated with resveratrol, a known activator of SIRT1 activity²⁹⁷ (see above). Quantitative cell death analyses demonstrated HCASMCs to have significantly decreased amounts of accumulated mono- and oligonucleosomes in the cytoplasm (Figure 59). Thus, stimulation of SIRT1 activity by the plant polyphenol slightly inhibited serum-starvation-mediated nuclear fragmentation dose-dependently.

This result suggests that endogenous SIRT1 activity can be pharmacologically increased in HCASMCs and that increased activity of SIRT1 protects the cells from apoptotic cell death caused by serum-starvation.

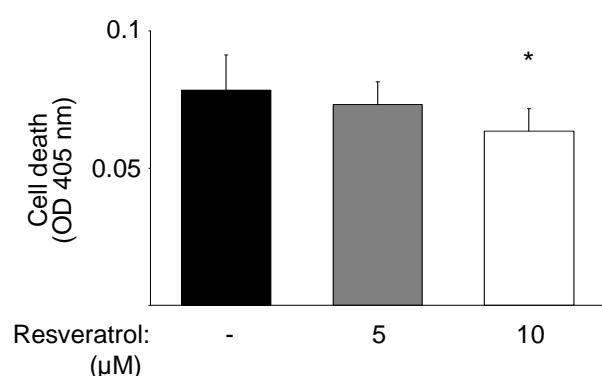


Figure 59. Resveratrol protects HCASMCs from apoptotic cell death

HCASMCs were silenced for 60 h and subsequently incubated in serum-free medium containing resveratrol at the indicated concentration for 16 h. Accumulation of mono- and oligonucleosomes in the cytoplasm was analyzed using commercially available Cell Death Detection ELISAs. Mean OD values were presented (* $p < 0.01$ vs serum-free control, $n=3$). Experiments were performed twice with similar results. Statistical significance was determined by ANOVA.

Adenoviral overexpression of active or inactive SIRT1 affects HCASMC viability and apoptotic cell death

Since inhibition of SIRT1 function increases HCASMC apoptosis, the question arose whether stimulation of SIRT1 function can reduce the number of cells committing suicide in response to serum-starvation. Therefore, our group transduced cells with adenoviruses either encoding functionally active SIRT1 or the catalytically inactive SIRT1 mutant H335A (see Figure 46). Overexpression of functional active SIRT1 decreased HCASMC apoptosis as compared to cells transduced with a control-adenovirus (data not shown). No significant differences in cell death were observed in cell populations exposed to control-adenovirus or adenovirus encoding functional inactive SIRT1 (data not shown).

Consistently with my previous results our groups' data suggest that SIRT1 is an important regulator of VSMC apoptosis and increases in cell death seem to be due to a lack of SIRT1 function.

SIRT1 protein expression is upregulated during apoptosis induction

After having shown that SIRT1 function plays an important role in HCASMC survival, I was interested in the expression levels of SIRT1 and its localization during the cells stress response. Therefore, protein expression levels of SIRT1 in response to peroxide stress were assayed by immunoblotting with an antibody for SIRT1 (Figure 60a). SIRT1 expression was significantly upregulated 24 to 48 h after application of H_2O_2 . Scanning densitometry of two immunoblots was used to quantify relative SIRT1 protein levels (normalized to vinculin) (Figure 60b). To verify induction of programmed cell death in response to oxidative stress stimuli, immunoblot analysis of PARP protein levels were performed (Figure 60a). Cleavage of PARP, a characteristic process during apoptosis, was depicted by a decrease in PARP levels in the course of H_2O_2 treatment.

Regarding the cells stress response, this experiment clearly demonstrated SIRT1 expression to increase over time in response to apoptotic stress stimuli such as peroxide treatment.

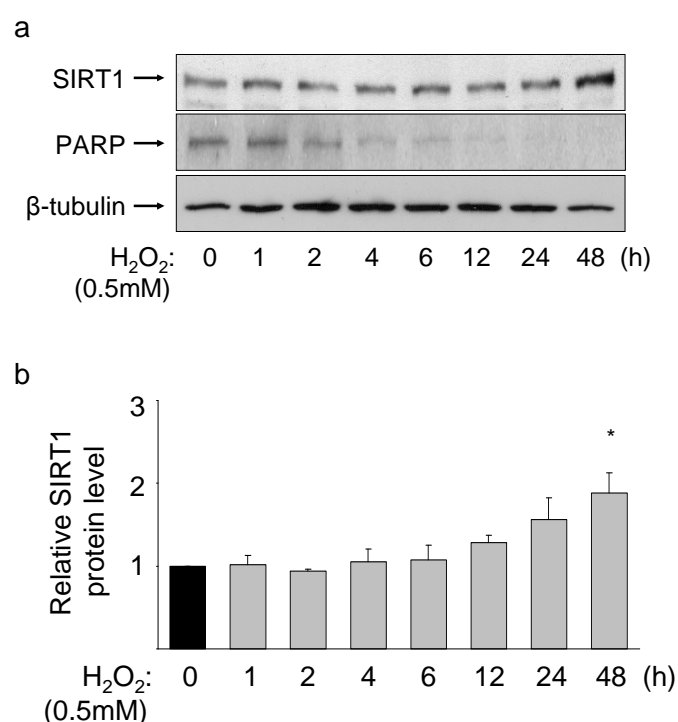


Figure 60. SIRT1 expression is upregulated in response to apoptotic stimuli

a) HCASMCs were cultured in the absence of serum for 48 h and subsequently treated with 0.5 mM H_2O_2 for the indicated time periods. Afterwards, cells were lysed and subjected to immunoblot analysis with antibodies for SIRT1, PARP or vinculin. **b)** Changes in SIRT1 protein levels during peroxide treatment were quantified with BioDoc Analyzer software. SIRT1 level (normalized to β -tubulin loading control) at time 0 h was arbitrarily set 1. Mean values and standard deviations of two independent immunoblots are shown (* $p < 0.005$ vs. 0 h).

SIRT1 and FoxOs are localized to the nuclei of peroxide stressed HCASMCs

The cellular distribution of SIRT1 under stress stimuli was determined by immunostaining as described in the “Materials and Methods”-part of this thesis. SIRT1 localized within the nuclei of H_2O_2 -treated quiescent HCASMCs (Figure 61a). Since SIRT1 was already shown to localize preferentially to the nucleus both under serum-free and serum conditions (Figure 38a), the deacetylase SIRT1 maintains its position in response to oxidative stress.

The next step of my research was to identify potential SIRT1 interaction partners. Recently, I excluded an interaction of SIRT1 with the FoxO1a transcription factors under pro-proliferative conditions. Since oxidative stress stimuli trigger different intracellular pathways than serum stimulation does, an interaction of SIRT1 with FoxO transcription factors upon peroxide treatment seemed to be possible and needed to be explored. The cellular distribution of endogenous FoxO1a transcription factor under stress stimuli was determined by immunostaining. Interestingly, treatment of quiescent HCASMCs with H_2O_2 caused nuclear accumulation of FoxO1a (Figure 61b) similar to serum-starvation (fig). Furthermore, immunohistochemical studies with double-staining for SIRT1 and FoxO1a showed that endogenous FoxO1a co-localized with SIRT1 within the nucleus during H_2O_2 treatment (Figure 61c), a phenomenon that was already show previously in quiescent cells (Figure 52).

Thus, the requirements for a possible SIRT1/FoxO1a interaction in peroxide stressed cell were fulfilled.

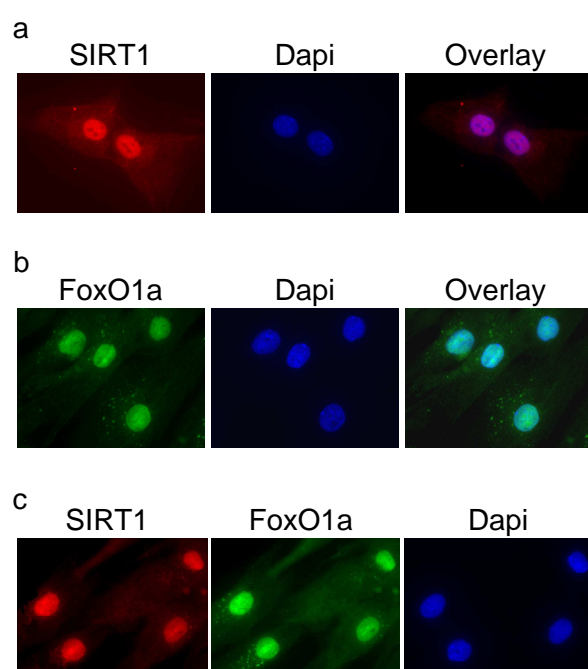


Figure 61. Localization of SIRT1 and FoxO1a in response to peroxide stress

Qualitative analysis of endogenous SIRT1 and FoxO1a localization in silenced HCASMCs treated with H_2O_2 (0.5 mM) for 30 min. **a)** SIRT1 was labeled with a Cy3-conjugated antibody (red). **b)** FoxO1a was detected by an Alexa 488-coupled antibody (green). **c)** FoxO1a-SIRT1 doublestaining in HCASMCs treated with H_2O_2 . DAPI was always used to stain the cells nuclei. Each staining was performed at least 3 times with the same results.

SIRT1 interacts with FoxO1a during peroxide stress

After having shown that under conditions of oxidative stress, both FoxO1a and SIRT1 are present within the nucleus, I next examined if there is a physiological interaction between both endogenous proteins. Conventional double-labeling immunofluorescence followed by FRET-CLSM analysis was performed with quiescent HCASMCs treated with or without H_2O_2 (Figure 62). A clear increase of fluorescence was detected in the bleached area of stress-stimulated HCASMCs (mean $\Delta IF = 8.24$) as compared to quiescent ones (SF) (mean $\Delta IF = 4.96$) (Figure 62f). The difference between both ΔIF s was highly significant ($*p < 0.000$ (Figure 62f)). For H_2O_2

measurements 31 ROIs of HCASMCs obtained from 5 independent aliquots were observed, whereas for SF 44 ROIs were measured. To exclude a false-positive FRET signal which might be caused by antibody cross-reactivity, both secondary antibodies were applied to sections that were incubated with the primary anti-FoxO1a antibody only. The control ΔIF quantified in the same region was low (mean for H_2O_2 : $\Delta IF = 0.46$; for SF: $\Delta IF = 0.28$). As compared to their corresponding controls the differences between the ΔIF observed in both experimental group was also highly significant ($*p < 0.000$ (Figure 62)).

With this experiment, a strong interaction between endogenous FoxO1a and SIRT1 in serum-starved HCASMCs was detected (additionally see Figure 52) and oxidative stress treatment further enhanced the FoxO1a/SIRT1 association.

To identify whether FoxO3a as a second important FoxO transcription factors interacts with SIRT1 in response to peroxide stress, FRET analysis of FoxO3a and SIRT1 were performed.

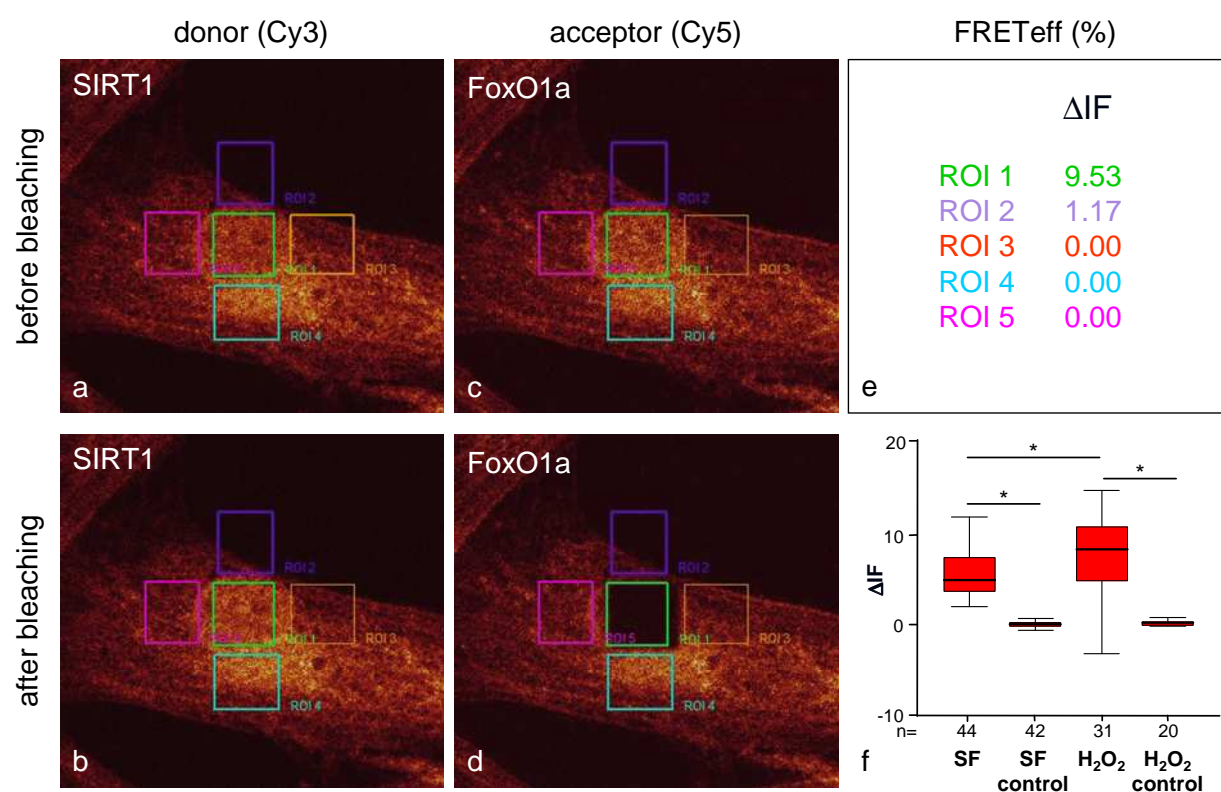


Figure 62. Detection of close association of SIRT1 and FoxO1a in HCASMCs

Close association between SIRT1 and FoxO1a in the nucleus of serum-starved (SF) or H_2O_2 -treated HCASMCs was determined by double-labeling indirect immunofluorescence with subsequent FRET analysis. Representative images of donor (SIRT1 labeled with Cy3-conjugated antibody) (a, b), and acceptor (FoxO1a labeled with Cy5-conjugated antibody) (c, d) fluorescence of a H_2O_2 -treated nucleus. Cy5 was bleached in a region of interest 1 (compare ROI 1 in c and d). e) ΔIF for each ROI of this representative measurement. ROI 1: bleached area (compare c-d). ROI 2-6: control area outside the bleached area. f) ΔIF in the nuclei of serum-starved (SF) and H_2O_2 treated HCASMCs as compared to their respective control group. Data represent mean values of 5 independent experiments. At least 20 ROIs were measured per condition ($*p < 0.000$, Mann-Whitney test; n=number of measurements). Boxplots: percentiles 0, 25, median, 75, 100.

Interestingly, treatment with H₂O₂ did not only affect FoxO1a/SIRT1 interaction but also increased a FoxO3a/SIRT1 interplay (data not shown). Thus, it seems that different FoxO transcription factors contribute to the transmission of intracellular stress signals.

FoxO1a is deacetylated by SIRT1 in response to peroxide induced stress

The observation that SIRT1 and FoxO1a interact in response to oxidative stress and that FoxO1a is a deacetylation product in HCASMCs (Figure 53) raised the possibility that, within this complex, FoxO1a is a substrate of SIRT1. To determine if SIRT1 directly deacetylates FoxO1a upon peroxide treatment, silenced HCASMCs were treated with H₂O₂ (0.5 mM) and acetylated proteins were immunoprecipitated with an antibody for acetylated-lysines. Acetylated FoxO1a was assessed by Western blot with an antibody for FoxO1a. Oxidative stress stimuli slightly increased the amount of acetylated FoxO1a in the cells (Figure 63), which is not surprisingly since H₂O₂ is known to promote acetylation of different proteins including FoxOs²³³,

263

Incubation of NAM-pretreated HCASMCs with H₂O₂ significant increased the amount of acetylated FoxO1a as compared to non-pretreated HCASMCs (Figure 63), and acetylation levels of FoxO1a in NAM/H₂O₂-treated cells are comparable to those from cells completely missing HDAC activity (TSA/NAM treatment) (Figure 63, see also Figure 53).

These observations thus indeed indicate that the enhanced nuclear location and interaction of FoxO1a and SIRT1 during peroxide stress is important for a SIRT1-mediated deacetylation of FoxO1a. In summary SIRT1 reverses H₂O₂-induced acetylation of the transcription factor.

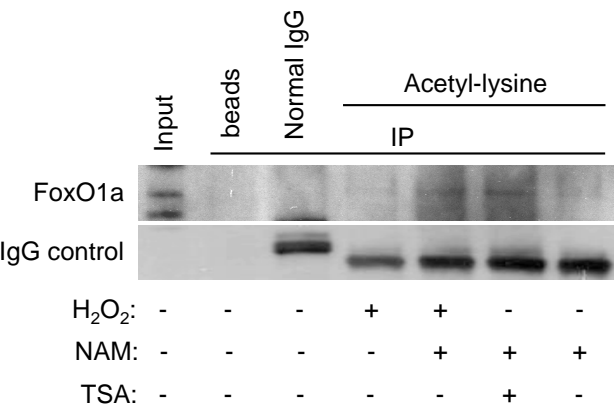


Figure 63. Acetylation levels of FoxO1a during peroxide stress

HCASMCs were serum-starved for 60 h, incubated for 12 h in the absence or presence of NAM (10 mM) or TSA (10 μM) and subsequently treated with H₂O₂ (0.5 mM) for 1 h. Cell lysates were subjected to immunoprecipitation with an antibody for acetylated-lysines and resulting precipitates were subjected to immunoblot analysis with an antibody for FoxO1a. The upper IgG control panel indicates the IgG that correlates to the anti-acetylated antibodies and monitors the addition of the same quantity of anti-acetylated antibodies in every sample.

SIRT1 enhances cell survival following exposure to oxidative stress by shifting FoxO1a-induced responses away from apoptotic cell death and towards cell-cycle arrest and survival

We and others have previously shown that members of the FoxO family transactivate a number of target genes that have crucial roles in the cell's response to stress stimuli, e.g. genes that control repair of damaged DNA (GADD45)^{168, 169} and ROS detoxification (MnSOD and catalase)¹⁶⁸⁻¹⁷¹. After having already proven that SIRT1-mediated deacetylation of FoxO1a results in an increased activity of the transcription factor, and that SIRT1 function protects HCASMCs from programmed cell death, the question arose whether SIRT1 affects FoxO1a-dependent transcription of pro-survival genes in response to H₂O₂ treatment. To clarify the role of endogenous SIRT1 on FoxO1a-mediated GADD45 induction in response to oxidative stress, HCASMCs depleted of SIRT1 using siRNA and control cells were treated with 0.5 mM H₂O₂ for the indicated times (Figure 64a, b). Subsequently, FoxO-mediated pro-survival target gene induction was monitored by immunoblot analysis. In control-transfected HCASMCs, GADD45 protein levels rose in response peroxide stimulation (Figure 64a, b). Interestingly, this induction was inhibited in HCASMCs depleted of endogenous SIRT1 (Figure 64a, b); in these cells almost no GADD45 was expressed.

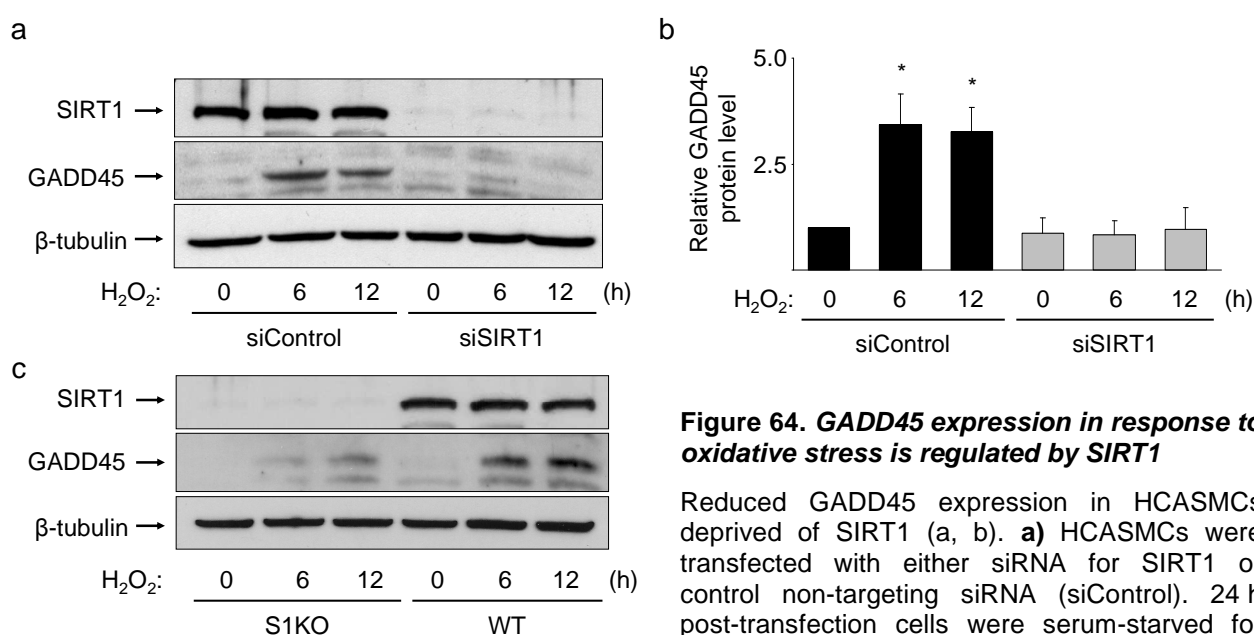


Figure 64. GADD45 expression in response to oxidative stress is regulated by SIRT1

Reduced GADD45 expression in HCASMCs deprived of SIRT1 (a, b). **a)** HCASMCs were transfected with either siRNA for SIRT1 or control non-targeting siRNA (siControl). 24 h post-transfection cells were serum-starved for 24 h and subsequently treated with 0.5 mM H₂O₂ for the indicated time periods. Non-stressed cells

were used for the 0 h sample. Cells were lysed and subjected to immunoblot analysis with specific antibodies for SIRT1 and GADD45. β-tubulin-staining was used for controlling equal loading. The blot shown is representative of five independent experiments. **b)** GADD45 expression levels were quantified with BioDoc Analyzer software (normalized to β-tubulin loading control) at time 0 h was arbitrarily set to 1.0. Mean values and standard deviations of four independent immunoblots are shown (*p < 0.001 vs. 0 h siControl). **c)** Reduced GADD45 expression in SIRT1^{-/-} cells. MEFs derived from wild-type (WT) or SIRT1-knockout mice were treated with H₂O₂ (1 mM) for the indicated times. The amounts of GADD45 and SIRT1 protein levels were quantified by Western blot. Equal loading was verified by β-tubulin staining. The represented blot corresponds to two independent experiments.

This result demonstrates that SIRT1 is essential for FoxO-mediated GADD45 induction in response to oxidative stress, thus suggesting that peroxide-induced apoptosis of HCASMCs is abandoned by SIRT1 through triggering FoxO-mediated GADD45 expression.

To further assess the role of endogenous SIRT1 in GADD45 gene expression, we analyzed expression of this protein in wild-type or SIRT1-null MEFs that were treated with H_2O_2 . Western blot analysis revealed H_2O_2 -treatment of wild-type MEFs to induce expression of the stress resistance gene GADD45 (Figure 64c). This response to H_2O_2 was strongly attenuated in the SIRT1-knockout fibroblast cell line (Figure 64c).

Thus, endogenous SIRT1 seems to contribute to enhanced expression of the genotoxic stress-responsive gene GADD45 in response to oxidative stress by increased FoxO1a deacetylation. Since GADD45 is not only involved in DNA repair but also in cell cycle arrest (see Introduction), regulation of this protein has a dual effect on protecting cells from apoptosis: the delayed progression of the cell cycle allows time for the repair of damaged DNA by GADD45.

Besides GADD45, the mitochondrial MnSOD protein is another known pro-survival genes whose transcription is regulated by FoxO-transcription factors¹⁶⁸⁻¹⁷¹. To investigate whether SIRT1 affects FoxO1a-mediated MnSOD transcription, cell lysates from peroxide-treated HCASMCs - deprived with or without SIRT1 – were analyzed for MnSOD (Figure 65a). Surprisingly, the amount of MnSOD is upregulated both in control transfected and SIRT1-lacking HCASMCs after H_2O_2 -treatment (Figure 65a, b), thus FoxO1a-induced expression of the survival gene MnSOD was not inhibited by treatment of cells with siRNA for SIRT1 as it was shown for GADD45.

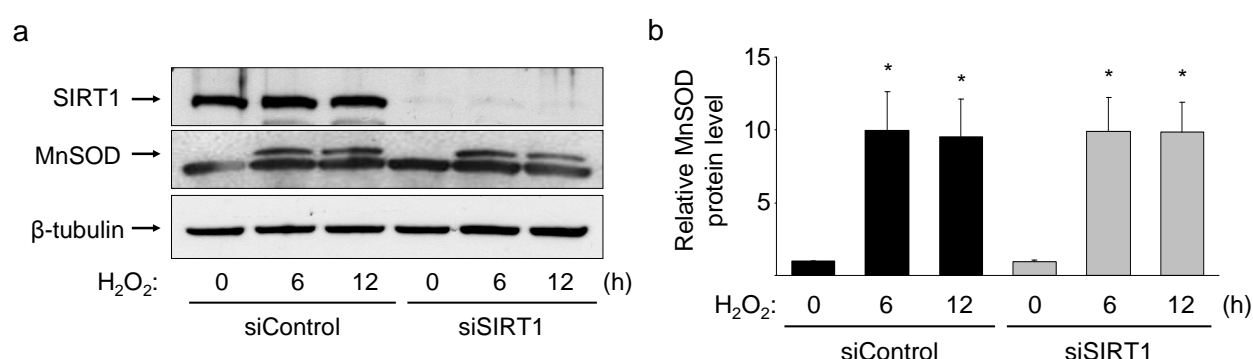


Figure 65. MnSOD expression in response to H_2O_2 treatment is not regulated by SIRT1

HCASMCs were transfected with either siRNA for SIRT1 or control non-targeting siRNA (siControl) and treated as in Figure 64a. Non-stressed cells were used for the 0 h sample. Cells were lysed at the indicated times after peroxide treatment and subjected to Western blot analysis for SIRT1 and MnSOD (a). Equal protein loadings were confirmed by the use of an anti- β -tubulin antibody. (b) Densitometric data from four independent immunoblots demonstrated MnSOD expression levels. Data are normalized to β -tubulin and represent means and standard deviations of four independent experiments. Timepoint 0 h of siControl transfected cells was arbitrarily set 1 (*p < 0.000 compared to 0h siControl). Statistical significance of the densitogram was determined by ANOVA.

Together these results indicate that not all FoxO target genes are affected in the same way by SIRT1 activity.

Consistent with the possibility that the deacetylase may differentially affect various FoxO target genes, I could not identify SIRT1 to affect FoxO-dependent expression of the pro-apoptotic genes Bim and FasL (data not shown).

The discovery that the presence of SIRT1 attenuates H₂O₂-induced HCASMC apoptosis by enhancing expression of a FoxO1a target protein involved in stress resistance (GADD45) but appears to have no impact on the expression of pro-apoptotic FoxO1a target genes (such as Bim and FasL), led me think about the possibility that SIRT1 is able to shift FoxO-induced responses away from cell death toward stress resistance and survival.

Discussion

Psammaplysene A and its analogues regulate HCASMC homeostasis *in vitro* and *in vivo*

Vasculo-proliferative disorders such as atherosclerosis, postangioplasty restenosis, vein graft failure upon bypass surgery and pulmonary hypertension are complex process that are especially related to vascular smooth muscle cells (VSMCs)^{45, 78}. In the arterial media, VSMC are normally quiescent, however, for the development and progression of the above mentioned diseases it is prerequisite that quiescent VSMCs start to proliferate, migrate and commit suicide. Different stimuli such as physical injury or mechanical stress are responsible for VSMC activation with subsequent changes in behavior (Sedding *et al.*, unpublished data)²¹¹.

Upon activation, VSMC migrate out of the media into the vessels intima⁸⁵. The subsequent proliferation of these neointimal VSMC dramatically increases the size of this vessel layer and can lead to occlusion of the vessel. This then represents the basis for the development of vasculo-proliferative disorders^{45, 78}. Understanding the mechanisms and signal transduction pathways manipulating VSMC behavior upon vessel injury will help to identify strategies for the prevention and treatment of vascular disease processes.

Accumulating evidence indicates that the phosphatidylinositol 3-kinase (PI3K)/Akt signaling pathway plays an essential role in critically regulating VSMC homeostasis in the blood vessel as well as vascular remodeling^{65, 66}. Dysfunction of the PI3K/Akt signaling pathway contributes to the pathogenesis of many diseases, including heart and vascular diseases, diabetes, inflammatory disorders and cancer. Various environmental inducers, e.g. increased strain stress induced by arterial hypertension or growth factors, are known to activate this pathway resulting in the subsequent Akt-mediated phosphorylation and inactivation of the forkhead box O (FoxO) subfamily of forkhead transcription factors. In mammals, there are four evolutionarily conserved FoxO family members (FoxO1a, FoxO3a, FoxO4 and FoxO6)^{148, 166, 167}. They are crucial downstream targets of the PI3K/Akt signaling pathway and critically regulate cell fate. Knockout studies done by Hosaka *et al.* revealed especially the importance of FoxO1a for the vascular development and remodeling, since FoxO1a-null embryos failed to establish normal vasculature¹⁵⁸. Previous work done by our group supported these observations by demonstrating the involvement of phosphorylated FoxO1a in regulating VSMC behavior under pathological conditions (Sedding *et al.*, unpublished data)⁶⁵.

The crucial function of FoxO transcription factors is based on their ability to control processes such as cell cycle progression and proliferation (p27^{KIP1}²²⁶, p21^{CIP1}²⁰⁵, p130¹⁶⁴, cyclin D1 and D2^{168, 215, 332} and cyclin B²¹⁴), DNA repair and defense against oxidative stress (GADD45^{168, 169}, MnSOD¹⁷⁰, catalase¹⁷¹), as well as apoptosis and aging (FasL¹⁶⁶, Bim^{191, 194}, TRAIL¹⁹³, TRADD¹⁹⁶ and caveolin-1 (Sedding *et al.*, unpublished data)). For review see (¹⁴⁰).

Intervening VSMC function by affecting FoxO1a function may represent an attractive approach for future therapeutic strategies in the prevention of vasculo-proliferative diseases.

The status of FoxO transcription factors in quiescent cells is defined as being localized to the cells nucleus actively repressing cell cycle progression³³⁸. Since the translocalization of FoxOs to the cytoplasm in response to diverse stimuli is the basis for their disability to further restrain cell cycle transition and other processes, one way to reconstitute FoxO function would be to enforce its nuclear re-localization and its stabilization.

With having this in mind, the group of John Clardy, Department of Biological Chemistry and Molecular Pharmacology, Harvard Medical School, Boston, USA, performed a cell-based, visual, chemical genetic screen to identify small molecules able to maintain FoxO1a in the nucleus of cancer-derived cells with PTEN loss-of-function mutations^{330, 331, 334}. Psammaplysene A, a natural product from the marine sponge *Psammaplysilla* sp. was amongst the strongest screening positives out of >18'000 synthetic and natural molecules. Thus, this compound compensated for lost tumor suppressor functionality in the mentioned cell line. Whether Psammaplysene A retains FoxO1a in the nucleus of VSMCs of the human coronary system was investigated in this thesis.

Previous studies done by our group demonstrated endogenous FoxO1a of being constitutively localized to the nucleus of silenced mouse VSMCs *in vitro* and *in vivo* (Sedding *et al.*, unpublished data) with my data supporting this observation in VSMCs from human coronary arteries (HCASMCs). In response to stimulation by mitogens, FoxO1a proteins become phosphorylated by Akt at three serine and threonine residues (Thr24, Ser256 and Ser319). This leads to an inhibited transcriptional activity of FoxO1a due to altered DNA binding activity, as well as to nuclear exclusion by enhancing interaction with 14-3-3 chaperone proteins (Sedding *et al.*, unpublished data)^{166, 167, 238, 239}. Regarding the existence of serum-induced FoxO1a translocation in HCASMCs, Psammaplysene A was demonstrated in this study to prevent this process dose-dependently, with 10 μ M showing the strongest effect as compared to lower concentrations. According to this observation, Kau *et al.* described Psammaplysene A at a concentration of 5-10 μ M to inhibit FoxO1a translocation in PTEN-deficient cells³³⁰, thus I found Psammaplysene A of being at least as potent in VSMCs as in other cell types.

Importantly, Kau and colleagues reported the marine compound to inhibit FoxO1a translocation not by interacting with the general nuclear export machinery, but by affecting a still unknown target in the PI3K/Akt/FoxO signaling pathway³³⁰. With my studies, I tried to explore the detailed mechanisms of action of Psammaplysene A in VSMCs from the human coronary system. I was able to demonstrate that Psammaplysene A acts downstream of Akt, since the

sponge compound did not abolish phospho-Akt levels induced by serum-stimulation. Additionally, Psammaplysene A did not affect serum-induced FoxO1a phosphorylation, thus impact of the molecule on FoxO1a translocation was not due to abrogated PI3K/Akt function. Consequently, FoxO1a is present in the nucleus of Psammaplysene A-treated HCASMCs in a phosphorylated state. In this regard it is noteworthy to mention, that recent publications demonstrated phosphorylation of FoxO proteins not to be necessarily connected with their susceptibility for inactivation, nuclear exclusion and degradation^{253, 257}.

However, the question remained how Psammaplysene A retained FoxO1a in the nucleus? Since Psammaplysene A did not prevent FoxO1a phosphorylation but somehow inhibited its cytoplasmic translocation, it was suggested that Psammaplysene A prevents adherence of FoxO1a to 14-3-3 proteins. However, preliminary data from me exclude this option, since the sponge compound did not interfere with FoxO1a/14-3-3 binding in immunoprecipitation experiments.

Kau *et al.* suggested the Ca^{2+} /calmodulin pathway to regulate FoxO1a's cellular location, since treatment with the intracellular Ca^{2+} -chelator BAPTA-AM relocalized FoxO1a to the nucleus of PTEN-deficient cells³³⁰. Psammaplysene A is a bromotyrosine and resembles the bastadins, a family of natural products that have been shown to modulate Ca^{2+} release channels. Though untested, it seems possible that Psammaplysene A reduces the intracellular Ca^{2+} concentration by blocking Ca^{2+} -channels³³⁰. Decreases in Ca^{2+} might prevent Ca^{2+} from binding to calmodulin and therefore inactivating calmodulin. There are some possibilities how inactivated calmodulin might influence FoxO1a translocation: One the one hand, several publications identified the Ca^{2+} /calmodulin-pathway to contribute to Akt phosphorylation, thus Kau and colleagues hypothesized Psammaplysene A to inhibit FoxO1a translocation by inhibiting its phosphorylation³³⁰. However as already mentioned above, my results indicated FoxO1a phosphorylation despite Psammaplysene A treatment. Therefore, this possibility was disproved in my model. On the other hand, calmodulin is known to affect various nuclear transport mechanisms³³⁰. Therefore, the idea of calmodulin being involved in FoxO1a subcellular localization and of Psammaplysene A affecting calmodulin activity by decreasing intracellular Ca^{2+} concentration seems to be promising and warrants further investigations.

Besides impairing FoxO1a translocation, data represented in this thesis pointed out a role for Psammaplysene A in affecting HCASMCs homeostasis. By using several *in vitro* and *in vivo* experimentations, I was able to demonstrate Psammaplysene A to attenuate HCASMC proliferation and migration as well as to decrease femoral artery neointimal hyperplasia after wire-injury in mice.

As determined by FACS analysis of propidium iodide-stained HCASMCs, Psammaplysene A inhibited serum-induced cell cycle progression by preventing G1/S-phase transition, with 10 μM of the compound showing the most significant effect. Consequently, Psammaplysene A also affected BrdU incorporation during DNA synthesis dose-dependently. Despite serum-stimulation, treatment of cells with 5 μM Psammaplysene A almost reduced DNA synthesis rates by 50%, and 10 μM completely abolishing them. These findings are consistent with studies from Kau *et al.* revealing Psammaplysene A to inhibit proliferation of PTEN-deficient cells with an IC_{50} of 5-10 μM ³³⁰.

As a result of reduced cell cycle progression rates due to Psammaplysene A-treatment, HCASMCs cell numbers were decreased, too. Cell counting after exposure to 5 μM Psammaplysene A revealed significant decreases in cell numbers as compared to non-treated cells. Interestingly, numbers of HCASMCs treated with Psammaplysene A at 10 μM was below that of quiescent cells. This phenomenon can be explained when considering data derived from both proliferation and apoptosis assays. At 10 μM , DNA replication was significantly inhibited by Psammaplysene A. Additionally, the compound strongly induced apoptotic cell death at the same concentration. Thus, a lack of VSMC growth was due to both an almost complete inhibition of cell cycle progression and a strong increase in apoptotic cell death. Psammaplysene A doses above 10 μM further increased cell death with no cells remaining viable. By using Psammaplysene A in the following *in vivo* experiments at therapeutically relevant doses < 10 μM , the specific effect of the molecule on HCASMC proliferation inhibition was suggested not to be overwhelmed by apoptosis-induced cell death.

Western blot analyses of cell cycle regulating proteins were performed to clarify the observed inhibitory role of Psammaplysene A on cell cycle transition from G0/G1- to S-phase. As already mentioned above, quiescent HCASMCs re-enter the cell cycle upon diverse stimuli such as mitogens. Different protein-complexes control progression through the cell cycle at G0/G1 to S, including cyclin D1-CDK4 and cyclin E-CDK2^{45, 78, 110}. Cyclin-dependent kinase inhibitors (CKIs), such as p27^{KIP1}, regulate the activity of the cyclin - cyclin-dependent kinase (CDK)-complexes. Cyclin D1 is expressed in low abundance in quiescent cells, whereas the “gatekeeper” p27^{KIP1} is highly present. Upon mitogen stimulation, cyclin D1 quickly accumulates within the nucleus and p27^{KIP1} disappears due to abrogate new-synthesis, providing requirements for cell cycle transition into S-phase⁹⁸. Importantly, we and others have shown both p27^{KIP1} and cyclin D1 to be transcriptionally regulated by FoxO1a^{78, 168, 215, 226, 339}, with our study describing this observation in VSMCs *in vitro* and *in vivo* (Sedding *et al.*, unpublished data). In this regard, p27^{KIP1}-deficient cells were partially resistant to G1-arrest induced by FoxO4²²⁶ and ectopic expression of cyclin D1 could partly overcome the anti-proliferative effect of FoxO-transcription factors²¹⁵. Nevertheless, regulation of both proteins by FoxO transcription

factors differs: whereas activation of p27^{KIP1} transcription requires binding of FoxO to specific DNA elements in the p27^{KIP1} promoter^{78, 226, 339}, the exact mechanism of transcriptional repression of cyclin D1 by active FoxOs has not been elucidated yet. A direct binding of FoxO transcription factors to the cyclin D1 promoter region could not be demonstrated, therefore, the most likely model for the FoxO-dependent cyclin D1 regulation is that - yet unidentified - transcription factors bound to the cyclin D promoter recruit FoxO transcription factors, which in turn repress transcription^{168, 215}. In this respect it is of interest that FoxO factors were reported to interact with a variety of nuclear receptors, thus functioning as transcriptional corepressors^{168, 215}.

Since Psammaplysene A-treatment was demonstrated to result in FoxO1a nuclear sequestration and to inhibit G1/S transition, I suggested this compound to affect FoxO1a activity and thereby influencing p27^{KIP1} and cyclin D1 protein levels. Indeed, immunoblot analyses revealed a decline in cyclin D1 levels in serum-stimulated HCASMCs treated with 10 μ M Psammaplysene A. Since phosphorylation of the retinoblastoma gene product (pRb) is initiated by cyclin D1-CDK4 complexes, hypo-phosphorylation of pRb in response to Psammaplysene A-treatment as detected can be explained by low cyclin D1 levels. Consequently, upregulation of protein levels of genes involved in cell cycle control downstream of cyclin D1 and pRb, such as proliferating cell nuclear antigen (PCNA), cyclin A and cyclin B, was prevented by Psammaplysene A.

Downregulated cyclin D1 protein levels after application of Psammaplysene A suggested that the sponge molecule somehow influenced FoxO1a transcriptional activity. Interestingly, Psammaplysene A-treatment was not able to retract FoxO1a's promoter binding activity in serum-stimulated HCASMCs: Neither did I observe increases in p27^{KIP1} transactivation upon Psammaplysene A-treatment, nor could I reveal general changes in the promoter binding capacity of FoxO1a. An explanation for that observation can be the dependency of reduced DNA binding activity on FoxO1a phosphorylation^{162, 267, 340}. Whether the phosphorylation status of FoxO1a influences its function as a transcriptional corepressor has - to my knowledge - never been examined. Therefore, it can be assumed that the Psammaplysene A-mediated presence of phosphorylated FoxO1a within the nucleus is sufficient for maintaining its corepressor function but not for transcription of direct target genes.

Unpublished studies from our group suggested a combined effect of FoxO1a-mediated p27^{KIP1} upregulation and cyclin D1 transcriptional repression in preventing VSMC cell cycle progression and proliferation (Sedding *et al.*, unpublished data). However, data presented by Ramaswamy *et al.* in a different cellular system indicated the transcriptional repression of D-

type cyclins rather than the activation of genes regulated by a insulin response sequence (IRS) promoter elements (such as p27^{KIP1}) to be required for FoxO1a mediated cell cycle stop¹⁶⁸. Thus, it definitely seems possible that Psammaplysene A's influence on HCASMCs function *in vitro* and *in vivo* as demonstrated in this thesis arose from the compound-induced prevention of cyclin D1 expression!

The importance of a reduced Psammaplysene A-mediated VSMC proliferation *in vivo* was also demonstrated in the present study: Treatment with Psammaplysene A significantly reduced development of postangioplasty restenosis due to reduced cell proliferation as determined by PCNA staining. This favors Psammaplysene A as a promising compound for local application to eliminate restenosis after PTCA. Unpublished data from our group also revealed the fractional involvement of apoptotic cell death on decreased restenosis development (Sedding *et al.*, unpublished data). Thus, in the future the influence of this compound on apoptotic cell death *in vivo* has to be examined too. However, it can be assumed that Psammaplysene A-mediated apoptosis plays only a minor role in the vessel injury model, since - as already mentioned above - Psammaplysene A at the doses used for *in vivo* application showed only small effects in *in vitro* cell death assays.

In response to atherogenic stimuli or vessel injury, VSMC migrate into the innermost layer of the arterial wall, where they re-enter the cell cycle thus leaving their quiescent state^{85, 86}. Thus, VSMC migration is another key event of vascular pathology and was shown in this thesis to be influenced by Psammaplysene A. At 5 μ M and 10 μ M, respectively, the sponge compound prevented cell migration along a chemoattractant gradient. Thus, besides decreasing cell proliferation, Psammaplysene A seemed to reduce neointima formation *in vivo* at least partially by inhibiting cell migration. Our group previously demonstrated functionally active FoxO1a to reduce the migratory capacity of VSMCs (Sedding *et al.*, unpublished data). Hence, the sponge molecule might influence cell chemotaxis via affecting FoxO1a function. Unfortunately, it is not clear, whether the anti-migratory effect caused by Psammaplysene A is a specific effect or whether it is a secondary effect due to the cell cycle arrest observed in G0/G1 (which in turn affects a number of other cellular functions, such as differentiation, inflammation and migration⁷⁸). Yet, the specific role of Psammaplysene A in the regulation of cell migration warrants further investigation.

In general, results pointed out in this thesis suggest Psammaplysene A to be a potent drug for treating vasculo-proliferative diseases. Unfortunately, Psammaplysene A is a pseudosymmetric bromotyrosine-derived alkaloid whose supply is limited. Thus Georgiades *et al.* developed an efficient synthesis of this compound³³³. In addition to being able to produce

large amounts of Psammaplysene A, this method provided the potential for synthesizing analogues and probes, creating a focused library of 28 Psammaplysene-like molecules. During my studies, I screened this library with regard to inhibit proliferation of HCASMCs. Out of all tested analogues, only one compound named F10 affected BrdU incorporation to a greater extent than Psammaplysene A. With an IC_{50} of $\sim 2.5 \mu M$, HCASMCs proliferation was inhibited at a clearly lower concentration as with Psammaplysene A. At $5 \mu M$ F10 prevented DNA synthesis upon serum-stimulation completely as determined by BrdU incorporation assays and by monitoring cell numbers. Importantly, unlike to what was revealed for Psammaplysene A, the analogue F10 did not induce apoptotic cell death at the tested concentrations as defined by apoptotic cell death ELISAs. Thus, F10 seems to exclusively affect HCASMCs proliferation at very low concentrations. This will be of advantage for a future therapeutic use, since functions of pharmaceuticals should be highly specific without having side effects.

As it was already shown for Psammaplysene A, the sponge analogue F10 was also revealed to prevent FoxO1a's nuclear exclusion upon serum-stimulation, thus it seems that F10's mode of action is similar to that of Psammaplysene A. However, for the future it will be interesting to analyze its impact on HCASMCs *in vitro* as well as on neointima formation *in vivo* in more detail. By now, a potential of F10 for future therapeutic uses can only be expected.

An alternative to the application of a single drug could be the combined application of different drugs striving for the same objective. With the present study, I was able to demonstrate this phenomenon when combining administration of F10 and Psammaplysene A. Whereas none of the compounds alone was able to prevent HCASMCs proliferation *in vitro* at a concentration of $2.5 \mu M$, a combined treatment with both agents at the same concentration completely inhibited BrdU incorporation. This observation could be promising for future therapeutic approaches, with regard to minimize unspecific side effects caused by high dosage of each compounds. Nevertheless, the combined effect of Psammaplysene A and F10 will be further examined in diverse biological assays both *in vitro* and *in vivo*.

My data given in this thesis have only focused on the influence of Psammaplysene A and F10 on the forkhead transcription factor FoxO1a. Nevertheless, similar results were obtained with regard to FoxO3a. Both compounds inhibited translocation of FoxO3a to the cytoplasm upon serum stimulation, and additionally, Psammaplysene A did not increase FoxO3a's transactivation activity. Thus, both Psammaplysene A and F10 were suggested to influence VSMC behavior by affecting all main members of the mammalian FoxO transcription factor family.

FoxO1a regulates PASMC proliferation, migration and apoptosis

Pulmonary hypertension is another vasculo-proliferative disorder depending on severity of injury⁷⁵. With increasing durability and persistence, pulmonary hypertension is connected to progressive vessel wall remodeling. Pulmonary artery smooth muscle cells (PASMC) in the lung artery wall contribute primarily to these remodeling processes⁷⁵. Understanding the molecular mechanisms that regulate human PASMC proliferation and migration will help to understand cellular responses to vascular injury and may provide novel aspects for future therapeutic interventions. Recent publications from Goncharova and coworkers identified the PI3K/Akt pathway to mediate proliferation and migration of human PASMCs³³⁵, and Fouty *et al.* noticed that overexpression of the FoxO target p27^{KIP1} attenuated PASMC proliferation⁷³. Since Pullamsetti *et al.* identified the forkhead transcription factor FoxO1a to be strongly downregulated at transcriptional levels in rat pulmonary hypertensive arteries as well as in lung homogenates from human patients with idiopathic pulmonary hypertension (unpublished data), I hypothesized FoxO1a to play a causal role in the development of pulmonary hypertension.

In the present study, I determined the importance of the transcription factor FoxO1a in controlling rat PASMCs behavior. My results suggested the transcription factor to be an interesting target for the development of future therapeutic strategies to prevent and/or treat vasculo-proliferative disorders such as pulmonary hypertension.

In this report, I was able to detect stable expression of FoxO1a within the nuclei of PASMCs, which was abolished after serum-stimulation due to FoxO1a translocation to the cytoplasm. Together with data from Pullamsetti *et al.* verifying expression of FoxO1a within the media of native and diseased pulmonary vessels, I demonstrated FoxO1a expression and translocation in vascular cells of pulmonary arteries for the first time.

Further on, this study demonstrated an important and specific role for FoxO1a in controlling cell proliferation of PASMCs. I demonstrated that serum stimulation increased mitogenesis of PASMCs, which correlated with an increase in cell cycle progression and cell number. In parallel, p27^{KIP1} protein levels declined and cyclin D1 rose when analyzing immunoblots. Levels of phosphorylated pRb increased due to enhanced presence of cyclin D1. As already mentioned, FoxO1a has been published to be involved in p27^{KIP1} transactivation as well as in repressing cyclin D1 expression^{78, 168, 215, 226, 339}, with our group demonstrating both genes being transcriptionally regulated by FoxO1a in VSMCs from the coronary system (Sedding *et al.*, unpublished data). Moreover, my results suggested that FoxO1a-mediated PASMC growth suppression is due, at least partially, to both the regulation of cyclin D1 and p27^{KIP1}.

The importance of p27^{KIP1} in controlling cellular proliferation of PASMC *in vitro* and in modulating the development of pulmonary vascular diseases was already described by Fouty *et al.*⁷³. In their study p27-deficient PASMCs revealed a 2-fold increase in [3H]thymidine incorporation and cell proliferation as compared with p27^{+/+}-PASMCs⁷³. The *in vivo* importance of p27^{KIP1} in the lung pulmonary system was demonstrated by Yu and coworkers⁷⁶. Downregulation of p27^{KIP1} upon serum-stimulation as observed in my studies correlated with increases in DNA replication, and demonstrated the importance of the CKI p27^{KIP1} in regulating PASMC proliferation.

Upon transduction of PASMC with the constitutive active form of FoxO1a (FoxO1a;AAA), p27^{KIP1} protein levels raised and cyclin D1 levels were diminished. Changes in protein levels were accompanied by attenuated proliferation rates as well as by reduced cell numbers of FoxO1a;AAA-transduced PASMCs. Thus, reconstitution of FoxO1a function seemed to restore the quiescent phenotype in PASMCs.

Interestingly, interference with p27^{KIP1} upon FoxO1a;AAA-transduction seemed to be selective, since p21^{CIP1} - another important FoxO1a-controlled inhibitor of G1-phase progression^{45, 205, 339} - was not affected. Additionally, no changes were observed in cyclin E protein levels upon FoxO1a;AAA-transduction. Besides cyclin D, cyclin E controls progression through the cell cycle at G0/G1- to S-phase. Since cyclin E gene expression is FoxO1a-independent, cell cycle arrest of PASMCs forced to express FoxO1a was FoxO1a-specific.

My results further suggested a combined effect of FoxO1a-mediated p27^{KIP1} upregulation and cyclin D1 transcriptional repression contributing to a robust inhibition of cell cycle progression in PASMCs *in vitro*. This effect was also observed in VSMCs from the coronary system (Sedding *et al.*, unpublished data). However, this study is the first describing FoxO1a's contribution to cell proliferation in VSMCs from the pulmonary system via regulating p27^{KIP1} and cyclin D1. Whether adenoviral transduction of FoxO1a;AAA has the same effects in the lung *in vivo* has to be investigated in the future.

Besides affecting proliferation, FoxO1a also attenuated PASMC migration, another critical step in the development of pulmonary hypertension⁷⁵. PDGF-BB-induced PASMC chemotaxis was significantly inhibited following transduction with FoxO1a;AAA. This is well in line with studies from our group reporting that overexpression of constitutive active FoxO1a inhibited migration of human coronary VSMCs along a PDGF-BB gradient (Sedding *et al.*, unpublished data). However, as it was the case for VSMC from the coronary system (see above), a detailed explanation on how the migratory process was inhibited by FoxO1a does not exist, and thus provides a promising area for future research. It might be possible that abrogated migration rates upon FoxO1a;AAA-transduction are only secondary effects caused by cell cycle arrest of PASMCs.

The data presented in this thesis also demonstrated FoxO1a to be important in regulating apoptotic cell death of PASMCs. As already mentioned, several FoxO transcription factor targets are involved in apoptosis, such as FasL¹⁶⁶, Bim^{191, 194}, TRAIL¹⁹³, TRADD¹⁹⁶. Recently, our group demonstrated FoxO1a to directly control caveolin-1 transactivation in SMCs from the arterial system (Sedding *et al.*, unpublished data). Since these experiments further revealed an increase in the number of apoptotic VSMCs upon ectopic expression of caveolin-1, FoxO1a's apoptotic effect on VSMCs seemed to be dependent, at least partly, on the increased expression of caveolin-1. My study now revealed a similar way for FoxO1a of regulating apoptosis in PASMCs. Upon transduction with FoxO1a;AAA neither FasL nor Bim protein levels increased, however, caveolin-1 protein levels significantly rose. Since transduction with FoxO1a;AAA significantly affected PASMC cell death rates, it was suggested that cell death in the pulmonary vessel system was, at least partially, dependent on caveolin-1 expression. In keeping with this data, recent publications have implicated the cellular caveolin-1 content to apoptosis in human coronary VSMCs³⁴¹. Other groups also revealed the major role of caveolin-1 in vascular homeostasis^{342, 343}. Their studies demonstrated caveolin-1 knockout mice to have lung abnormalities³⁴² and to develop pulmonary hypertension combined with secondary right ventricular hypertrophy, as well as cardiomyopathy³⁴³.

Caveolin-1 is the main structural component of organelles named caveolae in various cell types, such as smooth muscle cells, endothelial cells, fibroblasts, adipocytes and epithelial cells³⁴⁴. Caveolae are invaginations of the plasma membrane that have several functions in signal transduction. Several signaling molecules are known to interact with caveolin-1 including G-proteins (α and $\beta\gamma$), Ras-Stat, Janus kinase (Jak)-Stat and extracellular signal-regulated kinase (Erk) signaling pathways, protein kinase C isoforms, EGF-R and related receptor tyrosine kinases, Src family tyrosine kinases, and endothelial nitric oxide synthase (as reviewed in³⁴⁴). Taken together, caveolin-1 seems to be essential for normal cardiopulmonary function. However, the mechanism(s) by which caveolin-1 is able to facilitate and/or induce FoxO1a-mediated apoptosis in PASMCs is yet unknown and has to be investigated in the future.

In turns of my results, restoration of caveolin-1 expression by activated FoxO1a could resensitize hyperproliferative PASMCs to apoptotic stimuli, thereby contributing to the prevention of pulmonary vascular smooth muscle hyperplasia *in vitro* and pulmonary hypertension *in vivo*. However, induction of apoptosis with regard to avoid the impairment of vasculo-proliferative lung diseases is controversial and needs to be deliberated carefully.

Monocrotaline (MCT), a toxin isolated from plants of the *Crotalaria* species, is used to intentionally induce severe pulmonary hypertension in animals in order to generate an

experimental model for exploring the pathophysiology of pulmonary hypertension³³⁶. Accordingly, application of MCT fully established pulmonary hypertension in rats as it was shown by Pullamsetti *et al.*³³⁷. In detail, MCT treatment in rats provokes endothelial injury, proliferation, and migration of pulmonary VSMCs. Pulmonary vessels from MCT-treated rats show significant increases in media thickness similar to neointimal thickening during restenosis³³⁷.

In addition to studying FoxO1a function in regular PSMCs, I examined the effect of the transcription factor on pathologically modified PSMCs. Interestingly, there were no striking changes in behavior upon serum stimulation when comparing regular PSMCs and PSMCs derived from MCT-treated rats: Both cell types increased cell numbers due to induction of DNA synthesis and amplified their chemotactic responses when stimulated by serum. In addition, the incidence of apoptotic cell death was reduced. Following transduction of MCT-PSMCs with FoxO1a;AAA, serum-induced DNA replication rates declined. Subsequently, cell numbers decreased. Furthermore, other processes implicated in pulmonary vascular smooth muscle hyperplasia were affected, such as migration – which was attenuated - and apoptosis – which was strongly upregulated in PSMCs forced to express FoxO1a;AAA. This observation revealed the FoxO1a transcription factor to substantially regulate MCT-PSMC homeostasis in various ways.

With regard to the knowledge that FoxO1a phosphorylation and protein degradation is enhanced during the development of pulmonary hypertension in mice and man *in vivo* (Dr. Pullamsetti, personal communication) stabilization of FoxO1a activity by overexpressing a constitutive active form seems to represent an effective strategy to prevent pulmonary hyperplasia. However, for the future it will be important to analyze FoxO1a's mode of action in more detail before considering FoxO1a to be a target for medical therapy.

SIRT1 regulates HCASMC proliferation, migration and survival

Evidence suggests a role for FoxO1a activation in systemic VSMC cell cycle progression, proliferation, migration and apoptosis/cell survival. However, there potentially exist different cell-specific responses between VSMC from the pulmonary and from the coronary system. Thus, in the third part of my thesis, I come back to the coronary system for studying FoxO1a function in more detail and for identifying the influence of a specific mammalian deacetylase on these cells behavior.

In the latter part of this report I already mentioned that FoxO transcription factor activity is tightly controlled by Akt-mediated phosphorylation in SMCs of the vascular system. However, previous studies demonstrated FoxOs not only to be controlled by phosphorylation, but also by other posttranslational modifications, including ubiquitylation and – more importantly – acetylation. Especially the endogenous class III deacetylase SIRT1 has been reported to affect FoxO acetylation and thus function in various cell types^{233, 262, 263}. My results now suggested a model in which mammalian FoxO transcription factors were subject to reversible deacetylation by SIRT1 mainly under stress conditions. In doing so, SIRT1 activated FoxO1a and mediated HCASMC cell survival. The connection between stress and FoxO1a is of particular interest with respect to a possible role for FoxOs in vascular disease, as for example atherosclerotic lesions have been implicated with cytotoxic stress and apoptotic cell death^{24, 345}. Previous studies in other cell types have already demonstrated the involvement of SIRT1 in different biological processes, mainly in the context of longevity which is connected to stress resistance^{292, 303, 304}. However, this study is the first revealing SIRT1's pivotal importance in the vascular system *in vitro* and *in vivo*. In brief, I was able to show that SIRT1 plays an essential role in inhibiting cell growth, attenuating chemotaxis and cell death in HCASMCs, even though this effect was demonstrated not always to be FoxO1a-dependent.

Class III histone deacetylases (also called sirtuins) are phylogenetically conserved in organisms ranging from bacteria to complex eukaryotes, as e.g. humans²⁸¹. They were named after the first protein observed in *Saccharomyces cerevisiae*, the silent information regulator 2 (Sir2) protein³⁴⁶. In yeast, flies and worms, overexpression of the genes that encode class III histone deacetylases are demonstrated to enhance lifespan^{303, 304, 307}, thus suggesting sirtuins to be evolutionarily conserved and to mediate longevity. SIRT1, one of the seven human sirtuin family members with the closest homology to Sir2, is an NAD⁺-dependent histone deacetylase that catalyzes deacetylation of diverse histone and non-histone substrates^{278, 284}. In this regard, SIRT1 regulates various important biological processes^{277, 278}, including fat mobilization (NCoR, SMRT)³⁰⁹, differentiation (MyoD, PCAF)^{279, 290}, metabolism (PGC-1 α)³¹⁰, gene transcription and

heterochromatin formation (TAFI68, HES1 and HEY2, CTIP2, histones)²⁷⁹ as well as survival of neurons³¹¹ and survival under stress (p53³¹²⁻³¹⁴, NF- κ B³¹⁷, Ku70^{291, 318} and FoxOs^{233, 262}). SIRT1 knockout studies in mice revealed the deacetylase to promote survival rate and lifespan^{315, 316}. Since lifespan extension is closely linked to cell cycle arrest and stress resistance, SIRT1 was also suggested to have a potential role in the development of vasculo-proliferative diseases.

In this study, I reported SIRT1 to be a nuclear enzyme that plays an important role in HCASMCs *in vitro* and *in vivo*. Several other publications already described SIRT1 to be a nuclear protein^{233, 263, 314, 347, 348}. However, recent findings by Tanno and coworkers indicated a nucleocytoplasmic shuttling of SIRT1 during development and in response to physiological and pathological stimuli, thus representing a novel regulatory mechanism for SIRT1²⁸³. The nuclear localization of SIRT1 in HCASMCs as observed in this study was stable and independent of cellular stimulation - neither pro-proliferative nor pro-apoptotic stimuli affected intracellular SIRT1 distribution. Whether the mechanism of nucleocytoplasmic SIRT1 shuttling plays a role in other cells of the vascular system or under yet unevaluated circumstances in VSMCs needs to be explored in the future.

An important observation in this work is that inhibiting nicotinamide adenine dinucleotide (NAD)-dependent SIRT1 activity, either pharmacologically by applying nicotinamide (NAM)^{292, 293} and splitomicin²⁹⁴, respectively, or by siRNA-mediated downregulation of SIRT1 increased both basal and serum-induced HCASMC proliferation rate *in vitro*. Out of these three compounds, NAM, a form of vitamin B3 and a product of sirtuin-catalyzed deacetylation, is the only inhibitor of SIRT1 activity being present in living organisms^{285, 286}. Internal metabolic processes influence its concentration, thus the degree of SIRT1 inhibition in nature can be regulated by the organism itself (see below). However, the molecular mechanisms of NAM function remain unknown until date and need to be explored in the future. Increasing SIRT1 function by overexpressing functional active SIRT1 using adenoviral vectors had the opposite effect: HCASMC proliferation was decreased.

Furthermore, my experiments indicated that besides affecting proliferation, active SIRT1 attenuated HCASMC migration as well. Inhibiting SIRT1 function pharmacologically or by using siRNA specific for SIRT1 resulted in an enhanced chemotactic response. Since HCASMC migration is a key event in neointima development^{85, 349}, prevention of cell migration by pharmacologically inhibiting SIRT1 activity or by adenovirally manipulating SIRT1 levels may additionally contribute to reduced lesion formation *in vivo*. To my knowledge, this is the first description of SIRT1's inhibitory effect on cell migration. It is not clear so far whether the anti-migratory effect was a SIRT1-specific effect or whether it was a general response to cell cycle

arrest in G1, since cell cycle inhibition is known to prevent not only cellular proliferation but can modulate numerous cellular functions such as differentiation, inflammation and migration, too⁷⁸. Therefore, for the future the role of SIRT1 in regulating cell migration needs to be further investigated.

So far my results only demonstrated SIRT1 influence on HCASMC cell fate *in vitro*. The *in vivo* effect of SIRT1 was demonstrated using our implemented murine wire-injury model. Adenoviral transfer of SIRT1 to the denudated vessel was revealed to result in significant inhibition of neointima formation due to attenuated neointimal cell proliferation.

In mice arteries, SIRT1 was expressed within the nuclei of VSMCs of the media as well as within the growing neointima. Likewise, SIRT1 was present in the nuclei of human cells from the aortic media and in neointimal tissue generated during postangioplasty restenosis formation. In coincidence with SIRT1's effect on decreasing VSMC proliferation and migration, its verified presence in the vascular system and its downregulation in hyperproliferative tissues was hypothesized to be a sign for the importance of the deacetylase in mammals *in vivo*.

In cell culture, both SIRT1 protein level and mRNA expression was downregulated upon serum stimulation. With having in mind that SIRT1 represses cell proliferation, a downregulation of SIRT1 levels *in vitro* as well as its absence in hyperproliferative tissue is suggested to promote exceeding cell proliferation. Possible mechanisms underlying this regulatory feedback are discussed below.

Apoptosis, as a third component of vascular pathology was influenced by SIRT1 as well. The exposure to reactive oxygen species (ROS) by hydrogen peroxide (H₂O₂) treatment, an apoptosis-inducing stimulus for HCASMCs, mimics the stresses that the vascular system experiences under pathological conditions, such as atherosclerosis and restenosis. Recent publications described the influence of SIRT1 on cell survival in different cell types^{233, 263, 347}. My data now supported the contention that SIRT1 is an endogenous suppressor of apoptotic cell death in HCASMCs. Furthermore, the results given in this thesis extended previous findings since I showed for the first time that SIRT1 promotes cell survival in the mammalian vascular system by manipulating pro-survival gene expression.

Downregulation of SIRT1 using specific siRNA resulted in a significant increase in the number of apoptotic VSMCs. Studies with pharmacologically inhibiting SIRT1 function supported these results: Inhibiting SIRT1 function by applying NAM and sirtinol²⁹²⁻²⁹⁵, respectively, resulted in impaired HCASMC survival rates. Likewise, overexpression of SIRT1 by adenoviruses or stimulation of SIRT1 function using resveratrol significantly reduced HCASMC apoptosis rates. Thus, my results pointed out SIRT1 to protect VSMCs from cell death induced by serum starvation or hydrogen peroxide. These results are congruent with data

from other groups also demonstrating SIRT1 impact on cell survival^{233, 261-263, 268, 269, 347, 350}, however, my data demonstrated this effect in cells of the vascular system for the first time.

The importance of cell survival and/or apoptosis during the development of atherosclerosis and restenosis is still a matter of debate. Previous studies have reported that VSMC apoptosis alone (without the presence of inhibited proliferation and migration) is sufficient to prevent postangioplasty restenosis³⁵¹, thus increased SIRT1-mediated cell survival would exacerbate the process of neointimal lesion formation. On the other hand, survival of cells forming the fibrous cap is beneficial for plaque stability, whereas apoptosis of these cells will contribute to plaque vulnerability and, finally, to acute coronary events due to plaque rupture^{4, 21, 352}. Additionally, the anti-proliferative effect of activated SIRT1 must not be forgotten. Therefore, manipulating SIRT1 activity as a therapeutic approach for curing vascular diseases has to be carefully considered with regard to the syndrome and the disease state.

My results revealed the effect of SIRT1 on cell survival, however, the oxidative stress-response pathway influencing SIRT1 function is hitherto uncharacterized. It was previously mentioned that the deacetylase activity of SIRT1 critically depends on the NAD level and, thus, can be influenced by the cellular NADH/NAD⁺ ratio. It is postulated that stress affects SIRT1 function by altering the cellular concentration of NADH and NAD⁺. Poly (ADP-ribose) polymerase (PARP), a nuclear enzyme that is activated by DNA strand breaks, uses NAD as a substrate³⁵³. Thus, excessive activation of PARP depletes NAD⁺ stored in the tissue. Since SIRT1 activity depends on the presence of NAD⁺, decreases in NAD⁺ levels result in attenuated SIRT1 activity. PARP additionally elevates intracellular NAM levels. High dosages of NAM inhibit SIRT1 function as it was demonstrated in this thesis. Thus, DNA damage caused by oxidative stress or other triggers should shift the nuclear ratio away from NAD⁺ towards NAM through activation of the PARP enzyme, what then negatively affects SIRT1 activity³⁵⁴. The oxidative stress-induced upregulation of SIRT1 in VSMCs observed in this study could therefore be of biological importance, since it could be seen as a compensatory mechanism to prevent apoptotic cell death in response to double-stranded DNA breaks caused by hydrogen peroxide.

Resveratrol, a polyphenol compound found in grapes and grape products has been identified recently as one of the most potent stimulators of SIRT1²⁹⁷. In yeast, resveratrol treatment resulted in increased DNA stability, extending lifespan by 70%²⁹⁷. Also in *C. elegans* and *D. melanogaster* lifespan is extended by resveratrol in a Sir2-dependent manner^{298, 299}. In mammals, the polyphenol can improve SIRT1-dependent cellular processes as for example fat mobilization³⁰⁹, inhibition of NF- κ B-dependent transcription³¹⁷ and axonal protection³¹¹. In 2006, Baur *et al.* demonstrated resveratrol to improve health and survival of mice³⁰⁰. However,

whether the observed effects were due to a direct impact of resveratrol on SIRT1, or through a combination of different protein interactions remains to be investigated in the future.

In contrast to the above mentioned reports, Kaeberlein *et al.* revealed that resveratrol-treatment failed to enhance Sir2 activity *in vitro* and in yeast cells *in vivo*, thus speculating that activation of SIRT1 by resveratrol might be substrate-specific³⁵⁵.

In my study, resveratrol treatment was demonstrated to decrease HCASMCs cell growth by interfering with proliferation dose-dependently. Moreover, DNA synthesis of embryonic fibroblasts (MEF) isolated from WT mice was attenuated upon resveratrol treatment. Since the polyphenol had almost no effect on DNA synthesis as well as on migration of SIRT1-deprived HCASMCs and SIRT1^{-/-} MEF, resveratrol's effect on manipulating HCASMC function was shown to be SIRT1 specific. Consequently, it seemed that the polyphenol was able to specifically enhance SIRT1 activity in the vascular system. Araim and colleagues investigated the inhibitory effect of resveratrol on proliferation of calf VSMCs³⁵⁶. According to their results resveratrol's effect on mammalian VSMCs proliferation was verified.

In addition to decrease cell cycle progression, treatment of HCASMCs with resveratrol also significantly attenuated chemotaxis.

Coming to the influence of resveratrol on cell survival, I identified the plant polyphenol to reduce HCASMCs apoptosis in response to oxidative stress. Moreover, MEF isolated from SIRT1-null mice were more sensitive to both serum-starvation and H₂O₂-induced cell death as compared to WT-MEFs. These findings were in agreement with previous reports from Brunet *et al.*²³³. Preliminary data suggest deacetylation of p53 to play a role in this process, since acetylation of p53 at the known SIRT1 lysine residue 382, was decreased following resveratrol treatment²⁹⁷.

Taken together, my studies doubtlessly revealed the influence of resveratrol on SIRT1 activity and thus are well in line with studies from other groups.

The development of coronary heart diseases such as atherosclerosis and restenosis is mainly dependent on the proliferation and migration of VSMCs. Thus, reduction of these processes by resveratrol may have a potential beneficial effect on the development of atherosclerotic disease. In addition, resveratrol-mediated inhibition of apoptotic cell death of cells forming the fibrous cap is hypothesized to contribute to decreased cardio-vascular incident-rates. Regular consumption of red wine – containing resveratrol – is still proposed to have cardio-protective effects³⁰¹, however amounts of this polyphenol found in the alcoholic beverage are not sufficient to support this hypothesis.

The molecular mechanisms of how resveratrol influences SIRT1 activity are until now only poorly understood. M. Borra *et al.* tried to elucidate how resveratrol activates SIRT1³⁵⁷. They showed that the polyphenole is not a general activator of SIRT1 but that the covalent attachment of a fluorophore on the SIRT1 substrate is needed for activation³⁵⁷. Additionally they revealed that binding of resveratrol to the deacetylase initiates a conformational change in the protein which leads to tight binding of SIRT1 to the fluorophore-containing paptide³⁵⁷. With regard to my studies where resveratrol acts on SIRT1 in a fluorophore-free environment, other endogenous molecules might mimic the fluorophore's function thus supporting resveratrol's impact on SIRT1 activity. For the future, resveratrol's mode of action will therefore be of particular interest and thus needs to be determined.

In previous parts of this report, I investigated the mechanisms of how endogenous SIRT1 was able to affect VSMC behavior *in vitro* and *in vivo*. Extensive studies of our group revealed regulation of FoxO transcription factors via Akt-mediated phosphorylation in SMCs of the vascular system affecting cell proliferation, migration, cell cycle progression and/or cell survival (Sedding *et al.*, unpublished data). Meanwhile, research presented in this thesis demonstrated FoxO transcription factors to be direct substrates of SIRT1 in various cell types^{233, 262, 263}. Since SIRT1 was revealed in this report to play a major role in regulating HCASMCs cell fate, my further research concentrated on a possible connection between endogenous FoxO1a and SIRT1. Indeed, I could report SIRT1-mediated deacetylation of the forkhead transcription factor FoxO1a upon oxidative stress. As a prerequisite for a possible interaction of endogenous SIRT1 and FoxO1a, the accumulation of both proteins within the nucleus was demonstrated in stressed HCASMCs.

As determined by FRET analysis, FoxO1a directly interacted with the deacetylation enzyme SIRT1 in quiescent HCASMCs, and connection of both proteins increased following treatment of HCASMCs with hydrogen peroxide. Binding of SIRT1 to FoxO1a resulted in removal of the acetyl moiety, whose formation was induced by hydrogen peroxide treatment. Acetylation of FoxO1a led to inhibition of its transcriptional and biological activities, as it was proven by decreased promoter binding capacity as well as attenuated p27^{KIP1} target gene readout. Thus, SIRT1 regulates the transactivation activity of FoxO1a by catalyzing its deacetylation and counteracts the acetylation-mediated FoxO1a suppression. As a result, FoxO1a specific genes can be transcribed.

These results are congruent with data from other groups, however, there are controversial explanations regarding the effect of SIRT1-mediated deacetylation on FoxO transcription factor regulation. While Motta *et al.* reported SIRT1 function to repress FoxO activity²⁶², several other studies suggest that acetylation inhibits and SIRT1 function activates FoxO^{261, 263, 268, 269, 350}.

Brunet and coworkers even go one step further and proposed that the effects of acetylation and SIRT1 are target gene-specific, such that the expression of pro-apoptotic genes is inhibited or not affected, while genes that regulate cell cycle arrest and resistance to oxidative stress are increased²³³. This differential gene regulation model was named ‘tipping the balance towards survival’ and shifts the balance of FoxO-driven genes in favor of cytoprotection³⁵⁸.

My results now support Brunet's hypothesis. Several pro-survival genes have been described to be regulated by nuclear FoxOs, including GADD45, MnSOD and catalase. Furthermore, FoxOs are responsible for inducing transcription of pro-apoptotic genes, such as FasL, Bim, TRAIL, and TRADD^{178, 359, 360}. Unpublished data from our group identified caveolin-1 as another FoxO1a target regulating apoptosis in VSMCs. Thus, FoxO transcription factors have a dual cellular function. Upon NAM-treatment, I was able to reveal a decrease in p27^{KIP1} protein expression within HCASMCs. This cyclin inhibitory protein plays an important role in regulating VSMC proliferation as published by our group⁶⁵. Additionally, depletion of endogenous SIRT1 by siRNA resulted in impaired FoxO1a-mediated GADD45 expression in response to oxidative stress. This finding suggested that an augmented ability to repair damaged DNA mediated by FoxO and SIRT1 advances endurance and slows oxidative damage. The observation that GADD45 expression was SIRT1-dependent was in agreement with data from Kobayashi *et al.*²⁶⁸, who demonstrated that SIRT1 directly controls FoxO1a-mediated GADD45 expression in Saos2 cells. Whether the regulation of GADD45 expression is relevant to cytoprotection of the vasculature *in vivo* will be an attractive area for future investigation.

By increasing endogenous SIRT1 levels upon peroxide treatment as detected by immunoblot analyses and PCR, the cell seemed to have developed an internal feedback-mechanism to further enhance cell survival. With my studies I also provided evidence that not all FoxO-regulated cell survival genes are influenced by SIRT1 activity. For example FoxO1a-induced MnSOD transactivation was not affected by SIRT1. Interestingly, preliminary data from me pointed out that expression of different pro-apoptotic FoxO-target genes such as FasL and Bim were also not influenced by the presence or absence of SIRT1 during oxidative stress treatment. Therefore, my data supported Brunet's theory of a differential gene regulation and provided insights into SIRT1-dependend cellular processes regulating FoxO function in the vascular system for the first time (Figure 66). Nevertheless, the molecular mechanisms that underlie this differential gene regulation are yet unknown and more work is needed to elucidate conclusively the role of acetylation and SIRT1 on the dual function of FoxO. The only thing that has been verified so far is that acetylation-mediated inhibition of FoxO1a in VSMCs is

functionally equivalent to inhibition of FoxOs by Akt-mediated phosphorylation as displayed earlier.

Already in 2002 Kops *et al.* published observations concerning stress-induced FoxO-mediated pro-survival gene expression. The group provided evidence that even in the absence of Akt-mediated survival signals cells protect themselves against oxidative damage by activating the forkhead transcription factor FoxO3a, which directly increased expression of MnSOD in human colon carcinoma cells¹⁷⁰. Unfortunately, the group around Kops had no explanation for this phenomenon at that time, but it can now be claimed that SIRT1 participates in this observation.

In the vascular system, the impact of MnSOD under stress conditions warrants further investigation, since preliminary data of mine predict MnSOD expression in HCASMCs in the presence of ROS to be SIRT1-independent. Nevertheless, SIRT1-mediated expression of MnSOD could play a role in other cells of the vasculature contributing to the development of vasculo-proliferative diseases.

Beyond all mentioned observations, it will be interesting to know in the future whether other cell death-triggering stimuli that induce stresses similar to those the vasculature experiences under pathological conditions, such as exposure to ROS and hypoxia, also stimulate SIRT1 to induce pro-survival gene expression. Maybe other stress factors differentially affect SIRT1 function, thus shifting the cellular response rather towards apoptosis than protection.

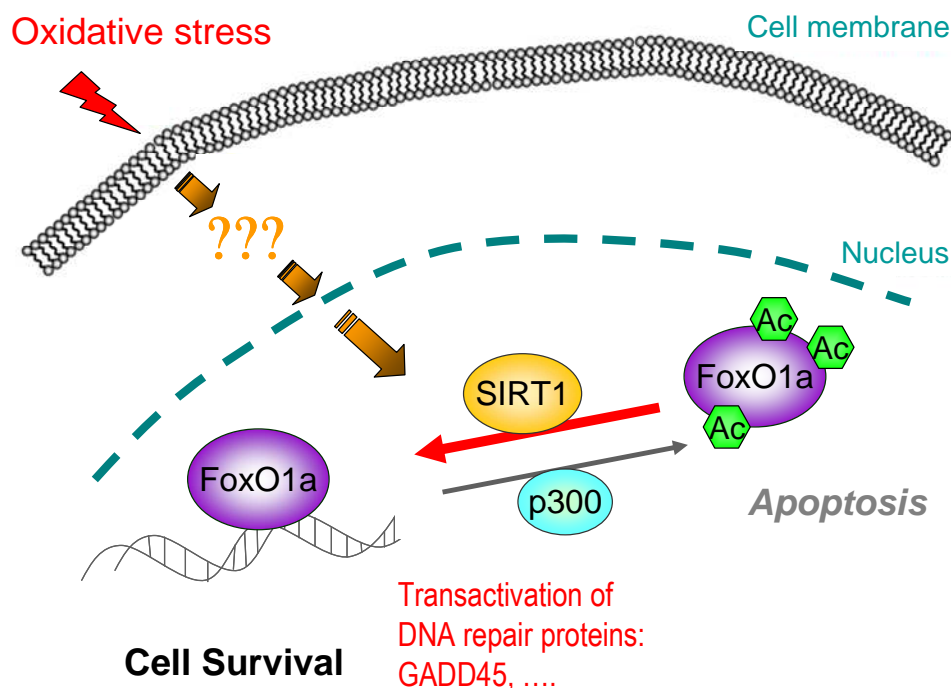


Figure 66. *SIRT1-dependent modulation of FoxO1a*

A FoxO1a/SIRT1 interaction as determined in stressed cells (induced either by serum withdrawal or by peroxide treatment) was not visible in serum-stimulated ones. The missing interaction of SIRT1 and FoxO1a under serum stimulation was not very surprisingly, because we and others have already demonstrated FoxO1a to become phosphorylated upon FBS treatment *in vitro* and *in vivo* (unpublished data)²³⁸⁻²⁴⁰, which then typically leads to its nuclear exclusion and degradation. Nevertheless, in my studies SIRT1 was demonstrated to affect cellular responses triggered by both serum and stress, thus it seems that SIRT1 has different mechanisms of action dependent on the stimulus. Whereas the stress-induced mechanism was suggested to operate via FoxO1a, the second one mediated by serum was demonstrated to be FoxO-independent.

But how does endogenous SIRT1 regulate cell cycle progression, proliferation and migration in HCASMCs *in vitro* and *in vivo*? One explanation could be that SIRT1 modulated other proteins, which in turn regulated the mentioned cellular processes. Until date, our group has identified several possible targets, including signaling pathway components and transcription factors (personal communication). However, the detailed mechanisms have to be identified in the future.

Other explanations that have already been published emphasized on the original identified function of SIRT1 as a histone deacetylase: SIRT1 contributes to gene silencing by interacting with histones and by deacetylating them³⁴⁸. Thus, another idea on how SIRT1 regulates VSMC gene transcription is by promoting facultative heterochromatin formation. Whether this point is important in the vascular system has not been investigated yet.

In regard with phosphorylation leading to FoxO1a's subcellular translocation, some publications described H₂O₂ to have insulin-mimetic effects, including enhanced Akt activity and exclusion of FoxO1a from the nucleus¹⁷¹. Nevertheless, the effects of peroxide in cultured cells are complex and other groups already showed a predominantly nuclear localization of FoxO1a upon peroxide treatment²³³. Thus, results reported are controversial. Since I showed deacetylated FoxO1a to be localized within the nucleus under oxidative stress conditions and displayed increased transcriptional activity on some of FoxO1a's specific target genes, nuclear exclusion due to possible H₂O₂-induced phosphorylation can be excluded in HCASMCs.

While the above mentioned studies have focused on the forkhead transcription factor FoxO1a, additional unpublished results of mine indicated that SIRT1 also adheres to FoxO3a, thereby deacetylating and inactivating this family member as well. SIRT1 may thus generally deacetylate FoxO transcription factors in VSMCs and therefore leads to upregulation of genes that are normally activated by forkhead proteins.

Recently, accumulating evidence indicated that considerable analogies exist between FoxOs and p53, not only in their common capability to regulate cell death and cell cycle arrest, but obviously also in their mode of action. Both proteins, p53 and FoxOs, were demonstrated to be regulated by p300/CBP-mediated acetylation and by deacetylation through SIRT1^{233, 261-263, 268, 312-315, 347}. SIRT1-mediated deacetylation of p53 was shown to inhibit apoptosis against a myriad of stress types, including DNA damage and oxidative stress, resulting in cellular protection.

Additionally, p53 seems to parallel FoxO in its functions, as it controls multiple analogous mechanisms, such as DNA repair, cell cycle arrest and apoptosis. Depending on the degree of DNA damage and the general cellular background, the pro-apoptotic effects might be favored. Additionally to be regulated by phosphorylation and/or acetylation, van der Horst and colleagues extended the list of similarities by revealing regulation of both proteins by monoubiquitination²⁶⁶.

Preliminary data from our group demonstrated SIRT1 to affect p53 function in HCASMCs. Thus, the shared regulatory network of both p53 and FoxO may have essential impacts on our understanding of the development of vascular disorders, as this process is expected to involve both the p53 and the FoxO pathway³⁶¹. How far SIRT1 is involved in this regulation will be of main interest, especially with regard to future therapeutic approaches manipulating SIRT1 activation.

In contrast to the effect on FoxOs and p53 - two proteins demonstrated to promote cell survival - SIRT1-mediated deacetylation of NF- κ B was suggested to stimulate NF- κ B signaling and thus induce cell death³¹⁷. This result demonstrates that the role of SIRT1 during cellular stress responses is complex and that the impact of its activation is expected to be cell context specific. The fact that SIRT1 influences numerous molecular pathways indicates that this type of histone deacetylase has an incomprehensible role in the cellular system what affords much room for future research.

Summary

Vasculopathic disorders are the major causes of death in Western civilization. Diseases such as atherosclerosis, postangioplasty restenosis and vein graft failure upon bypass surgery, as well as pulmonary hypertension result in myocardial infarction, stroke or peripheral artery diseases. VSMCs are closely correlated with the pathogenesis of these diseases. Previous data from our group as well as data presented in this thesis suggest that the forkhead transcription factor FoxO1a contributes to the regulation of cell cycle progression, VSMC proliferation, chemotactic migration, neointimal hyperplasia, vascular remodeling and apoptotic cell death. Regulation of FoxO1a by post-translational modification is important for its activity. Since the influence of FoxO1a phosphorylation was already investigated by our group, deacetylation of FoxO1a by the

class III deacetylase SIRT1 is a novel phenomenon, which was examined in this study. My data indicate that SIRT1-dependent deacetylation of FoxO1a has a major influence on vascular development and homeostasis, pointing towards a central role of the deacetylase in the pathogenesis of diseases affecting the vasculature. Adequate functions of both proteins are important for adapting VSMCs to the environmental demands. Taken together, my data imply that both FoxO1a and SIRT1 may represent potentially attractive targets for future therapeutic strategies in the prevention of vasculo-proliferative diseases.

References

References

1. Rosamond W, Flegal K, Friday G, et al. Heart disease and stroke statistics--2007 update: a report from the American Heart Association Statistics Committee and Stroke Statistics Subcommittee. *Circulation*. Feb 6 2007;115(5):e69-171.
2. Truelsen T, Piechowski-Jozwiak B, Bonita R, et al. Stroke incidence and prevalence in Europe: a review of available data. *Eur J Neurol*. Jun 2006;13(6):581-598.
3. Murray CJ, Lopez AD. Global mortality, disability, and the contribution of risk factors: Global Burden of Disease Study. *Lancet*. May 17 1997;349(9063):1436-1442.
4. Ross R. Atherosclerosis--an inflammatory disease. *N Engl J Med*. Jan 14 1999;340(2):115-126.
5. Libby P, Ridker PM, Maseri A. Inflammation and atherosclerosis. *Circulation*. Mar 5 2002;105(9):1135-1143.
6. Lusis AJ. Atherosclerosis. *Nature*. Sep 14 2000;407(6801):233-241.
7. McGill HC, Jr., McMahan CA, Herderick EE, et al. Origin of atherosclerosis in childhood and adolescence. *Am J Clin Nutr*. Nov 2000;72(5 Suppl):1307S-1315S.
8. Davies PF, Barbee KA, Volin MV, et al. Spatial relationships in early signaling events of flow-mediated endothelial mechanotransduction. *Annu Rev Physiol*. 1997;59:527-549.
9. Wissler RW, Vesselinovitch D. Atherosclerosis--relationship to coronary blood flow. *Am J Cardiol*. Jul 20 1983;52(2):2A-7A.
10. McMillan DE. Blood flow and the localization of atherosclerotic plaques. *Stroke*. Jul-Aug 1985;16(4):582-587.
11. Ross R. The pathogenesis of atherosclerosis--an update. *N Engl J Med*. Feb 20 1986;314(8):488-500.
12. Chiesa G, Sirtori CR. Apolipoprotein A-I(Milano): current perspectives. *Curr Opin Lipidol*. Apr 2003;14(2):159-163.
13. Majors A, Ehrhart LA, Pezacka EH. Homocysteine as a risk factor for vascular disease. Enhanced collagen production and accumulation by smooth muscle cells. *Arterioscler Thromb Vasc Biol*. Oct 1997;17(10):2074-2081.
14. Nygard O, Nordrehaug JE, Refsum H, et al. Plasma homocysteine levels and mortality in patients with coronary artery disease. *N Engl J Med*. Jul 24 1997;337(4):230-236.
15. Vaughan DE. PAI-1 and atherothrombosis. *J Thromb Haemost*. Aug 2005;3(8):1879-1883.
16. Koenig W. Fibrin(ogen) in cardiovascular disease: an update. *Thromb Haemost*. Apr 2003;89(4):601-609.
17. Fox SL. *Human Physiology, 8/e*: McGraw-Hill Higher Education; 2003.
18. Ross R, Glomset JA. Atherosclerosis and the arterial smooth muscle cell: Proliferation of smooth muscle is a key event in the genesis of the lesions of atherosclerosis. *Science*. Jun 29 1973;180(93):1332-1339.
19. Ross R, Faggitotto A, Bowen-Pope D, et al. The role of endothelial injury and platelet and macrophage interactions in atherosclerosis. *Circulation*. Nov 1984;70(5 Pt 2):III77-82.
20. Harrison DG. Cellular and molecular mechanisms of endothelial cell dysfunction. *J Clin Invest*. Nov 1 1997;100(9):2153-2157.
21. Libby P. Inflammation in atherosclerosis. *Nature*. Dec 19-26 2002;420(6917):868-874.
22. Navab M, Berliner JA, Watson AD, et al. The Yin and Yang of oxidation in the development of the fatty streak. A review based on the 1994 George Lyman Duff Memorial Lecture. *Arterioscler Thromb Vasc Biol*. Jul 1996;16(7):831-842.
23. Steinberg D. Low density lipoprotein oxidation and its pathobiological significance. *J Biol Chem*. Aug 22 1997;272(34):20963-20966.
24. Griending KK, Alexander RW. Oxidative stress and cardiovascular disease. *Circulation*. Nov 18 1997;96(10):3264-3265.
25. Steinberg D, Parthasarathy S, Carew TE, et al. Beyond cholesterol. Modifications of low-density lipoprotein that increase its atherogenicity. *N Engl J Med*. Apr 6 1989;320(14):915-924.

26. Rajavashisth TB, Andalibi A, Territo MC, et al. Induction of endothelial cell expression of granulocyte and macrophage colony-stimulating factors by modified low-density lipoproteins. *Nature*. Mar 15 1990;344(6263):254-257.
27. Cybulsky MI, Gimbrone MA, Jr. Endothelial expression of a mononuclear leukocyte adhesion molecule during atherogenesis. *Science*. Feb 15 1991;251(4995):788-791.
28. Cybulsky MI, Iiyama K, Li H, et al. A major role for VCAM-1, but not ICAM-1, in early atherosclerosis. *J Clin Invest*. May 2001;107(10):1255-1262.
29. Gu L, Okada Y, Clinton SK, et al. Absence of monocyte chemoattractant protein-1 reduces atherosclerosis in low density lipoprotein receptor-deficient mice. *Mol Cell*. Aug 1998;2(2):275-281.
30. Ross R. The pathogenesis of atherosclerosis: a perspective for the 1990s. *Nature*. Apr 29 1993;362(6423):801-809.
31. Berliner JA, Navab M, Fogelman AM, et al. Atherosclerosis: basic mechanisms. Oxidation, inflammation, and genetics. *Circulation*. May 1 1995;91(9):2488-2496.
32. Smith JD, Trogan E, Ginsberg M, et al. Decreased atherosclerosis in mice deficient in both macrophage colony-stimulating factor (op) and apolipoprotein E. *Proc Natl Acad Sci U S A*. Aug 29 1995;92(18):8264-8268.
33. Hansson GK, Jonasson L, Lojsthe B, et al. Localization of T lymphocytes and macrophages in fibrous and complicated human atherosclerotic plaques. *Atherosclerosis*. Aug 1988;72(2-3):135-141.
34. Clinton SK, Underwood R, Hayes L, et al. Macrophage colony-stimulating factor gene expression in vascular cells and in experimental and human atherosclerosis. *Am J Pathol*. Feb 1992;140(2):301-316.
35. Rosenfeld ME, Yla-Herttuala S, Lipton BA, et al. Macrophage colony-stimulating factor mRNA and protein in atherosclerotic lesions of rabbits and humans. *Am J Pathol*. Feb 1992;140(2):291-300.
36. Schwartz SM, deBlois D, O'Brien ER. The intima. Soil for atherosclerosis and restenosis. *Circ Res*. Sep 1995;77(3):445-465.
37. Faggiotto A, Ross R, Harker L. Studies of hypercholesterolemia in the nonhuman primate. I. Changes that lead to fatty streak formation. *Arteriosclerosis*. Jul-Aug 1984;4(4):323-340.
38. Kockx MM, Herman AG. Apoptosis in atherosclerosis: beneficial or detrimental? *Cardiovasc Res*. Feb 2000;45(3):736-746.
39. Libby P. Inflammation and cardiovascular disease mechanisms. *Am J Clin Nutr*. Feb 2006;83(2):456S-460S.
40. Richardson PD, Davies MJ, Born GV. Influence of plaque configuration and stress distribution on fissuring of coronary atherosclerotic plaques. *Lancet*. Oct 21 1989;2(8669):941-944.
41. Davies MJ, Thomas A. Thrombosis and acute coronary-artery lesions in sudden cardiac ischemic death. *N Engl J Med*. May 3 1984;310(18):1137-1140.
42. Toschi V, Gallo R, Lettino M, et al. Tissue factor modulates the thrombogenicity of human atherosclerotic plaques. *Circulation*. Feb 4 1997;95(3):594-599.
43. Gruntzig A. Transluminal dilatation of coronary-artery stenosis. *Lancet*. Feb 4 1978;1(8058):263.
44. Serruys PW, de Jaegere P, Kiemeneij F, et al. A comparison of balloon-expandable-stent implantation with balloon angioplasty in patients with coronary artery disease. Benestent Study Group. *N Engl J Med*. Aug 25 1994;331(8):489-495.
45. Dzau VJ, Braun-Dullaeus RC, Sedding DG. Vascular proliferation and atherosclerosis: new perspectives and therapeutic strategies. *Nat Med*. Nov 2002;8(11):1249-1256.
46. Farb A, Weber DK, Kolodgie FD, et al. Morphological predictors of restenosis after coronary stenting in humans. *Circulation*. Jun 25 2002;105(25):2974-2980.
47. Sousa JE, Serruys PW, Costa MA. New frontiers in cardiology: drug-eluting stents: Part I. *Circulation*. May 6 2003;107(17):2274-2279.
48. Sousa JE, Costa MA, Abizaid A, et al. Sirolimus-eluting stent for the treatment of in-stent restenosis: a quantitative coronary angiography and three-dimensional intravascular ultrasound study. *Circulation*. Jan 7 2003;107(1):24-27.

49. Granada JF, Kaluza GL, Raizner A. Drug-eluting stents for cardiovascular disorders. *Curr Atheroscler Rep*. Jul 2003;5(4):308-316.
50. Virmani R, Guagliumi G, Farb A, et al. Localized hypersensitivity and late coronary thrombosis secondary to a sirolimus-eluting stent: should we be cautious? *Circulation*. Feb 17 2004;109(6):701-705.
51. van Beusekom HM, Saia F, Zindler JD, et al. Drug-eluting stents show delayed healing: paclitaxel more pronounced than sirolimus. *Eur Heart J*. Apr 2007;28(8):974-979.
52. McBride W, Lange RA, Hillis LD. Restenosis after successful coronary angioplasty. Pathophysiology and prevention. *N Engl J Med*. Jun 30 1988;318(26):1734-1737.
53. Rajagopal V, Rockson SG. Coronary restenosis: a review of mechanisms and management. *Am J Med*. Nov 2003;115(7):547-553.
54. Costa MA, Simon DI. Molecular basis of restenosis and drug-eluting stents. *Circulation*. May 3 2005;111(17):2257-2273.
55. Welt FG, Rogers C. Inflammation and restenosis in the stent era. *Arterioscler Thromb Vasc Biol*. Nov 1 2002;22(11):1769-1776.
56. Rodriguez AE, Palacios IF, Fernandez MA, et al. Time course and mechanism of early luminal diameter loss after percutaneous transluminal coronary angioplasty. *Am J Cardiol*. Dec 1 1995;76(16):1131-1134.
57. Baumgartner HR, Haudenschild C. Adhesion of platelets to subendothelium. *Ann N Y Acad Sci*. Oct 27 1972;201:22-36.
58. Libby P, Simon DI. Inflammation and thrombosis: the clot thickens. *Circulation*. Apr 3 2001;103(13):1718-1720.
59. Goldberg ID, Stemerman MB, Handin RI. Vascular permeation of platelet factor 4 after endothelial injury. *Science*. Aug 1 1980;209(4456):611-612.
60. Rectenwald JE, Moldawer LL, Huber TS, et al. Direct evidence for cytokine involvement in neointimal hyperplasia. *Circulation*. Oct 3 2000;102(14):1697-1702.
61. Libby P, Schwartz D, Brogi E, et al. A cascade model for restenosis. A special case of atherosclerosis progression. *Circulation*. Dec 1992;86(6 Suppl):III47-52.
62. Bauters C, Isner JM. The biology of restenosis. *Prog Cardiovasc Dis*. Sep-Oct 1997;40(2):107-116.
63. Scott-Burden T VP. The endothelium as a regulator of vascular smooth muscle proliferation. *Circulation*. 1993;87(Suppl V):V-51- V-55.
64. Li C, Xu Q. Mechanical stress-initiated signal transductions in vascular smooth muscle cells. *Cell Signal*. Jul 2000;12(7):435-445.
65. Sedding DG, Seay U, Fink L, et al. Mechanosensitive p27Kip1 regulation and cell cycle entry in vascular smooth muscle cells. *Circulation*. Aug 5 2003;108(5):616-622.
66. Sedding DG, Hermesen J, Seay U, et al. Caveolin-1 facilitates mechanosensitive protein kinase B (Akt) signaling in vitro and in vivo. *Circ Res*. Apr 1 2005;96(6):635-642.
67. Bendeck MP, Irvin C, Reidy MA. Inhibition of matrix metalloproteinase activity inhibits smooth muscle cell migration but not neointimal thickening after arterial injury. *Circ Res*. Jan 1996;78(1):38-43.
68. Scott NA, Cipolla GD, Ross CE, et al. Identification of a potential role for the adventitia in vascular lesion formation after balloon overstretch injury of porcine coronary arteries. *Circulation*. Jun 15 1996;93(12):2178-2187.
69. Patel S, Shi Y, Niculescu R, et al. Characteristics of coronary smooth muscle cells and adventitial fibroblasts. *Circulation*. Feb 8 2000;101(5):524-532.
70. Mintz GS, Popma JJ, Pichard AD, et al. Arterial remodeling after coronary angioplasty: a serial intravascular ultrasound study. *Circulation*. Jul 1 1996;94(1):35-43.
71. Bennett MR, Schwartz SM. Antisense therapy for angioplasty restenosis. Some critical considerations. *Circulation*. Oct 1 1995;92(7):1981-1993.
72. Walker LN, Bowen-Pope DF, Ross R, et al. Production of platelet-derived growth factor-like molecules by cultured arterial smooth muscle cells accompanies proliferation after arterial injury. *Proc Natl Acad Sci U S A*. Oct 1986;83(19):7311-7315.
73. Fouty BW, Grimison B, Fagan KA, et al. p27(Kip1) is important in modulating pulmonary artery smooth muscle cell proliferation. *Am J Respir Cell Mol Biol*. Nov 2001;25(5):652-658.

74. Gurbanov E, Shiliang X. The key role of apoptosis in the pathogenesis and treatment of pulmonary hypertension. *Eur J Cardiothorac Surg*. Sep 2006;30(3):499-507.
75. Strange JW, Wharton J, Phillips PG, et al. Recent insights into the pathogenesis and therapeutics of pulmonary hypertension. *Clin Sci (Lond)*. Mar 2002;102(3):253-268.
76. Yu L, Quinn DA, Garg HG, et al. Cyclin-dependent kinase inhibitor p27Kip1, but not p21WAF1/Cip1, is required for inhibition of hypoxia-induced pulmonary hypertension and remodeling by heparin in mice. *Circ Res*. Oct 28 2005;97(9):937-945.
77. Orlandi A, Ehrlich HP, Ropraz P, et al. Rat aortic smooth muscle cells isolated from different layers and at different times after endothelial denudation show distinct biological features in vitro. *Arterioscler Thromb*. Jun 1994;14(6):982-989.
78. Braun-Dullaeus RC, Mann MJ, Dzau VJ. Cell cycle progression: new therapeutic target for vascular proliferative disease. *Circulation*. Jul 7 1998;98(1):82-89.
79. Owens GK, Kumar MS, Wamhoff BR. Molecular regulation of vascular smooth muscle cell differentiation in development and disease. *Physiol Rev*. Jul 2004;84(3):767-801.
80. Hao H, Gabbiani G, Bochaton-Piallat ML. Arterial smooth muscle cell heterogeneity: implications for atherosclerosis and restenosis development. *Arterioscler Thromb Vasc Biol*. Sep 1 2003;23(9):1510-1520.
81. Yoshida T, Owens GK. Molecular determinants of vascular smooth muscle cell diversity. *Circ Res*. Feb 18 2005;96(3):280-291.
82. Sata M. Role of circulating vascular progenitors in angiogenesis, vascular healing, and pulmonary hypertension: lessons from animal models. *Arterioscler Thromb Vasc Biol*. May 2006;26(5):1008-1014.
83. Zalewski A, Shi Y, Johnson AG. Diverse origin of intimal cells: smooth muscle cells, myofibroblasts, fibroblasts, and beyond? *Circ Res*. Oct 18 2002;91(8):652-655.
84. Clowes AW, Clowes MM. Kinetics of cellular proliferation after arterial injury. II. Inhibition of smooth muscle growth by heparin. *Lab Invest*. Jun 1985;52(6):611-616.
85. Casscells W. Migration of smooth muscle and endothelial cells. Critical events in restenosis. *Circulation*. Sep 1992;86(3):723-729.
86. Willis AI, Pierre-Paul D, Sumpio BE, et al. Vascular smooth muscle cell migration: current research and clinical implications. *Vasc Endovascular Surg*. Jan-Feb 2004;38(1):11-23.
87. Chandrasekar B, Tanguay JF. Platelets and restenosis. *J Am Coll Cardiol*. Mar 1 2000;35(3):555-562.
88. Sedding D, Daniel JM, Muhl L, et al. The G534E polymorphism of the gene encoding the factor VII-activating protease is associated with cardiovascular risk due to increased neointima formation. *J Exp Med*. Dec 25 2006;203(13):2801-2807.
89. Schwartz SM. Smooth muscle migration in atherosclerosis and restenosis. *J Clin Invest*. Dec 1 1997;100(11 Suppl):S87-89.
90. Casarosa P, Waldhoer M, LiWang PJ, et al. CC and CX3C chemokines differentially interact with the N terminus of the human cytomegalovirus-encoded US28 receptor. *J Biol Chem*. Feb 4 2005;280(5):3275-3285.
91. Nelson PR, Yamamura S, Kent KC. Extracellular matrix proteins are potent agonists of human smooth muscle cell migration. *J Vasc Surg*. Jul 1996;24(1):25-32; discussion 32-23.
92. Kokubo T, Uchida H, Choi ET. Integrin alpha(v)beta(3) as a target in the prevention of neointimal hyperplasia. *J Vasc Surg*. Jun 2007;45 Suppl A:A33-38.
93. O'Brien ER, Garvin MR, Stewart DK, et al. Osteopontin is synthesized by macrophage, smooth muscle, and endothelial cells in primary and restenotic human coronary atherosclerotic plaques. *Arterioscler Thromb*. Oct 1994;14(10):1648-1656.
94. Pompili VJ, Gordon D, San H, et al. Expression and function of a recombinant PDGF B gene in porcine arteries. *Arterioscler Thromb Vasc Biol*. Dec 1995;15(12):2254-2264.
95. Lindner V, Reidy MA. Proliferation of smooth muscle cells after vascular injury is inhibited by an antibody against basic fibroblast growth factor. *Proc Natl Acad Sci U S A*. May 1 1991;88(9):3739-3743.

96. Ignarro LJ, Buga GM, Wei LH, et al. Role of the arginine-nitric oxide pathway in the regulation of vascular smooth muscle cell proliferation. *Proc Natl Acad Sci U S A*. Mar 27 2001;98(7):4202-4208.
97. Braun-Dullaeus RC, Mann MJ, Seay U, et al. Cell cycle protein expression in vascular smooth muscle cells in vitro and in vivo is regulated through phosphatidylinositol 3-kinase and mammalian target of rapamycin. *Arterioscler Thromb Vasc Biol*. Jul 2001;21(7):1152-1158.
98. Sherr CJ, Roberts JM. CDK inhibitors: positive and negative regulators of G1-phase progression. *Genes Dev*. Jun 15 1999;13(12):1501-1512.
99. Hiromura K, Pippin JW, Fero ML, et al. Modulation of apoptosis by the cyclin-dependent kinase inhibitor p27(Kip1). *J Clin Invest*. Mar 1999;103(5):597-604.
100. Walsh K, Smith RC, Kim HS. Vascular cell apoptosis in remodeling, restenosis, and plaque rupture. *Circ Res*. Aug 4 2000;87(3):184-188.
101. Geng YJ. Molecular signal transduction in vascular cell apoptosis. *Cell Res*. Dec 2001;11(4):253-264.
102. McCarthy NJ, Bennett MR. The regulation of vascular smooth muscle cell apoptosis. *Cardiovasc Res*. Feb 2000;45(3):747-755.
103. Virchow R. Die Cellularpathologie: Sechzehnte verlesung, 14 April 1858. *George Olms, Hildesheim, Germany*.1966:317-329.
104. Isner JM, Kearney M, Bortman S, et al. Apoptosis in human atherosclerosis and restenosis. *Circulation*. Jun 1 1995;91(11):2703-2711.
105. Bennett MR, Evan GI, Schwartz SM. Apoptosis of human vascular smooth muscle cells derived from normal vessels and coronary atherosclerotic plaques. *J Clin Invest*. May 1995;95(5):2266-2274.
106. Bennett MR, Boyle JJ. Apoptosis of vascular smooth muscle cells in atherosclerosis. *Atherosclerosis*. May 1998;138(1):3-9.
107. Geng YJ, Wu Q, Muszynski M, et al. Apoptosis of vascular smooth muscle cells induced by in vitro stimulation with interferon-gamma, tumor necrosis factor-alpha, and interleukin-1 beta. *Arterioscler Thromb Vasc Biol*. Jan 1996;16(1):19-27.
108. Geng YJ, Libby P. Evidence for apoptosis in advanced human atheroma. Colocalization with interleukin-1 beta-converting enzyme. *Am J Pathol*. Aug 1995;147(2):251-266.
109. Han DK, Haudenschild CC, Hong MK, et al. Evidence for apoptosis in human atherogenesis and in a rat vascular injury model. *Am J Pathol*. Aug 1995;147(2):267-277.
110. Elledge SJ. Cell cycle checkpoints: preventing an identity crisis. *Science*. Dec 6 1996;274(5293):1664-1672.
111. Kerr JF, Wyllie AH, Currie AR. Apoptosis: a basic biological phenomenon with wide-ranging implications in tissue kinetics. *Br J Cancer*. Aug 1972;26(4):239-257.
112. Bauriedel G, Schluckebier S, Hutter R, et al. Apoptosis in restenosis versus stable-angina atherosclerosis: implications for the pathogenesis of restenosis. *Arterioscler Thromb Vasc Biol*. Jul 1998;18(7):1132-1139.
113. Bauriedel G, Hutter R, Welsch U, et al. Role of smooth muscle cell death in advanced coronary primary lesions: implications for plaque instability. *Cardiovasc Res*. Feb 1999;41(2):480-488.
114. Perlman H, Maillard L, Krasinski K, et al. Evidence for the rapid onset of apoptosis in medial smooth muscle cells after balloon injury. *Circulation*. Feb 18 1997;95(4):981-987.
115. Mallat Z, Tedgui A. Apoptosis in the vasculature: mechanisms and functional importance. *Br J Pharmacol*. Jul 2000;130(5):947-962.
116. Irani K. Oxidant signaling in vascular cell growth, death, and survival: a review of the roles of reactive oxygen species in smooth muscle and endothelial cell mitogenic and apoptotic signaling. *Circ Res*. Aug 4 2000;87(3):179-183.
117. Boyle JJ, Weissberg PL, Bennett MR. Human macrophage-induced vascular smooth muscle cell apoptosis requires NO enhancement of Fas/Fas-L interactions. *Arterioscler Thromb Vasc Biol*. Oct 1 2002;22(10):1624-1630.
118. Bennett MR. Apoptosis of vascular smooth muscle cells in vascular remodelling and atherosclerotic plaque rupture. *Cardiovasc Res*. Feb 1999;41(2):361-368.

119. Sato K, Niessner A, Kopecky SL, et al. TRAIL-expressing T cells induce apoptosis of vascular smooth muscle cells in the atherosclerotic plaque. *J Exp Med*. Jan 23 2006;203(1):239-250.
120. Thornberry NA, Lazebnik Y. Caspases: enemies within. *Science*. Aug 28 1998;281(5381):1312-1316.
121. Littlewood TD, Bennett MR. Apoptotic cell death in atherosclerosis. *Curr Opin Lipidol*. Oct 2003;14(5):469-475.
122. Rakesh K, Agrawal DK. Cytokines and growth factors involved in apoptosis and proliferation of vascular smooth muscle cells. *Int Immunopharmacol*. Sep 2005;5(10):1487-1506.
123. Bennett MR, Evan GI, Newby AC. Deregulated expression of the c-myc oncogene abolishes inhibition of proliferation of rat vascular smooth muscle cells by serum reduction, interferon-gamma, heparin, and cyclic nucleotide analogues and induces apoptosis. *Circ Res*. Mar 1994;74(3):525-536.
124. Cantley LC. The phosphoinositide 3-kinase pathway. *Science*. May 31 2002;296(5573):1655-1657.
125. Hawkins PT, Anderson KE, Davidson K, et al. Signalling through Class I PI3Ks in mammalian cells. *Biochem Soc Trans*. Nov 2006;34(Pt 5):647-662.
126. Vanhaesebroeck B, Alessi DR. The PI3K-PDK1 connection: more than just a road to PKB. *Biochem J*. Mar 15 2000;346 Pt 3:561-576.
127. Alessi DR, Deak M, Casamayor A, et al. 3-Phosphoinositide-dependent protein kinase-1 (PDK1): structural and functional homology with the Drosophila DSTPK61 kinase. *Curr Biol*. Oct 1 1997;7(10):776-789.
128. Jiang T, Qiu Y. Interaction between Src and a C-terminal proline-rich motif of Akt is required for Akt activation. *J Biol Chem*. May 2 2003;278(18):15789-15793.
129. Chen R, Kim O, Yang J, et al. Regulation of Akt/PKB activation by tyrosine phosphorylation. *J Biol Chem*. Aug 24 2001;276(34):31858-31862.
130. Brunet A, Datta SR, Greenberg ME. Transcription-dependent and -independent control of neuronal survival by the PI3K-Akt signaling pathway. *Curr Opin Neurobiol*. Jun 2001;11(3):297-305.
131. Liang J, Zubovitz J, Petrocelli T, et al. PKB/Akt phosphorylates p27, impairs nuclear import of p27 and opposes p27-mediated G1 arrest. *Nat Med*. Oct 2002;8(10):1153-1160.
132. Zhou BP, Liao Y, Xia W, et al. Cytoplasmic localization of p21Cip1/WAF1 by Akt-induced phosphorylation in HER-2/neu-overexpressing cells. *Nat Cell Biol*. Mar 2001;3(3):245-252.
133. Rossig L, Badorff C, Holzmann Y, et al. Glycogen synthase kinase-3 couples AKT-dependent signaling to the regulation of p21Cip1 degradation. *J Biol Chem*. Mar 22 2002;277(12):9684-9689.
134. Li Y, Dowbenko D, Lasky LA. AKT/PKB phosphorylation of p21Cip/WAF1 enhances protein stability of p21Cip/WAF1 and promotes cell survival. *J Biol Chem*. Mar 29 2002;277(13):11352-11361.
135. Zimmermann S, Moelling K. Phosphorylation and regulation of Raf by Akt (protein kinase B). *Science*. Nov 26 1999;286(5445):1741-1744.
136. Moelling K, Schad K, Bosse M, et al. Regulation of Raf-Akt Cross-talk. *J Biol Chem*. Aug 23 2002;277(34):31099-31106.
137. Reusch HP, Zimmermann S, Schaefer M, et al. Regulation of Raf by Akt controls growth and differentiation in vascular smooth muscle cells. *J Biol Chem*. Sep 7 2001;276(36):33630-33637.
138. Ozes ON, Mayo LD, Gustin JA, et al. NF-kappaB activation by tumour necrosis factor requires the Akt serine-threonine kinase. *Nature*. Sep 2 1999;401(6748):82-85.
139. Kane LP, Mollenauer MN, Xu Z, et al. Akt-dependent phosphorylation specifically regulates Cot induction of NF-kappa B-dependent transcription. *Mol Cell Biol*. Aug 2002;22(16):5962-5974.
140. Burgering BM, Kops GJ. Cell cycle and death control: long live Forkheads. *Trends Biochem Sci*. Jul 2002;27(7):352-360.

141. Kaestner KH, Knochel W, Martinez DE. Unified nomenclature for the winged helix/forkhead transcription factors. *Genes Dev.* Jan 15 2000;14(2):142-146.
142. Weigel D, Jurgens G, Kuttner F, et al. The homeotic gene fork head encodes a nuclear protein and is expressed in the terminal regions of the Drosophila embryo. *Cell.* May 19 1989;57(4):645-658.
143. Kaufmann E, Knochel W. Five years on the wings of fork head. *Mech Dev.* Jun 1996;57(1):3-20.
144. Lehmann OJ, Sowden JC, Carlsson P, et al. Fox's in development and disease. *Trends Genet.* Jun 2003;19(6):339-344.
145. Carter ME, Brunet A. FOXO transcription factors. *Curr Biol.* Feb 20 2007;17(4):R113-114.
146. Ogg S, Paradis S, Gottlieb S, et al. The Fork head transcription factor DAF-16 transduces insulin-like metabolic and longevity signals in *C. elegans*. *Nature.* Oct 30 1997;389(6654):994-999.
147. Lin K, Dorman JB, Rodan A, et al. daf-16: An HNF-3/forkhead family member that can function to double the life-span of *Caenorhabditis elegans*. *Science.* Nov 14 1997;278(5341):1319-1322.
148. Jacobs FM, van der Heide LP, Wijchers PJ, et al. FoxO6, a novel member of the FoxO class of transcription factors with distinct shuttling dynamics. *J Biol Chem.* Sep 19 2003;278(38):35959-35967.
149. Anderson MJ, Viars CS, Czekay S, et al. Cloning and characterization of three human forkhead genes that comprise an FKHR-like gene subfamily. *Genomics.* Jan 15 1998;47(2):187-199.
150. Furuyama T, Nakazawa T, Nakano I, et al. Identification of the differential distribution patterns of mRNAs and consensus binding sequences for mouse DAF-16 homologues. *Biochem J.* Jul 15 2000;349(Pt 2):629-634.
151. Biggs WH, 3rd, Cavenee WK, Arden KC. Identification and characterization of members of the FKHR (FOX O) subclass of winged-helix transcription factors in the mouse. *Mamm Genome.* Jun 2001;12(6):416-425.
152. Hoekman MF, Jacobs FM, Smidt MP, et al. Spatial and temporal expression of FoxO transcription factors in the developing and adult murine brain. *Gene Expr Patterns.* Jan 2006;6(2):134-140.
153. Galili N, Davis RJ, Fredericks WJ, et al. Fusion of a fork head domain gene to PAX3 in the solid tumour alveolar rhabdomyosarcoma. *Nat Genet.* Nov 1993;5(3):230-235.
154. Davis RJ, D'Cruz CM, Lovell MA, et al. Fusion of PAX7 to FKHR by the variant t(1;13)(p36;q14) translocation in alveolar rhabdomyosarcoma. *Cancer Res.* Jun 1 1994;54(11):2869-2872.
155. Parry P, Wei Y, Evans G. Cloning and characterization of the t(X;11) breakpoint from a leukemic cell line identify a new member of the forkhead gene family. *Genes Chromosomes Cancer.* Oct 1994;11(2):79-84.
156. Borkhardt A, Repp R, Haas OA, et al. Cloning and characterization of AFX, the gene that fuses to MLL in acute leukemias with a t(X;11)(q13;q23). *Oncogene.* Jan 16 1997;14(2):195-202.
157. Hillion J, Le Coniat M, Jonveaux P, et al. AF6q21, a novel partner of the MLL gene in t(6;11)(q21;q23), defines a forkhead transcriptional factor subfamily. *Blood.* Nov 1 1997;90(9):3714-3719.
158. Hosaka T, Biggs WH, 3rd, Tieu D, et al. Disruption of forkhead transcription factor (FOXO) family members in mice reveals their functional diversification. *Proc Natl Acad Sci U S A.* Mar 2 2004;101(9):2975-2980.
159. Furuyama T, Kitayama K, Shimoda Y, et al. Abnormal angiogenesis in Foxo1 (Fkhr)-deficient mice. *J Biol Chem.* Aug 13 2004;279(33):34741-34749.
160. Castrillon DH, Miao L, Kollipara R, et al. Suppression of ovarian follicle activation in mice by the transcription factor Foxo3a. *Science.* Jul 11 2003;301(5630):215-218.
161. Brownawell AM, Kops GJ, Macara IG, et al. Inhibition of nuclear import by protein kinase B (Akt) regulates the subcellular distribution and activity of the forkhead transcription factor AFX. *Mol Cell Biol.* May 2001;21(10):3534-3546.

162. Van Der Heide LP, Hoekman MF, Smidt MP. The ins and outs of FoxO shuttling: mechanisms of FoxO translocation and transcriptional regulation. *Biochem J*. Jun 1 2004;380(Pt 2):297-309.
163. Zhao X, Gan L, Pan H, et al. Multiple elements regulate nuclear/cytoplasmic shuttling of FOXO1: characterization of phosphorylation- and 14-3-3-dependent and -independent mechanisms. *Biochem J*. Mar 15 2004;378(Pt 3):839-849.
164. Kops GJ, Medema RH, Glassford J, et al. Control of cell cycle exit and entry by protein kinase B-regulated forkhead transcription factors. *Mol Cell Biol*. Apr 2002;22(7):2025-2036.
165. Xuan Z, Zhang MQ. From worm to human: bioinformatics approaches to identify FOXO target genes. *Mech Ageing Dev*. Jan 2005;126(1):209-215.
166. Brunet A, Bonni A, Zigmond MJ, et al. Akt promotes cell survival by phosphorylating and inhibiting a Forkhead transcription factor. *Cell*. Mar 19 1999;96(6):857-868.
167. Kops GJ, de Ruiter ND, De Vries-Smits AM, et al. Direct control of the Forkhead transcription factor AFX by protein kinase B. *Nature*. Apr 15 1999;398(6728):630-634.
168. Ramaswamy S, Nakamura N, Sansal I, et al. A novel mechanism of gene regulation and tumor suppression by the transcription factor FKHR. *Cancer Cell*. Jul 2002;2(1):81-91.
169. Tran H, Brunet A, Grenier JM, et al. DNA repair pathway stimulated by the forkhead transcription factor FOXO3a through the Gadd45 protein. *Science*. Apr 19 2002;296(5567):530-534.
170. Kops GJ, Dansen TB, Polderman PE, et al. Forkhead transcription factor FOXO3a protects quiescent cells from oxidative stress. *Nature*. Sep 19 2002;419(6904):316-321.
171. Nemoto S, Finkel T. Redox regulation of forkhead proteins through a p66shc-dependent signaling pathway. *Science*. Mar 29 2002;295(5564):2450-2452.
172. Greer EL, Brunet A. FOXO transcription factors at the interface between longevity and tumor suppression. *Oncogene*. Nov 14 2005;24(50):7410-7425.
173. Kajihara T, Jones M, Fusi L, et al. Differential expression of FOXO1 and FOXO3a confers resistance to oxidative cell death upon endometrial decidualization. *Mol Endocrinol*. Oct 2006;20(10):2444-2455.
174. Bakker WJ, Blazquez-Domingo M, Kolbus A, et al. FoxO3a regulates erythroid differentiation and induces BTG1, an activator of protein arginine methyl transferase 1. *J Cell Biol*. Jan 19 2004;164(2):175-184.
175. Birkenkamp KU, Essafi A, van der Vos KE, et al. FOXO3a induces differentiation of Bcr-Abl-transformed cells through transcriptional down-regulation of Id1. *J Biol Chem*. Jan 26 2007;282(4):2211-2220.
176. Hribal ML, Nakae J, Kitamura T, et al. Regulation of insulin-like growth factor-dependent myoblast differentiation by Foxo forkhead transcription factors. *J Cell Biol*. Aug 18 2003;162(4):535-541.
177. Nakae J, Kitamura T, Kitamura Y, et al. The forkhead transcription factor Foxo1 regulates adipocyte differentiation. *Dev Cell*. Jan 2003;4(1):119-129.
178. Accili D, Arden KC. FoxOs at the crossroads of cellular metabolism, differentiation, and transformation. *Cell*. May 14 2004;117(4):421-426.
179. Barthel A, Schmoll D, Unterman TG. FoxO proteins in insulin action and metabolism. *Trends Endocrinol Metab*. May-Jun 2005;16(4):183-189.
180. Nakae J, Kitamura T, Silver DL, et al. The forkhead transcription factor Foxo1 (Fkhr) confers insulin sensitivity onto glucose-6-phosphatase expression. *J Clin Invest*. Nov 2001;108(9):1359-1367.
181. Onuma H, Vander Kooi BT, Boustead JN, et al. Correlation between FOXO1a (FKHR) and FOXO3a (FKHRL1) binding and the inhibition of basal glucose-6-phosphatase catalytic subunit gene transcription by insulin. *Mol Endocrinol*. Nov 2006;20(11):2831-2847.
182. Yang Z, Whelan J, Babb R, et al. An mRNA splice variant of the AFX gene with altered transcriptional activity. *J Biol Chem*. Mar 8 2002;277(10):8068-8075.
183. Furuyama T, Kitayama K, Yamashita H, et al. Forkhead transcription factor FOXO1 (FKHR)-dependent induction of PDK4 gene expression in skeletal muscle during energy deprivation. *Biochem J*. Oct 15 2003;375(Pt 2):365-371.

184. Nadal A, Marrero PF, Haro D. Down-regulation of the mitochondrial 3-hydroxy-3-methylglutaryl-CoA synthase gene by insulin: the role of the forkhead transcription factor FKHL1. *Biochem J.* Aug 15 2002;366(Pt 1):289-297.
185. Kamei Y, Mizukami J, Miura S, et al. A forkhead transcription factor FKHR up-regulates lipoprotein lipase expression in skeletal muscle. *FEBS Lett.* Feb 11 2003;536(1-3):232-236.
186. Daitoku H, Yamagata K, Matsuzaki H, et al. Regulation of PGC-1 promoter activity by protein kinase B and the forkhead transcription factor FKHR. *Diabetes.* Mar 2003;52(3):642-649.
187. Puigserver P, Rhee J, Donovan J, et al. Insulin-regulated hepatic gluconeogenesis through FOXO1-PGC-1alpha interaction. *Nature.* May 29 2003;423(6939):550-555.
188. Rhee J, Inoue Y, Yoon JC, et al. Regulation of hepatic fasting response by PPARgamma coactivator-1alpha (PGC-1): requirement for hepatocyte nuclear factor 4alpha in gluconeogenesis. *Proc Natl Acad Sci U S A.* Apr 1 2003;100(7):4012-4017.
189. Durham SK, Suwanichkul A, Scheimann AO, et al. FKHR binds the insulin response element in the insulin-like growth factor binding protein-1 promoter. *Endocrinology.* Jul 1999;140(7):3140-3146.
190. Zhang W, Patil S, Chauhan B, et al. FoxO1 regulates multiple metabolic pathways in the liver: effects on gluconeogenic, glycolytic, and lipogenic gene expression. *J Biol Chem.* Apr 14 2006;281(15):10105-10117.
191. Dijkers PF, Medema RH, Lammers JW, et al. Expression of the pro-apoptotic Bcl-2 family member Bim is regulated by the forkhead transcription factor FKHR-L1. *Curr Biol.* Oct 5 2000;10(19):1201-1204.
192. Tang TT, Dowbenko D, Jackson A, et al. The forkhead transcription factor AFX activates apoptosis by induction of the BCL-6 transcriptional repressor. *J Biol Chem.* Apr 19 2002;277(16):14255-14265.
193. Modur V, Nagarajan R, Evers BM, et al. FOXO proteins regulate tumor necrosis factor-related apoptosis inducing ligand expression. Implications for PTEN mutation in prostate cancer. *J Biol Chem.* Dec 6 2002;277(49):47928-47937.
194. Gilley J, Coffey PJ, Ham J. FOXO transcription factors directly activate bim gene expression and promote apoptosis in sympathetic neurons. *J Cell Biol.* Aug 18 2003;162(4):613-622.
195. Real PJ, Benito A, Cuevas J, et al. Blockade of epidermal growth factor receptors chemosensitizes breast cancer cells through up-regulation of Bnip3L. *Cancer Res.* Sep 15 2005;65(18):8151-8157.
196. Rokudai S, Fujita N, Kitahara O, et al. Involvement of FKHR-dependent TRADD expression in chemotherapeutic drug-induced apoptosis. *Mol Cell Biol.* Dec 2002;22(24):8695-8708.
197. Nakamura N, Ramaswamy S, Vazquez F, et al. Forkhead transcription factors are critical effectors of cell death and cell cycle arrest downstream of PTEN. *Mol Cell Biol.* Dec 2000;20(23):8969-8982.
198. Sandri M, Sandri C, Gilbert A, et al. Foxo transcription factors induce the atrophy-related ubiquitin ligase atrogin-1 and cause skeletal muscle atrophy. *Cell.* Apr 30 2004;117(3):399-412.
199. Potente M, Urbich C, Sasaki K, et al. Involvement of Foxo transcription factors in angiogenesis and postnatal neovascularization. *J Clin Invest.* Sep 2005;115(9):2382-2392.
200. van den Heuvel AP, Schulze A, Burgering BM. Direct control of caveolin-1 expression by FOXO transcription factors. *Biochem J.* Feb 1 2005;385(Pt 3):795-802.
201. Nasrin N, Ogg S, Cahill CM, et al. DAF-16 recruits the CREB-binding protein coactivator complex to the insulin-like growth factor binding protein 1 promoter in HepG2 cells. *Proc Natl Acad Sci U S A.* Sep 12 2000;97(19):10412-10417.
202. Li P, Lee H, Guo S, et al. AKT-independent protection of prostate cancer cells from apoptosis mediated through complex formation between the androgen receptor and FKHR. *Mol Cell Biol.* Jan 2003;23(1):104-118.

203. Yang L, Xie S, Jamaluddin MS, et al. Induction of androgen receptor expression by phosphatidylinositol 3-kinase/Akt downstream substrate, FOXO3a, and their roles in apoptosis of LNCaP prostate cancer cells. *J Biol Chem*. Sep 30 2005;280(39):33558-33565.
204. Guo S, Sonenshein GE. Forkhead box transcription factor FOXO3a regulates estrogen receptor alpha expression and is repressed by the Her-2/neu/phosphatidylinositol 3-kinase/Akt signaling pathway. *Mol Cell Biol*. Oct 2004;24(19):8681-8690.
205. Seoane J, Le HV, Shen L, et al. Integration of Smad and forkhead pathways in the control of neuroepithelial and glioblastoma cell proliferation. *Cell*. Apr 16 2004;117(2):211-223.
206. Kortylewski M, Feld F, Kruger KD, et al. Akt modulates STAT3-mediated gene expression through a FKHR (FOXO1a)-dependent mechanism. *J Biol Chem*. Feb 14 2003;278(7):5242-5249.
207. Junger MA, Rintelen F, Stocker H, et al. The Drosophila forkhead transcription factor FOXO mediates the reduction in cell number associated with reduced insulin signaling. *J Biol*. 2003;2(3):20.
208. Puig O, Marr MT, Ruhf ML, et al. Control of cell number by Drosophila FOXO: downstream and feedback regulation of the insulin receptor pathway. *Genes Dev*. Aug 15 2003;17(16):2006-2020.
209. Skurk C, Izumiya Y, Maatz H, et al. The FOXO3a transcription factor regulates cardiac myocyte size downstream of AKT signaling. *J Biol Chem*. May 27 2005;280(21):20814-20823.
210. Stitt TN, Drujan D, Clarke BA, et al. The IGF-1/PI3K/Akt pathway prevents expression of muscle atrophy-induced ubiquitin ligases by inhibiting FOXO transcription factors. *Mol Cell*. May 7 2004;14(3):395-403.
211. Sedding DG, Braun-Dullaues RC. Caveolin-1: dual role for proliferation of vascular smooth muscle cells. *Trends Cardiovasc Med*. Feb 2006;16(2):50-55.
212. Martinez SC, Cras-Meneur C, Bernal-Mizrachi E, et al. Glucose Regulates Foxo1 Through Insulin Receptor Signaling in the Pancreatic Islet {beta}-cell. *Diabetes*. Jun 2006;55(6):1581-1591.
213. Mawal-Dewan M, Lorenzini A, Frisoni L, et al. Regulation of collagenase expression during replicative senescence in human fibroblasts by Akt-forkhead signaling. *J Biol Chem*. Mar 8 2002;277(10):7857-7864.
214. Alvarez B, Martinez AC, Burgering BM, et al. Forkhead transcription factors contribute to execution of the mitotic programme in mammals. *Nature*. Oct 18 2001;413(6857):744-747.
215. Schmidt M, Fernandez de Mattos S, van der Horst A, et al. Cell cycle inhibition by FoxO forkhead transcription factors involves downregulation of cyclin D. *Mol Cell Biol*. Nov 2002;22(22):7842-7852.
216. Martinez-Gac L, Marques M, Garcia Z, et al. Control of cyclin G2 mRNA expression by forkhead transcription factors: novel mechanism for cell cycle control by phosphoinositide 3-kinase and forkhead. *Mol Cell Biol*. Mar 2004;24(5):2181-2189.
217. Barthel A, Schmoll D, Kruger KD, et al. Differential regulation of endogenous glucose-6-phosphatase and phosphoenolpyruvate carboxykinase gene expression by the forkhead transcription factor FKHR in H4IIE-hepatoma cells. *Biochem Biophys Res Commun*. Jul 27 2001;285(4):897-902.
218. Furukawa-Hibi Y, Yoshida-Araki K, Ohta T, et al. FOXO forkhead transcription factors induce G(2)-M checkpoint in response to oxidative stress. *J Biol Chem*. Jul 26 2002;277(30):26729-26732.
219. Asselin-Labat ML, David M, Biola-Vidamment A, et al. GILZ, a new target for the transcription factor FoxO3, protects T lymphocytes from interleukin-2 withdrawal-induced apoptosis. *Blood*. Jul 1 2004;104(1):215-223.
220. Ayyadevara S, Dandapat A, Singh SP, et al. Lifespan extension in hypomorphic daf-2 mutants of *Caenorhabditis elegans* is partially mediated by glutathione transferase CeGSTP2-2. *Aging Cell*. Dec 2005;4(6):299-307.

221. Tang TT, Lasky LA. The forkhead transcription factor FOXO4 induces the down-regulation of hypoxia-inducible factor 1 alpha by a von Hippel-Lindau protein-independent mechanism. *J Biol Chem*. Aug 8 2003;278(32):30125-30135.
222. Kim HS, Skurk C, Maatz H, et al. Akt/FOXO3a signaling modulates the endothelial stress response through regulation of heat shock protein 70 expression. *Faseb J*. Jun 2005;19(8):1042-1044.
223. Puig O, Tjian R. Transcriptional feedback control of insulin receptor by dFOXO/FOXO1. *Genes Dev*. Oct 15 2005;19(20):2435-2446.
224. Kitamura YI, Kitamura T, Kruse JP, et al. FoxO1 protects against pancreatic beta cell failure through NeuroD and MafA induction. *Cell Metab*. Sep 2005;2(3):153-163.
225. Murakami S, Johnson TE. The OLD-1 positive regulator of longevity and stress resistance is under DAF-16 regulation in *Caenorhabditis elegans*. *Curr Biol*. Oct 2 2001;11(19):1517-1523.
226. Medema RH, Kops GJ, Bos JL, et al. AFX-like Forkhead transcription factors mediate cell-cycle regulation by Ras and PKB through p27kip1. *Nature*. Apr 13 2000;404(6779):782-787.
227. Dijkers PF, Medema RH, Pals C, et al. Forkhead transcription factor FKHR-L1 modulates cytokine-dependent transcriptional regulation of p27(KIP1). *Mol Cell Biol*. Dec 2000;20(24):9138-9148.
228. Collado M, Medema RH, Garcia-Cao I, et al. Inhibition of the phosphoinositide 3-kinase pathway induces a senescence-like arrest mediated by p27Kip1. *J Biol Chem*. Jul 21 2000;275(29):21960-21968.
229. Sandri M, Lin J, Handschin C, et al. PGC-1alpha protects skeletal muscle from atrophy by suppressing FoxO3 action and atrophy-specific gene transcription. *Proc Natl Acad Sci U S A*. Oct 31 2006;103(44):16260-16265.
230. Armoni M, Harel C, Karni S, et al. FOXO1 represses peroxisome proliferator-activated receptor-gamma1 and -gamma2 gene promoters in primary adipocytes. A novel paradigm to increase insulin sensitivity. *J Biol Chem*. Jul 21 2006;281(29):19881-19891.
231. Ookuma S, Fukuda M, Nishida E. Identification of a DAF-16 transcriptional target gene, scl-1, that regulates longevity and stress resistance in *Caenorhabditis elegans*. *Curr Biol*. Mar 4 2003;13(5):427-431.
232. Dansen TB, Kops GJ, Denis S, et al. Regulation of sterol carrier protein gene expression by the forkhead transcription factor FOXO3a. *J Lipid Res*. Jan 2004;45(1):81-88.
233. Brunet A, Sweeney LB, Sturgill JF, et al. Stress-dependent regulation of FOXO transcription factors by the SIRT1 deacetylase. *Science*. Mar 26 2004;303(5666):2011-2015.
234. Nemoto S, Fergusson MM, Finkel T. Nutrient availability regulates SIRT1 through a forkhead-dependent pathway. *Science*. Dec 17 2004;306(5704):2105-2108.
235. Essers MA, de Vries-Smits LM, Barker N, et al. Functional interaction between beta-catenin and FOXO in oxidative stress signaling. *Science*. May 20 2005;308(5725):1181-1184.
236. Vogt PK, Jiang H, Aoki M. Triple layer control: phosphorylation, acetylation and ubiquitination of FOXO proteins. *Cell Cycle*. Jul 2005;4(7):908-913.
237. van der Horst A, Burgering BM. Stressing the role of FoxO proteins in lifespan and disease. *Nat Rev Mol Cell Biol*. Jun 2007;8(6):440-450.
238. Rena G, Guo S, Cichy SC, et al. Phosphorylation of the transcription factor forkhead family member FKHR by protein kinase B. *J Biol Chem*. Jun 11 1999;274(24):17179-17183.
239. Biggs WH, 3rd, Meisenhelder J, Hunter T, et al. Protein kinase B/Akt-mediated phosphorylation promotes nuclear exclusion of the winged helix transcription factor FKHR1. *Proc Natl Acad Sci U S A*. Jun 22 1999;96(13):7421-7426.
240. Tang ED, Nunez G, Barr FG, et al. Negative regulation of the forkhead transcription factor FKHR by Akt. *J Biol Chem*. Jun 11 1999;274(24):16741-16746.
241. Takaishi H, Konishi H, Matsuzaki H, et al. Regulation of nuclear translocation of forkhead transcription factor AFX by protein kinase B. *Proc Natl Acad Sci U S A*. Oct 12 1999;96(21):11836-11841.

242. Guarente L, Kenyon C. Genetic pathways that regulate ageing in model organisms. *Nature*. Nov 9 2000;408(6809):255-262.
243. Kenyon C, Chang J, Gensch E, et al. A *C. elegans* mutant that lives twice as long as wild type. *Nature*. Dec 2 1993;366(6454):461-464.
244. van der Heide LP, Jacobs FM, Burbach JP, et al. FoxO6 transcriptional activity is regulated by Thr26 and Ser184, independent of nucleo-cytoplasmic shuttling. *Biochem J*. Nov 1 2005;391(Pt 3):623-629.
245. Brunet A, Kanai F, Stehn J, et al. 14-3-3 transits to the nucleus and participates in dynamic nucleocytoplasmic transport. *J Cell Biol*. Mar 4 2002;156(5):817-828.
246. Rena G, Prescott AR, Guo S, et al. Roles of the forkhead in rhabdomyosarcoma (FKHR) phosphorylation sites in regulating 14-3-3 binding, transactivation and nuclear targeting. *Biochem J*. Mar 15 2001;354(Pt 3):605-612.
247. Brunet A, Park J, Tran H, et al. Protein kinase SGK mediates survival signals by phosphorylating the forkhead transcription factor FKHL1 (FOXO3a). *Mol Cell Biol*. Feb 2001;21(3):952-965.
248. Woods YL, Rena G, Morrice N, et al. The kinase DYRK1A phosphorylates the transcription factor FKHR at Ser329 in vitro, a novel in vivo phosphorylation site. *Biochem J*. May 1 2001;355(Pt 3):597-607.
249. Rena G, Woods YL, Prescott AR, et al. Two novel phosphorylation sites on FKHR that are critical for its nuclear exclusion. *Embo J*. May 1 2002;21(9):2263-2271.
250. Hu MC, Lee DF, Xia W, et al. I kappa B kinase promotes tumorigenesis through inhibition of forkhead FOXO3a. *Cell*. Apr 16 2004;117(2):225-237.
251. Huang H, Regan KM, Lou Z, et al. CDK2-dependent phosphorylation of FOXO1 as an apoptotic response to DNA damage. *Science*. Oct 13 2006;314(5797):294-297.
252. Bois PR, Brochard VF, Salin-Cantegrel AV, et al. FoxO1a-cyclic GMP-dependent kinase I interactions orchestrate myoblast fusion. *Mol Cell Biol*. Sep 2005;25(17):7645-7656.
253. Essers MA, Weijzen S, de Vries-Smits AM, et al. FOXO transcription factor activation by oxidative stress mediated by the small GTPase Ral and JNK. *Embo J*. Dec 8 2004;23(24):4802-4812.
254. Oh SW, Mukhopadhyay A, Svrzikapa N, et al. JNK regulates lifespan in *Caenorhabditis elegans* by modulating nuclear translocation of forkhead transcription factor/DAF-16. *Proc Natl Acad Sci U S A*. Mar 22 2005;102(12):4494-4499.
255. Sunayama J, Tsuruta F, Masuyama N, et al. JNK antagonizes Akt-mediated survival signals by phosphorylating 14-3-3. *J Cell Biol*. Jul 18 2005;170(2):295-304.
256. Tsuruta F, Sunayama J, Mori Y, et al. JNK promotes Bax translocation to mitochondria through phosphorylation of 14-3-3 proteins. *Embo J*. Apr 21 2004;23(8):1889-1899.
257. Lehtinen MK, Yuan Z, Boag PR, et al. A conserved MST-FOXO signaling pathway mediates oxidative-stress responses and extends life span. *Cell*. Jun 2 2006;125(5):987-1001.
258. Legube G, Trouche D. Regulating histone acetyltransferases and deacetylases. *EMBO Rep*. Oct 2003;4(10):944-947.
259. Yang XJ. The diverse superfamily of lysine acetyltransferases and their roles in leukemia and other diseases. *Nucleic Acids Res*. 2004;32(3):959-976.
260. Fukuoka M, Daitoku H, Hatta M, et al. Negative regulation of forkhead transcription factor AFX (Foxo4) by CBP-induced acetylation. *Int J Mol Med*. Oct 2003;12(4):503-508.
261. Daitoku H, Hatta M, Matsuzaki H, et al. Silent information regulator 2 potentiates Foxo1-mediated transcription through its deacetylase activity. *Proc Natl Acad Sci U S A*. Jul 6 2004;101(27):10042-10047.
262. Motta MC, Divecha N, Lemieux M, et al. Mammalian SIRT1 represses forkhead transcription factors. *Cell*. Feb 20 2004;116(4):551-563.
263. van der Horst A, Tertoolen LG, de Vries-Smits LM, et al. FOXO4 is acetylated upon peroxide stress and deacetylated by the longevity protein hSir2(SIRT1). *J Biol Chem*. Jul 9 2004;279(28):28873-28879.
264. Perrot V, Rechler MM. The coactivator p300 directly acetylates the forkhead transcription factor Foxo1 and stimulates Foxo1-induced transcription. *Mol Endocrinol*. Sep 2005;19(9):2283-2298.

265. Yang Y, Hou H, Haller EM, et al. Suppression of FOXO1 activity by FHL2 through SIRT1-mediated deacetylation. *Embo J*. Mar 9 2005;24(5):1021-1032.
266. van der Horst A, de Vries-Smits AM, Brenkman AB, et al. FOXO4 transcriptional activity is regulated by monoubiquitination and USP7/HAUSP. *Nat Cell Biol*. Oct 2006;8(10):1064-1073.
267. Matsuzaki H, Daitoku H, Hatta M, et al. Acetylation of Foxo1 alters its DNA-binding ability and sensitivity to phosphorylation. *Proc Natl Acad Sci U S A*. Aug 9 2005;102(32):11278-11283.
268. Kobayashi Y, Furukawa-Hibi Y, Chen C, et al. SIRT1 is critical regulator of FOXO-mediated transcription in response to oxidative stress. *Int J Mol Med*. Aug 2005;16(2):237-243.
269. Frescas D, Valenti L, Accili D. Nuclear trapping of the forkhead transcription factor FoxO1 via Sirt-dependent deacetylation promotes expression of glucogenetic genes. *J Biol Chem*. May 27 2005;280(21):20589-20595.
270. Gan L, Han Y, Bastianetto S, et al. FoxO-dependent and -independent mechanisms mediate SirT1 effects on IGF1R gene expression. *Biochem Biophys Res Commun*. Dec 2 2005;337(4):1092-1096.
271. van der Heide LP, Smidt MP. Regulation of FoxO activity by CBP/p300-mediated acetylation. *Trends Biochem Sci*. Feb 2005;30(2):81-86.
272. Matsuzaki H, Daitoku H, Hatta M, et al. Insulin-induced phosphorylation of FKHR (Foxo1) targets to proteasomal degradation. *Proc Natl Acad Sci U S A*. Sep 30 2003;100(20):11285-11290.
273. Plas DR, Thompson CB. Akt activation promotes degradation of tuberlin and FOXO3a via the proteasome. *J Biol Chem*. Apr 4 2003;278(14):12361-12366.
274. Huang H, Regan KM, Wang F, et al. Skp2 inhibits FOXO1 in tumor suppression through ubiquitin-mediated degradation. *Proc Natl Acad Sci U S A*. Feb 1 2005;102(5):1649-1654.
275. Huang H, Muddiman DC, Tindall DJ. Androgens negatively regulate forkhead transcription factor FKHR (FOXO1) through a proteolytic mechanism in prostate cancer cells. *J Biol Chem*. Apr 2 2004;279(14):13866-13877.
276. Charvet C, Alberti I, Luciano F, et al. Proteolytic regulation of Forkhead transcription factor FOXO3a by caspase-3-like proteases. *Oncogene*. Jul 17 2003;22(29):4557-4568.
277. Gray SG, Ekstrom TJ. The human histone deacetylase family. *Exp Cell Res*. Jan 15 2001;262(2):75-83.
278. Imai S, Armstrong CM, Kaeblerlein M, et al. Transcriptional silencing and longevity protein Sir2 is an NAD-dependent histone deacetylase. *Nature*. Feb 17 2000;403(6771):795-800.
279. Blander G, Guarente L. The Sir2 family of protein deacetylases. *Annu Rev Biochem*. 2004;73:417-435.
280. Grozinger CM, Schreiber SL. Deacetylase enzymes: biological functions and the use of small-molecule inhibitors. *Chem Biol*. Jan 2002;9(1):3-16.
281. Frye RA. Phylogenetic classification of prokaryotic and eukaryotic Sir2-like proteins. *Biochem Biophys Res Commun*. Jul 5 2000;273(2):793-798.
282. Frye RA. Characterization of five human cDNAs with homology to the yeast SIR2 gene: Sir2-like proteins (sirtuins) metabolize NAD and may have protein ADP-ribosyltransferase activity. *Biochem Biophys Res Commun*. Jun 24 1999;260(1):273-279.
283. Tanno M, Sakamoto J, Miura T, et al. Nucleocytoplasmic shuttling of the NAD+-dependent histone deacetylase SIRT1. *J Biol Chem*. Mar 2 2007;282(9):6823-6832.
284. Landry J, Sutton A, Tafrov ST, et al. The silencing protein SIR2 and its homologs are NAD-dependent protein deacetylases. *Proc Natl Acad Sci U S A*. May 23 2000;97(11):5807-5811.
285. Tanny JC, Moazed D. Coupling of histone deacetylation to NAD breakdown by the yeast silencing protein Sir2: Evidence for acetyl transfer from substrate to an NAD breakdown product. *Proc Natl Acad Sci U S A*. Jan 16 2001;98(2):415-420.

286. Tanner KG, Landry J, Sternglanz R, et al. Silent information regulator 2 family of NAD-dependent histone/protein deacetylases generates a unique product, 1-O-acetyl-ADP-ribose. *Proc Natl Acad Sci U S A*. Dec 19 2000;97(26):14178-14182.
287. Grubisha O, Raftly LA, Takanishi CL, et al. Metabolite of SIR2 reaction modulates TRPM2 ion channel. *J Biol Chem*. May 19 2006;281(20):14057-14065.
288. Liou GG, Tanny JC, Kruger RG, et al. Assembly of the SIR complex and its regulation by O-acetyl-ADP-ribose, a product of NAD-dependent histone deacetylation. *Cell*. May 20 2005;121(4):515-527.
289. Lin SJ, Ford E, Haigis M, et al. Calorie restriction extends yeast life span by lowering the level of NADH. *Genes Dev*. Jan 1 2004;18(1):12-16.
290. Fulco M, Schiltz RL, Iezzi S, et al. Sir2 regulates skeletal muscle differentiation as a potential sensor of the redox state. *Mol Cell*. Jul 2003;12(1):51-62.
291. Cohen HY, Miller C, Bitterman KJ, et al. Calorie restriction promotes mammalian cell survival by inducing the SIRT1 deacetylase. *Science*. Jul 16 2004;305(5682):390-392.
292. Anderson RM, Bitterman KJ, Wood JG, et al. Nicotinamide and PNC1 govern lifespan extension by calorie restriction in *Saccharomyces cerevisiae*. *Nature*. May 8 2003;423(6936):181-185.
293. Bitterman KJ, Anderson RM, Cohen HY, et al. Inhibition of silencing and accelerated aging by nicotinamide, a putative negative regulator of yeast sir2 and human SIRT1. *J Biol Chem*. Nov 22 2002;277(47):45099-45107.
294. Bedalov A, Gatabonton T, Irvine WP, et al. Identification of a small molecule inhibitor of Sir2p. *Proc Natl Acad Sci U S A*. Dec 18 2001;98(26):15113-15118.
295. Grozinger CM, Chao ED, Blackwell HE, et al. Identification of a class of small molecule inhibitors of the sirtuin family of NAD-dependent deacetylases by phenotypic screening. *J Biol Chem*. Oct 19 2001;276(42):38837-38843.
296. Sauve AA, Wolberger C, Schramm VL, et al. The Biochemistry of Sirtuins. *Annu Rev Biochem*. Mar 3 2006.
297. Howitz KT, Bitterman KJ, Cohen HY, et al. Small molecule activators of sirtuins extend *Saccharomyces cerevisiae* lifespan. *Nature*. Sep 11 2003;425(6954):191-196.
298. Wood JG, Rogina B, Lavu S, et al. Sirtuin activators mimic caloric restriction and delay ageing in metazoans. *Nature*. Aug 5 2004;430(7000):686-689.
299. Viswanathan M, Kim SK, Berdichevsky A, et al. A role for SIR-2.1 regulation of ER stress response genes in determining *C. elegans* life span. *Dev Cell*. Nov 2005;9(5):605-615.
300. Baur JA, Pearson KJ, Price NL, et al. Resveratrol improves health and survival of mice on a high-calorie diet. *Nature*. Nov 16 2006;444(7117):337-342.
301. Middleton E, Jr., Kandaswami C, Theoharides TC. The effects of plant flavonoids on mammalian cells: implications for inflammation, heart disease, and cancer. *Pharmacol Rev*. Dec 2000;52(4):673-751.
302. Haigis MC, Guarente LP. Mammalian sirtuins--emerging roles in physiology, aging, and calorie restriction. *Genes Dev*. Nov 1 2006;20(21):2913-2921.
303. Kaeberlein M, McVey M, Guarente L. The SIR2/3/4 complex and SIR2 alone promote longevity in *Saccharomyces cerevisiae* by two different mechanisms. *Genes Dev*. Oct 1 1999;13(19):2570-2580.
304. Tissenbaum HA, Guarente L. Increased dosage of a sir-2 gene extends lifespan in *Caenorhabditis elegans*. *Nature*. Mar 8 2001;410(6825):227-230.
305. Wang Y, Oh SW, Deplancke B, et al. *C. elegans* 14-3-3 proteins regulate life span and interact with SIR-2.1 and DAF-16/FOXO. *Mech Ageing Dev*. Sep 2006;127(9):741-747.
306. Berdichevsky A, Guarente L. A stress response pathway involving sirtuins, forkheads and 14-3-3 proteins. *Cell Cycle*. Nov 2006;5(22):2588-2591.
307. Rogina B, Helfand SL. Sir2 mediates longevity in the fly through a pathway related to calorie restriction. *Proc Natl Acad Sci U S A*. Nov 9 2004;101(45):15998-16003.
308. Blander G, Olejnik J, Krzymanska-Olejnik E, et al. SIRT1 shows no substrate specificity in vitro. *J Biol Chem*. Mar 18 2005;280(11):9780-9785.
309. Picard F, Kurtev M, Chung N, et al. Sirt1 promotes fat mobilization in white adipocytes by repressing PPAR-gamma. *Nature*. Jun 17 2004;429(6993):771-776.

310. Rodgers JT, Lerin C, Haas W, et al. Nutrient control of glucose homeostasis through a complex of PGC-1 α and SIRT1. *Nature*. Mar 3 2005;434(7029):113-118.
311. Araki T, Sasaki Y, Milbrandt J. Increased nuclear NAD biosynthesis and SIRT1 activation prevent axonal degeneration. *Science*. Aug 13 2004;305(5686):1010-1013.
312. Luo J, Nikolaev AY, Imai S, et al. Negative control of p53 by Sir2 α promotes cell survival under stress. *Cell*. Oct 19 2001;107(2):137-148.
313. Vaziri H, Dessain SK, Ng Eaton E, et al. hSIR2(SIRT1) functions as an NAD-dependent p53 deacetylase. *Cell*. Oct 19 2001;107(2):149-159.
314. Langley E, Pearson M, Faretta M, et al. Human SIR2 deacetylates p53 and antagonizes PML/p53-induced cellular senescence. *Embo J*. May 15 2002;21(10):2383-2396.
315. Cheng HL, Mostoslavsky R, Saito S, et al. Developmental defects and p53 hyperacetylation in Sir2 homolog (SIRT1)-deficient mice. *Proc Natl Acad Sci U S A*. Sep 16 2003;100(19):10794-10799.
316. McBurney MW, Yang X, Jardine K, et al. The mammalian SIR2 α protein has a role in embryogenesis and gametogenesis. *Mol Cell Biol*. Jan 2003;23(1):38-54.
317. Yeung F, Hoberg JE, Ramsey CS, et al. Modulation of NF- κ B-dependent transcription and cell survival by the SIRT1 deacetylase. *Embo J*. Jun 16 2004;23(12):2369-2380.
318. Jeong J, Juhn K, Lee H, et al. SIRT1 promotes DNA repair activity and deacetylation of Ku70. *Exp Mol Med*. Feb 28 2007;39(1):8-13.
319. Sedding D, Haendeler J. Do we age on Sirt1 expression? *Circ Res*. May 25 2007;100(10):1396-1398.
320. Braun-Dullaeus RC, Mann MJ, Ziegler A, et al. A novel role for the cyclin-dependent kinase inhibitor p27(Kip1) in angiotensin II-stimulated vascular smooth muscle cell hypertrophy. *J Clin Invest*. Sep 1999;104(6):815-823.
321. Förster T. Intramolecular energy migration and fluorescence. *Ann Phys. (Leipzig)*. 1948;2:55-75.
322. Jares-Erijman EA, Jovin TM. FRET imaging. *Nat Biotechnol*. Nov 2003;21(11):1387-1395.
323. Gastard M. FRET Acceptor Bleaching (AB). *Confocal Application Notes*. February 2006 2006;5.
324. Gastard M. FRET Acceptor PhotoBleaching (AB) in LASAF. *Confocal Application Notes*. September 2006 2006;4.
325. Krasteva G, Pfeil U, Drab M, et al. Caveolin-1 and -2 in airway epithelium: expression and in situ association as detected by FRET-CLSM. *Respir Res*. 2006;7:108.
326. König P, Krasteva G, Tag C, et al. FRET-CLSM and double-labeling indirect immunofluorescence to detect close association of proteins in tissue sections. *Lab Invest*. Aug 2006;86(8):853-864.
327. Held P. An Introduction to Fluorescence Resonance Energy Transfer (FRET) Technology and its Application in Bioscience. *BioTek Application Note*. June 2005 2005.
328. Sata M, Maejima Y, Adachi F, et al. A mouse model of vascular injury that induces rapid onset of medial cell apoptosis followed by reproducible neointimal hyperplasia. *J Mol Cell Cardiol*. Nov 2000;32(11):2097-2104.
329. Laemmli UK. Cleavage of structural proteins during the assembly of the head of bacteriophage T4. *Nature*. Aug 15 1970;227(5259):680-685.
330. Kau TR, Schroeder F, Ramaswamy S, et al. A chemical genetic screen identifies inhibitors of regulated nuclear export of a Forkhead transcription factor in PTEN-deficient tumor cells. *Cancer Cell*. Dec 2003;4(6):463-476.
331. Schroeder FC, Kau TR, Silver PA, et al. The psammaplysenes, specific inhibitors of FOXO1 α nuclear export. *J Nat Prod*. Apr 2005;68(4):574-576.
332. Fernandez de Mattos S, Essafi A, Soeiro I, et al. FoxO3 α and BCR-ABL regulate cyclin D2 transcription through a STAT5/BCL6-dependent mechanism. *Mol Cell Biol*. Nov 2004;24(22):10058-10071.
333. Georgiades SN, Clardy J. Total synthesis of psammaplysenes A and B, naturally occurring inhibitors of FOXO1 α nuclear export. *Org Lett*. Sep 15 2005;7(19):4091-4094.

334. Georgiades SN, Clardy J. Preparation of a psammaphysene-based library. *Org Lett*. Sep 14 2006;8(19):4251-4254.
335. Goncharova EA, Ammit AJ, Irani C, et al. PI3K is required for proliferation and migration of human pulmonary vascular smooth muscle cells. *Am J Physiol Lung Cell Mol Physiol*. Aug 2002;283(2):L354-363.
336. Olschewski H, Olschewski A, Rose F, et al. Physiologic basis for the treatment of pulmonary hypertension. *J Lab Clin Med*. Nov 2001;138(5):287-297.
337. Pullamsetti S, Krick S, Yilmaz H, et al. Inhaled tolafertrine reverses pulmonary vascular remodeling via inhibition of smooth muscle cell migration. *Respir Res*. 2005;6:128.
338. Burgering BM, Medema RH. Decisions on life and death: FOXO Forkhead transcription factors are in command when PKB/Akt is off duty. *J Leukoc Biol*. Jun 2003;73(6):689-701.
339. Braun-Dullaeus RC, Mann MJ, Sedding DG, et al. Cell cycle-dependent regulation of smooth muscle cell activation. *Arterioscler Thromb Vasc Biol*. May 2004;24(5):845-850.
340. Zhang X, Gan L, Pan H, et al. Phosphorylation of serine 256 suppresses transactivation by FKHR (FOXO1) by multiple mechanisms. Direct and indirect effects on nuclear/cytoplasmic shuttling and DNA binding. *J Biol Chem*. Nov 22 2002;277(47):45276-45284.
341. Peterson TE, Guicciardi ME, Gulati R, et al. Caveolin-1 can regulate vascular smooth muscle cell fate by switching platelet-derived growth factor signaling from a proliferative to an apoptotic pathway. *Arterioscler Thromb Vasc Biol*. Sep 1 2003;23(9):1521-1527.
342. Razani B, Engelman JA, Wang XB, et al. Caveolin-1 null mice are viable but show evidence of hyperproliferative and vascular abnormalities. *J Biol Chem*. Oct 12 2001;276(41):38121-38138.
343. Zhao YY, Liu Y, Stan RV, et al. Defects in caveolin-1 cause dilated cardiomyopathy and pulmonary hypertension in knockout mice. *Proc Natl Acad Sci U S A*. Aug 20 2002;99(17):11375-11380.
344. Okamoto T, Schlegel A, Scherer PE, et al. Caveolins, a family of scaffolding proteins for organizing "preassembled signaling complexes" at the plasma membrane. *J Biol Chem*. Mar 6 1998;273(10):5419-5422.
345. Thompson EB, Ayala-Torres S. Oxysterols and apoptosis: evidence for gene regulation outside the cholesterol pathway. *Crit Rev Biochem Mol Biol*. 1999;34(1):25-32.
346. Brachmann CB, Sherman JM, Devine SE, et al. The SIR2 gene family, conserved from bacteria to humans, functions in silencing, cell cycle progression, and chromosome stability. *Genes Dev*. Dec 1 1995;9(23):2888-2902.
347. Alcendor RR, Kirshenbaum LA, Imai S, et al. Silent information regulator 2alpha, a longevity factor and class III histone deacetylase, is an essential endogenous apoptosis inhibitor in cardiac myocytes. *Circ Res*. Nov 12 2004;95(10):971-980.
348. Vaquero A, Scher M, Lee D, et al. Human SirT1 interacts with histone H1 and promotes formation of facultative heterochromatin. *Mol Cell*. Oct 8 2004;16(1):93-105.
349. Ross R. Cell biology of atherosclerosis. *Annu Rev Physiol*. 1995;57:791-804.
350. Ross R, Wight TN, Strandness E, et al. Human atherosclerosis. I. Cell constitution and characteristics of advanced lesions of the superficial femoral artery. *Am J Pathol*. Jan 1984;114(1):79-93.
351. Luo Z, Sata M, Nguyen T, et al. Adenovirus-mediated delivery of fas ligand inhibits intimal hyperplasia after balloon injury in immunologically primed animals. *Circulation*. Apr 13 1999;99(14):1776-1779.
352. Libby P. Molecular bases of the acute coronary syndromes. *Circulation*. Jun 1 1995;91(11):2844-2850.
353. Pieper AA, Verma A, Zhang J, et al. Poly (ADP-ribose) polymerase, nitric oxide and cell death. *Trends Pharmacol Sci*. Apr 1999;20(4):171-181.
354. Zhang J. Are poly(ADP-ribosylation) by PARP-1 and deacetylation by Sir2 linked? *Bioessays*. Aug 2003;25(8):808-814.
355. Kaeberlein M, McDonagh T, Heltweg B, et al. Substrate-specific activation of sirtuins by resveratrol. *J Biol Chem*. Apr 29 2005;280(17):17038-17045.

356. Araim O, Ballantyne J, Waterhouse AL, et al. Inhibition of vascular smooth muscle cell proliferation with red wine and red wine polyphenols. *J Vasc Surg.* Jun 2002;35(6):1226-1232.
357. Borra MT, Smith BC, Denu JM. Mechanism of human SIRT1 activation by resveratrol. *J Biol Chem.* Apr 29 2005;280(17):17187-17195.
358. Giannakou ME, Partridge L. The interaction between FOXO and SIRT1: tipping the balance towards survival. *Trends Cell Biol.* Aug 2004;14(8):408-412.
359. Tran H, Brunet A, Griffith EC, et al. The many forks in FOXO's road. *Sci STKE.* Mar 4 2003;2003(172):RE5.
360. Suhara T, Kim HS, Kirshenbaum LA, et al. Suppression of Akt signaling induces Fas ligand expression: involvement of caspase and Jun kinase activation in Akt-mediated Fas ligand regulation. *Mol Cell Biol.* Jan 2002;22(2):680-691.
361. Mercer J, Mahmoudi M, Bennett M. DNA damage, p53, apoptosis and vascular disease. *Mutat Res.* Mar 1 2007.

Appendix

Summary

Vasculo-proliferative disorders such as atherosclerosis, postangioplasty restenosis, and pulmonary hypertension are complex processes that are especially related to vascular smooth muscle cells (VSMCs)^{45, 78}. In the arterial media, VSMC are normally quiescent, however, for the development and progression of the above mentioned diseases it is prerequisite that quiescent VSMCs start to proliferate, migrate and undergo apoptosis. Different extracellular stimuli are responsible for regulating VSMC homeostasis, including growth factors, cytokines and mechanic stress. Through activating the intracellular phosphatidylinositol 3-kinase (PI3K)/Akt-pathway these factors critically regulate the transcriptional activity of the forkhead box O (FoxO) transcription factors via phosphorylation. FoxOs have crucial roles in different biological processes such as proliferation, differentiation, metabolism, aging, cell survival and stress resistance. Intervening VSMC function by affecting FoxO1a function may represent an attractive approach for future therapeutic strategies in the prevention of vasculo-proliferative diseases.

Part 1: Upon Akt-mediated phosphorylation under mitogenic conditions, FoxOs depart from the nucleus. However, stabilization and localization of the transcription factors in the nucleus is a prerequisite for executing their regulatory function. Psammaplysene A, a natural product from the marine sponge *Psammaplysilla* sp., was revealed to promote retention of FoxO1a in the nucleus of VSMCs by directly regulating FoxO1a localization. The marine compound was demonstrated to affect cell viability and to inhibit VSMC proliferation *in vitro* and *in vivo* by inhibiting S-phase due to attenuating cyclin D1 expression. A Psammaplysene A-analogue named F10 similarly affected VSMC behavior. By applying Psammaplysene A and F10 simultaneously, single doses of each compound could be reduced.

Dysfunction of pulmonary VSMCs (PAMCs) contributes to the development of pulmonary hypertension. In **Part 2** of this thesis I identified FoxO1a to simultaneously modulate proliferation, migration and cell death of PAMCs. Following transduction with constitutive active FoxO1a, proliferation and migration were significantly attenuated, whereas the number of apoptotic cells increased. Caveolin-1 was suggested to mainly mediate this pro-apoptotic response, since only protein expression of caveolin-1 - but not that of any other FoxO1a target involved in apoptosis - was elevated. The effect of FoxO1a on pathologically modified PAMCs was comparable to that on normal cells. This demonstrates FoxO transcription factors to be important in the disease state as well.

In **Part 3**, I showed that SIRT1, a class III histone deacetylase known for controlling longevity in organisms ranging from bacteria to complex eukaryotes, was able to regulate vascular homeostasis and remodeling processes *in vitro* and *in vivo*. It did so by deacetylating FoxO factors, thereby inducing their transcriptional activity. Under native conditions, SIRT1 physiologically interacts with FoxO1a. Pharmacological inhibition of SIRT1, as well as

knockdown of SIRT1 reduced FoxO1a's DNA-binding and transactivation capacity leading to attenuated FoxO1a target gene expression. In contrast, the SIRT1 activator resveratrol enhanced FoxO1a's transcriptional activity. Upon stress conditions, the observed SIRT1/FoxO1a interaction was increased and led to expression of target genes involved in regulating the cells oxidative stress response (e.g. GADD45), thus, shifting FoxO1a's transcriptional activity towards cell survival. Application of resveratrol protected from apoptotic cell death, whereas inhibition of SIRT1 activity by pharmacologic drugs or siRNA enhanced the apoptotic response. Moreover, embryonic fibroblasts derived from SIRT1 knockout mice were more resistant to oxidative stress-induced apoptosis as compared to wildtype cells.

Zusammenfassung

Vaskulo-proliferative Erkrankungen wie Atherosklerose, Restenose nach Koronarintervention sowie pulmonale Hypertonie sind komplexe Erkrankungen der Gefäßwand, bei denen vor allem glatte Gefäßmuskelzellen eine wichtige Rolle spielen. In der Regel befinden sich in der arteriellen Gefäßwand ruhende Gefäßmuskelzellen, unter pathologischen Bedingungen hingegen fangen diese Zellen an zu proliferieren, aus der Media auszuwandern und sogar apoptotisch zu werden. Verschiedenste extrazelluläre Faktoren, wie Wachstumsfaktoren, Zytokine und mechanischen Dehnungsreize, regulieren die Homöostase der glatten Gefäßmuskelzellen. Über diverse Transmembranrezeptoren aktivieren die genannten Faktoren die Phosphatidylinositol-3-Kinase (PI3K)/Akt Signaltransduktionskaskade, an deren Ende die Phosphorylierung und Deaktivierung von FoxO-Transkriptionsfaktoren steht. FoxO-Transkriptionsfaktoren wiederum spielen eine wichtige Rolle in den unterschiedlichsten biologischen Prozessen, wie Zellproliferation, Metabolismus-Kontrolle, zellulärem Überleben und Stresstoleranz. Eine Wiederherstellung der normalen Gefäßmuskelzell-Funktion durch Regulierung der FoxO-Aktivität könnte eine vielversprechende Strategie zur gezielten Therapie vaskulo-proliferativer Erkrankungen bilden.

Teil 1: Die Akt-vermittelte Phosphorylierung der FoxO-Transkriptionsfaktoren sorgt für deren Ausschleusung aus dem Nukleus. Ihre regulatorische Funktion können die FoxO-Transkriptionsfaktoren allerdings nur dann ausführen, wenn sie sich im dephosphorylierten Zustand im Nukleus befinden. In meinen Experimenten konnte gezeigt werden, dass Psammaphysene A, ein natürliches Produkt aus dem Meeresschwamm *Psammaphysilla* sp., das Ausschleusen von FoxO1a aus dem Nukleus verhindern kann. Zusätzlich konnte aufgezeigt werden, dass die Schwammsubstanz sowohl die Lebensfähigkeit als auch die Proliferation von glatten Gefäßmuskelzellen *in vitro* und *in vivo* beeinflusste. Voraussetzung hierfür war eine verminderte Zyklin D1 Expression, die den Eintritt der Zellen in die S-Phase des Zellzyklus verhinderte. Eine Psammaphysene A-analoge Substanz namens F10 beeinflusste auf ähnliche Weise das Verhalten der glatten Gefäßmuskelzellen. Durch die simultane Verabreichung von Psammaphysene A und F10 konnten die Einzeldosen – bei gleich bleibender Wirkung auf die Zellen - reduziert werden.

Dysfunktionen von pulmonalen Gefäßmuskelzellen legen den Grundstein für die Entwicklung von pulmonaler Hypertonie. In **Teil 2** meiner Arbeit konnte gezeigt werden, dass FoxO1a sowohl die Proliferation und Migration, als auch den apoptotischen Zelltod von pulmonalen Gefäßmuskelzellen beeinflusst. Eine Transduktion dieser Zellen mit einer konstitutiv aktiven FoxO1a-Form führte zu einer stark verminderten Zellproliferation und -migration, wohingegen die Anzahl apoptotischer Zellen signifikant anstieg. Von allen pro-apoptotischen FoxO1a-Zielgenen konnte in diesen Zellen nur die Expression von Caveolin-1 als gesteigert aufgezeigt

werden, und wurde somit als Hauptmediator der FoxO1a-vermittelten Apoptose identifiziert. Pathologisch veränderte pulmonale Gefäßmuskelzellen reagierten ähnlich wie normale Zellen auf die verstärkte Expression von inaktivem FoxO1a, was vielversprechend für eine zukünftige FoxO-bezogene Therapie bei pulmonaler Hypertonie ist.

In **Teil 3** konnte gezeigt werden, dass SIRT1 - eine Histondeazetylase der Klasse III, die für ihren Einfluss auf die Lebensdauer von Organismen bekannt ist – auch eine regulierende Funktion in arteriellen Gefäßmuskelzellen hat. SIRT1 sorgte hierbei für die Deazetylierung von FoxO Transkriptionsfaktoren, die daraufhin eine verstärkte Transkriptionsaktivität aufwiesen. Unter natürlichen Bedingungen interagierten beide Proteine physiologisch miteinander. Eine pharmakologische Inhibition der SIRT1-Aktivität brachte, genauso wie eine siRNA-vermittelte Runterregulation von SIRT1, eine reduzierte FoxO1a-Aktivität mit sich. Im Gegensatz dazu führte eine Behandlung mit dem SIRT1-Aktivator Resveratrol zu einer verstärkten transkriptionalen Aktivität von FoxO1a. Unter oxidativem Stress verstärkte sich die beobachtete SIRT1/FoxO1a-Interaktion noch weiter. Die dadurch gesteigerte Expression von an der Zellreparatur beteiligten Proteinen wie GADD45 erhöhte die Wahrscheinlichkeit eines Überlebens der Zelle. Die Gabe von Resveratrol schützte die glatten Gefäßmuskelzellen vor apoptotischem Zelltod, wohingegen eine Inhibition der SIRT1 Aktivität durch pharmakologische Substanzen oder siRNA zu einer Verstärkung der Apoptose führte. Darüber hinaus konnte gezeigt werden, dass embryonische Fibroblasten aus SIRT1-defizienten Mäusen resistenter gegenüber oxidativem Stress und der dadurch induzierten Apoptose waren als vergleichbare Wildtyp-Zellen.

Acronyms and Abbreviations

Acronym	Meaning
(ox)LDL	(oxidized) low-density lipoprotein
(V)SMCs	(Vascular) smooth muscle cell(s)
ACS	acute coronary syndrome
AR	androgen receptor
bFGF	basic fibroblast growth factor
bNIP3L	Bcl2/adenovirus E1B 19 kDa interacting protein 3-like
BTG1	B-cell translocation gene 1
CAM(s)	cell adhesion molecule(s)
CBP	CREB-binding protein
CDK2	cyclin-dependent kinase 2
cGKI	cyclic GMP-dependent protein kinase I
CK1	casein kinase
CMV	human cytomegalovirus
Cot	cancer Osaka thyroid
cyt-c	cytochrome c
DBE	DAF-16 family member-binding element
DYRK1	Tyrosine phosphorylated and -regulated kinase 1
ECM	extra-cellular matrix
ECs	endothelial cells
EGF	epidermal growth factor
eNOS	endothelial nitric oxide synthase
EPC	endothelial progenitor cells
ER	estrogen receptor
FasL	Fas ligand
FBS	Fetal bovine serum
FoxO	forkhead box O
g	gravity
G6Pase	glucose-6-phosphatase
GADD45	DNA damage-inducible protein 45
GM-CSF	Granulocyte-macrophage colony-stimulating factor
GSK3	glycogen synthase kinase 3
h	hour(s)
H ₂ O ₂	hydrogen peroxide
HAT(s)	histone acetyltransferase(s)
HAUSP	herpesvirus-associated ubiquitin-specific protease
HDAC(s)	Histone deacetylase(s)
HMGCS2	3-hydroxy-3-methylglutaryl-CoA synthase
hTERT	telomerase catalytic subunit

Id1	inhibitor of differentiation 1
IFN- γ	interferon gamma
IGF-1	insulin-like growth factor 1
IGFBP1	IGF-binding protein 1
IKK	I κ B kinase
IL-2	Interleukin 2
JNK	c-Jun N-terminal kinase
LPL	lipoprotein lipase
MCP-1	monocyte chemoattractant protein-1
M-CSF	macrophage colony-stimulating factor
MHC	myosin heavy chain
min	minutes
MMP	matrix metalloproteinase
MnSOD	manganese superoxide dismutase
MST1	mammalian sterile 20-like kinase-1
mTOR	mammalian target of rapamycin
NAM	nicotinamide
NCoR	nuclear receptor co-repressor
NES	nuclear export signal
NLS	nuclear localization signal
NO	nitric oxide
NO ₃ ⁻	peroxynitrite
O ²⁻	hydroxyl radical
PAI-1	plasminogen activator inhibitor 1
PASMC(s)	Pulmonary artery smooth muscle cell(s)
PCAF	CBP-associated factor
PCI	percutaneous coronary intervention
PDGF	platelet-derived growth factor
PDK-1	phosphoinositide-dependent kinase-1
PDK4	pyruvate dehydrogenase kinase 4
PEP	phosphoenolpyruvate
PEPCK	phosphoenolpyruvate carboxykinase
PGC-1	PPAR- γ coactivator 1
PH	pleckstrin-homology
PHT	pulmonary hypertension
PI(s)	phosphatidylinositol lipid(s)
PI3K	phosphatidylinositol 3-kinase
PKB	protein kinase B
Plk	Polo-like kinase
PPAR	Peroxisome proliferator-activated receptor
PS	phosphatidylserine

PTCA	Percutaneous transluminal coronary angioplasty
PTEN	phosphatase and tensin homologue deleted on chromosome 10
ROS	reactive oxygen species
rpm	Rounds per minutes
SGK	serum and glucocorticoid inducible kinase
SH2	Src-homology 2
Sir2	silent mating type information regulator 2
SIRT1	sirtuin1
SMRT	silencing mediator of retinoid and thyroid hormone receptors
TGF	transforming growth factor
TGF- β	transforming growth factor beta
TNFR1	TNF receptor-1
TNF- α	Tumor necrosis factor alpha
tPA	tissue plasminogen activator
TRADD	TNF receptor-associated death domain
TRAIL	TNF- related apoptosis-inducing ligand
TSA	Trichostatin A
uPA	urokinase plasminogen activator
VCAM-1	vascular cell adhesion molecule-1
vs	versus

Table 7. List of acronyms and abbreviations

Declaration

I declare that this dissertation represents my own work except where otherwise stated. This work has not been submitted to any other university for any degree or examination.

Heike König

Publications

Role of Sirt1 in Vascular Homeostasis and Pathologic Remodelling

Sedding DG, Vogel S, Daniel JM, Koenig H, Tillmanns H

Deutsche Gesellschaft für Kardiologie, Frühjahrstagung 2009

Functional and Molecular Effects of Resveratrol on Vascular Smooth Muscle Cells

Krämer F, Koenig H, Erdogan A, Tillmanns H, Preissner K, Sedding DG

Deutsche Gesellschaft für Kardiologie, Frühjahrstagung 2009

Sirt1 Modulates Foxo-dependent Transcription and Prevents Smooth Muscle Cell Apoptosis in Response to Oxidative Stress.

Sedding DG, Vogel S, Koenig H, Daniel JM, Tillmanns H

Deutsche Gesellschaft für Kardiologie, Frühjahrstagung 2008

Sirt1 Modulates Foxo-dependent Transcription and Prevents Smooth Muscle Cell Apoptosis in Response to Oxidative Stress

Sedding DG, Vogel S, Koenig H, Daniel JM, Tillmanns H

Scientific Sessions der American Heart Association 2007

Role of SIRT1 in VSMC Function and Vascular Remodeling

Sedding DG, Vogel S, Koenig H, Daniel JM, Tillmanns H

Scientific Sessions der American Heart Association 2007

Sirt1 Modulates Foxo-Dependent Transactivation and Prevents Smooth Muscle Cell Apoptosis in Response to Oxidative Stress

Sedding DG, Koenig H, Vogel S, Krasteva G, Kummer W, Tillmanns H

European Meeting on Vascular Biology and Medicine 2007

Sirt1 Modulates Foxo-dependent Transcription and Prevents Smooth Muscle Cell Apoptosis in Response to Oxidative Stress

Sedding DG, Vogel S, Koenig H, Daniel JM, Tillmanns H

Annual Meeting of the European Society of Cardiology 2007

Role of Foxo Transcription Factors in the Pathogenesis of Pulmonary Hypertension

Sedding DG, Pullamsetti S, Koenig H, Vogel S, Tillmanns H

Deutsche Gesellschaft für Kardiologie, Frühjahrstagung 2007

Role of SIRT1 in VSMC Function and Vascular Remodeling

Sedding DG, Vogel S, Koenig H, Daniel JM, Tillmanns H

Deutsche Gesellschaft für Kardiologie, Frühjahrstagung 2007

Sirt1 Modulates Foxo-dependent Transcription and Prevents Smooth Muscle Cell Apoptosis in Response to Oxidative Stress

Vogel S, Koenig H, Daniel JM, Tillmanns H, Sedding DG

Deutsche Gesellschaft für Kardiologie, Frühjahrstagung 2007

The Interaction between FoxO1a and SIRT1: Surviving Oxidative Stress

Koenig H

Annual Meeting of the Research Training Group 534 "Biological Basis of Vascular Medicine" 2007

Assessment of Transfection Parameters for Efficient siRNA-Mediated Gene Knock-Down in the Vascular System

Koenig H

Joint-Meeting of the Research Training Group 534 "Biological Basis of Vascular Medicine" 2006

Acknowledgements

After finishing my dissertation, I would like to thank all the persons who helped me to reach this target:

First, I would like to express my appreciation to Prof. Dr. H. Tillmanns, head of Internal Medicine I for providing me with a position in the lab for molecular cardiology and supporting my PhD thesis, and to Prof. Dr. W. Clauss from the faculty of biology for supporting my external dissertation for the Justus-Liebig-University, Giessen, Germany.

I am most grateful to my supervisor Dr. D. Sedding, head of the molecular cardiology lab, for backing me with his suggestions, knowledge and experience, and for carefully reviewing this thesis.

My thesis was financially supported by a DFG scholarship in the research training group 534 “Biological Basis of Vascular Medicine”. Therefore, Prof. Dr. H. M. Piper and PD Dr. T. Noll are also acknowledged for supporting this thesis and for providing scientific education.

Special thanks go to Dr. G. Krasteva and Prof. Dr. W. Kummer from the Institute for Anatomy for the cooperation with the FRET experiments, and to Dr. S. Pullamsetti and Prof. Dr. R. Schermuly from the University of Giessen Lung Center (UGLC) for the close collaboration concerning the PHT experiments.

Thanks to J.-M. Daniel and A. Prock for teaching me everything about mice dilatation operations and for their support with the *in vivo* experiments. Thanks also to all the other collaborators who made working not only a duty but also fun.

Special thanks go to Roche Diagnostics Austria for supporting me finishing this thesis

I would like to thank all my friends, especially S. Wößner, for helping me succeeding this dissertation and carefully reviewing it.

I am also grateful to my boyfriend Richard Stolz for his love and patience, for cheering me up during hard times and for providing me with food both inland and abroad.

Last but not least I wish to thank my parents, Reinhard and Rita König, and my sister Silke, for their enormous mental and financial support.